Supporting Information

One-Pot Method for Synthesis of 1-Aryl-2-Aminoalkanol Derivatives from the Corresponding Amides or Nitriles

Jan Otevrel,*[§] David Svestka,[§] Pavel Bobal*

Department of Chemical Drugs, Faculty of Pharmacy
Masaryk University, Palackeho 1946/1, 612 42 Brno, Czech Republic

*pbobal@icloud.com, *otevrel@icloud.com
§Both authors contributed equally to this work and appear here in alphabetical order

TABLE OF CONTENTS

1. Optimization of the Reaction Conditions S2
2. Substrate Scope S5
3. Determination of the Enantiomeric Purity of **8a**, **8b**, and **5a** S45
4. Identification of the Reaction Intermediates S50
5. References S61
6. HRMS and NMR Data S62

1. Optimization of the Reaction Conditions

1.1 Optimization of the Hydride Loading and the Reaction Temperature

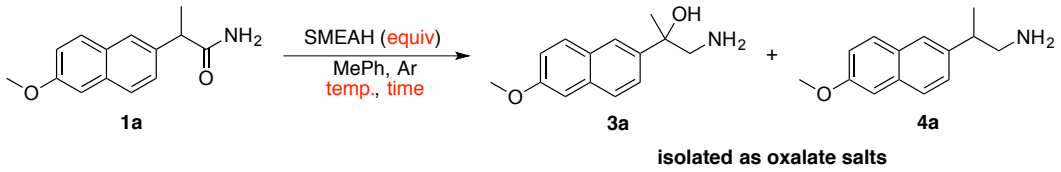

Optimization experiments were performed as follows: A solution of **1a** (0.3 g, 1.31 mmol) in an appropriate anhydrous solvent was treated with the corresponding hydride dropwise/portionwise at 0 °C (foaming). The resulting mixture was left to stir under the argon/air/oxygen-filled rubber balloon at ambient or slightly elevated temperature (55 °C) for 3–48 h (please, see **Tab. S1–S3** for further details). The initially formed deep-red color gradually disappeared during the reaction time, leaving the light-yellow colored solution.

TLC (SiO_2) CH_2Cl_2–MeOH (90:10) or $CHCl_3$–MeOH–NH_4OH (79:20:1).

Then the reaction mixture was carefully quenched by a dropwise addition of an aqueous solution of NaOH (5 M, 1 mL) at 0 °C and further diluted with an aqueous solution of NaOH (5 M, 15 mL). The organic and aqueous layers were separated and the aqueous phase was reextracted with toluene (5 × 15 mL). The combined organic phase was dried over anhydrous Na_2SO_4, filtered, and evaporated in vacuo.
The yellow oily residue was dissolved in 5 mL of Et_2O–MeOH, 5:1 and a solution of anhydrous oxalic acid (0.13 g, 1.1 equiv) in 5 mL of Et_2O–MeOH (5:1) was added dropwise. The resulting white precipitate was filtered off, washed several times with fresh Et_2O–MeOH (5:1), Et_2O, and dried in vacuo.

Table S1. Optimization of the hydride loading and the reaction temperature

entry	hydride	solvent	atm.	temp.	time	yield [a]	3a/4a ratio [b]	variable
1	**SMEAH** [70% in MePh, 5 equiv]	MePh [5 mL]	Ar	25 °C	48 h	30 mg	74:26	Hydride Load
2	**SMEAH** [70% in MePh, 10 equiv]	MePh [5 mL]	Ar	25 °C	48 h	60 mg	84:16	
3	**SMEAH** [70% in MePh, 15 equiv]	MePh [5 mL]	Ar	25 °C	48 h	145 mg	84:16	
4	**SMEAH** [70% in MePh, 20 equiv]	MePh [5 mL]	Ar	25 °C	48 h	162 mg	85:15	
5	**SMEAH** [70% in MePh, 10 equiv]	MePh [5 mL]	Ar	55 °C	24 h	79 mg	58:42	Temp.

Footnotes: Experiments were performed at the 1.3 mmol scale; SMEAH = sodium bis(2-methoxyethoxy)aluminum hydride; [a] based on the isolated yields, [b] measured by ^{1}H NMR (400 MHz, DMSO-d_6, 35 °C) analyses of the isolated products (**Fig. S1**).

1.2 Alteration of the Hydride Type

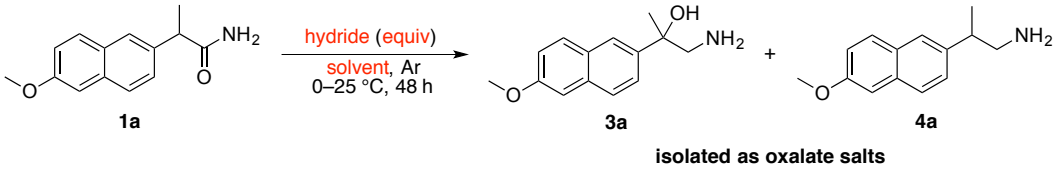

Table S2. Alteration of the Hydride Type

entry	hydride	solvent	atm.	temp.	time	yield [a]	3a/4a ratio [b]	variable
6	**DIBAH** [25% in MePh, 30 equiv]	MePh [5 mL]	Ar	25 °C	48 h	252 mg	1:99	Hydride Type
7	**LAH** [7.5 equiv]	THF–MePh [1:1, 8 mL]	Ar	25 °C	48 h	74 mg	5:95	
8	**LMAH** [15 equiv]	THF–MePh [1:1, 8 mL]	Ar	25 °C	48 h	214 mg	48:52	

Footnotes: Experiments were performed at the 1.3 mmol scale; DIBAH = diisobutylaluminum hydride, LAH = lithium aluminum hydride, LMAH = lithium dimethoxyaluminum hydride; [a] based on the isolated yields, [b] measured by ^{1}H NMR (400 MHz, DMSO-d_6, 35 °C) analyses of the isolated products (**Fig. S1**).

1.3 Optimization of the Solvent Type and the Reaction Atmosphere

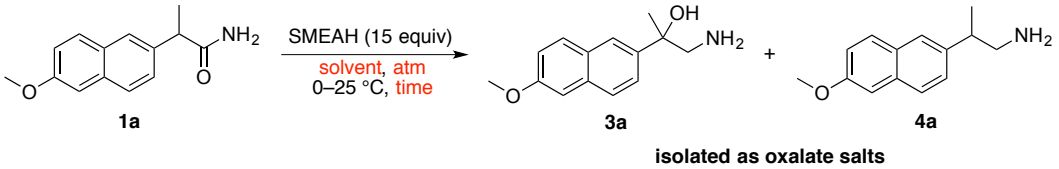

Table S3. Optimization of the Solvent Type

entry	hydride	solvent	atm.	temp.	time	yield [a]	3a/4a ratio [b]	variable
9	**SMEAH** [70% in MePh, 15 equiv]	THF [5 mL]	Ar	25 °C	48 h	87 mg	92:8	Solvent Type
10	**SMEAH** [70% in MePh, 15 equiv]	Et_2O [5 mL]	Ar	25 °C	48 h	120 mg	89:11	
11	**SMEAH** [70% in MePh, 15 equiv]	dioxane [5 mL]	Ar	25 °C	48 h	50 mg	93:7	
12	**SMEAH** [70% in MePh, 15 equiv]	DME [5 mL]	Ar	25 °C	48 h	61 mg	92:8	
13	**SMEAH** [70% in MePh, 15 equiv]	THF [5 mL]	Dry air	25 °C	3 h	75 mg	93:7	Atm.
14	**SMEAH** [70% in MePh, 15 equiv]	THF [5 mL]	O_2	25 °C	3 h	182 mg	94:6	

Footnotes: Experiments were performed at the 1.3 mmol scale; SMEAH = sodium bis(2-methoxyethoxy)aluminium hydride, DME = dimethoxyethane; [a] based on the isolated yields, [b] measured by ^{1}H NMR (400 MHz, DMSO-d_6, 35 °C) analyses of the isolated products (**Fig. S1**).

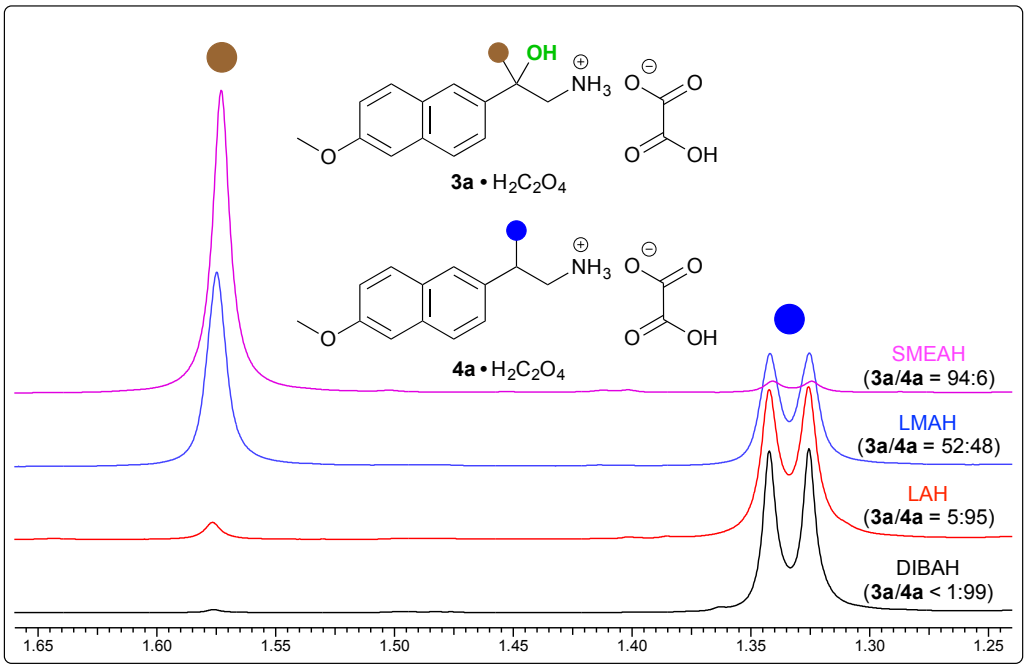

Figure S1. ^{1}H NMR (400 MHz, DMSO-d_6, 35 °C) analysis of the isolated product mixtures of **Entries 6–8** and **14** (in detail).

HPLC conditions: an YMC-Triart C_{18} column (3 μm, 150 × 2.0 mm), MeCN–50mM $HCOONH_4$ (pH = 9.30), 40:60, 0.2 mL/min, 40 °C (λ = 230 nm).

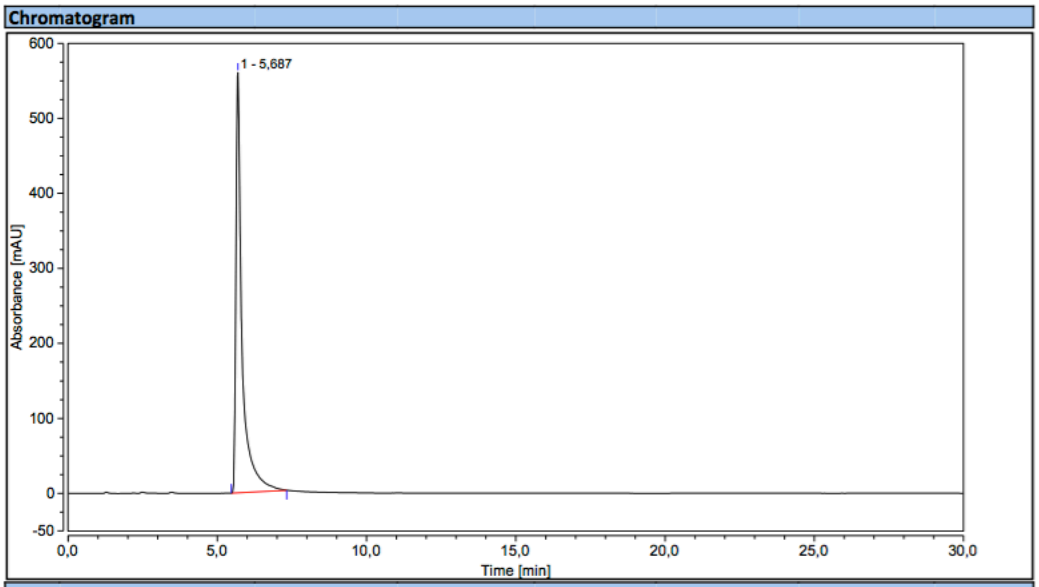

Integration Results

No.	Peak Name	Retention Time min	Area mAU*min	Height mAU	Relative Area %	Relative Height %	Amount n.a.
1		5,687	134,108	560,368	100,00	100,00	n.a.
Total:			**134,108**	**560,368**	**100,00**	**100,00**	

Figure S2. RP-HPLC analysis of the **4a** prepared according to the **Entry 6** (**Tab. S2**).

2. Substrate Scope

2.1 The reduction of **1a**

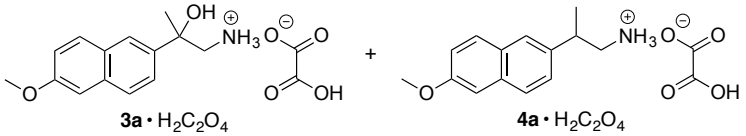

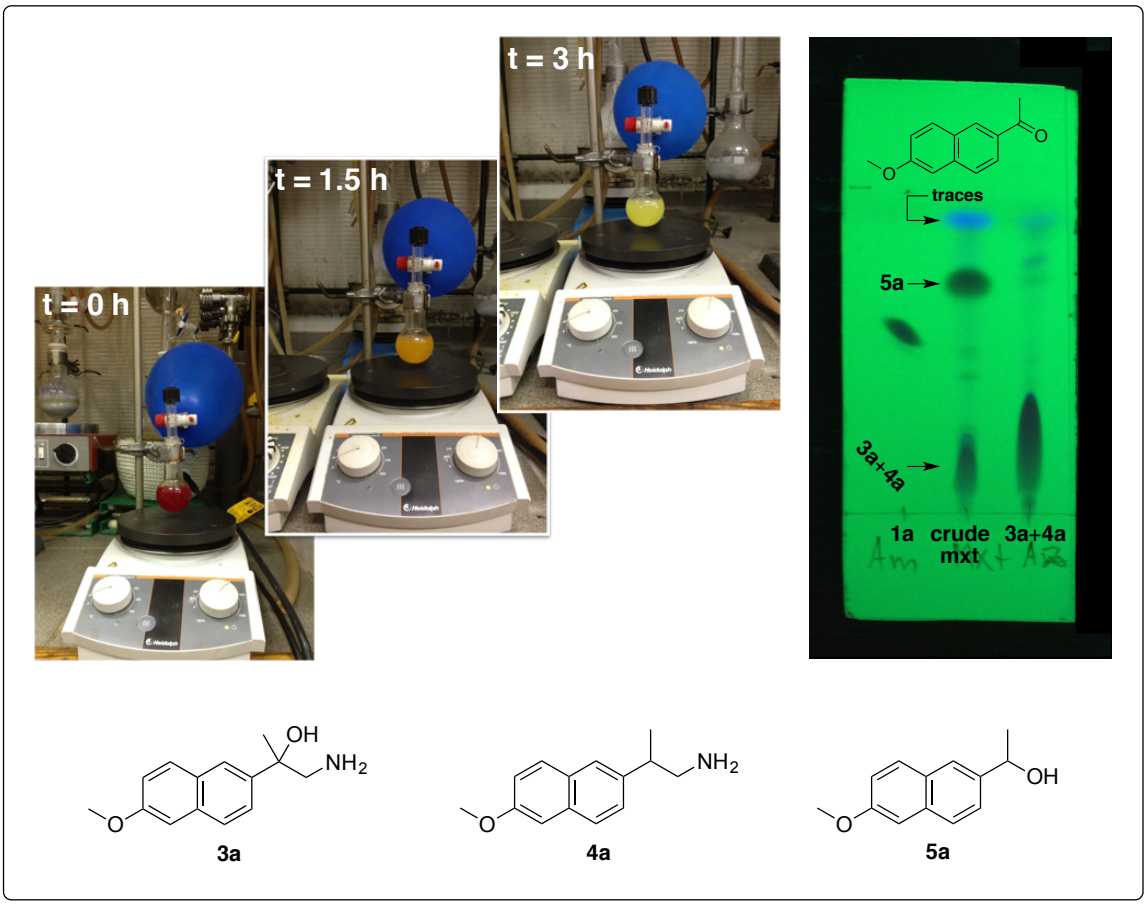

Figure S3. Visual progress and TLC analysis of the crude reaction mixture of **1a** after 3 h (SiO_2, CH_2Cl_2–MeOH, 9:1).

HPLC conditions: an YMC-Triart C_{18} column (3 μm, 150 × 2.0 mm), MeCN–50mM $HCOONH_4$ (pH = 9.30), 40:60, 0.2 mL/min, 40 °C (λ = 230 nm).

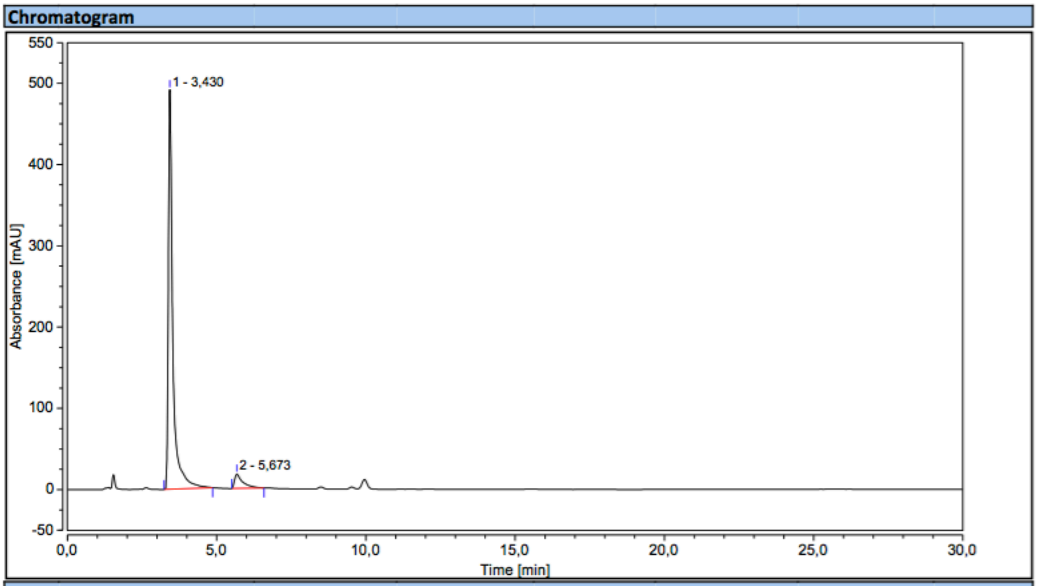

Integration Results

No.	Peak Name	Retention Time min	Area mAU*min	Height mAU	Relative Area %	Relative Height %	Amount n.a.
1		3,430	85,115	491,736	93,81	96,53	n.a.
2		5,673	5,619	17,653	6,19	3,47	n.a.
Total:			**90,734**	**509,389**	**100,00**	**100,00**	

Figure S4. RP-HPLC analysis of the precipitate from the reduction of **1a** showing **3a**/**4a** = 94:6 (external standard calibration method).

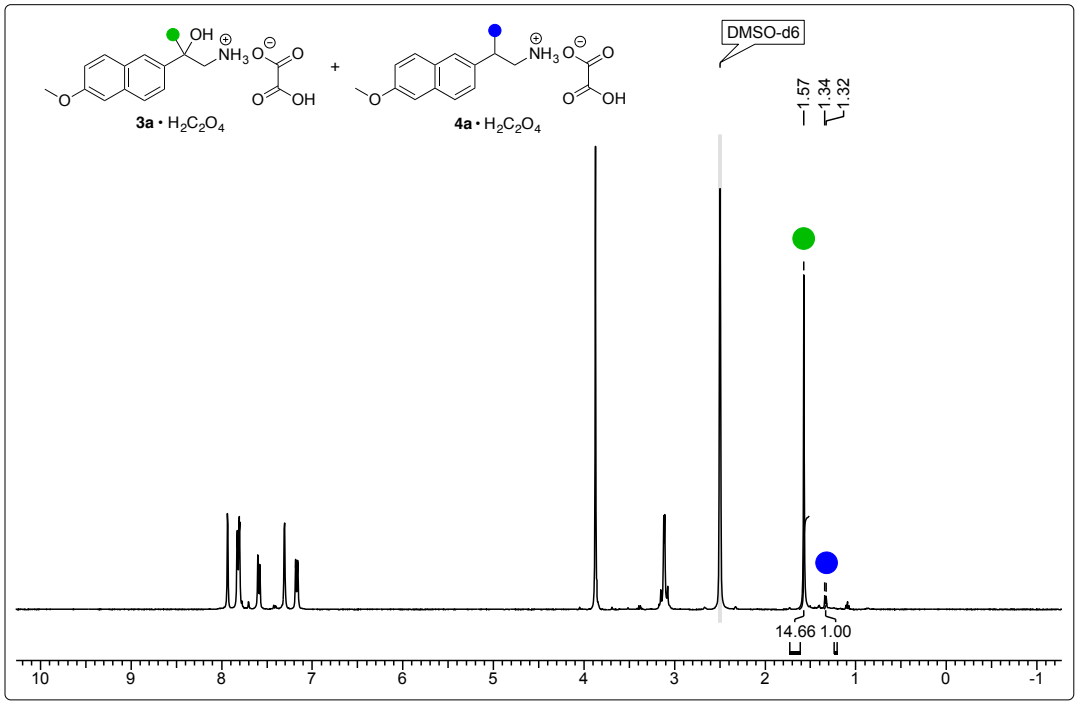

Figure S5. ^{1}H NMR (400 MHz, DMSO-d_6, 35 °C) analysis of the precipitate from the reduction of **1a** showing **3a**/**4a** = 94:6.

2.2 The reduction of **1ad**

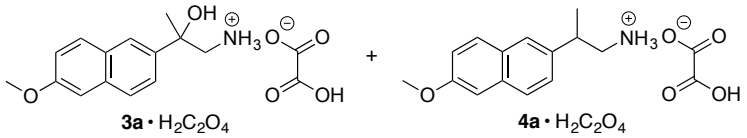

3a · $H_2C_2O_4$ **4a** · $H_2C_2O_4$

HPLC conditions: an YMC-Triart C_{18} column (3 μm, 150 × 2.0 mm), MeCN–50mM $HCOONH_4$ (pH = 9.30), 40:60, 0.2 mL/min, 40 °C (λ = 230 nm).

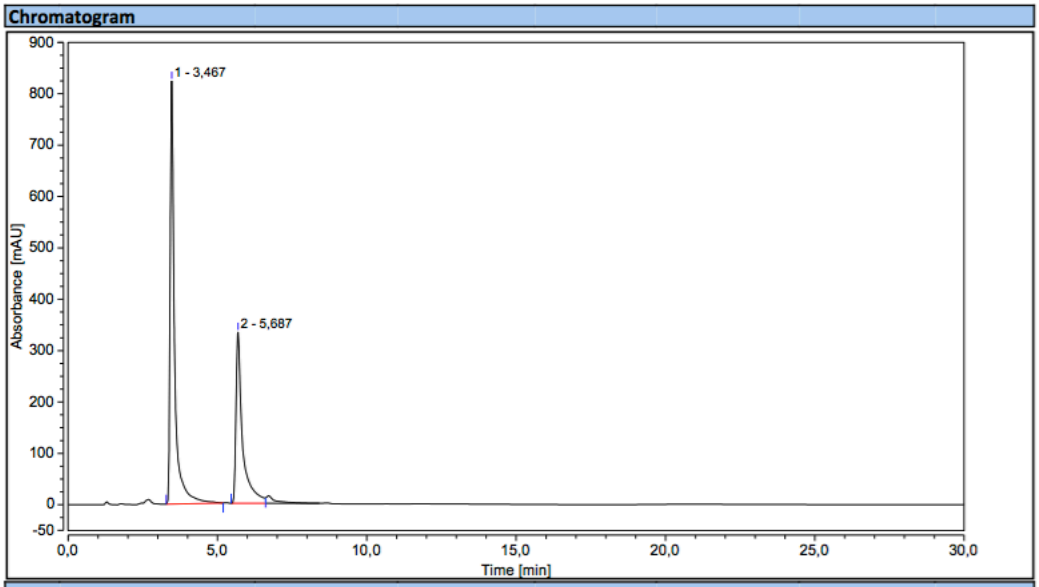

Integration Results

No.	Peak Name	Retention Time min	Area mAU*min	Height mAU	Relative Area %	Relative Height %	Amount n.a.
1		3,467	143,261	823,540	63,05	71,21	n.a.
2		5,687	83,940	332,988	36,95	28,79	n.a.
Total:			**227,201**	**1156,529**	**100,00**	**100,00**	

Figure S6. RP-HPLC analysis of the precipitate from the reduction of **1ad** showing **3a**/**4a** = 63:37 (external standard calibration method).

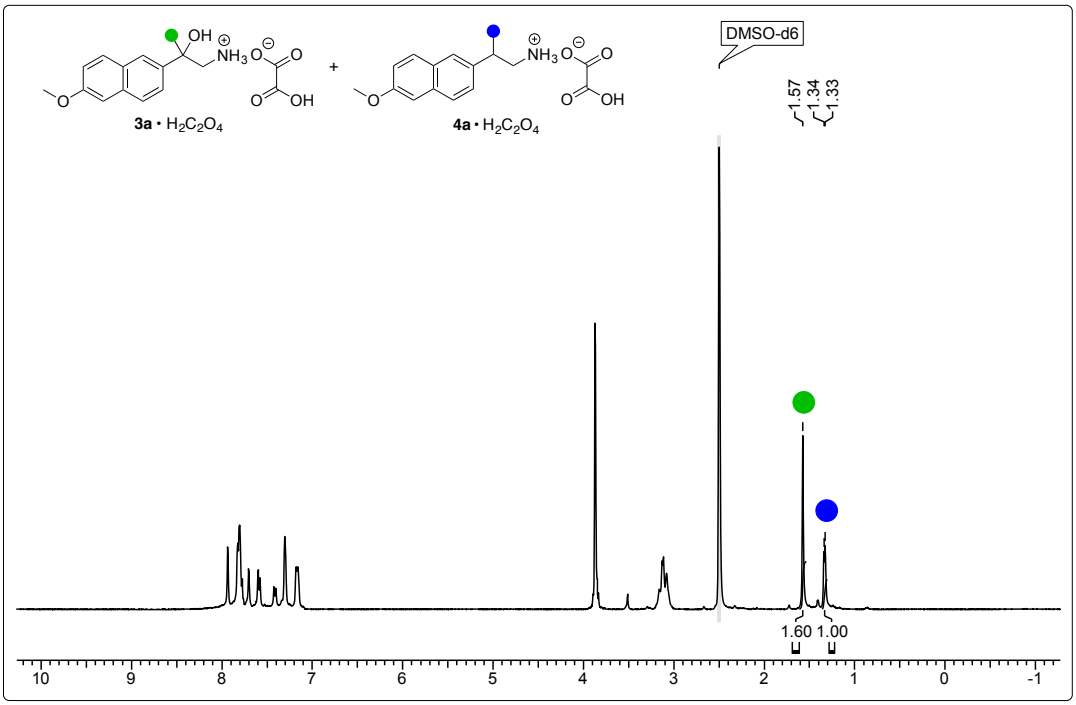

Figure S7. ^{1}H NMR (400 MHz, DMSO-d_6, 35 °C) analysis of the precipitate from the reduction of **1ad** showing **3a**/**4a** = 62:38.

2.3 The reduction of **1b**

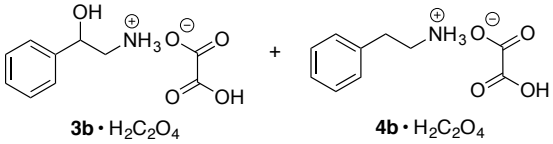

HPLC conditions: an YMC-Triart C_{18} column (3 μm, 150 × 2.0 mm), MeCN–50mM $HCOONH_4$ (pH = 9.30), 20:80, 0.2 mL/min, 40 °C (λ = 210 nm).

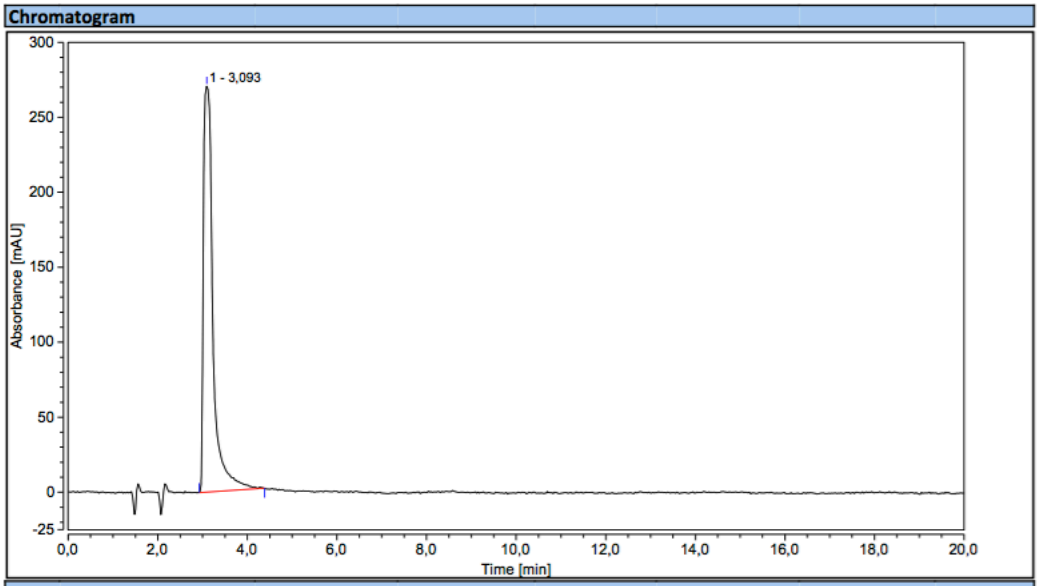

Integration Results

No.	Peak Name	Retention Time min	Area mAU*min	Height mAU	Relative Area %	Relative Height %	Amount n.a.
1		3,093	66,950	270,666	100,00	100,00	n.a.
Total:			**66,950**	**270,666**	**100,00**	**100,00**	

Figure S8. HPLC analysis of the authentic sample of **3b**.

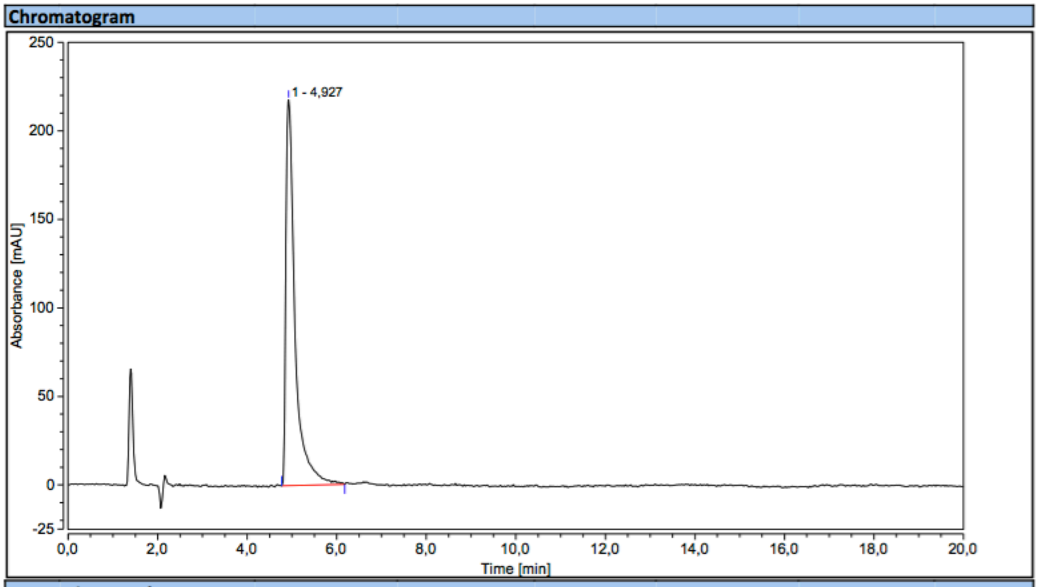

Integration Results

No.	Peak Name	Retention Time min	Area mAU*min	Height mAU	Relative Area %	Relative Height %	Amount n.a.
1		4,927	51,935	217,932	100,00	100,00	n.a.
Total:			**51,935**	**217,932**	**100,00**	**100,00**	

Figure S9. HPLC analysis of the authentic sample of **4b**. Note: the first peak corresponds to oxalic acid.

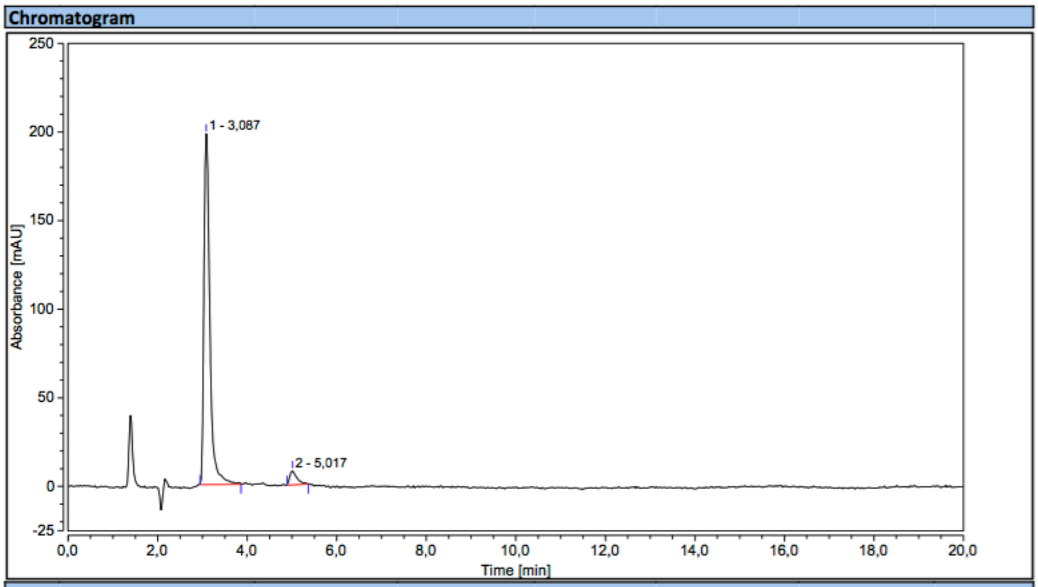

Integration Results

No.	Peak Name	Retention Time min	Area mAU*min	Height mAU	Relative Area %	Relative Height %	Amount n.a.
1		3,087	30,397	197,921	95,36	96,06	n.a.
2		5,017	1,478	8,120	4,64	3,94	n.a.
Total:			**31,875**	**206,041**	**100,00**	**100,00**	

Figure S10. HPLC analysis of the precipitate from the reduction of **1b** under O_2 atmosphere showing **3b**/**4b** = 95:5 (external standard calibration method). Note: the first peak corresponds to oxalic acid.

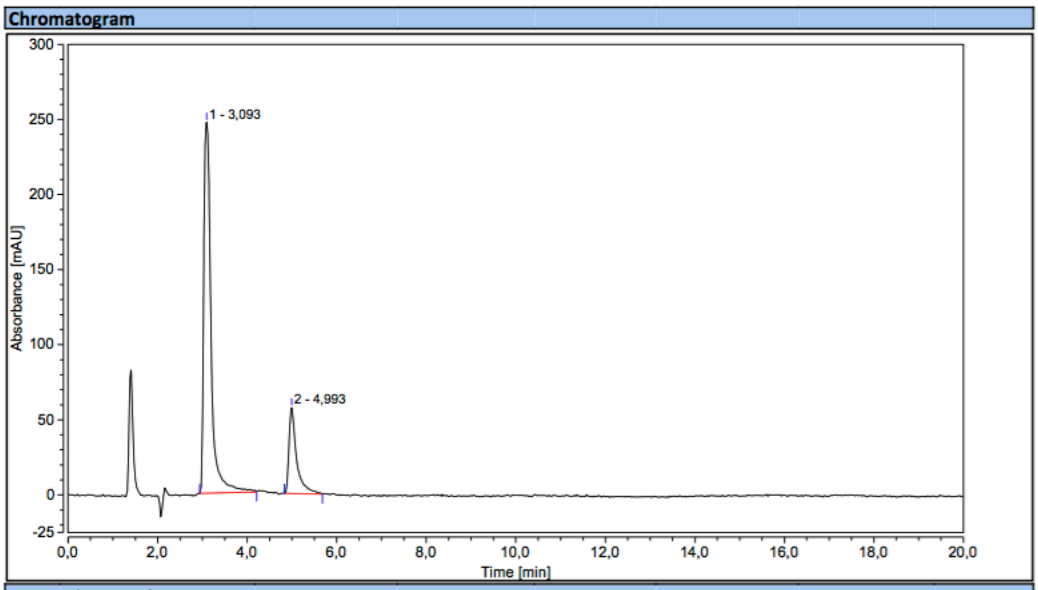

Integration Results

No.	Peak Name	Retention Time min	Area mAU*min	Height mAU	Relative Area %	Relative Height %	Amount n.a.
1		3,093	46,891	246,930	80,58	81,21	n.a.
2		4,993	11,301	57,122	19,42	18,79	n.a.
Total:			**58,192**	**304,052**	**100,00**	**100,00**	

Figure S11. HPLC analysis of the precipitate from the reduction of **1b** under Ar atmosphere showing **3b**/**4b** = 81:19 (external standard calibration method). Note: the first peak corresponds to oxalic acid.

2.4 The reduction of **1ba**

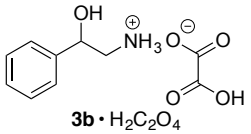

HPLC conditions: an YMC-Triart C_{18} column (3 μm, 150 × 2.0 mm), MeCN–50mM $HCOONH_4$ (pH = 9.30), 20:80, 0.2 mL/min, 40 °C (λ = 210 nm).

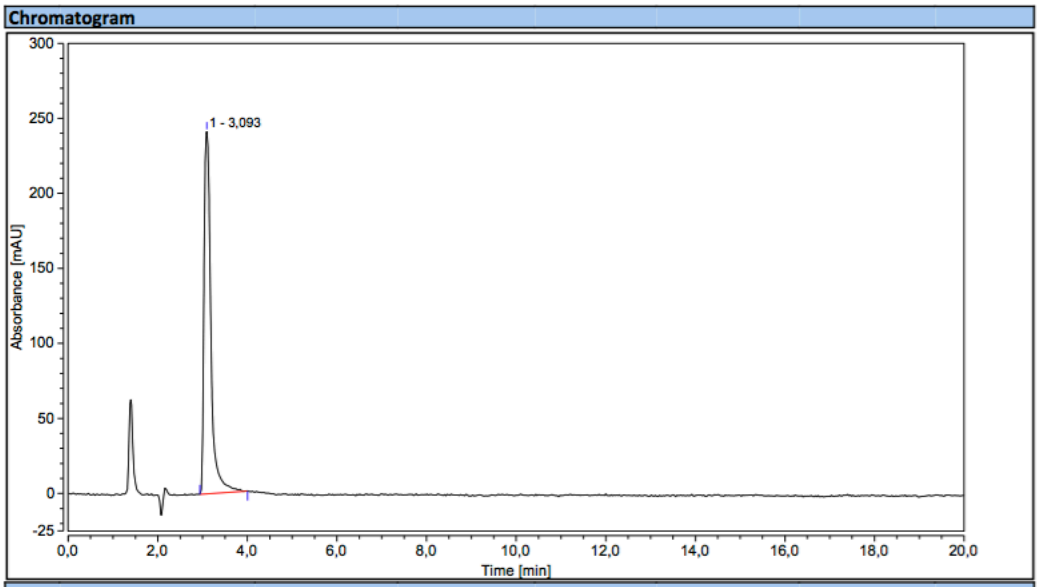

Integration Results

No.	Peak Name	Retention Time min	Area mAU*min	Height mAU	Relative Area %	Relative Height %	Amount n.a.
1		3,093	43,146	241,390	100,00	100,00	n.a.
Total:			**43,146**	**241,390**	**100,00**	**100,00**	

Figure S12. HPLC analysis of the precipitate from the reduction of **1ba** showing **3b**. Note: the first peak corresponds to oxalic acid.

2.5 The reduction of **1bb**

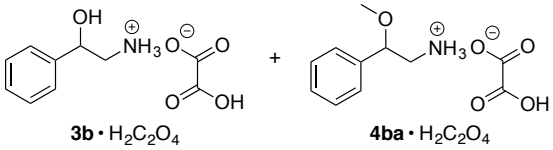

HPLC conditions: an YMC-Triart C_{18} column (3 μm, 150 × 2.0 mm), MeCN–50mM $HCOONH_4$ (pH = 9.30), 20:80, 0.2 mL/min, 40 °C (λ = 210 nm).

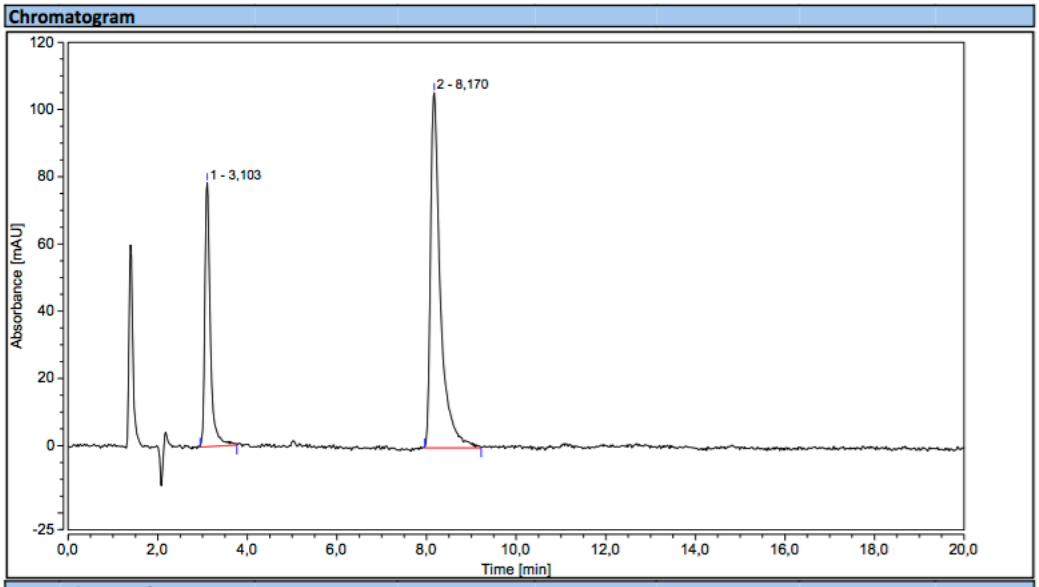

Integration Results

No.	Peak Name	Retention Time min	Area mAU*min	Height mAU	Relative Area %	Relative Height %	Amount n.a.
1		3,103	11,260	78,573	29,41	42,65	n.a.
2		8,170	27,024	105,653	70,59	57,35	n.a.
Total:			**38,285**	**184,226**	**100,00**	**100,00**	

Figure S13. HPLC analysis of the precipitate from the reduction of **1bb** showing **3b**/**4ba** = 29:71 (external standard calibration method). Note: the first peak corresponds to oxalic acid.

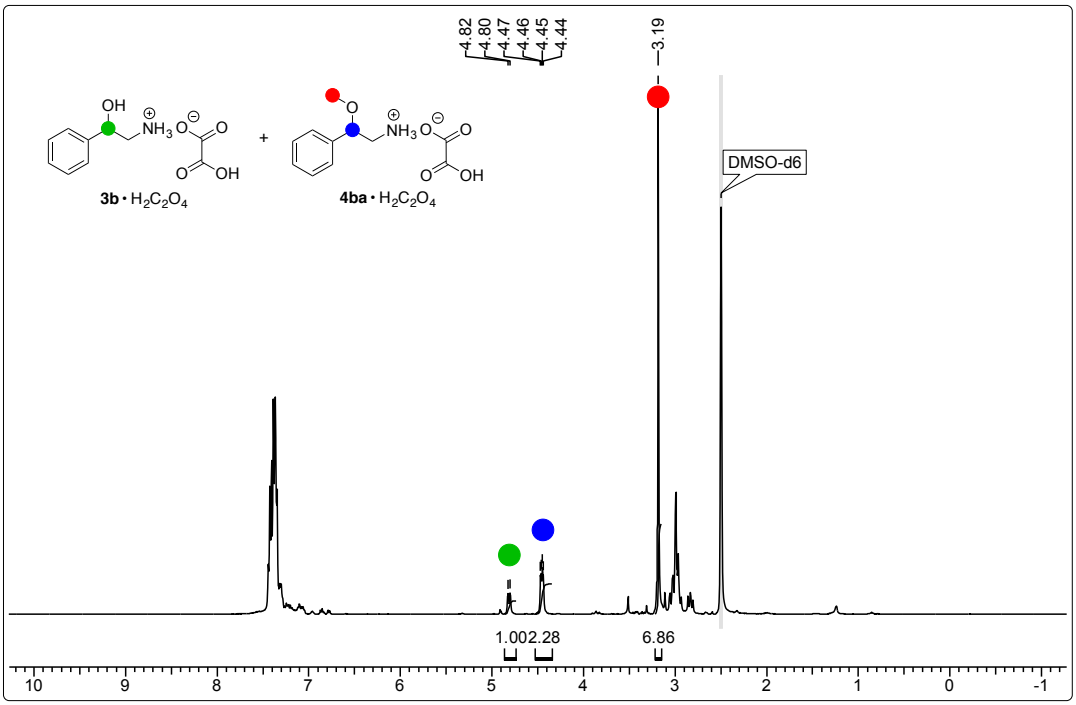

Figure S14. ^{1}H NMR (400 MHz, DMSO-d_6, 35 °C) analysis of the precipitate from the reduction of **1bb** showing **3b**/**4ba** = 30:70.

2.6 The reduction of **1bc**

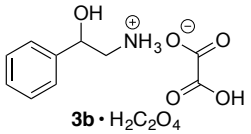

HPLC conditions: an YMC-Triart C_{18} column (3 µm, 150 × 2.0 mm), MeCN–50mM $HCOONH_4$ (pH = 9.30), 20:80, 0.2 mL/min, 40 °C (λ = 210 nm).

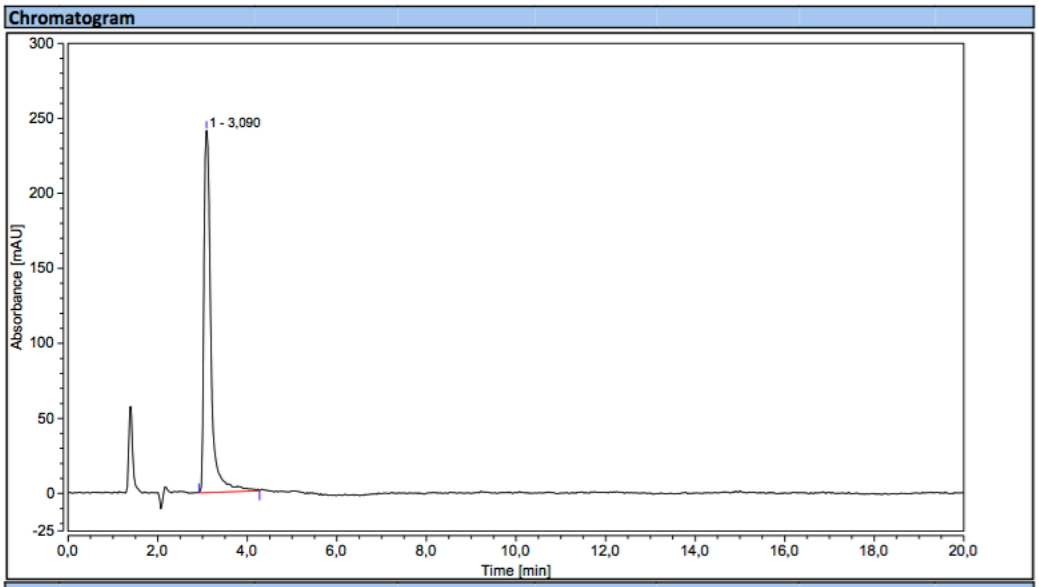

Integration Results

No.	Peak Name	Retention Time min	Area mAU*min	Height mAU	Relative Area %	Relative Height %	Amount n.a.
1		3,090	43,968	241,363	100,00	100,00	n.a.
Total:			**43,968**	**241,363**	**100,00**	**100,00**	

Figure S15. HPLC analysis of the precipitate from the reduction of **1bc** showing **3b**. Note: the first peak corresponds to oxalic acid.

2.7 The reduction of **1c**

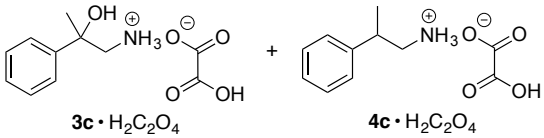

HPLC conditions: an YMC-Triart C_{18} column (3 μm, 150 × 2.0 mm), MeCN–50mM $HCOONH_4$ (pH = 9.30), 30:70, 0.2 mL/min, 40 °C (λ = 210 nm).

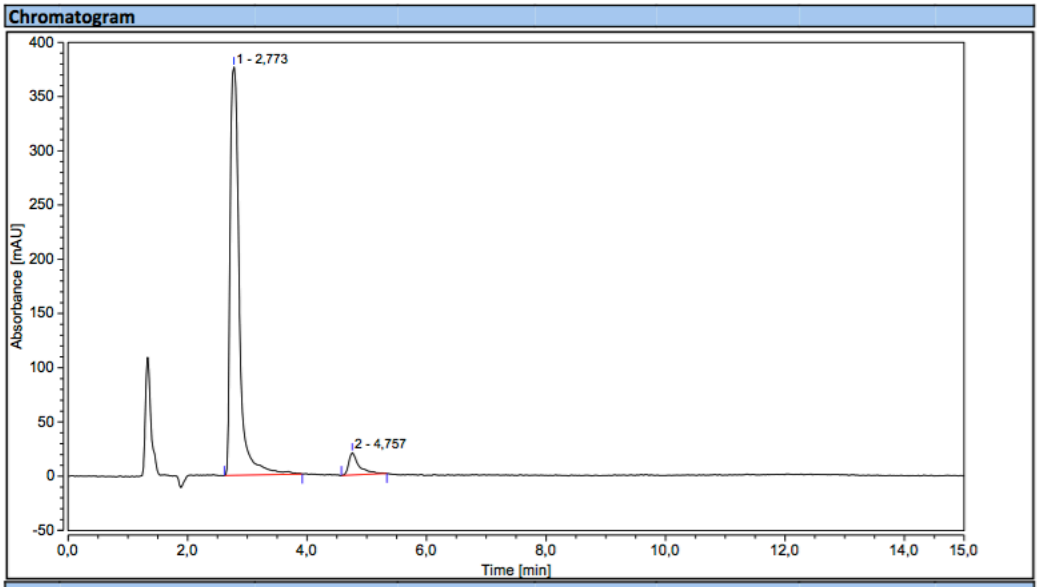

Integration Results

No.	Peak Name	Retention Time min	Area mAU*min	Height mAU	Relative Area %	Relative Height %	Amount n.a.
1		2,773	66,981	376,654	94,23	94,82	n.a.
2		4,757	4,100	20,581	5,77	5,18	n.a.
Total:			**71,080**	**397,234**	**100,00**	**100,00**	

Figure S16. HPLC analysis of the precipitate from the reduction of **1c** showing **3c**/**4c** = 95:5 (external standard calibration method). Note: the first peak corresponds to oxalic acid.

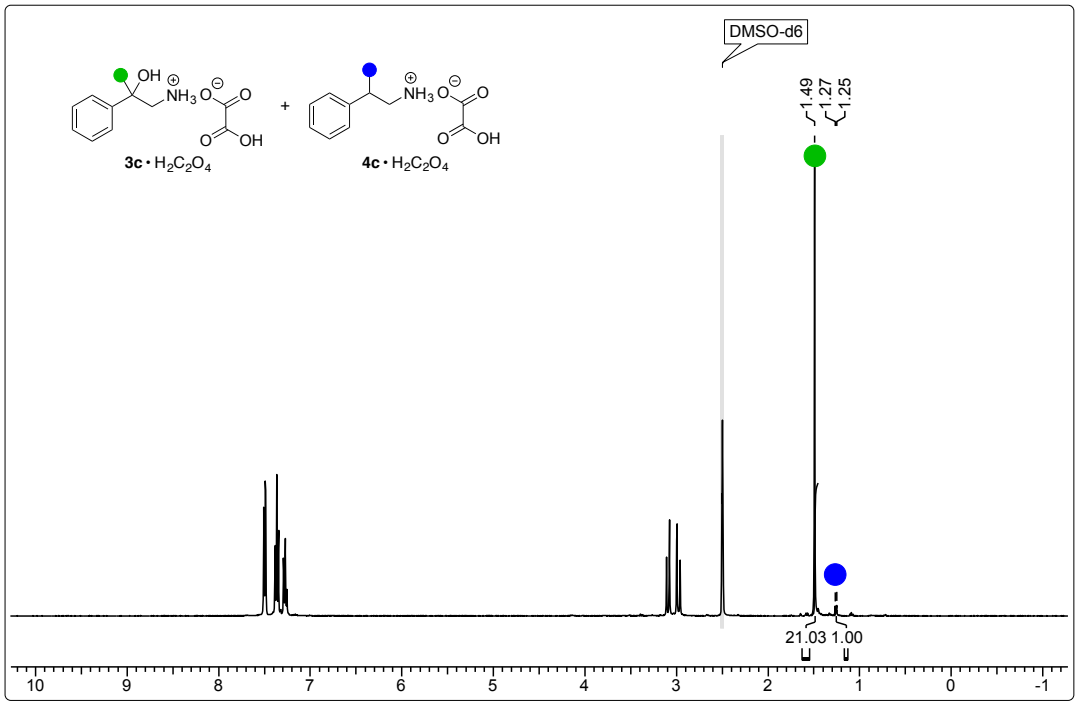

Figure S17. ^{1}H NMR (400 MHz, DMSO-d_6, 35 °C) analysis of the precipitate from the reduction of **1c** showing **3c**/**4c** = 95:5.

2.8 The reduction of **1ca**

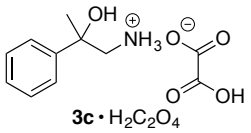

HPLC conditions: an YMC-Triart C_{18} column (3 μm, 150 × 2.0 mm), MeCN–50mM $HCOONH_4$ (pH = 9.30), 30:70, 0.2 mL/min, 40 °C (λ = 210 nm).

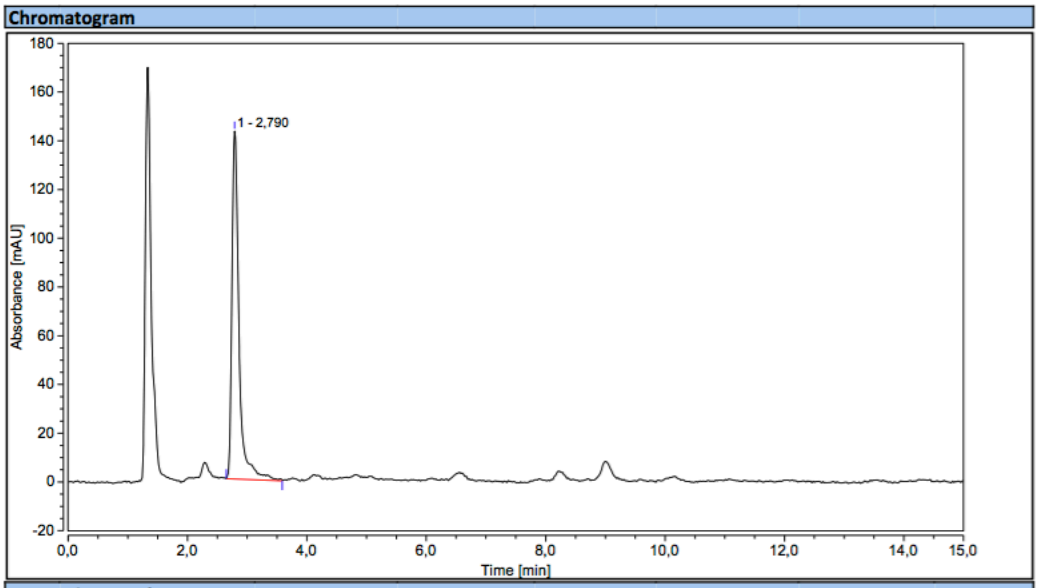

Integration Results

No.	Peak Name	Retention Time min	Area mAU*min	Height mAU	Relative Area %	Relative Height %	Amount n.a.
1		2,790	19,438	142,736	100,00	100,00	n.a.
Total:			**19,438**	**142,736**	**100,00**	**100,00**	

Figure S18. HPLC analysis of the precipitate from the reduction of **1ca** showing **3c**. Note: the first peak corresponds to oxalic acid.

2.9 The reduction of **1cb**

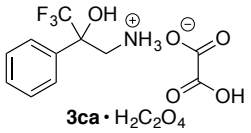

HPLC conditions: an YMC-Triart C_{18} column (3 μm, 150 × 2.0 mm), MeCN–50mM $HCOONH_4$ (pH = 9.30), 30:70, 0.2 mL/min, 40 °C (λ = 210 nm).

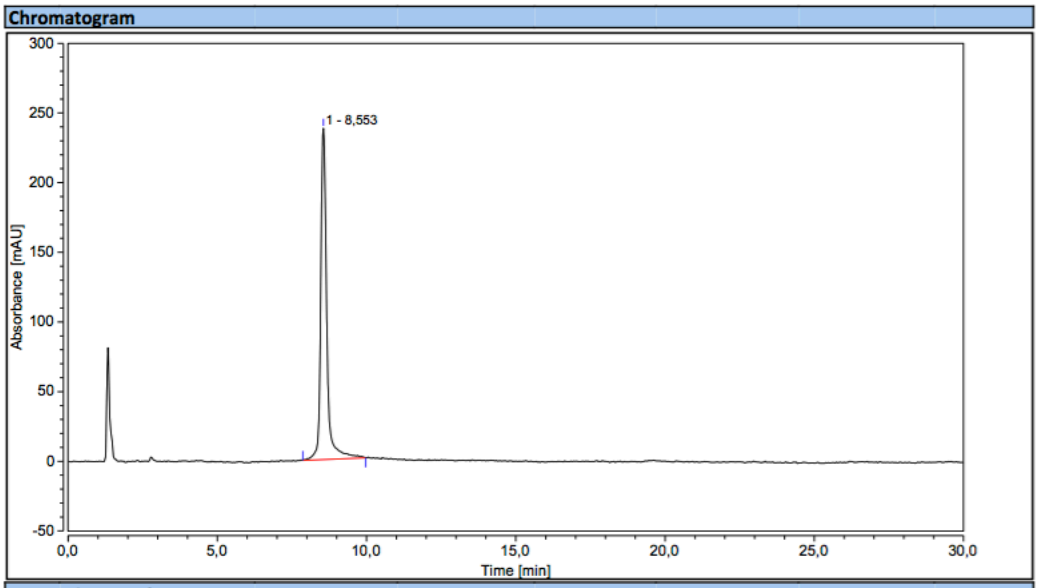

Integration Results

No.	Peak Name	Retention Time min	Area mAU*min	Height mAU	Relative Area %	Relative Height %	Amount n.a.
1		8,553	55,694	237,707	100,00	100,00	n.a.
Total:			**55,694**	**237,707**	**100,00**	**100,00**	

Figure S19. HPLC analysis of the precipitate from the reduction of **1cb** showing **3ca**. Note: the first peak corresponds to oxalic acid.

2.10 The reduction of **1cc**

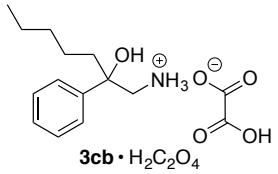

HPLC conditions: an YMC-Triart C_{18} column (3 μm, 150 × 2.0 mm), MeCN–50mM $HCOONH_4$ (pH = 9.30), 40:60, 0.2 mL/min, 40 °C (λ = 210 nm).

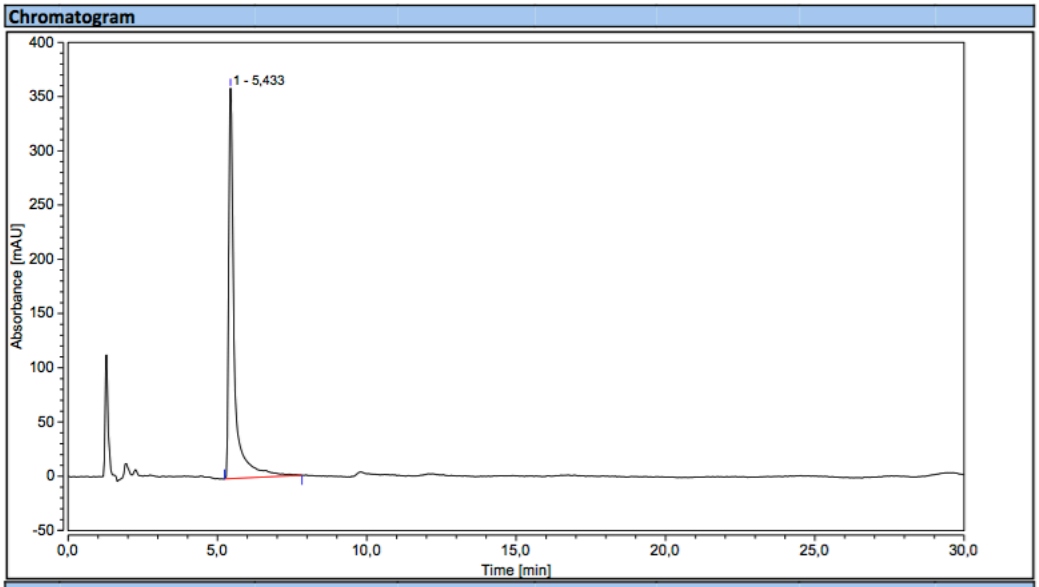

Integration Results

No.	Peak Name	Retention Time min	Area mAU*min	Height mAU	Relative Area %	Relative Height %	Amount n.a.
1		5,433	79,538	359,918	100,00	100,00	n.a.
Total:			**79,538**	**359,918**	**100,00**	**100,00**	

Figure S20. HPLC analysis of the precipitate from the reduction of **1cc** showing **3cb**. Note: the first peak corresponds to oxalic acid.

2.11 The reduction of **1d**

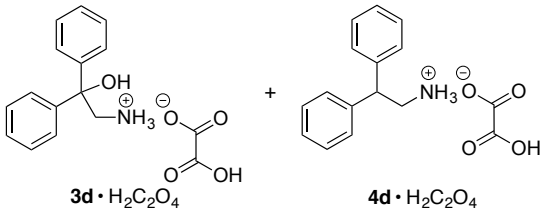

HPLC conditions: an YMC-Triart C_{18} column (3 μm, 150 × 2.0 mm), MeCN–50mM $HCOONH_4$ (pH = 9.30), 40:60, 0.2 mL/min, 40 °C (λ = 210 nm).

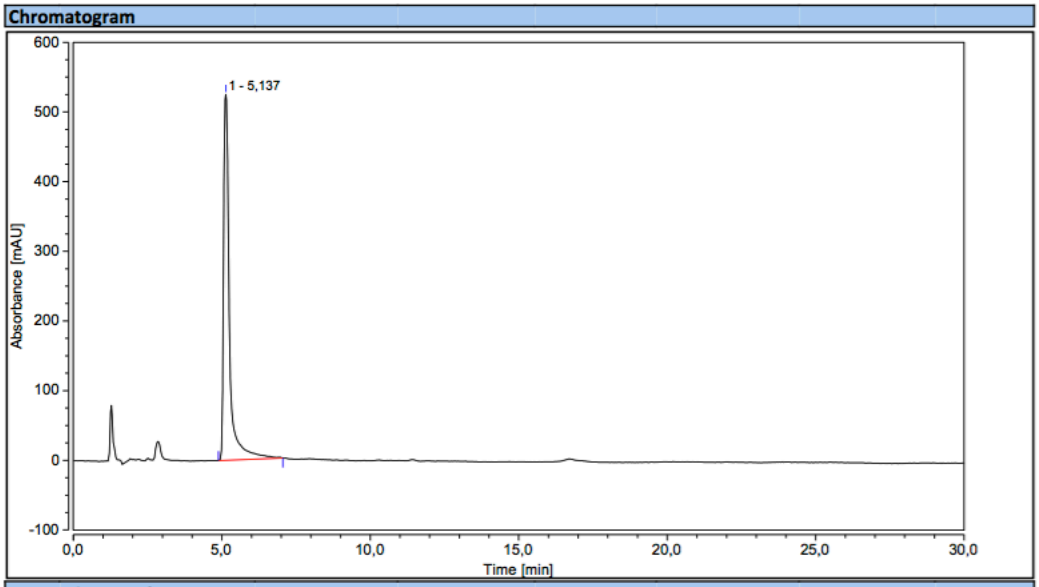

Integration Results

No.	Peak Name	Retention Time min	Area mAU*min	Height mAU	Relative Area %	Relative Height %	Amount n.a.
1		5,137	121,105	525,330	100,00	100,00	n.a.
Total:			**121,105**	**525,330**	**100,00**	**100,00**	

Figure S21. HPLC analysis of the precipitate from the reduction of **1d** showing **3d**. Note: the first peak corresponds to oxalic acid.

2.12 The reduction of **1da**

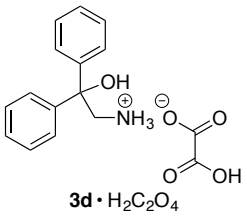

HPLC conditions: an YMC-Triart C_{18} column (3 μm, 150 × 2.0 mm), MeCN–50mM $HCOONH_4$ (pH = 9.30), 40:60, 0.2 mL/min, 40 °C (λ = 210 nm).

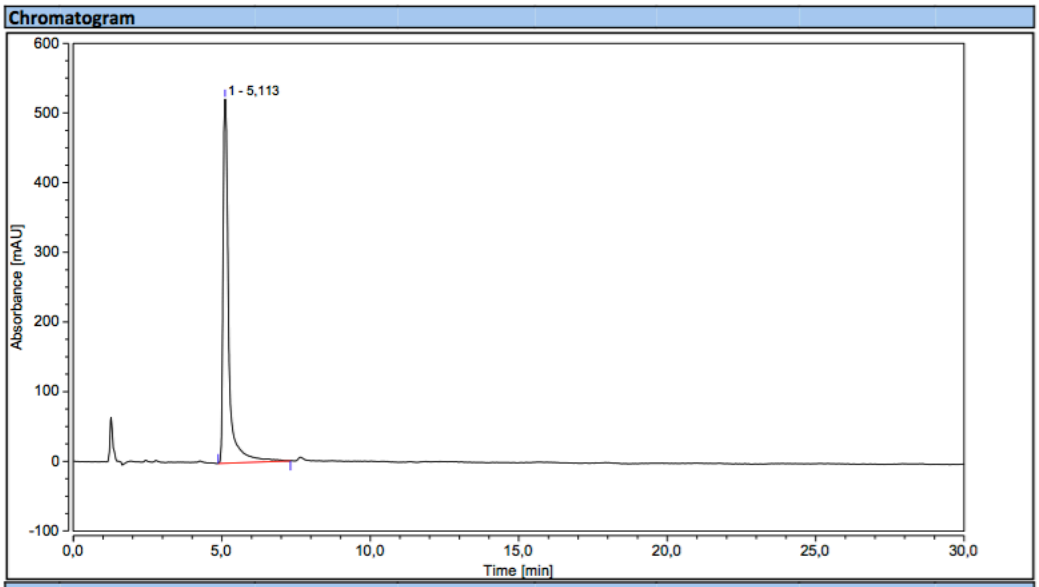

Integration Results

No.	Peak Name	Retention Time min	Area mAU*min	Height mAU	Relative Area %	Relative Height %	Amount n.a.
1		5,113	117,777	522,732	100,00	100,00	n.a.
Total:			**117,777**	**522,732**	**100,00**	**100,00**	

Figure S22. HPLC analysis of the precipitate from the reduction of **1da** showing **3d**. Note: the first peak corresponds to oxalic acid.

2.13 The reduction of **1e**

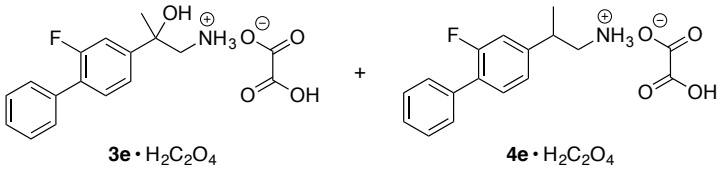

HPLC conditions: an YMC-Triart C_{18} column (3 μm, 150 × 2.0 mm), MeCN–50mM $HCOONH_4$ (pH = 9.30), 50:50, 0.2 mL/min, 40 °C (λ = 210 nm).

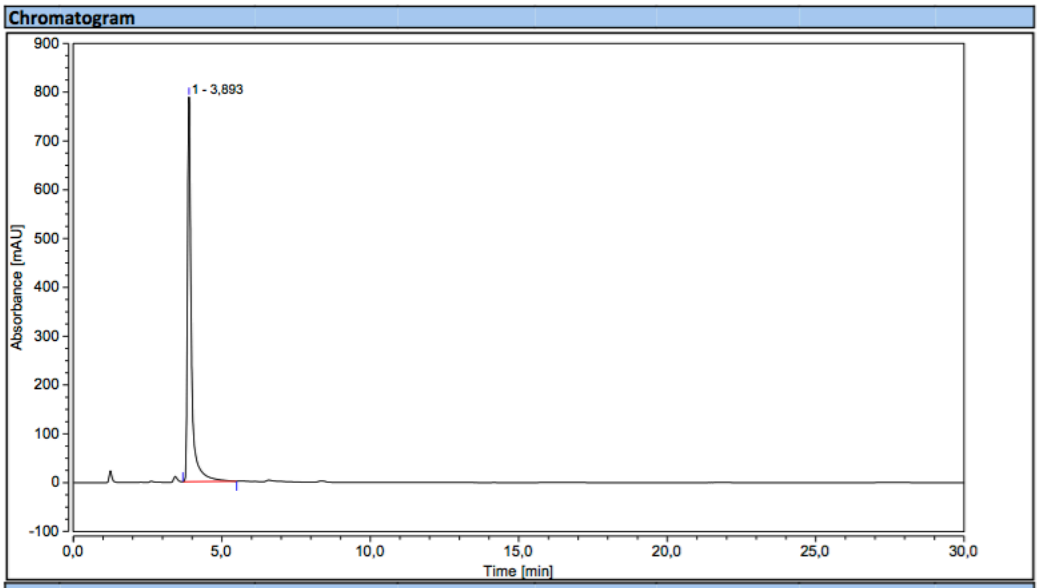

Integration Results

No.	Peak Name	Retention Time min	Area mAU*min	Height mAU	Relative Area %	Relative Height %	Amount n.a.
1		3,893	120,117	788,085	100,00	100,00	n.a.
Total:			**120,117**	**788,085**	**100,00**	**100,00**	

Figure S23. HPLC analysis of the precipitate from the reduction of **1e** showing **3e**.

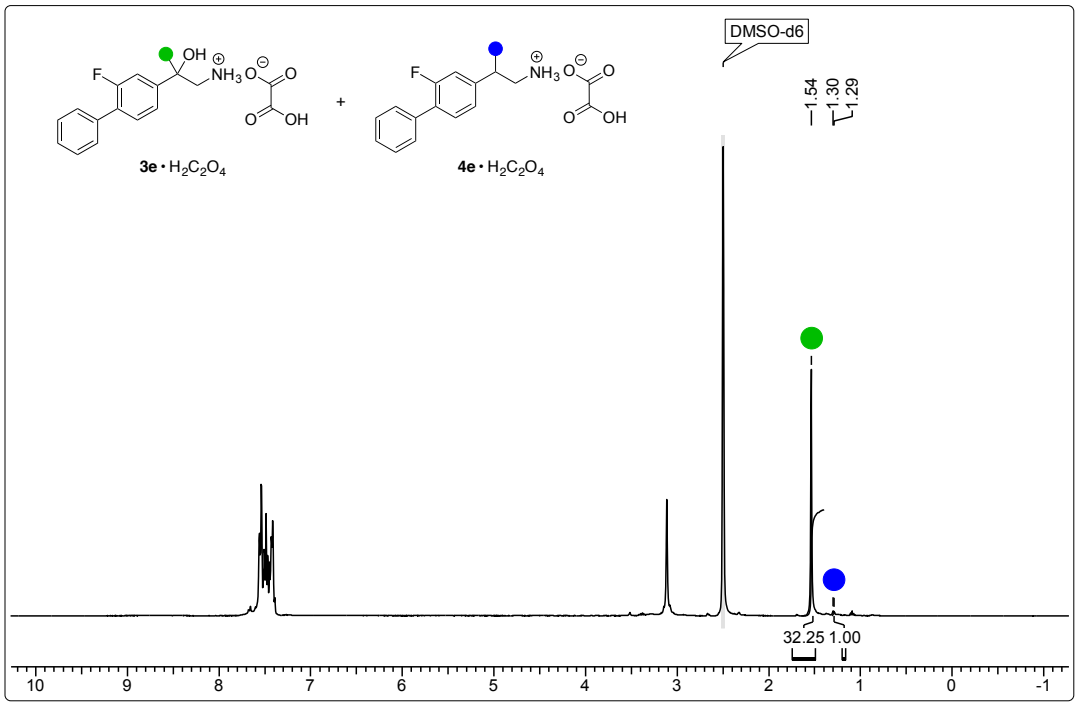

Figure S24. ^{1}H NMR (400 MHz, DMSO-d_6, 35 °C) analysis of the precipitate from the reduction of **1e** showing **3e**/**4e** = 97:3.

2.14 The reduction of **1f**

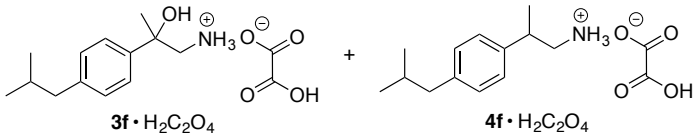

HPLC conditions: an YMC-Triart C_{18} column (3 μm, 150 × 2.0 mm), MeCN–50mM $HCOONH_4$ (pH = 9.30), 50:50, 0.2 mL/min, 40 °C (λ = 210 nm).

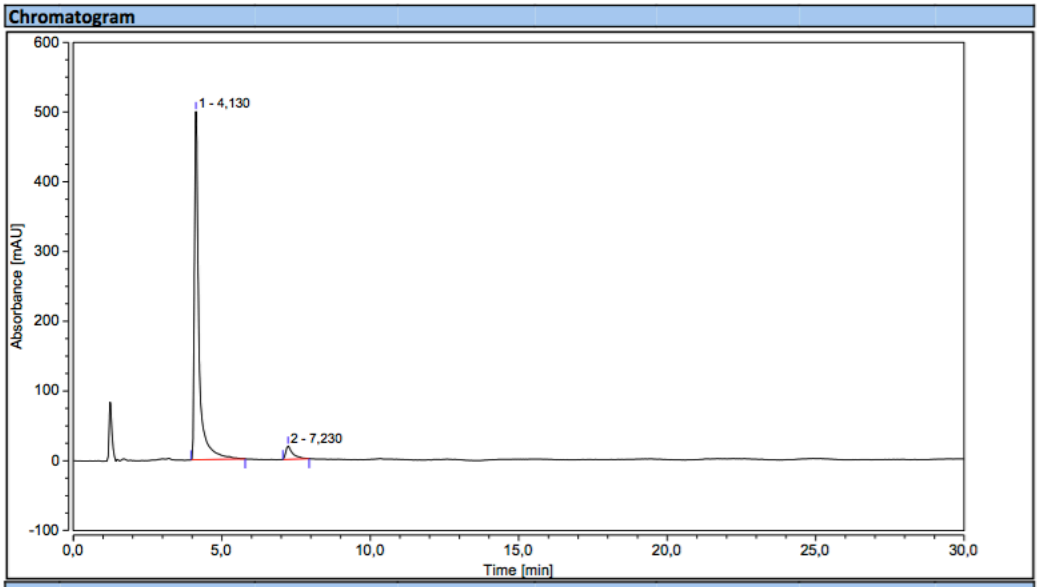

Integration Results

No.	Peak Name	Retention Time min	Area mAU*min	Height mAU	Relative Area %	Relative Height %	Amount n.a.
1		4,130	89,718	499,674	94,48	96,34	n.a.
2		7,230	5,237	19,007	5,52	3,66	n.a.
Total:			**94,956**	**518,681**	**100,00**	**100,00**	

Figure S25. HPLC analysis of the precipitate from the reduction of **1f** showing **3f**/**4f** = 94:6 (external standard calibration method).

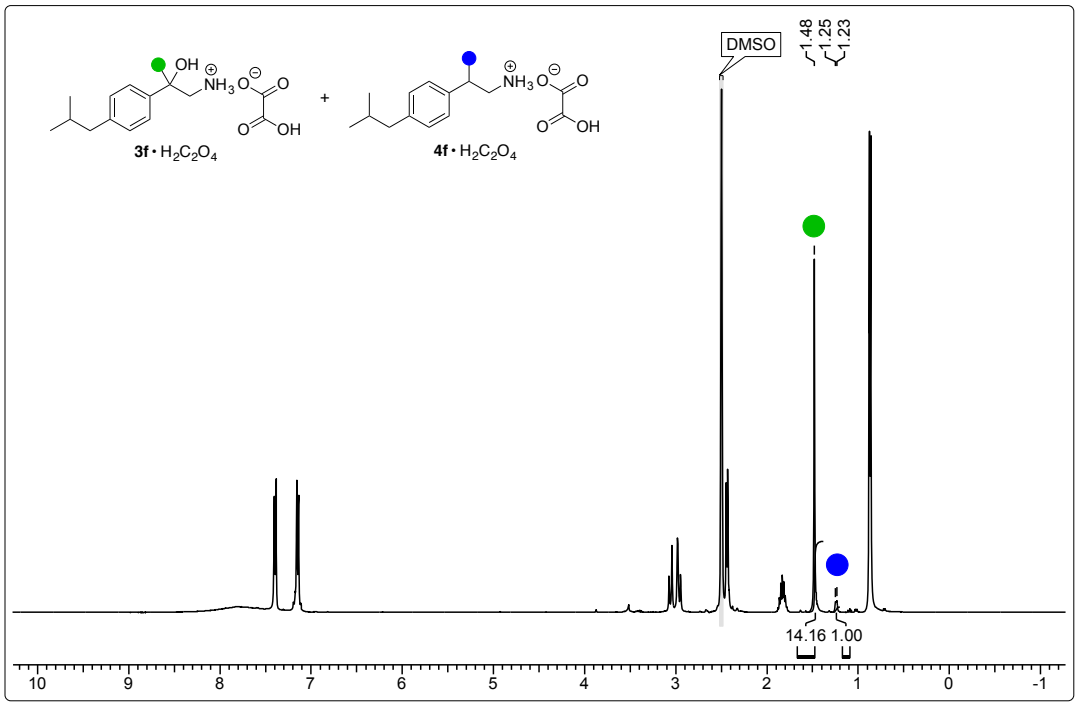

Figure S26. ^{1}H NMR (400 MHz, DMSO-d_6, 35 °C) analysis of the precipitate from the reduction of **1f** showing **3f**/**4f** = 93:7.

2.15 The reduction of **1g**

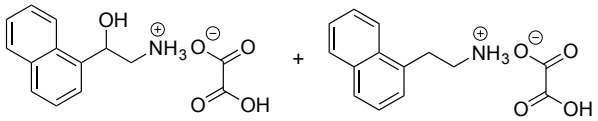

3g · $H_2C_2O_4$ **4g** · $H_2C_2O_4$

HPLC conditions: an YMC-Triart C_{18} column (3 μm, 150 × 2.0 mm), MeCN–50mM $HCOONH_4$ (pH = 9.30), 30:70, 0.2 mL/min, 40 °C (λ = 230 nm).

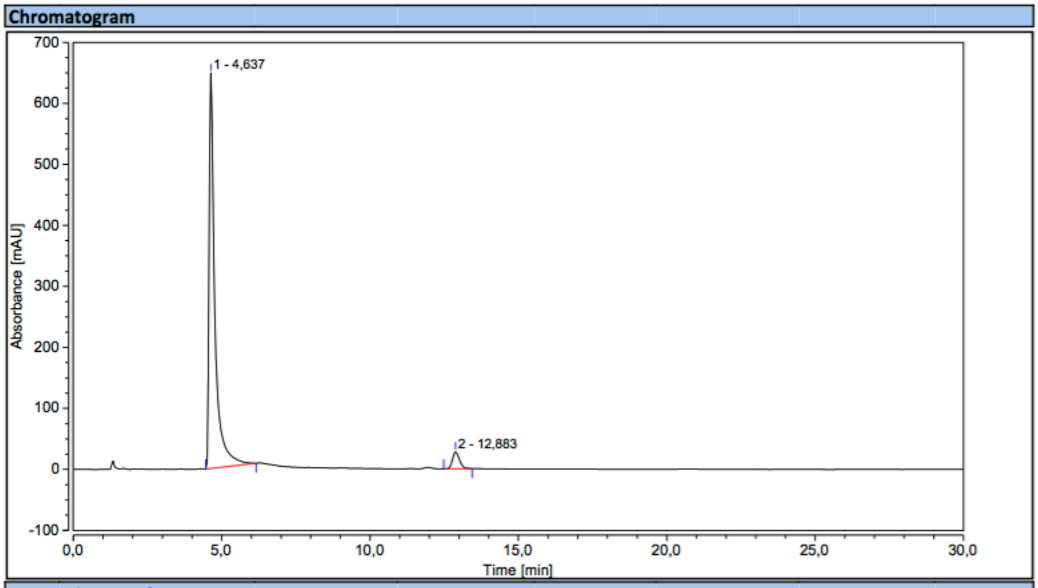

Integration Results

No.	Peak Name	Retention Time min	Area mAU*min	Height mAU	Relative Area %	Relative Height %	Amount n.a.
1		4,637	146,386	648,017	95,14	95,90	n.a.
2		12,883	7,480	27,739	4,86	4,10	n.a.
Total:			**153,865**	**675,756**	**100,00**	**100,00**	

Figure S27. HPLC analysis of the precipitate from the reduction of **1g** showing **3g**/**4g** = 95:5 (external standard calibration method).

2.16 The reduction of **1h**

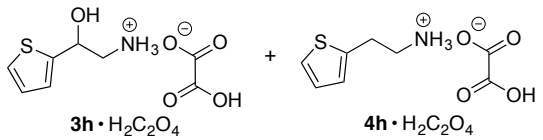

HPLC conditions: an YMC-Triart C_{18} column (3 μm, 150 × 2.0 mm), MeCN–50mM $HCOONH_4$ (pH = 9.30), 20:80, 0.2 mL/min, 40 °C (λ = 230 nm).

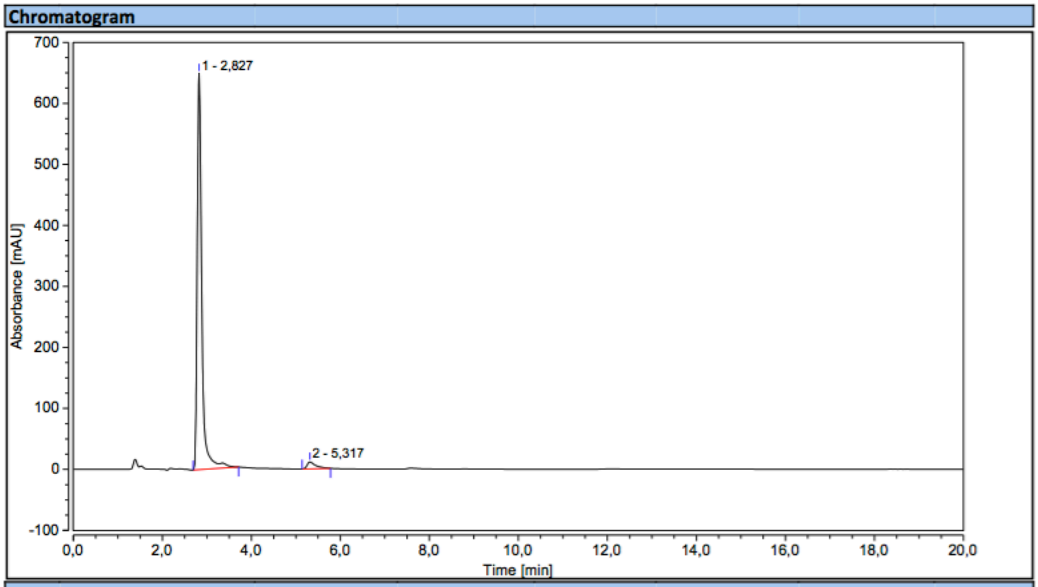

Integration Results

No.	Peak Name	Retention Time min	Area mAU*min	Height mAU	Relative Area %	Relative Height %	Amount n.a.
1		2,827	76,745	649,625	96,77	98,28	n.a.
2		5,317	2,559	11,364	3,23	1,72	n.a.
Total:			**79,304**	**660,989**	**100,00**	**100,00**	

Figure S28. HPLC analysis of the precipitate from the reduction of **1h** showing **3h**/**4h** = 97:3 (external standard calibration method).

2.17 The reduction of **2a**

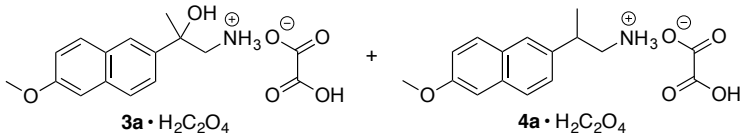

HPLC conditions: an YMC-Triart C_{18} column (3 μm, 150 × 2.0 mm), MeCN–50mM $HCOONH_4$ (pH = 9.30), 40:60, 0.2 mL/min, 40 °C (λ = 230 nm).

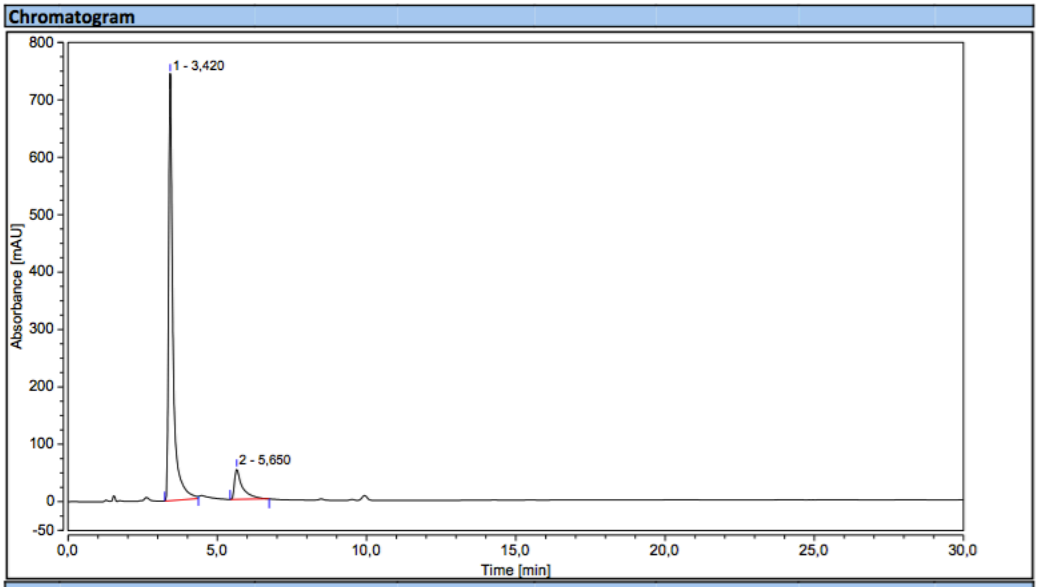

Integration Results

No.	Peak Name	Retention Time min	Area mAU*min	Height mAU	Relative Area %	Relative Height %	Amount n.a.
1		3,420	125,732	744,092	88,50	93,33	n.a.
2		5,650	16,338	53,195	11,50	6,67	n.a.
Total:			**142,071**	**797,287**	**100,00**	**100,00**	

Figure S29. RP-HPLC analysis of the precipitate from the reduction of **1a** showing **3a**/**4a** = 89:11 (external standard calibration method).

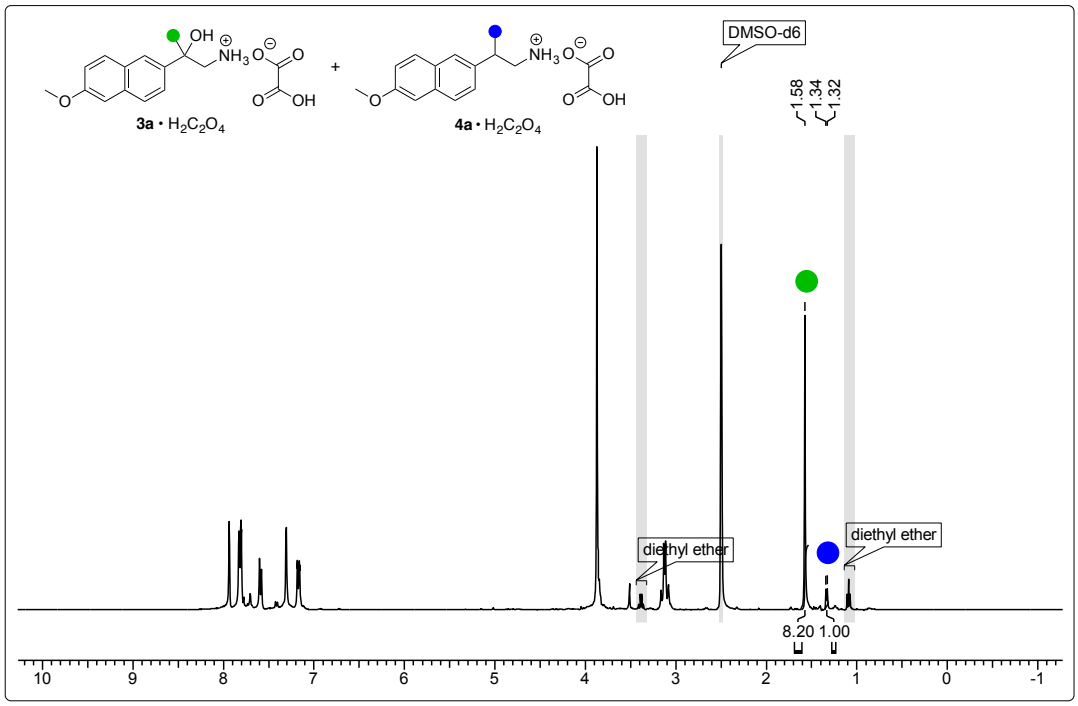

Figure S30. ^{1}H NMR (400 MHz, DMSO-d_6, 35 °C) analysis of the precipitate from the reduction of **1a** showing **3a**/**4a** = 89:11.

2.18 The reduction of **2b**

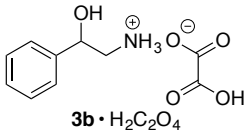

HPLC conditions: an YMC-Triart C_{18} column (3 μm, 150 × 2.0 mm), MeCN–50mM $HCOONH_4$ (pH = 9.30), 20:80, 0.2 mL/min, 40 °C (λ = 210 nm).

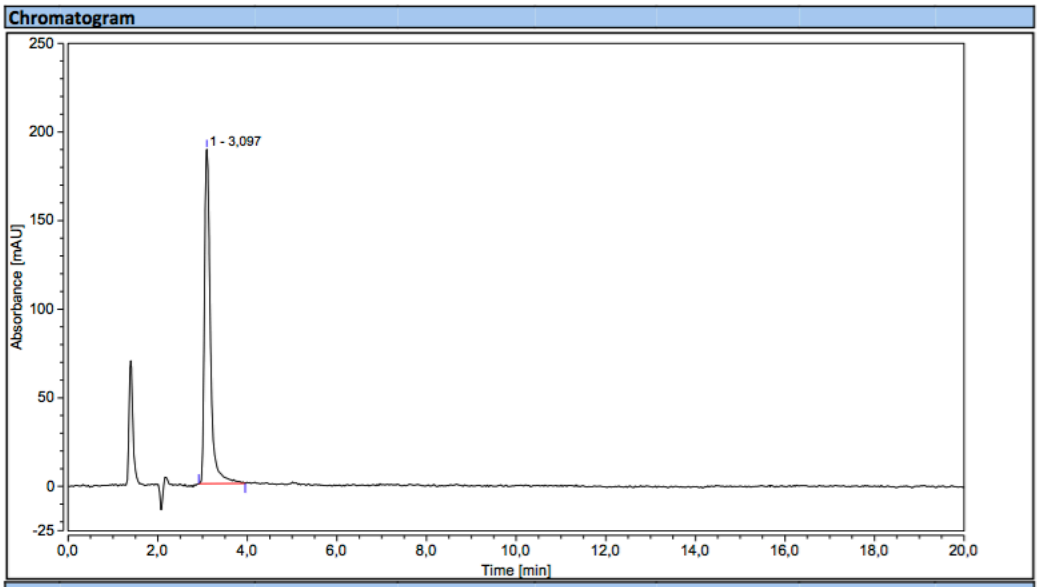

Integration Results

No.	Peak Name	Retention Time min	Area mAU*min	Height mAU	Relative Area %	Relative Height %	Amount n.a.
1		3,097	29,267	188,652	100,00	100,00	n.a.
Total:			**29,267**	**188,652**	**100,00**	**100,00**	

Figure S31. HPLC analysis of the precipitate from the reduction of **2b** showing **3b**. Note: the first peak corresponds to oxalic acid.

2.19 The reduction of **2ba**

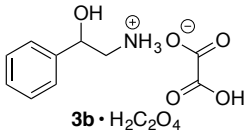

HPLC conditions: an YMC-Triart C_{18} column (3 μm, 150 × 2.0 mm), MeCN–50mM $HCOONH_4$ (pH = 9.30), 20:80, 0.2 mL/min, 40 °C (λ = 210 nm).

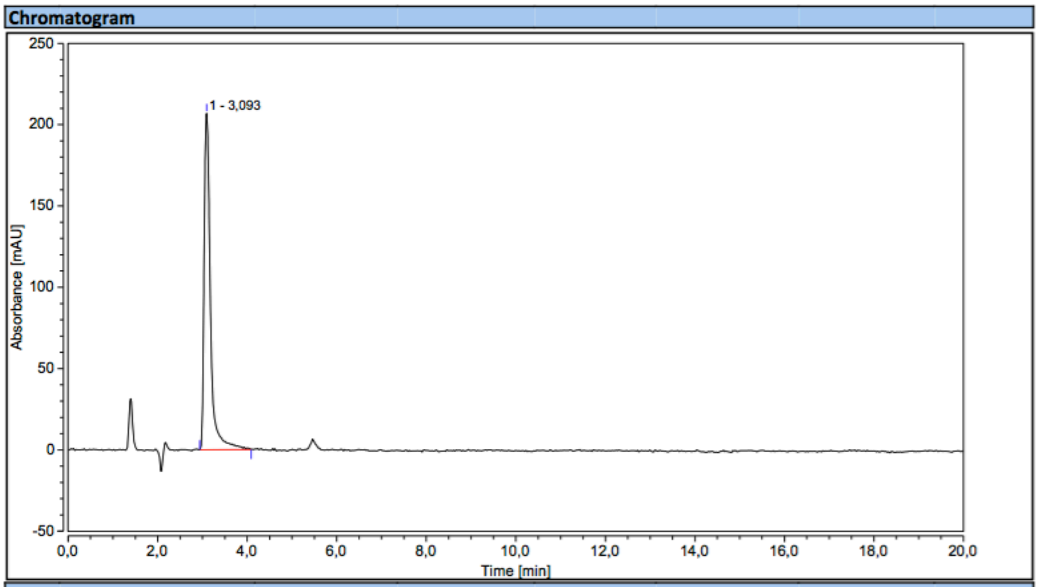

Integration Results

No.	Peak Name	Retention Time min	Area mAU*min	Height mAU	Relative Area %	Relative Height %	Amount n.a.
1		3,093	33,963	206,880	100,00	100,00	n.a.
Total:			**33,963**	**206,880**	**100,00**	**100,00**	

Figure S32. HPLC analysis of the precipitate from the reduction of **2ba** showing **3b**. Note: the first peak corresponds to oxalic acid.

2.20 The reduction of **2c**

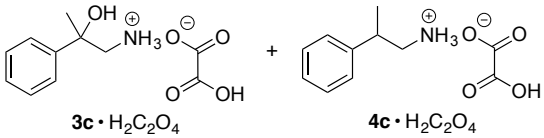

HPLC conditions: an YMC-Triart C_{18} column (3 μm, 150 × 2.0 mm), MeCN–50mM $HCOONH_4$ (pH = 9.30), 30:70, 0.2 mL/min, 40 °C (λ = 210 nm).

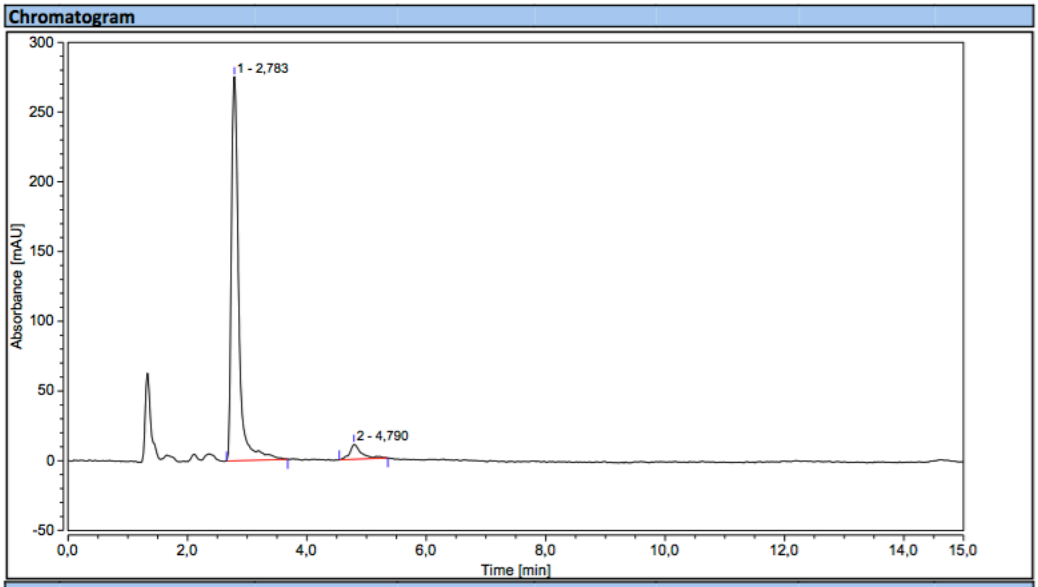

Integration Results

No.	Peak Name	Retention Time min	Area mAU*min	Height mAU	Relative Area %	Relative Height %	Amount n.a.
1		2,783	39,042	275,521	94,20	96,24	n.a.
2		4,790	2,404	10,761	5,80	3,76	n.a.
Total:			**41,445**	**286,282**	**100,00**	**100,00**	

Figure S33. RP-HPLC analysis of the precipitate from the reduction of **2c** showing **3c**/**4c** = 94:6 (external standard calibration method). Note: the first peak corresponds to oxalic acid.

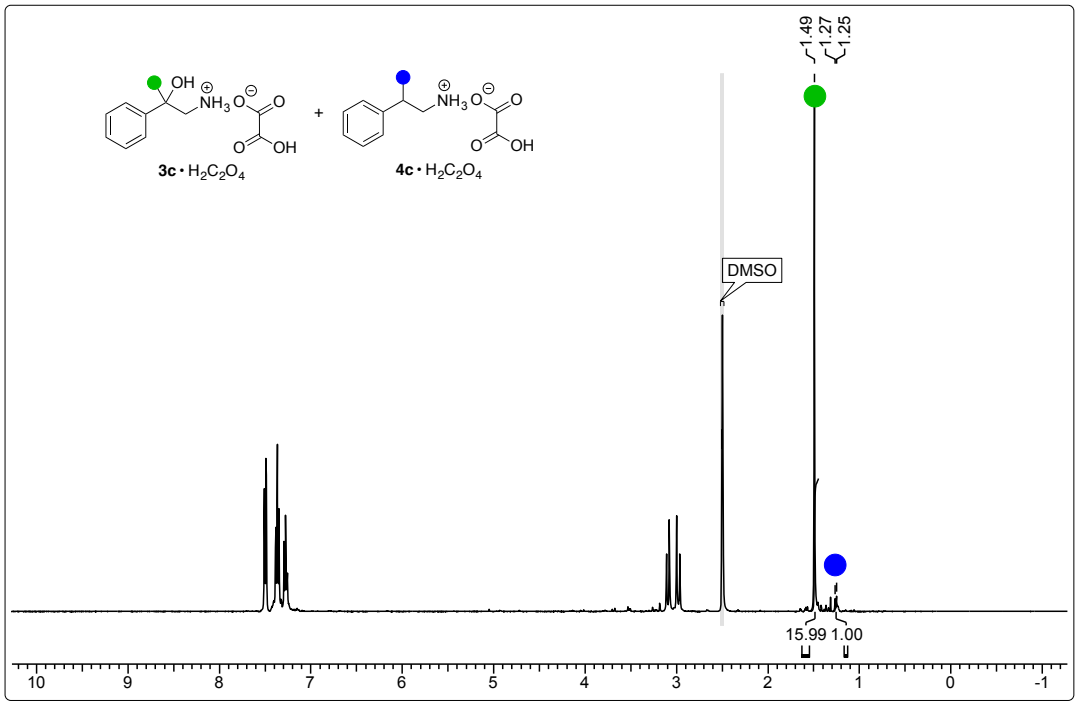

Figure S34. ^{1}H NMR (400 MHz, DMSO-d_6, 35 °C) analysis of the precipitate from the reduction of **1c** showing **3c**/**4c** = 94:6.

2.21 The reduction of **2d**

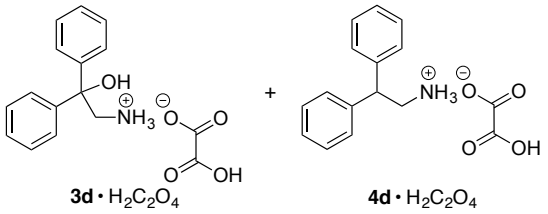

HPLC conditions: an YMC-Triart C_{18} column (3 μm, 150 × 2.0 mm), MeCN–50mM $HCOONH_4$ (pH = 9.30), 40:60, 0.2 mL/min, 40 °C (λ = 210 nm).

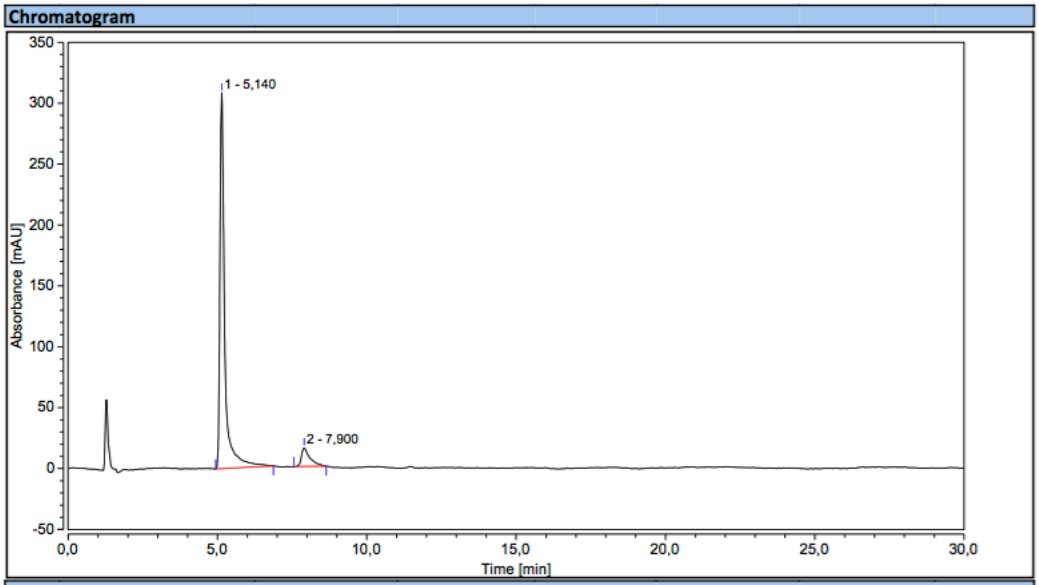

Integration Results

No.	Peak Name	Retention Time min	Area mAU*min	Height mAU	Relative Area %	Relative Height %	Amount n.a.
1		5,140	57,526	308,623	91,99	95,23	n.a.
2		7,900	5,011	15,444	8,01	4,77	n.a.
Total:			**62,537**	**324,066**	**100,00**	**100,00**	

Figure S35. RP-HPLC analysis of the precipitate from the reduction of **2d** showing **3d**/**4d** = 92:8 (external standard calibration method). Note: the first peak corresponds to oxalic acid.

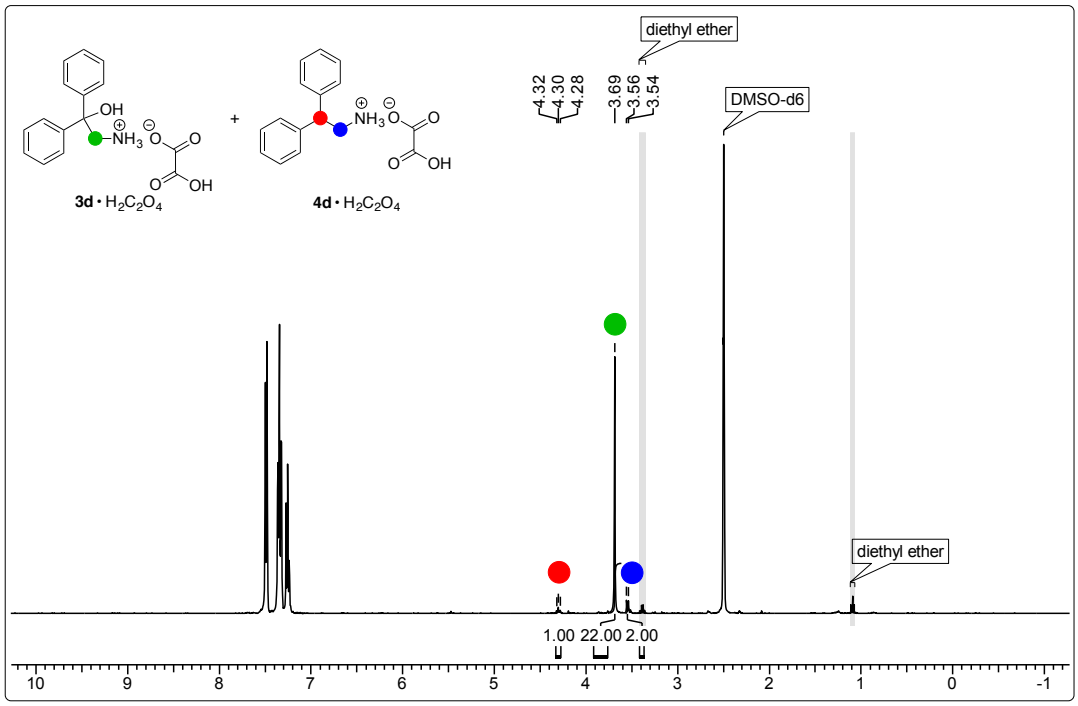

Figure S36. ^{1}H NMR (400 MHz, DMSO-d_6, 35 °C) analysis of the precipitate from the reduction of **2d** showing **3d**/**4d** = 92:8.

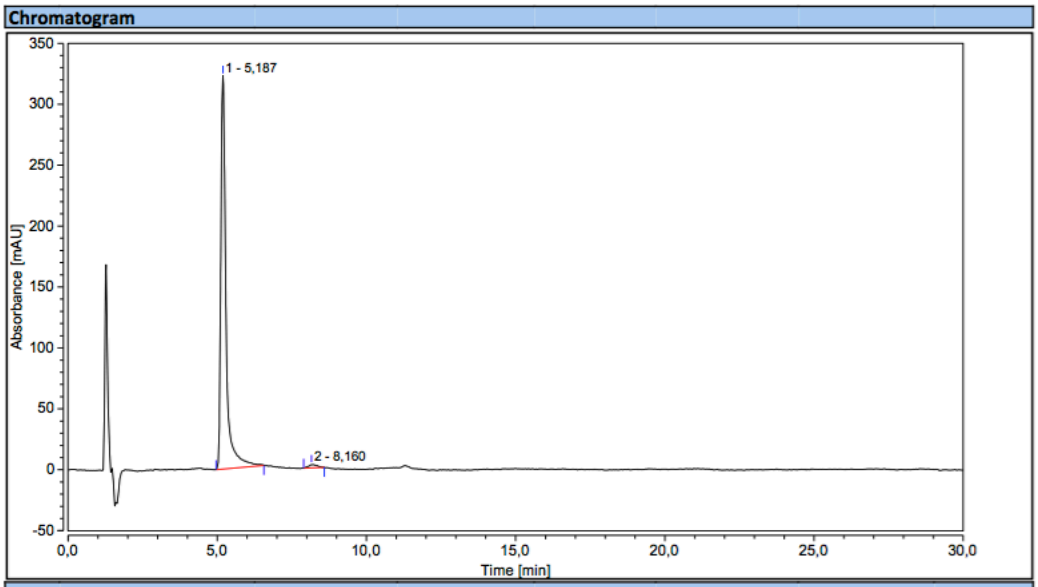

Integration Results

No.	Peak Name	Retention Time min	Area mAU*min	Height mAU	Relative Area %	Relative Height %	Amount n.a.
1		5,187	64,920	323,081	98,59	99,12	n.a.
2		8,160	0,926	2,863	1,41	0,88	n.a.
Total:			**65,846**	**325,944**	**100,00**	**100,00**	

Figure S37. RP-HPLC analysis of the precipitate from the reduction of **2d** with added NaCN (10 equiv) showing **3d**/**4d** = 99:1 (external standard calibration method). Note: the first peak corresponds to oxalic acid.

2.22 The reduction of **2da**

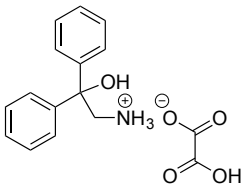

3d • $H_2C_2O_4$

HPLC conditions: an YMC-Triart C_{18} column (3 μm, 150 × 2.0 mm), MeCN–50mM $HCOONH_4$ (pH = 9.30), 40:60, 0.2 mL/min, 40 °C (λ = 210 nm).

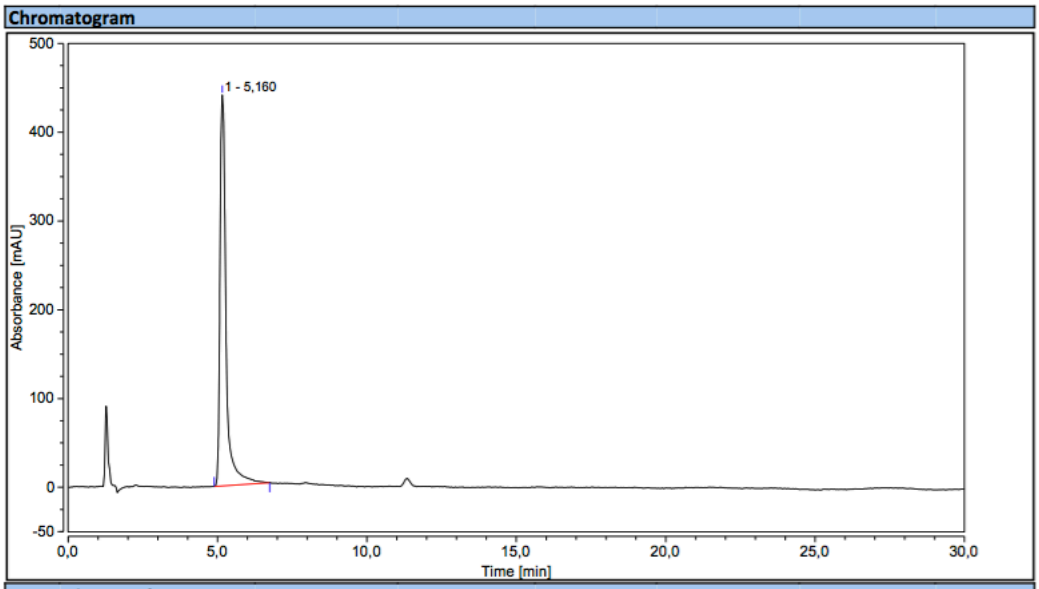

Integration Results

No.	Peak Name	Retention Time min	Area mAU*min	Height mAU	Relative Area %	Relative Height %	Amount n.a.
1		5,160	104,384	440,306	100,00	100,00	n.a.
Total:			**104,384**	**440,306**	**100,00**	**100,00**	

Figure S38. RP-HPLC analysis of the precipitate from the reduction of **2da** showing **3d**. Note: the first peak corresponds to oxalic acid.

2.23 The reduction of **2e**

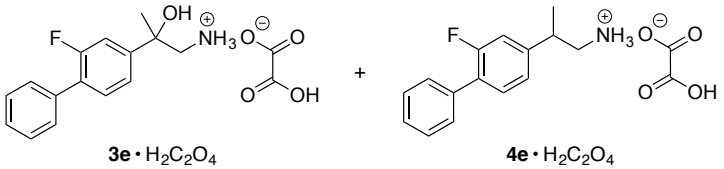

HPLC conditions: an YMC-Triart C_{18} column (3 μm, 150 × 2.0 mm), MeCN–50mM $HCOONH_4$ (pH = 9.30), 50:50, 0.2 mL/min, 40 °C (λ = 210 nm).

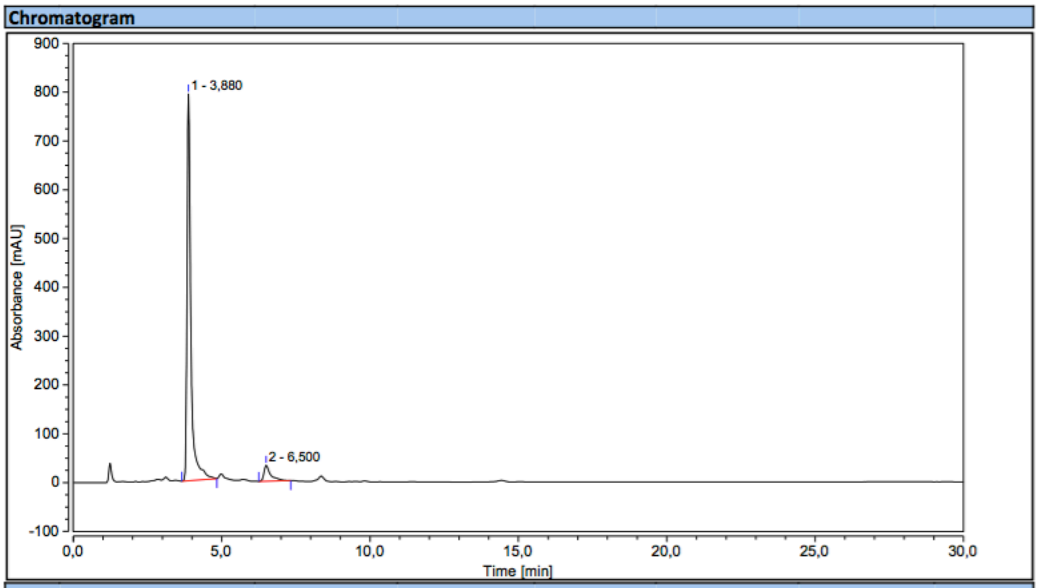

Integration Results

No.	Peak Name	Retention Time min	Area mAU*min	Height mAU	Relative Area %	Relative Height %	Amount n.a.
1		3,880	119,667	792,171	93,26	96,03	n.a.
2		6,500	8,651	32,762	6,74	3,97	n.a.
Total:			**128,318**	**824,933**	**100,00**	**100,00**	

Figure S39. RP-HPLC analysis of the precipitate from the reduction of **2e** showing **3e**/**4e** = 93:7 (external standard calibration method). Note: the first peak corresponds to oxalic acid.

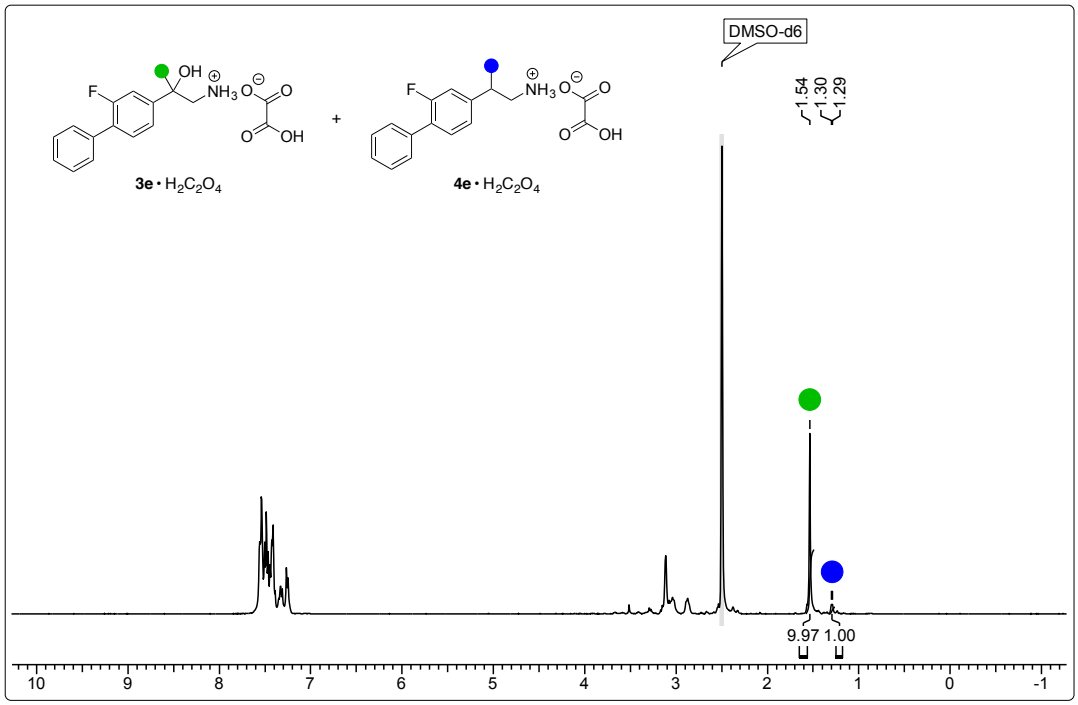

Figure S40. ^{1}H NMR (400 MHz, DMSO-d_6, 35 °C) analysis of the precipitate from the reduction of **1e** showing **3e**/**4e** = 91:9.

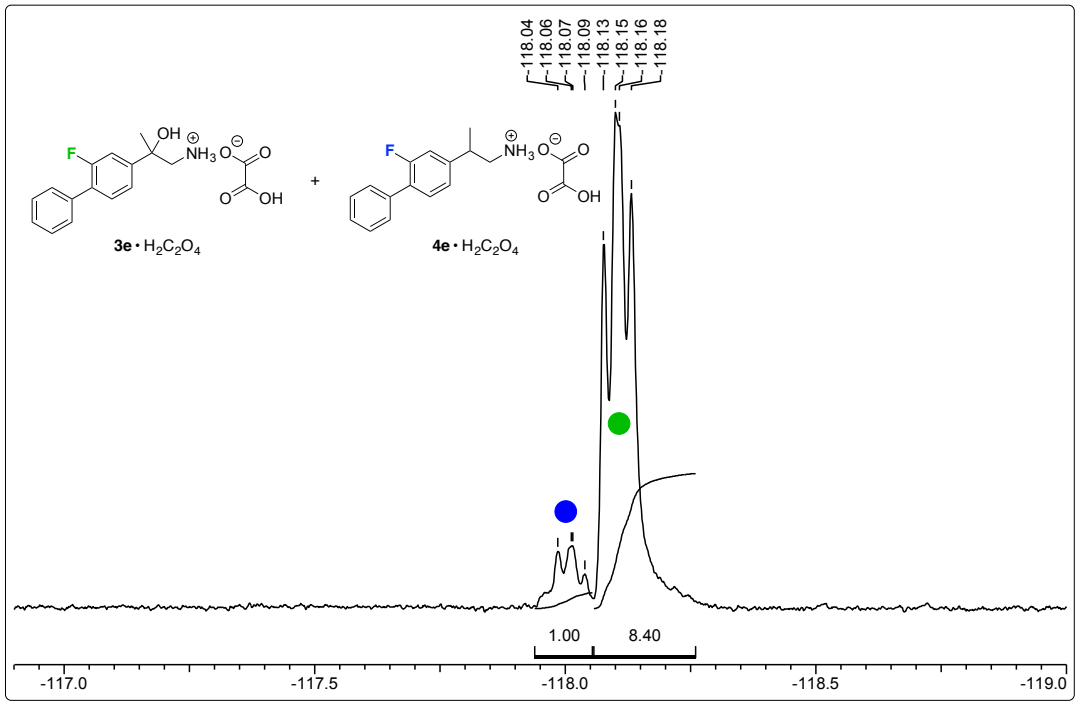

Figure S41. ^{19}F NMR (376 MHz, DMSO-d_6, 35 °C) analysis of the precipitate from the reduction of **1e** showing **3e**/**4e** = 89:11.

2.24 The reduction of **2f**

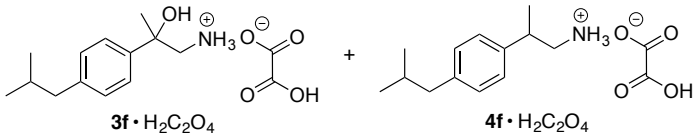

HPLC conditions: an YMC-Triart C_{18} column (3 μm, 150 × 2.0 mm), MeCN–50mM $HCOONH_4$ (pH = 9.30), 50:50, 0.2 mL/min, 40 °C (λ = 210 nm).

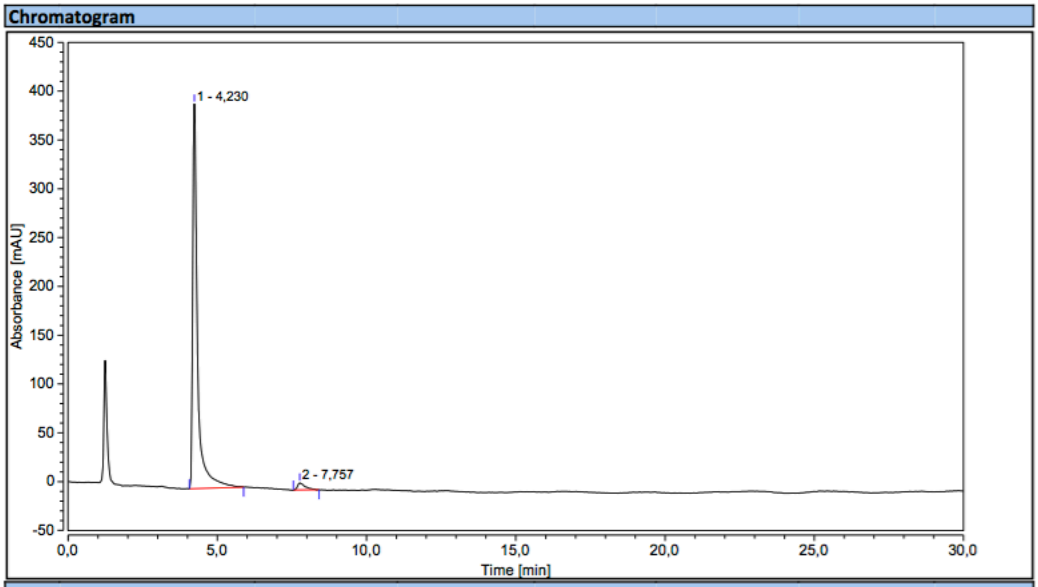

Integration Results

No.	Peak Name	Retention Time min	Area mAU*min	Height mAU	Relative Area %	Relative Height %	Amount n.a.
1		4,230	73,925	394,082	97,18	98,20	n.a.
2		7,757	2,145	7,218	2,82	1,80	n.a.
Total:			**76,070**	**401,301**	**100,00**	**100,00**	

Figure S42. HPLC analysis of the precipitate from the reduction of **2f** showing **3f**/**4f** = 97:3 (external standard calibration method). Note: the first peak corresponds to oxalic acid.

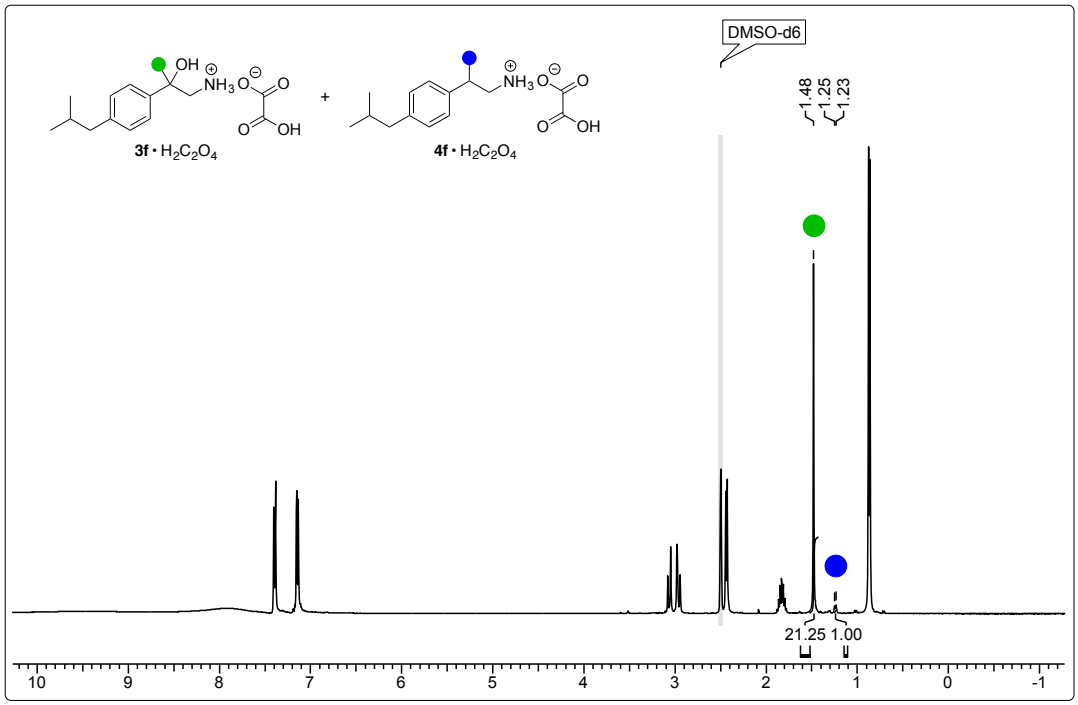

Figure S43. ^{1}H NMR (400 MHz, DMSO-d_6, 35 °C) analysis of the precipitate from the reduction of **1f** showing **3f**/**4f** = 96:4.

2.25 The reduction of **2g**

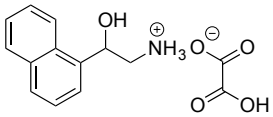

3g · $H_2C_2O_4$

HPLC conditions: an YMC-Triart C_{18} column (3 μm, 150 × 2.0 mm), MeCN–50mM $HCOONH_4$ (pH = 9.30), 30:70, 0.2 mL/min, 40 °C (λ = 230 nm).

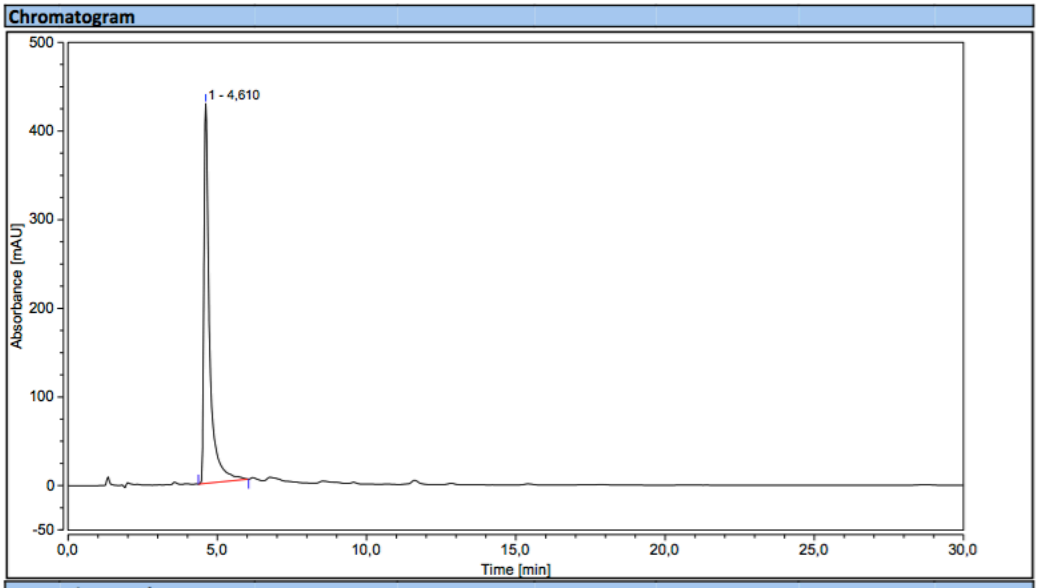

Integration Results

No.	Peak Name	Retention Time min	Area mAU*min	Height mAU	Relative Area %	Relative Height %	Amount n.a.
1		4,610	94,037	428,345	100,00	100,00	n.a.
Total:			**94,037**	**428,345**	**100,00**	**100,00**	

Figure S44. HPLC analysis of the precipitate from the reduction of **2g** showing **3g**.

2.26 The reduction of **2h**

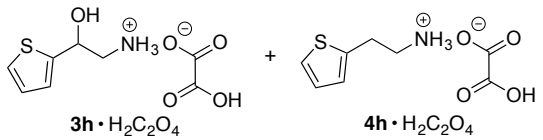

HPLC conditions: an YMC-Triart C_{18} column (3 μm, 150 × 2.0 mm), MeCN–50mM $HCOONH_4$ (pH = 9.30), 20:80, 0.2 mL/min, 40 °C (λ = 230 nm).

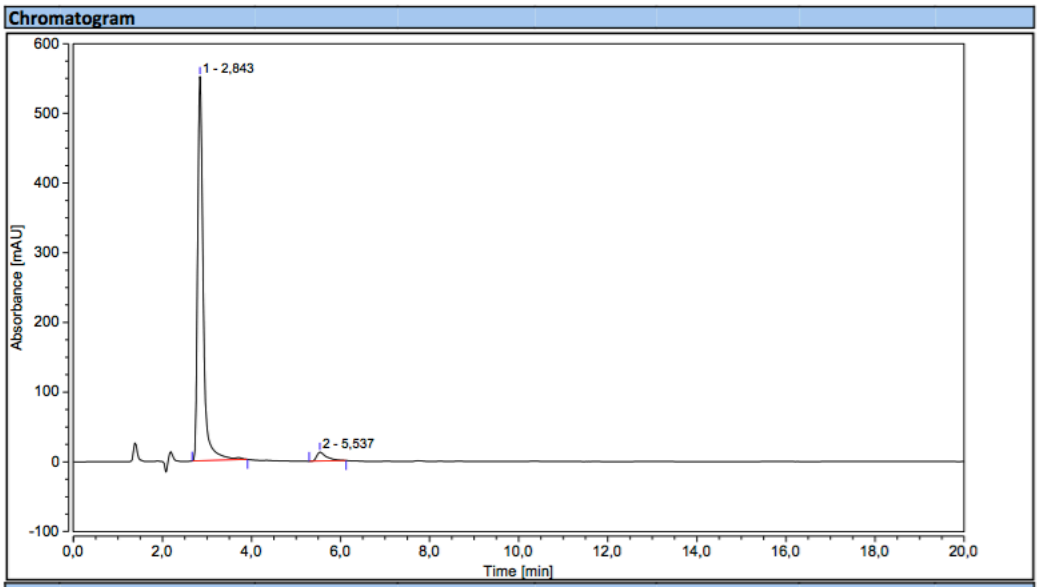

Integration Results

No.	Peak Name	Retention Time min	Area mAU*min	Height mAU	Relative Area %	Relative Height %	Amount n.a.
1		2,843	80,428	551,468	96,08	97,72	n.a.
2		5,537	3,278	12,862	3,92	2,28	n.a.
Total:			**83,706**	**564,331**	**100,00**	**100,00**	

Figure S45. HPLC analysis of the precipitate from the reduction of **2h** showing **3h**/**4h** = 96:4 (external standard calibration method).

3. Determination of the Enantiomeric Purity of 8a, 8b, and 5a

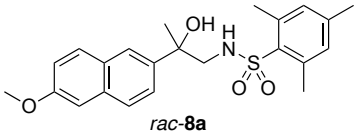

rac-**8a**

HPLC conditions: a Hypersil silica column (3 µm, 100 × 4.6 mm used as a precolumn, which was connected via the standard blue PEEK capillary tubing (L 300 mm, ID 0.01", OD 1/16") to a Daicel Chiralpak IA column (5 µm, 250 × 4.6 mm), *i*-PrOH–*n*-heptane, 10:90, 0.5 mL/min, 25 °C (λ = 230 nm).

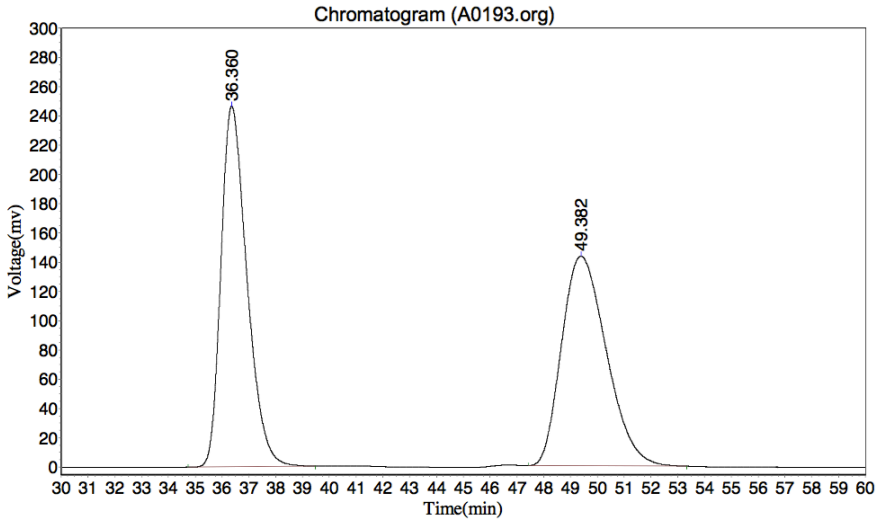

Results

Peak No.	Peak ID	Ret Time	Height	Area	Conc.
1		36.360	246387.406	16595349.000	49.9440
2		49.382	143238.063	16632589.000	50.0560
Total			389625.469	33227938.000	100.0000

Figure S46. Chiral HPLC chromatogram of **8a** (0% ee).

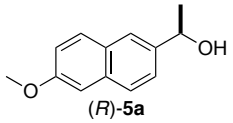

(*R*)-**5a**

Stereochemical assignment: Absolute configuration of (*R*)-**5** was established by comparison of the sign of specific rotation and the relative elution order of the resolved peaks with literature data.[1]

HPLC conditions: a Hypersil silica column (3 µm, 100 × 4.6 mm used as a precolumn, which was connected via the standard blue PEEK capillary tubing (L 300 mm, ID 0.01", OD 1/16") to a Daicel Chiralpak IB column (5 µm, 250 × 4.6 mm), *i*-PrOH–*n*-heptane, 5:95, 0.5 mL/min, 25 °C (λ = 230 nm).

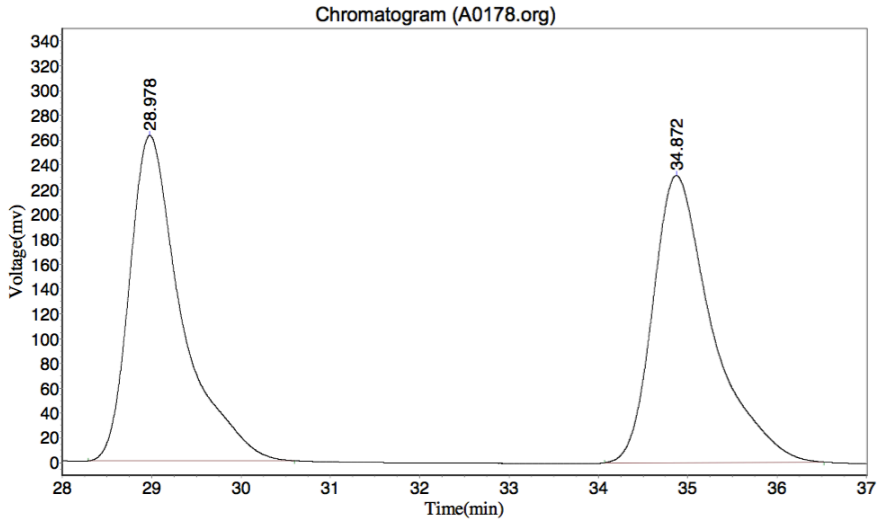

Results

Peak No.	Peak ID	Ret Time	Height	Area	Conc.
1		28.978	262292.688	10607185.000	49.8585
2		34.872	231386.391	10667406.000	50.1415
Total			493679.078	21274591.000	100.0000

Figure S47. Chiral HPLC chromatogram of *rac*-**5a** (0% ee).

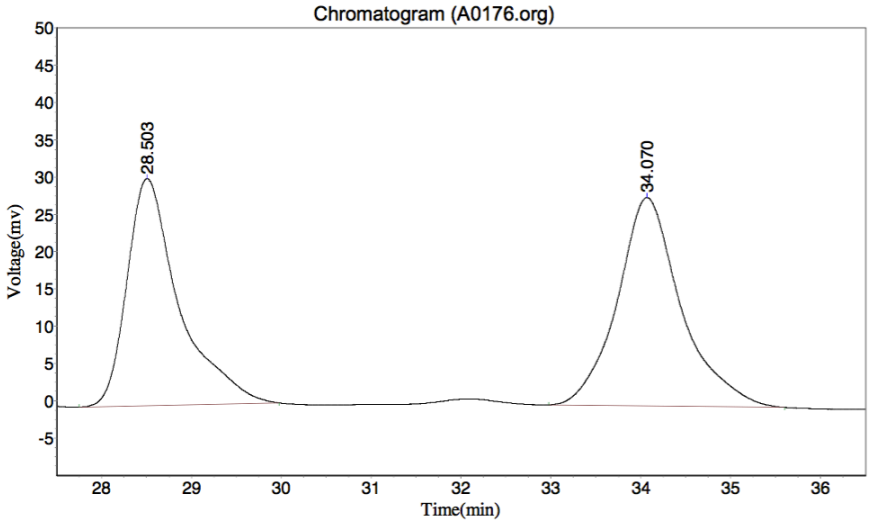

Results

Peak No.	Peak ID	Ret Time	Height	Area	Conc.
1		28.503	30436.004	1223150.625	47.0368
2		34.070	27920.609	1377261.625	52.9632
Total			58356.613	2600412.250	100.0000

Figure S48. Chiral HPLC chromatogram of (*R*)-**5a** (6% ee).

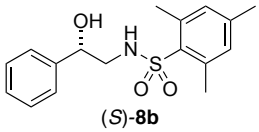

(*S*)-**8b**

Stereochemical assignment: Absolute configuration of (*S*)-**8b** was established by chemical correlation with (*S*)-**1ba**.

HPLC conditions: a Hypersil silica column (3 µm, 100 × 4.6 mm used as a precolumn, which was connected via the standard blue PEEK capillary tubing (L 300 mm, ID 0.01", OD 1/16") to a Daicel Chiralpak IA column (5 µm, 250 × 4.6 mm), *i*-PrOH–*n*-heptane, 10:90, 0.5 mL/min, 25 °C (λ = 230 nm).

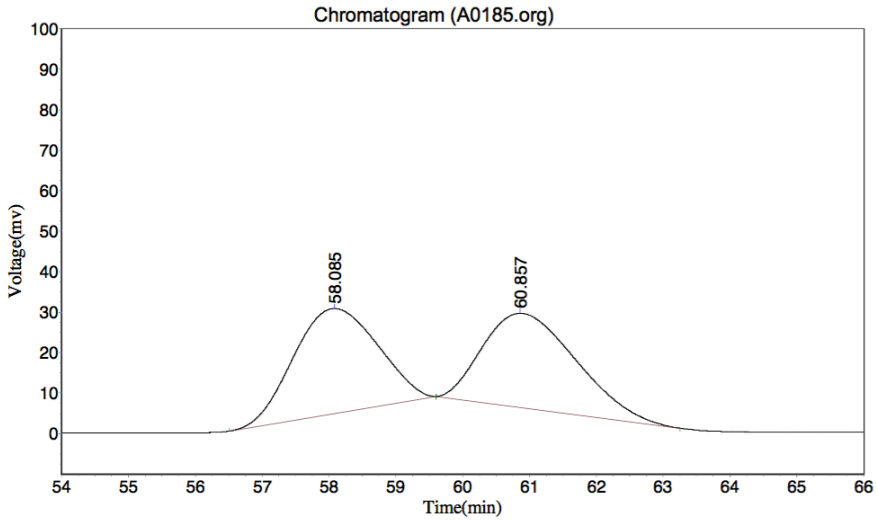

Results

Peak No.	Peak ID	Ret Time	Height	Area	Conc.
1		58.085	25900.541	2261213.750	49.9107
2		60.857	23239.223	2269307.250	50.0893
Total			49139.764	4530521.000	100.0000

Figure S49. Chiral HPLC chromatogram of *rac*-**8b** (0% ee).

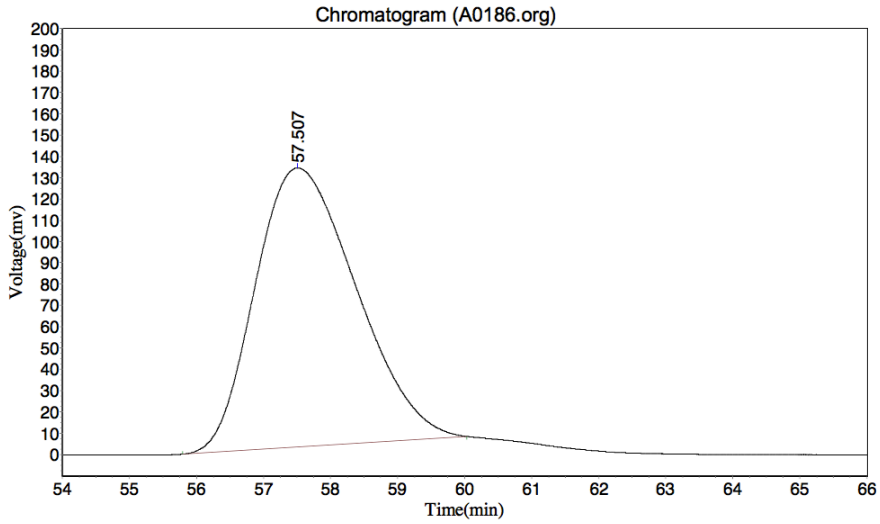

Results

Peak No.	Peak ID	Ret Time	Height	Area	Conc.
1		57.507	130975.086	13684664.000	100.0000
Total			130975.086	13684664.000	100.0000

Figure S50. Chiral HPLC chromatogram of (*S*)-**8b** (> 99% ee).

4. Identification of the Reaction Intermediates

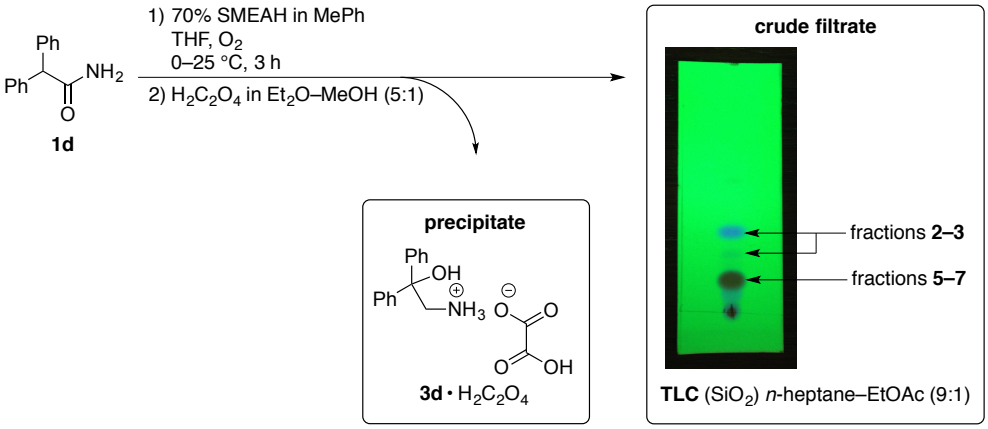

The reduction of **1d** (275 mg, 1.3 mmol) was performed according to **GP**. The precipitated salt was filtered off and afforded 101 mg of **3d**·$H_2C_2O_4$ as a white hygroscopic powder (26% yield). The crude filtrate was treated according to **GP** and provided 130 mg of the yellowish waxy residue, which contained **5c** as a major component (HPLC purity > 90%). Then the residue (120 mg) was subjected to column chromatography (120 × 15 mm), 10 g of SiO_2, *n*-heptane–EtOAc (9:1), and fractions of 10 mL each were collected.

The combined fractions **2–3** gave after evaporation 6 mg of the residue, which was subjected to NMR and GC-MS analysis. Therein, compounds **2d**, **6**, and **7** were successfully identified. The combined fractions **5–7** provided 81 mg of the pure **5c**.

HPLC conditions: an YMC-Triart C_{18} column (3 µm, 150 × 2.0 mm), MeCN–H_2O, 50:50 → 90:10, 0.2 mL/min, 40 °C (λ = 210 nm).

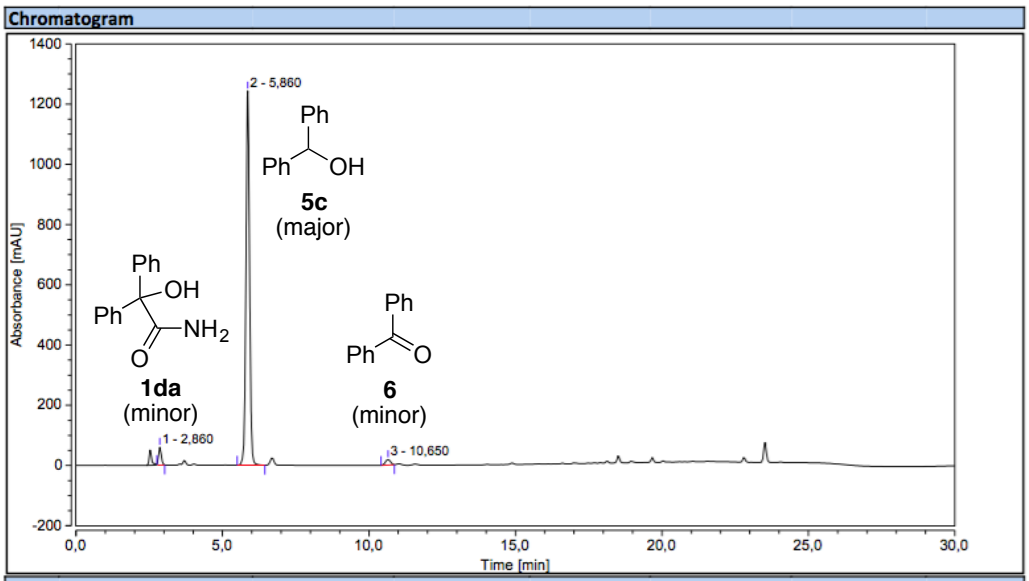

Integration Results

No.	Peak Name	Retention Time min	Area mAU*min	Height mAU	Relative Area %	Relative Height %	Amount n.a.
1		2,860	6,302	59,579	3,32	4,51	n.a.
2		5,860	179,631	1242,675	94,74	94,11	n.a.
3		10,650	3,675	18,259	1,94	1,38	n.a.
Total:			**189,608**	**1320,512**	**100,00**	**100,00**	

Figure S51. HPLC profile of the crude filtrate (210 nm).

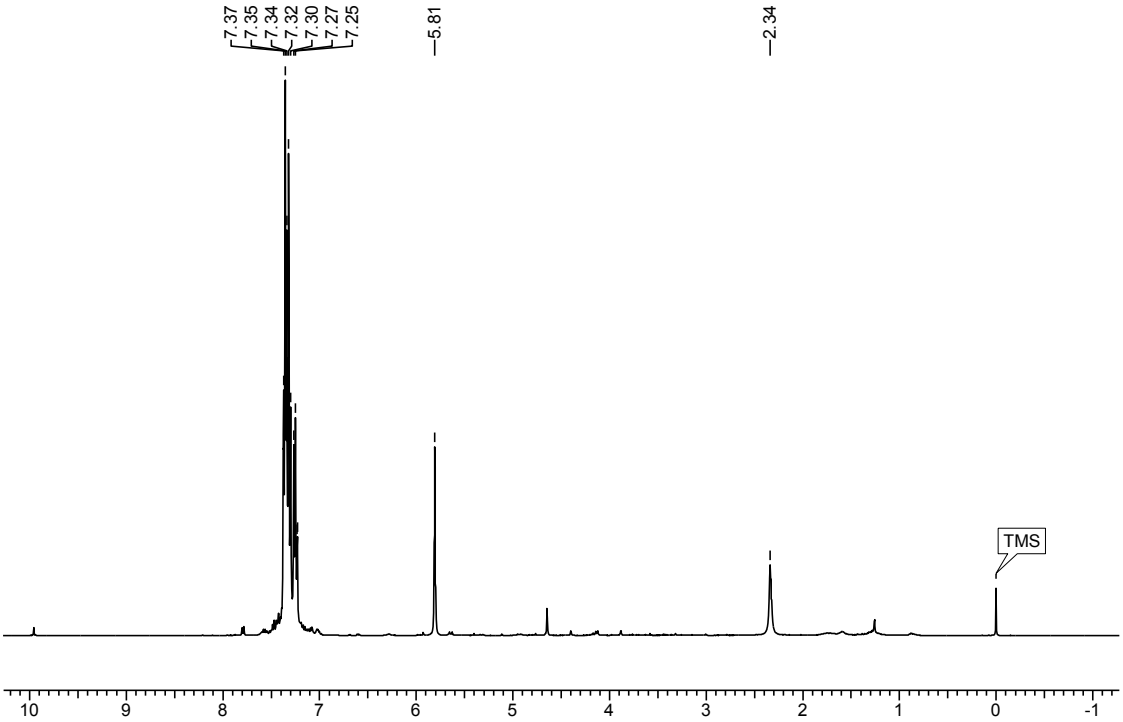

Figure S52. ^{1}H NMR ($CDCl_3$, 400 MHz) profile of the crude filtrate.

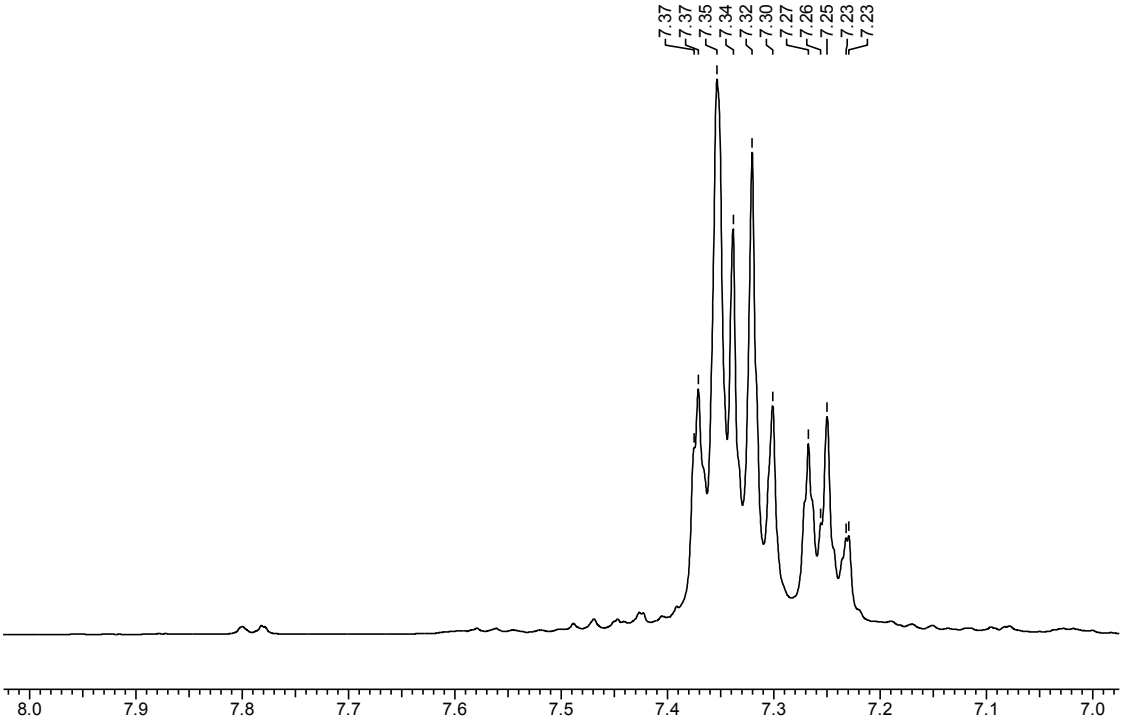

Figure S53. ^{1}H NMR ($CDCl_3$, 400 MHz) profile of the crude filtrate (in detail).

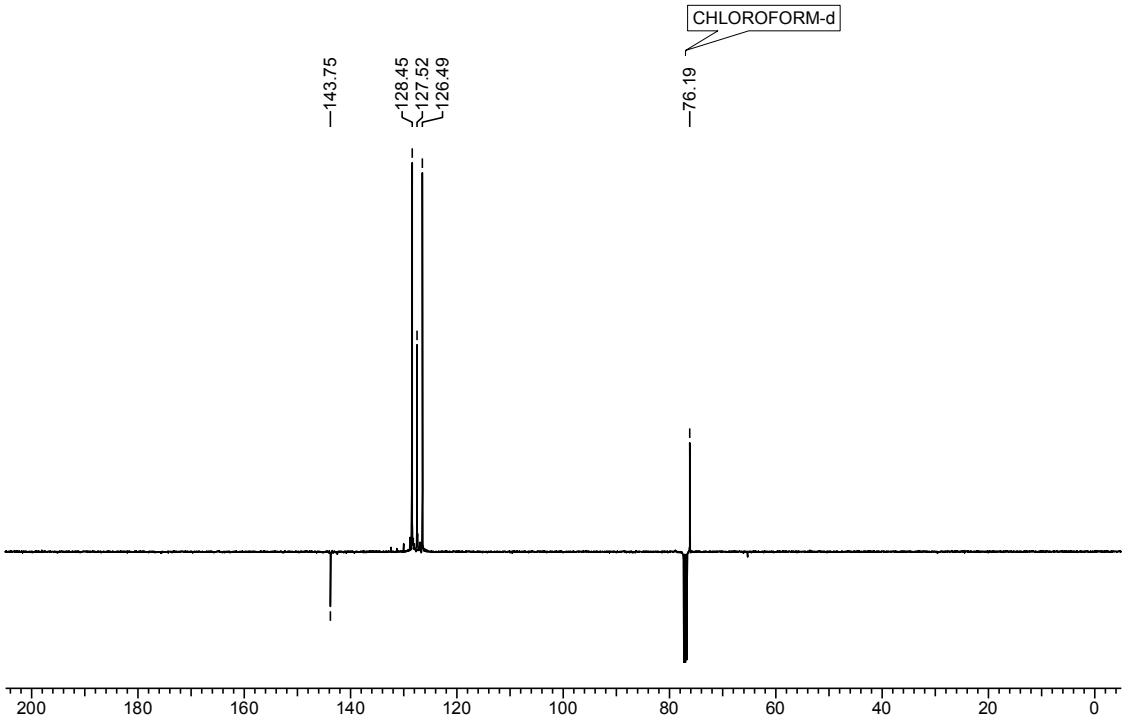

Figure S54. ^{13}C NMR ($CDCl_3$, 100 MHz) profile of the crude filtrate.

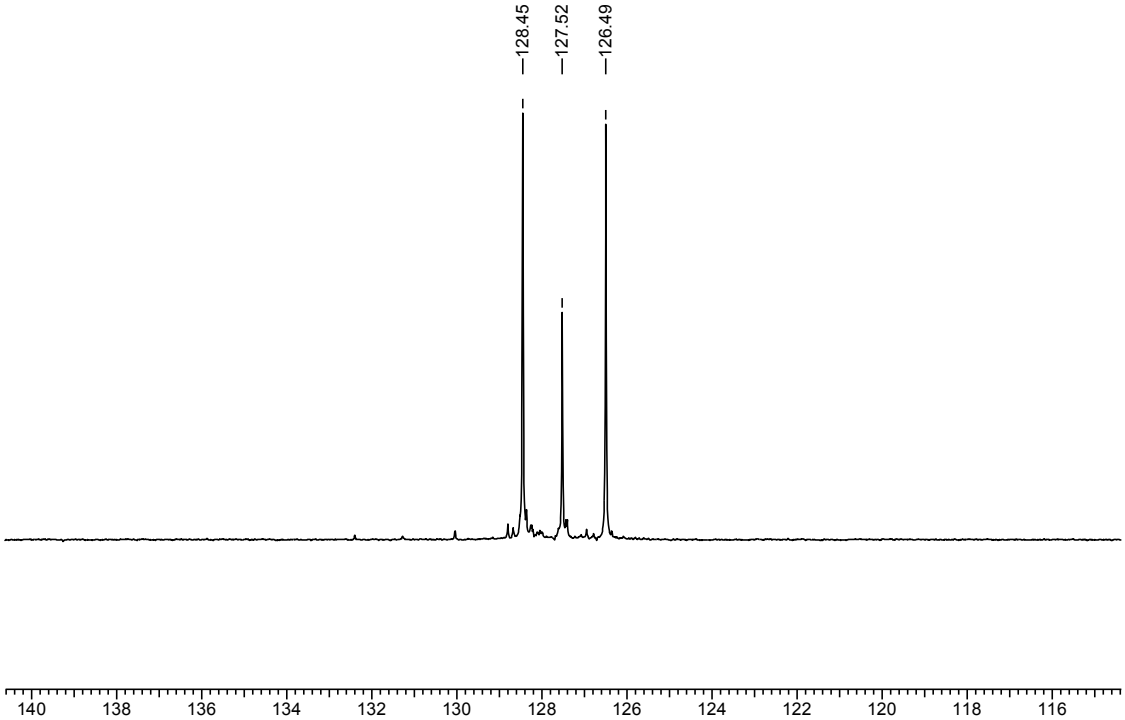

Figure S55. ^{13}C NMR ($CDCl_3$, 100 MHz) profile of the crude filtrate (in detail).

GC conditions: a DB-5MS column (0.25 µm, 30 m × 0.25 mm), He (constant flow 1 mL/min), temperature program (50 °C | hold 2 min; 10 °C/min rate to 300°C | hold 15 min).

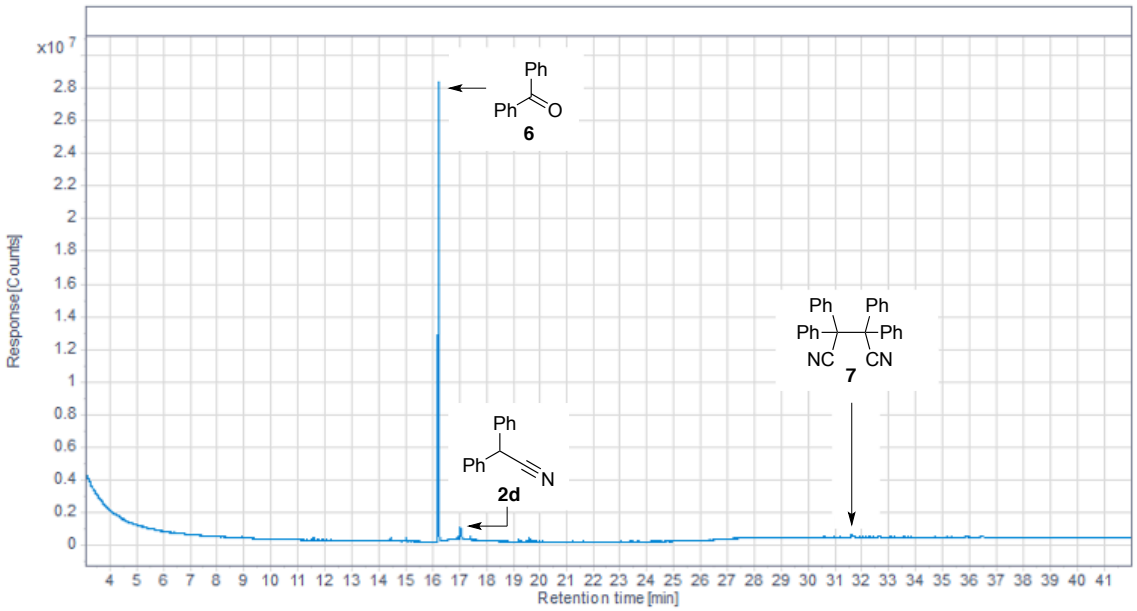

Figure S56. GC profile of the fractions **2–3**.

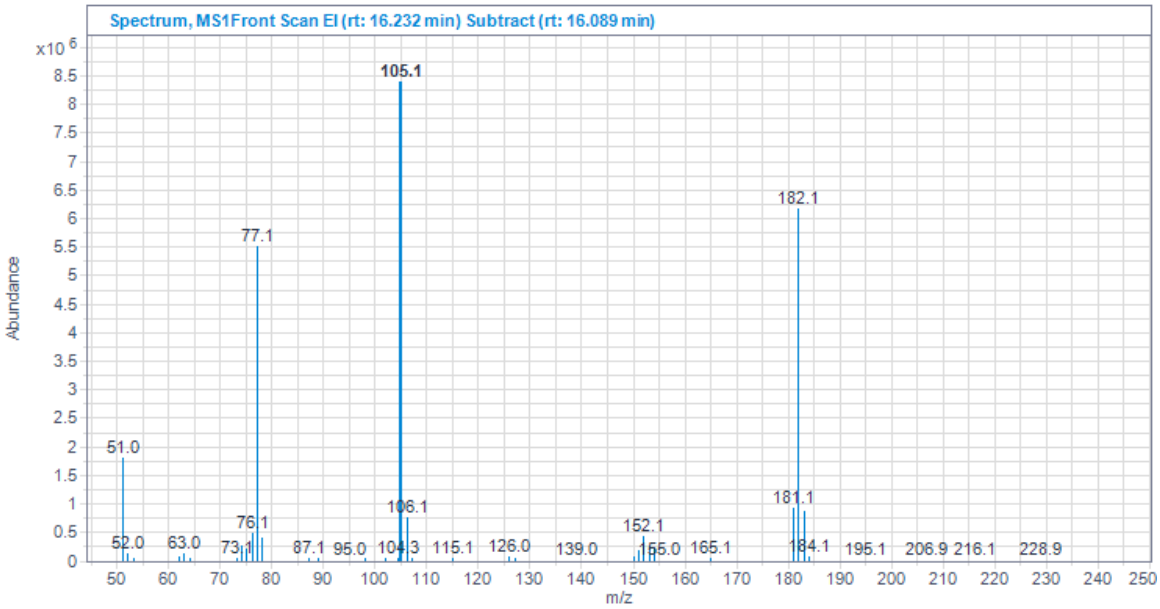

Figure S57. MS spectrum of the peak 16.23 min corresponding to the compound **6**.

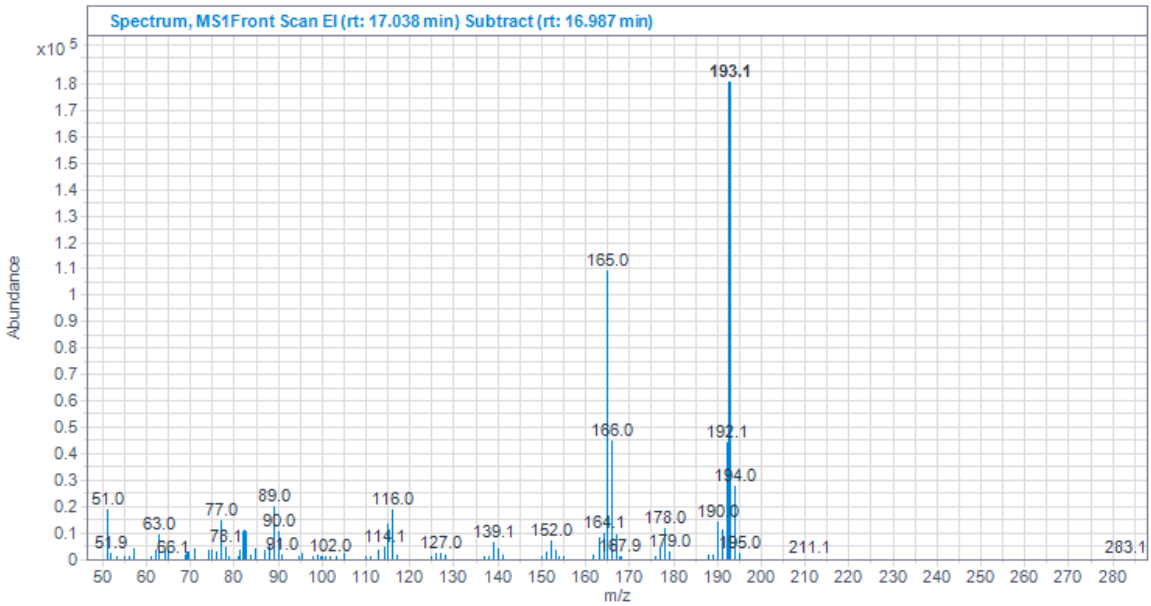

Figure S58. MS spectrum of the peak 17.04 min corresponding to the compound **2d**.

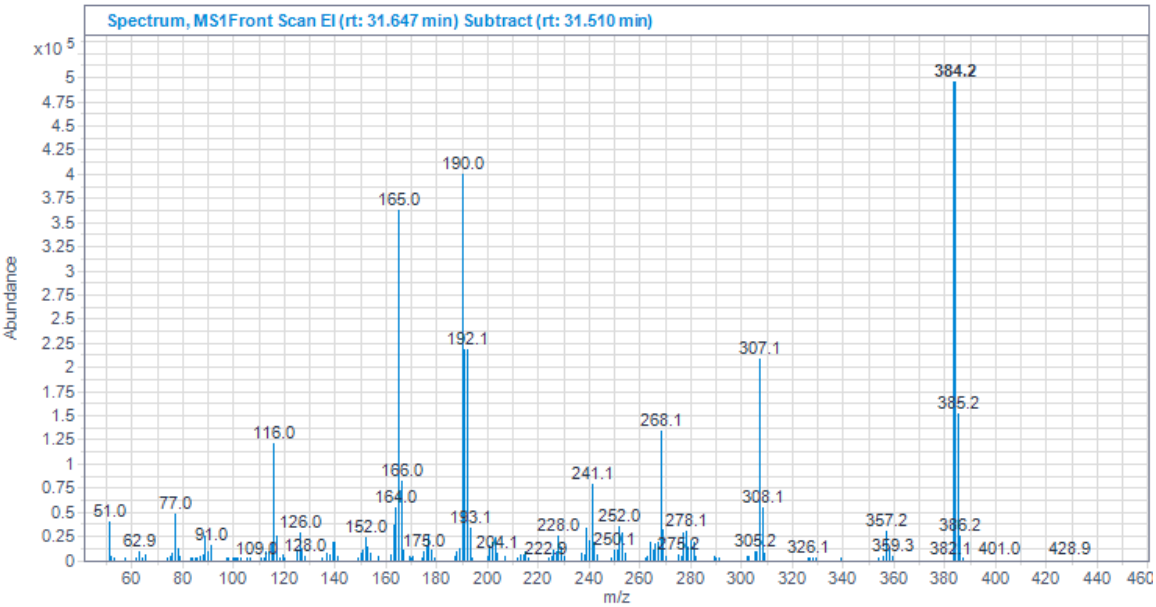

Figure S59. MS spectrum of the peak 31.65 min corresponding to the compound **7**.

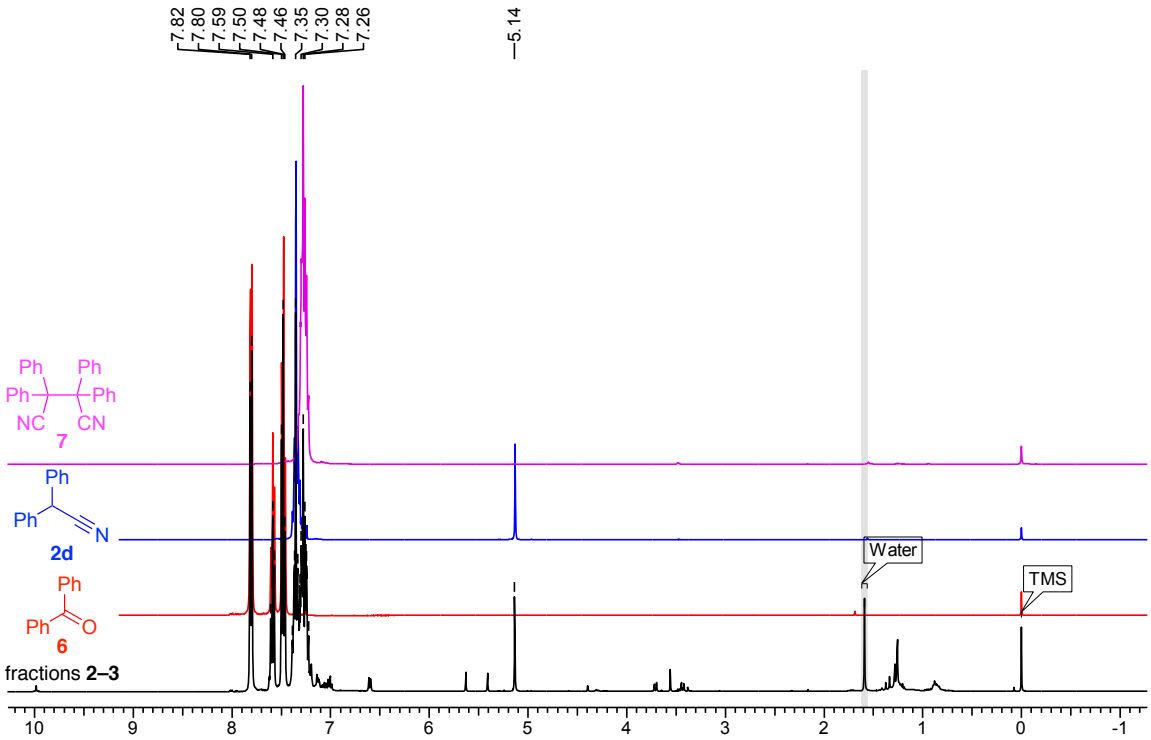

Figure S60. ^{1}H NMR ($CDCl_3$, 400 MHz) profile of the fractions **2–3** in comparison with the authentic spectra of **6**, **2d**, and **7**.

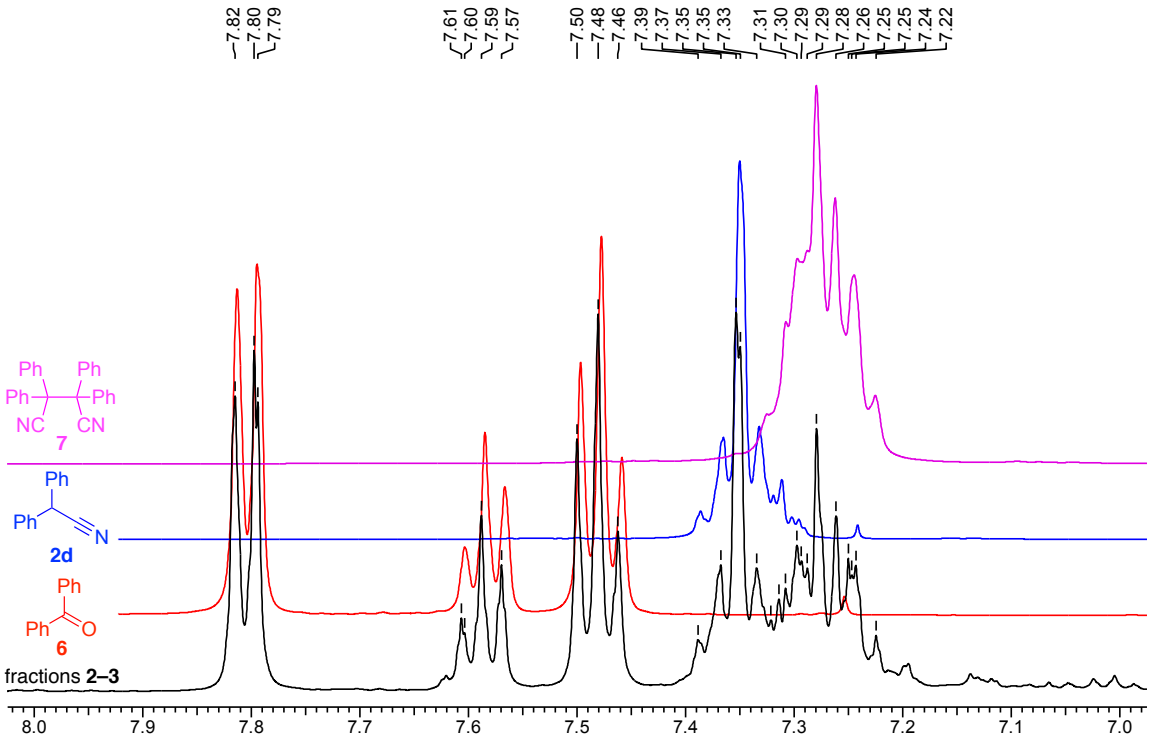

Figure S61. ^{1}H NMR ($CDCl_3$, 400 MHz) profile of the fractions **2–3** in comparison with the authentic spectra of **6**, **2d**, and **7** (in detail).

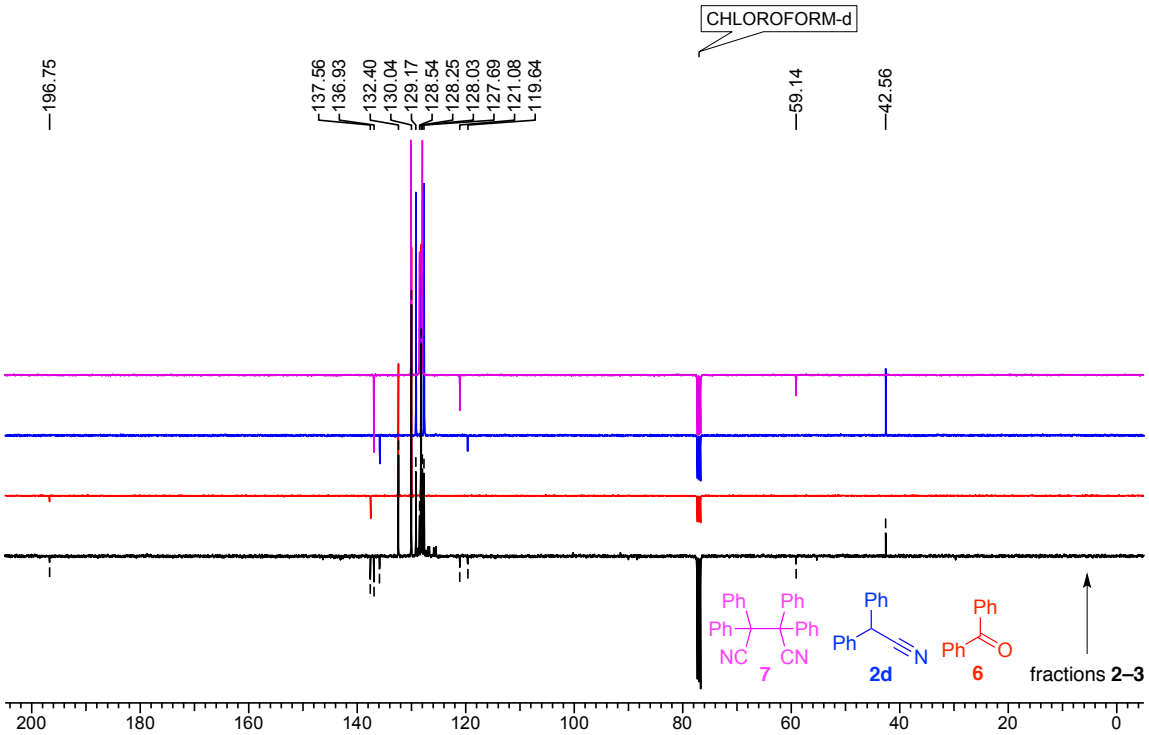

Figure S62. ^{13}C NMR ($CDCl_3$, 100 MHz) profile of the fractions **2–3** in comparison with the authentic spectra of **6**, **2d**, and **7**.

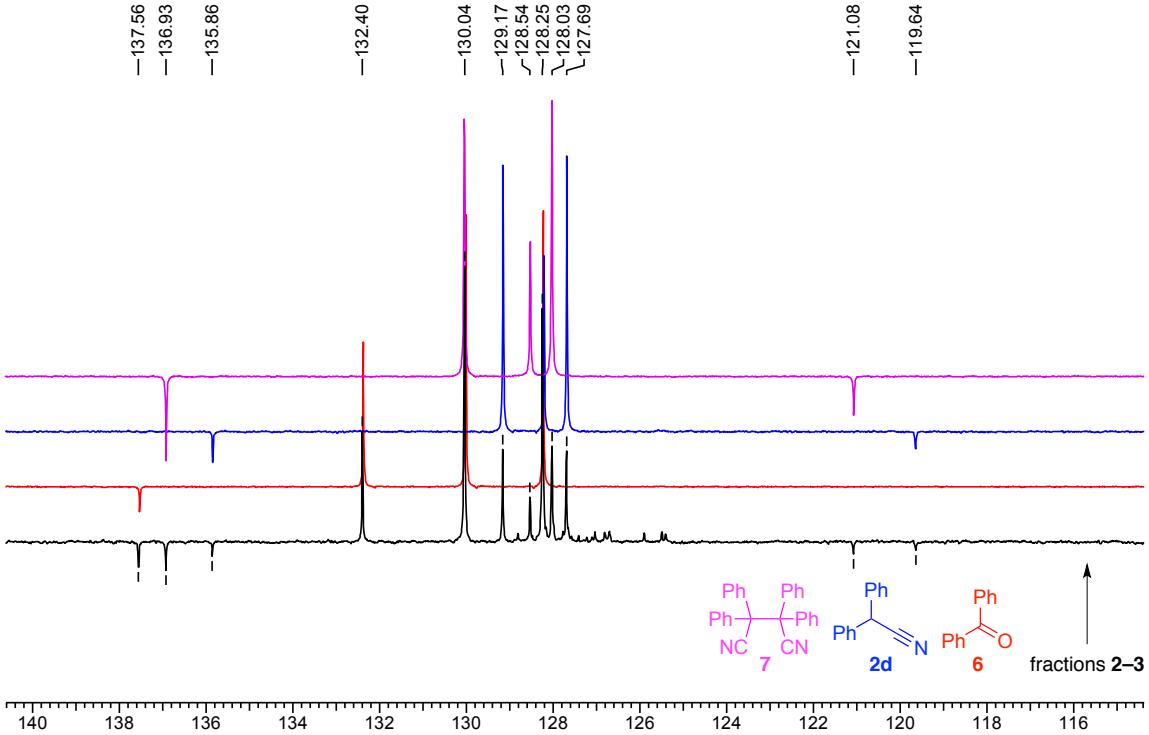

Figure S63. ^{13}C NMR ($CDCl_3$, 100 MHz) profile of the fractions **2–3** in comparison with the authentic spectra of **6**, **2d**, and **7** (in detail).

GC conditions: a DB-5MS column (0.25 µm, 30 m × 0.25 mm), He (constant flow 1 mL/min), temperature program (50 °C | hold 2 min; 10 °C/min rate to 300°C | hold 15 min).

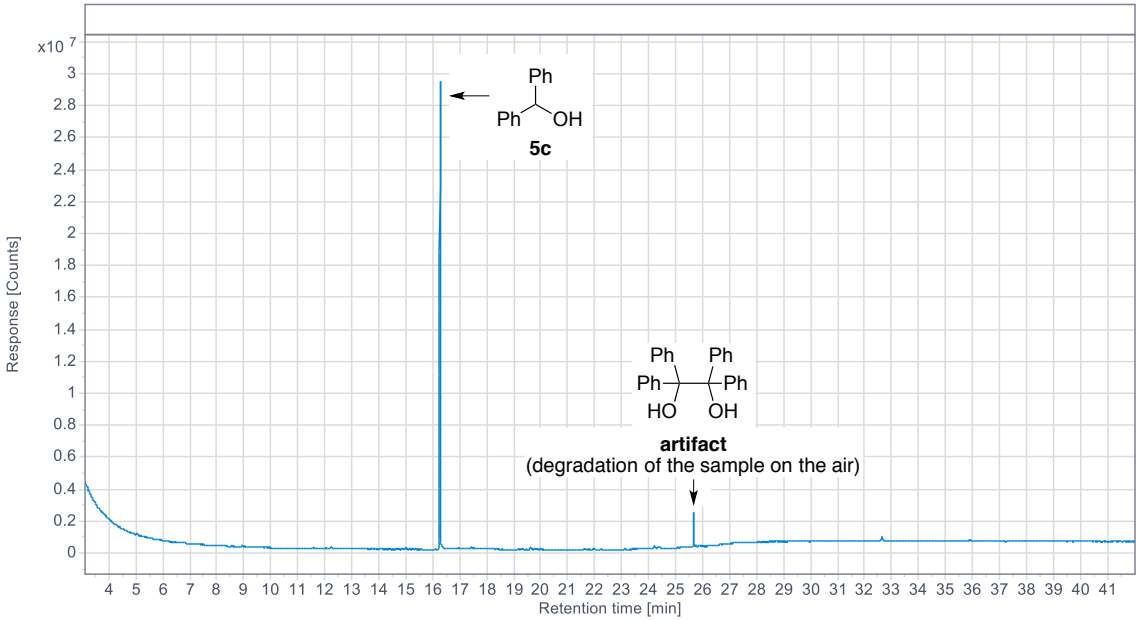

Figure S64. GC profile of the fractions **5–7** corresponding to the compound **5c**.

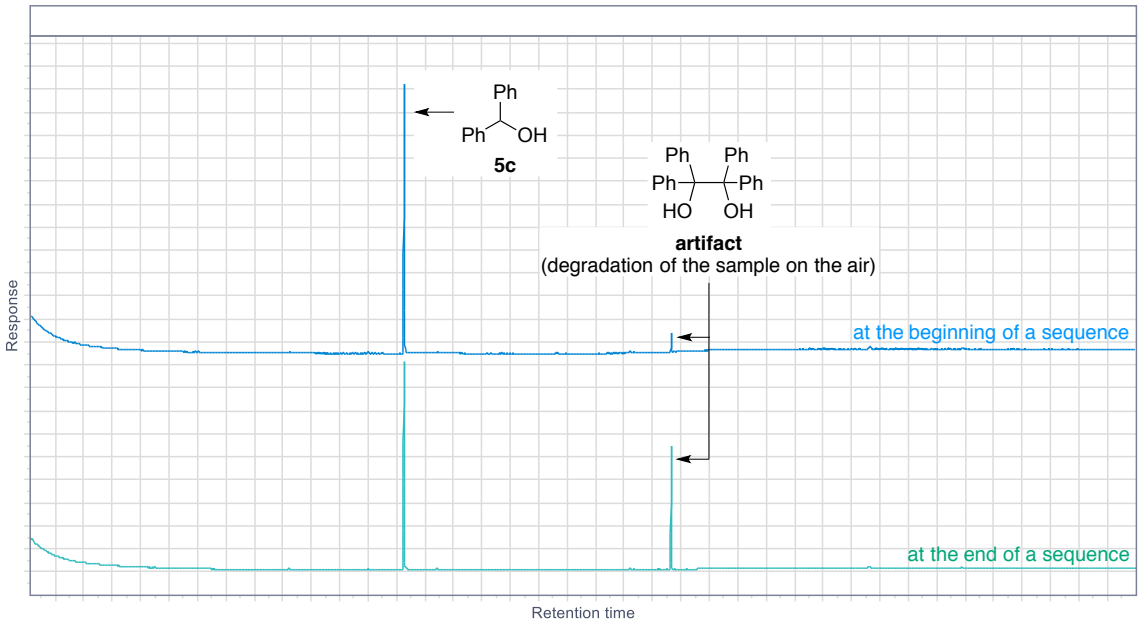

Figure S65. GC spectrum showing slow degradation of the sample containing **5c** on the air.

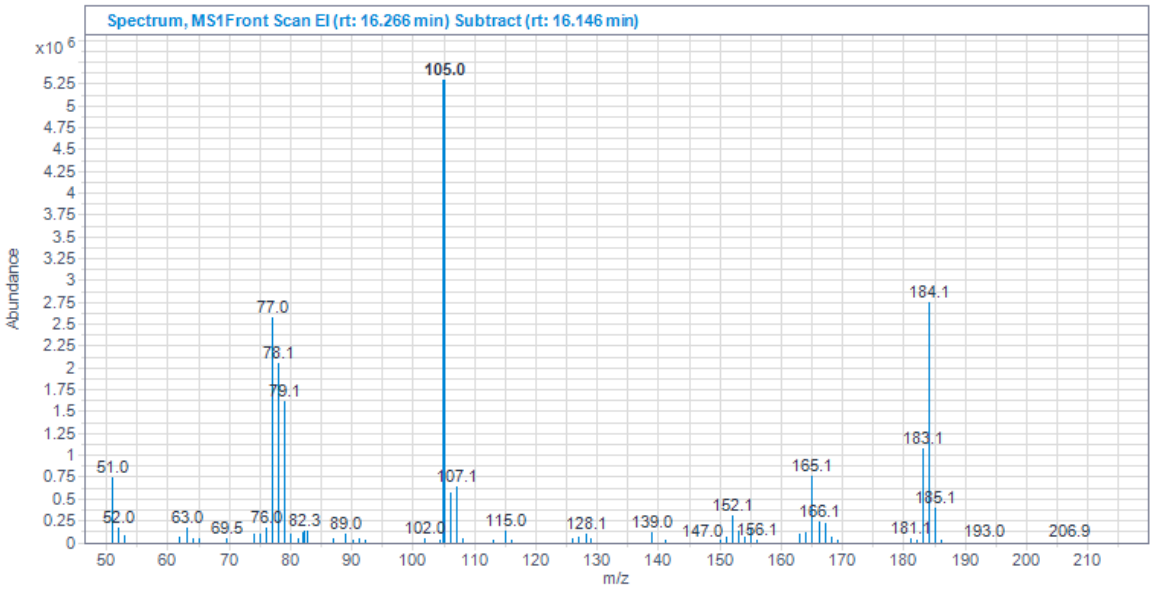

Figure S66. MS spectrum of the peak 16.27 min corresponding to the compound **5c**.

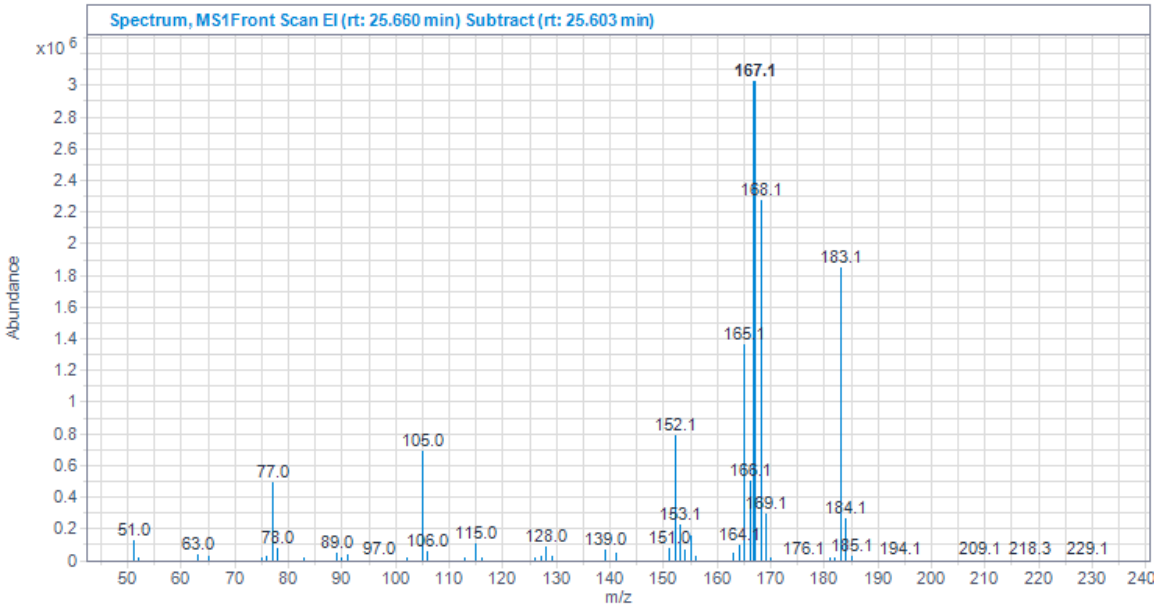

Figure S67. MS spectrum of the peak 25.66 min corresponding to the the benzopinacol artifact.

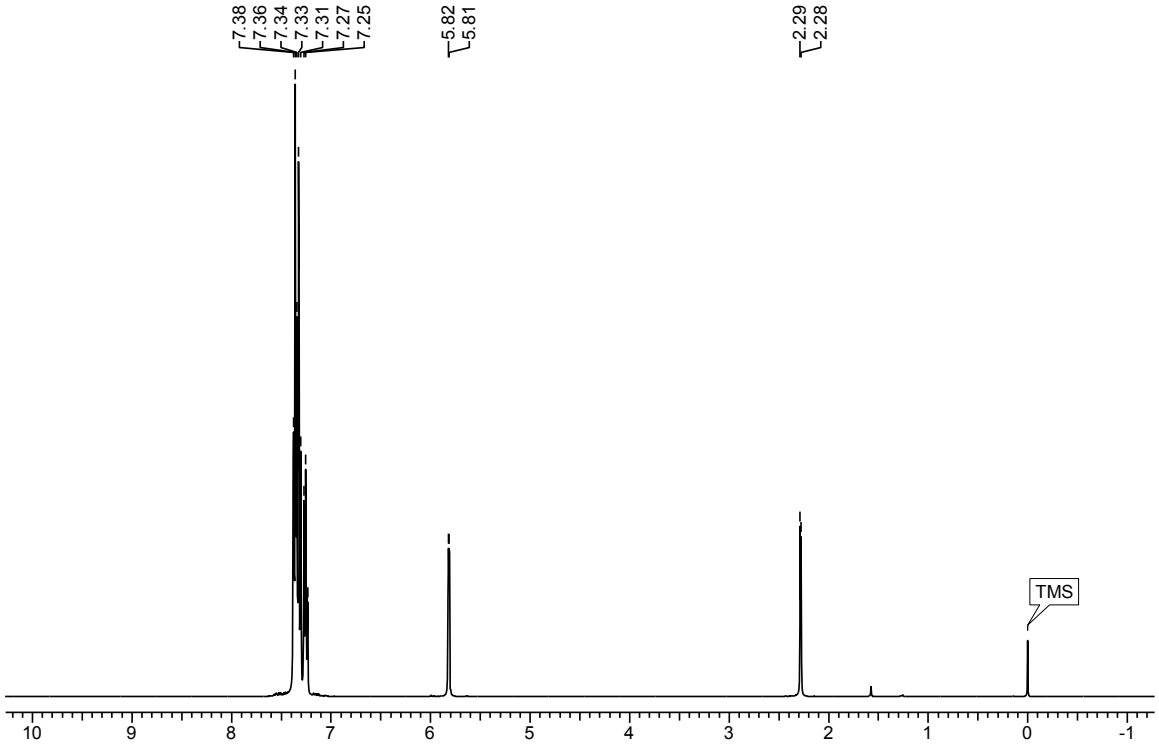

Figure S68. ^{1}H NMR ($CDCl_3$, 400 MHz) profile of the fractions **5–7** corresponding to the compound **5c**.

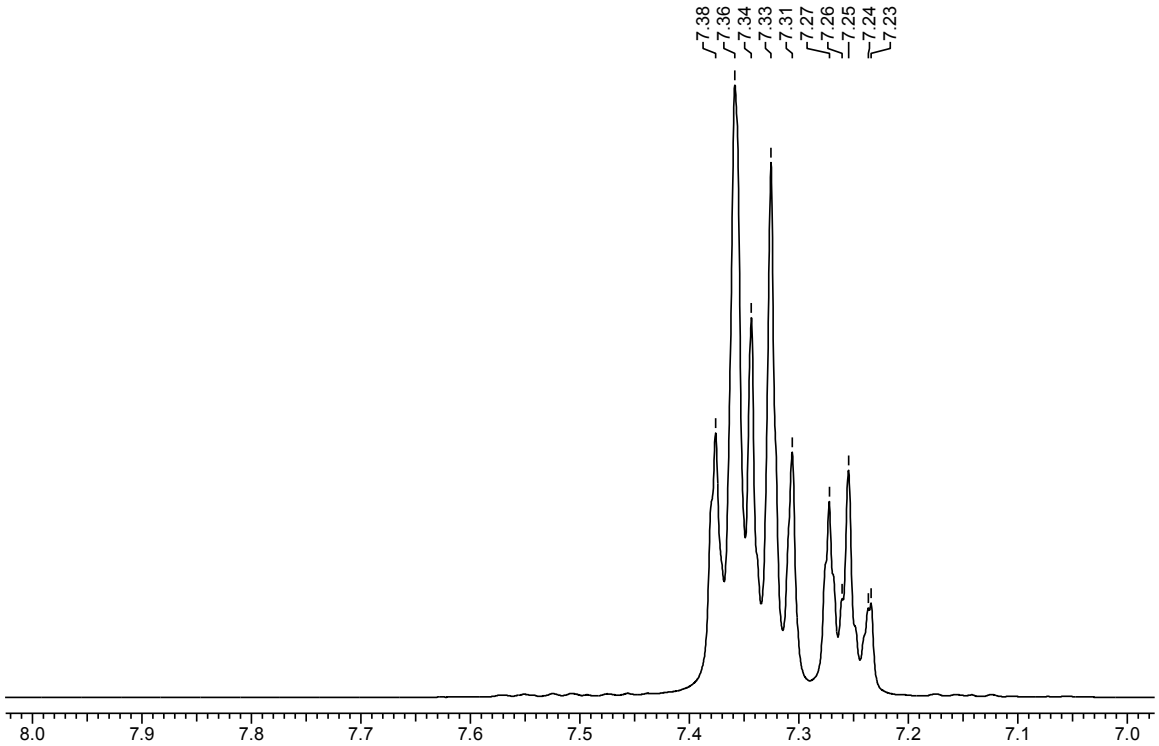

Figure S69. ^{1}H NMR ($CDCl_3$, 400 MHz) profile of the fractions **5–7** corresponding to the compound **5c** (in detail).

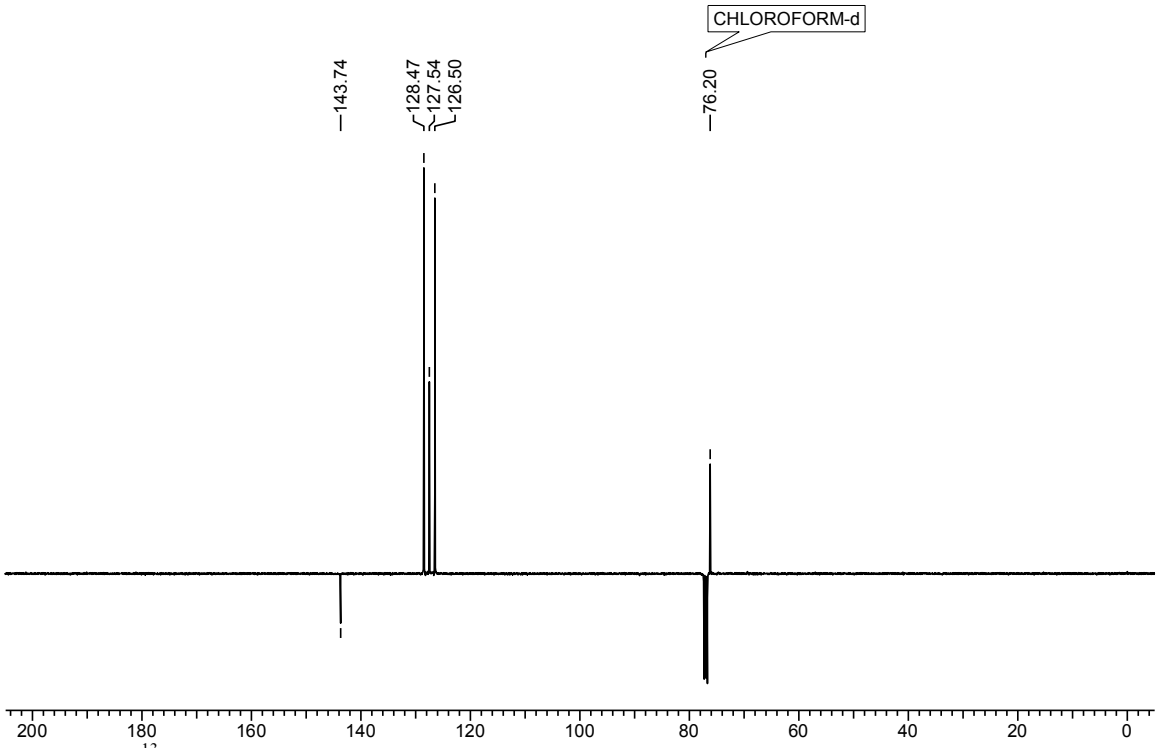

Figure S70. ^{13}C NMR ($CDCl_3$, 100 MHz) profile of the fractions **5–7** corresponding to the compound **5c**.

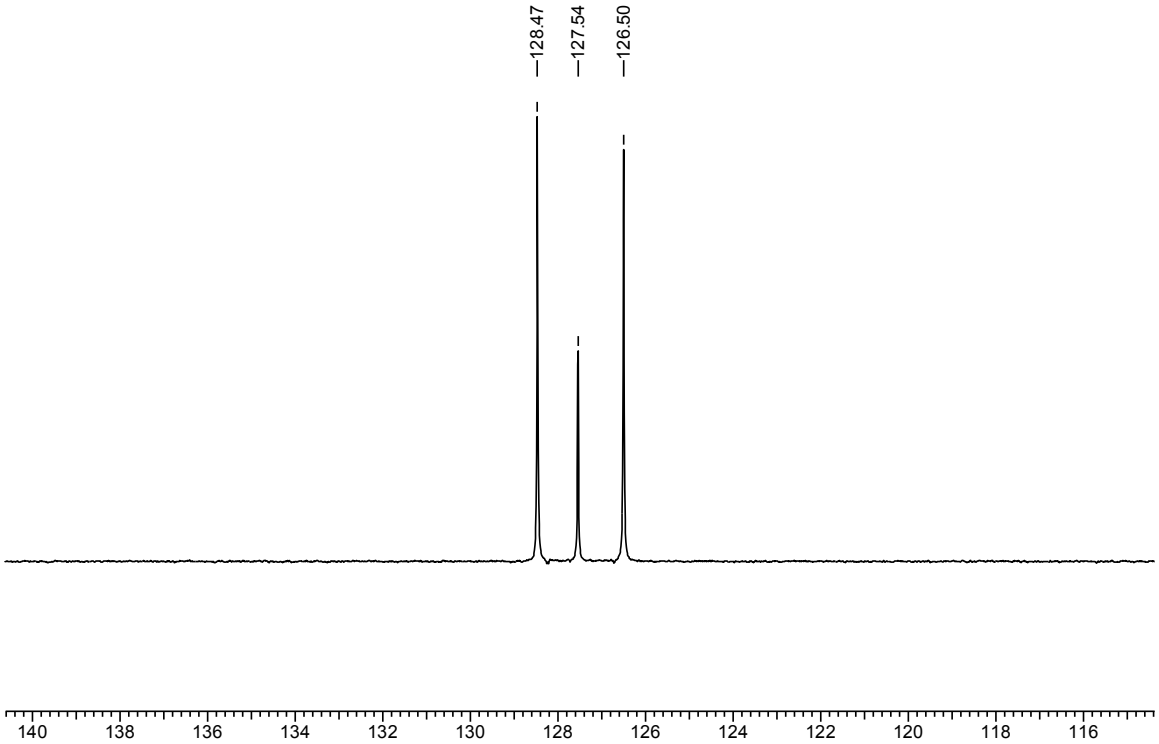

Figure S71. ^{13}C NMR ($CDCl_3$, 100 MHz) profile of the fractions **5–7** corresponding to the compound **5c** (in detail).

5. References

(1) J. Xiao, Z. Z. Wong, Y. P. Lu and T. P. Loh, *Adv. Synth. Catal.* 2010, **352**, 1107.

6. HRMS and NMR Data

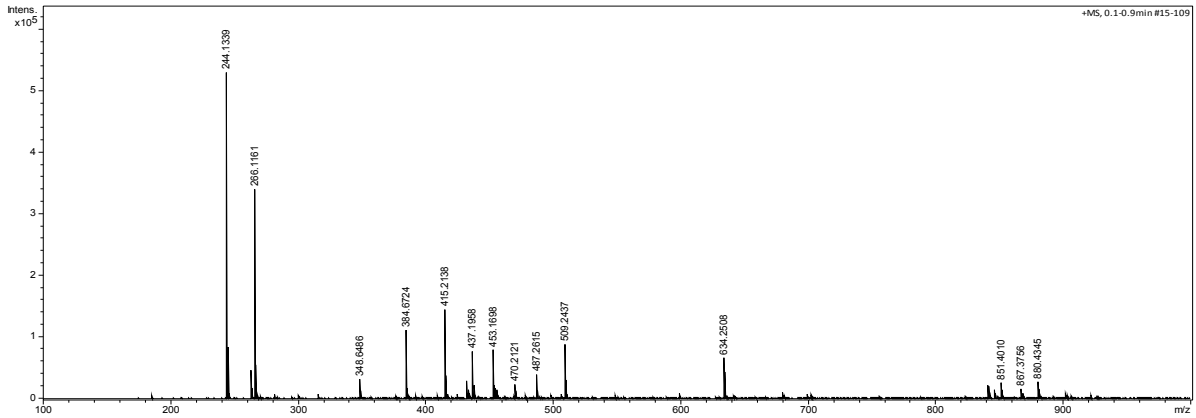

Figure S72. HRMS (ESI–Q-TOF) spectrum of **1aa** $[M+H]^+$.

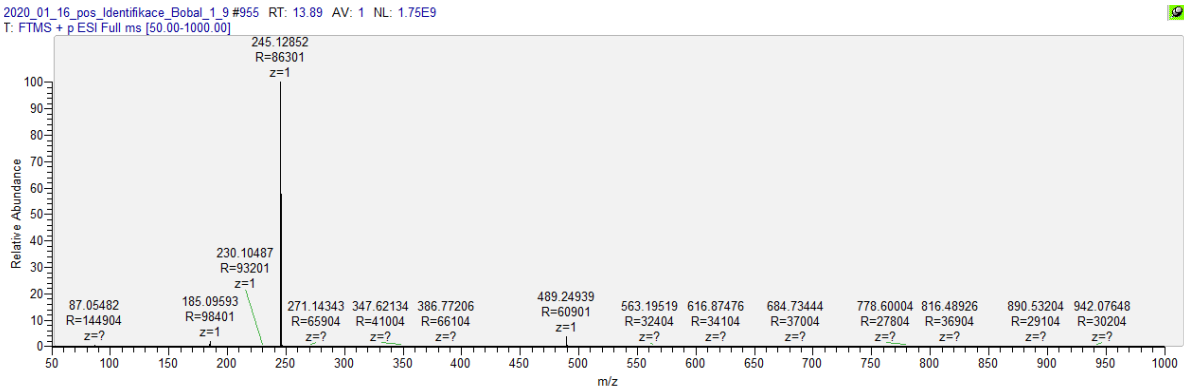

Figure S73. HRMS (ESI-Orbitrap) spectrum of **1ab** $[M+H]^+$.

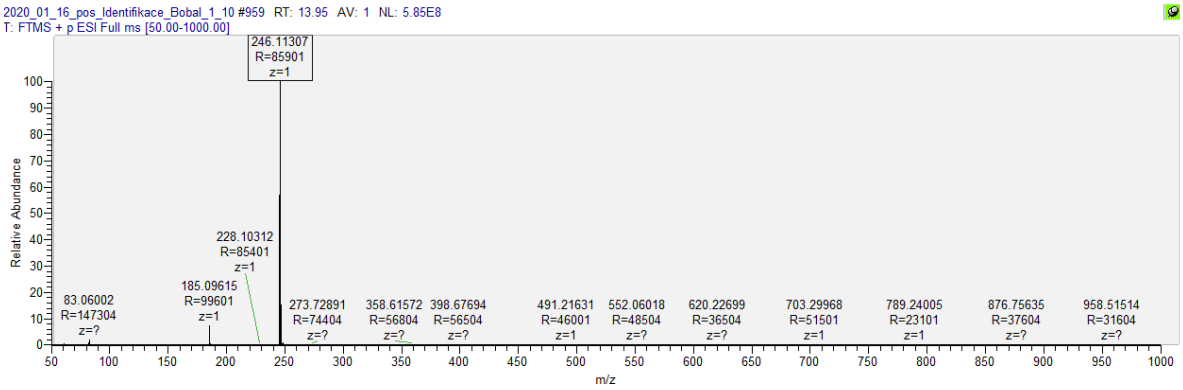

Figure S74. HRMS (ESI-Orbitrap) spectrum of **1ac** $[M+H]^+$.

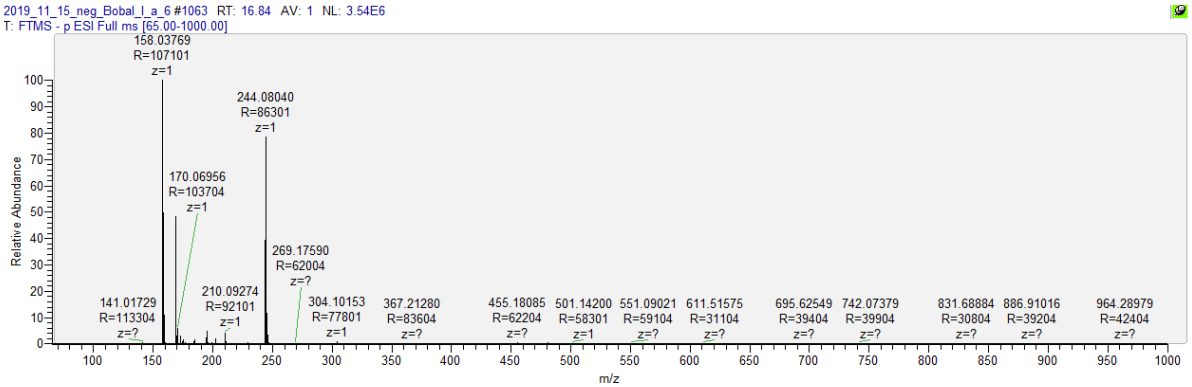

Figure S75. HRMS (ESI-Orbitrap) spectrum of **1ad** $[M-H]^-$.

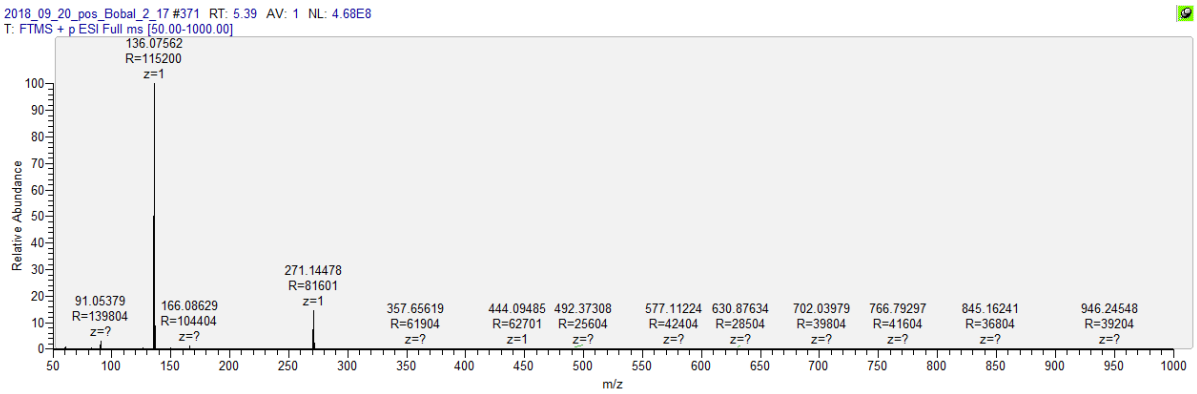

Figure S76. HRMS (ESI-Orbitrap) spectrum of **1b** $[M+H]^+$.

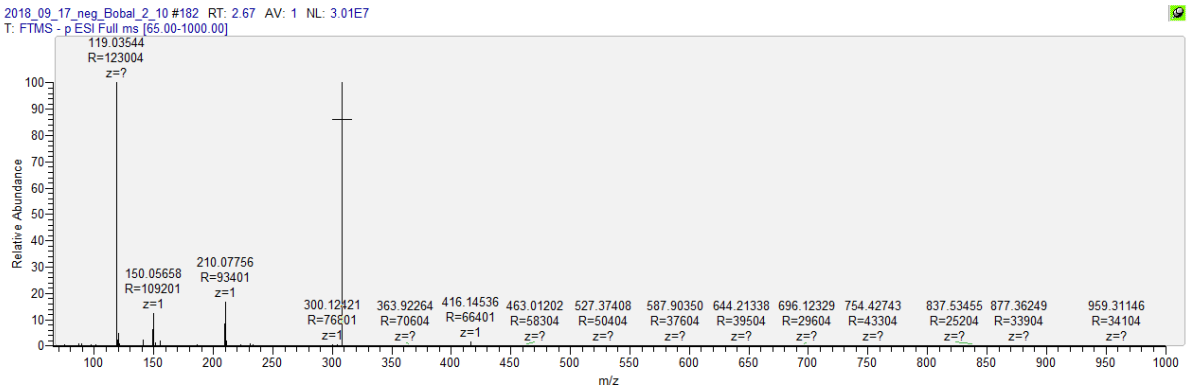

Figure S77. HRMS (ESI-Orbitrap) spectrum of **1ba** $[M-H]^-$.

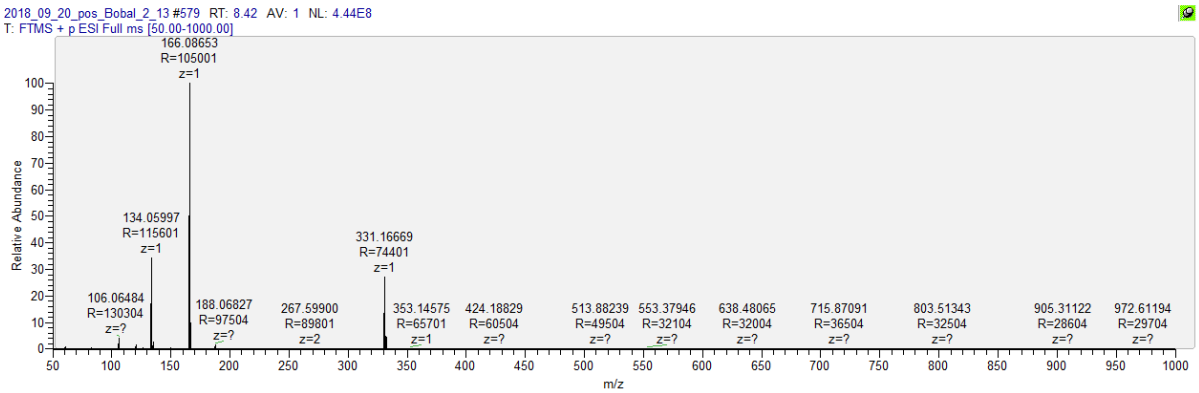

Figure S78. HRMS (ESI-Orbitrap) spectrum of **1bb** $[M+H]^+$.

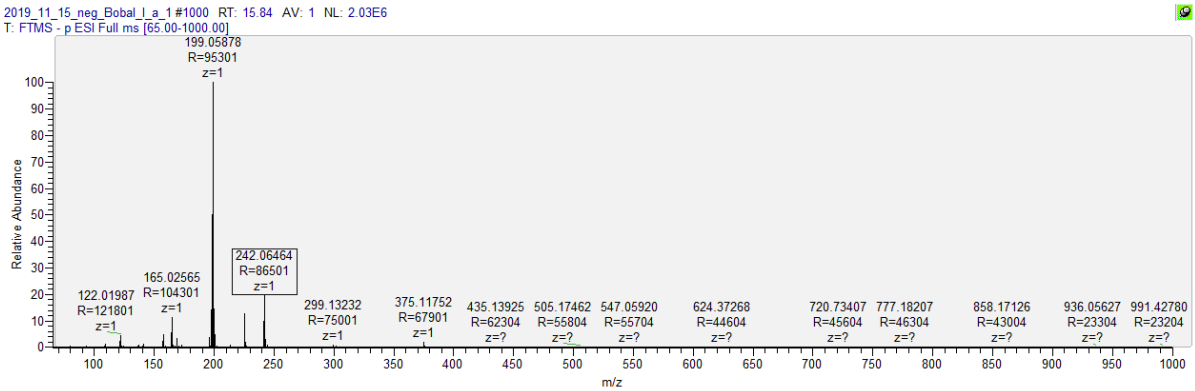

Figure S79. HRMS (ESI-Orbitrap) spectrum of **1bc** $[M-H]^-$.

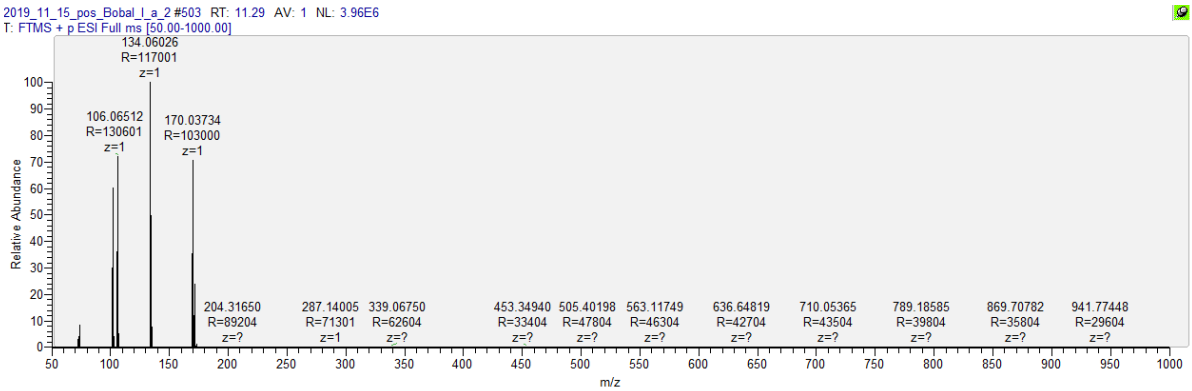

Figure S80. HRMS (ESI-Orbitrap) spectrum of **1bd** $[M+H]^+$.

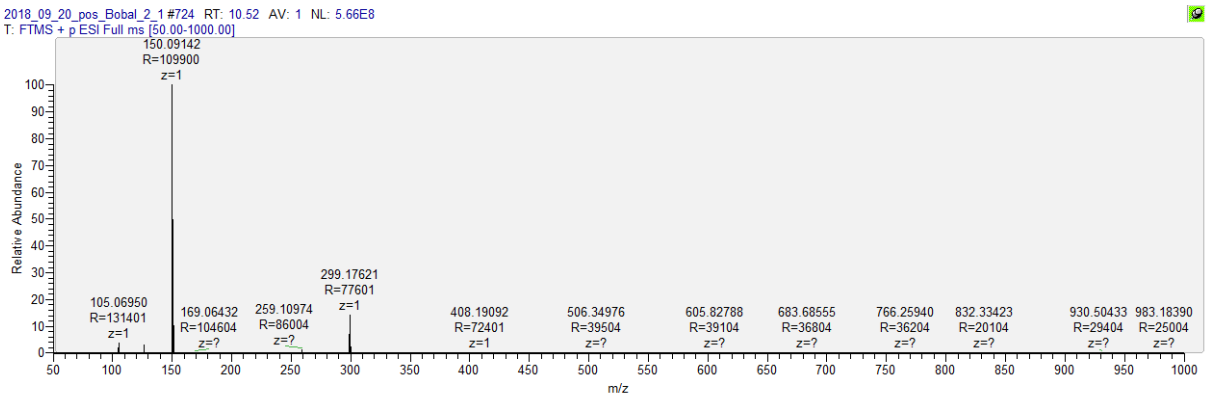

Figure S81. HRMS (ESI-Orbitrap) spectrum of **1c** $[M+H]^+$.

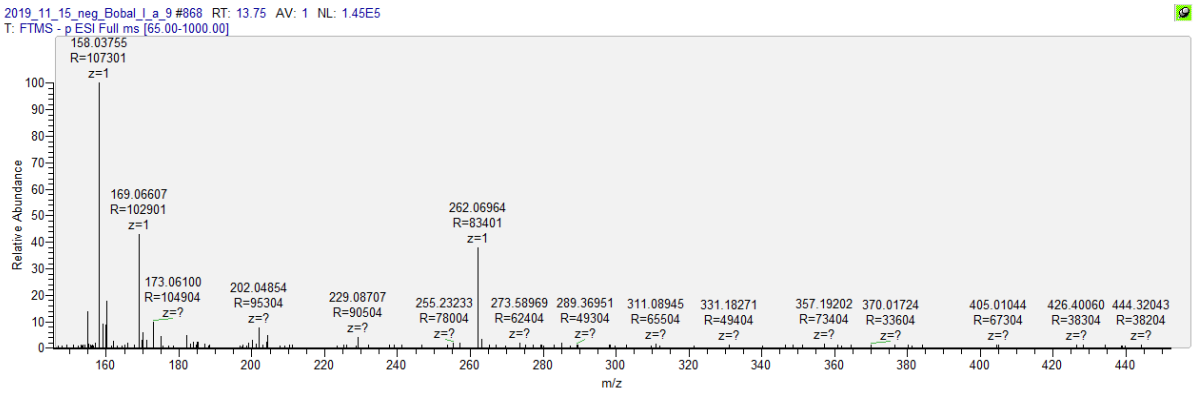

Figure S82. HRMS (ESI-Orbitrap) spectrum of **1ca** $[M-H]^-$.

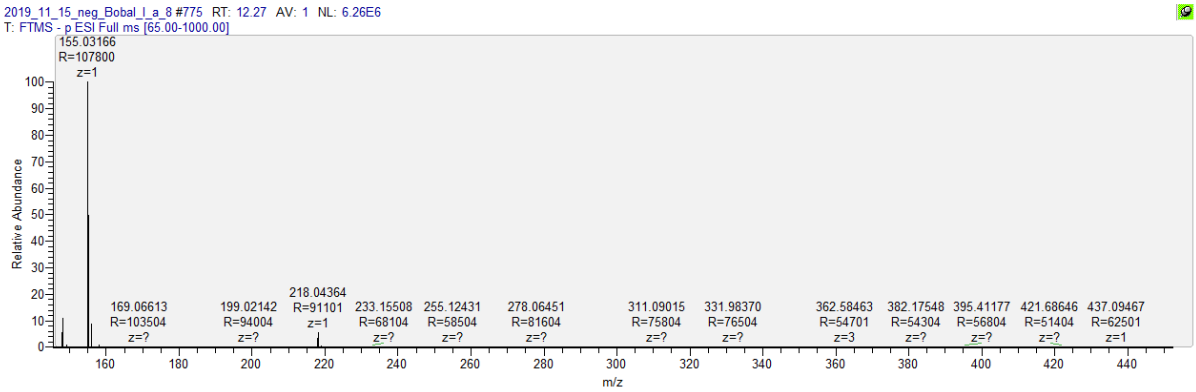

Figure S83. HRMS (ESI-Orbitrap) spectrum of **1cb** $[M-H]^-$.

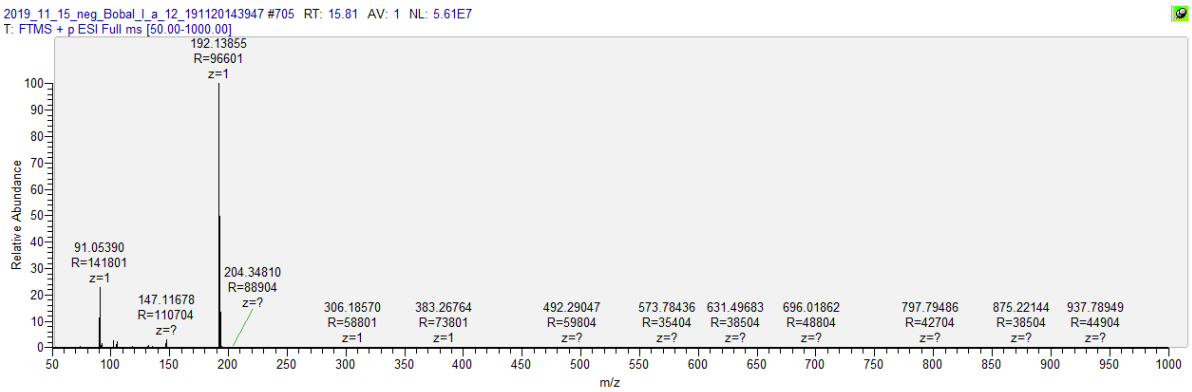

Figure S84. HRMS (ESI-Orbitrap) spectrum of **1cc** $[M+H]^+$.

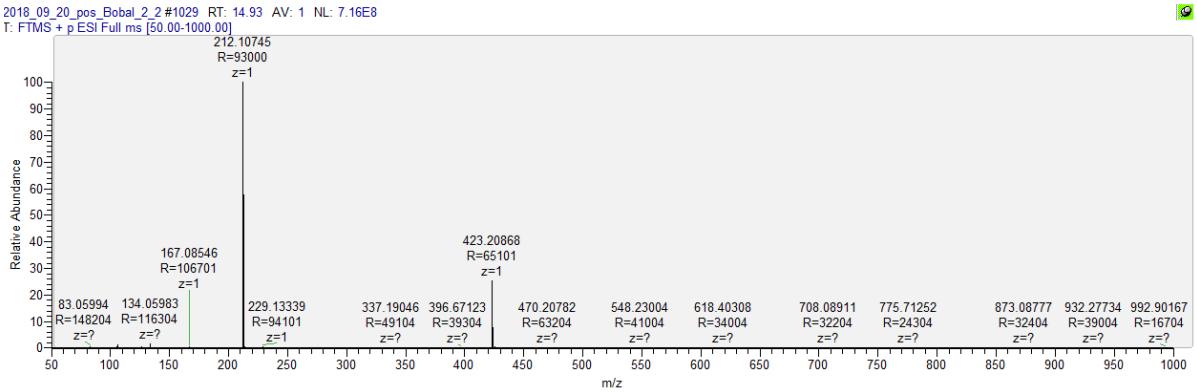

Figure S85. HRMS (ESI-Orbitrap) spectrum of **1d** $[M+H]^+$.

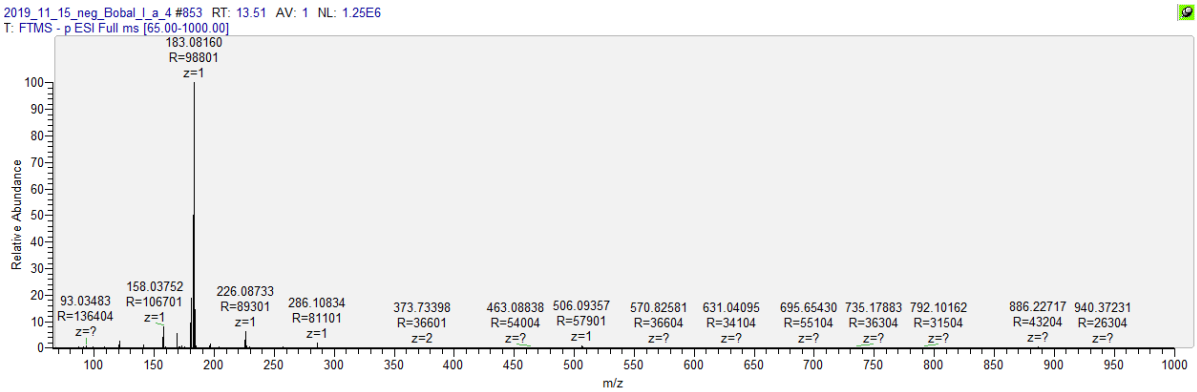

Figure S86. HRMS (ESI-Orbitrap) spectrum of **1da** $[M-H]^-$.

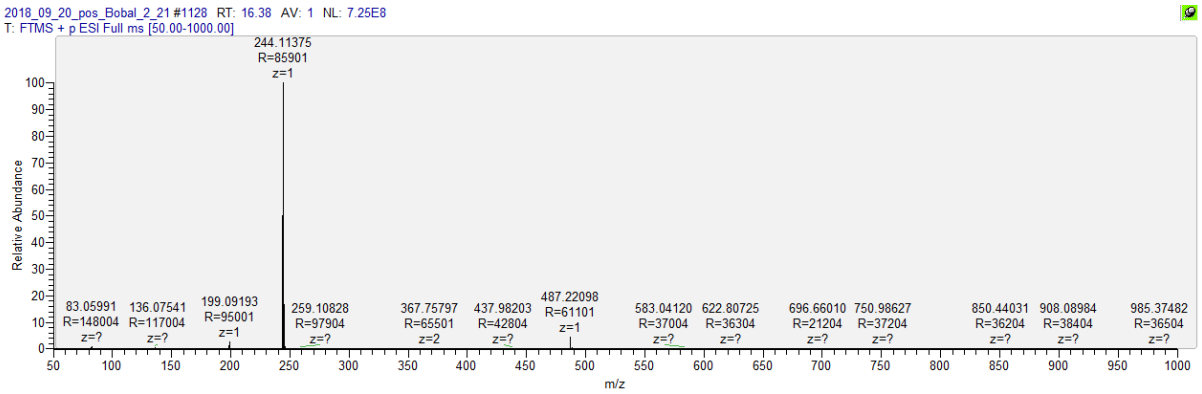

Figure S87. HRMS (ESI-Orbitrap) spectrum of **1e** $[M+H]^+$.

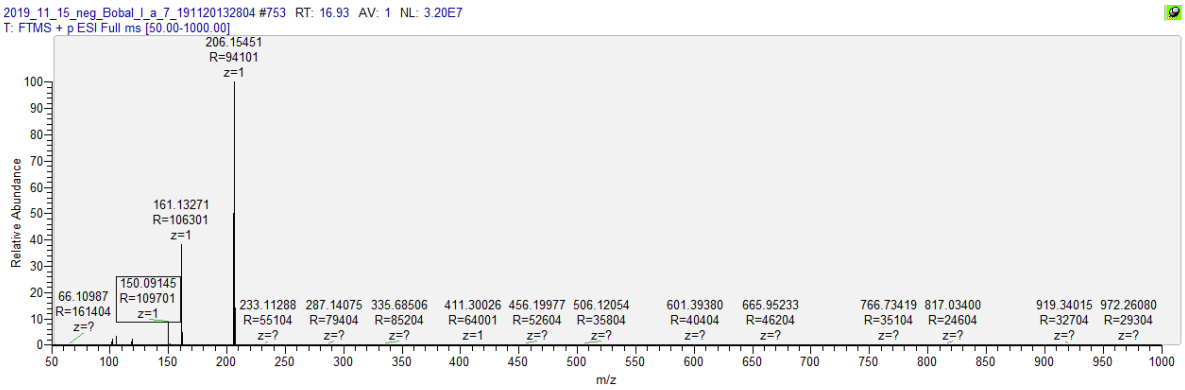

Figure S88. HRMS (ESI-Orbitrap) spectrum of **1f** $[M+H]^+$.

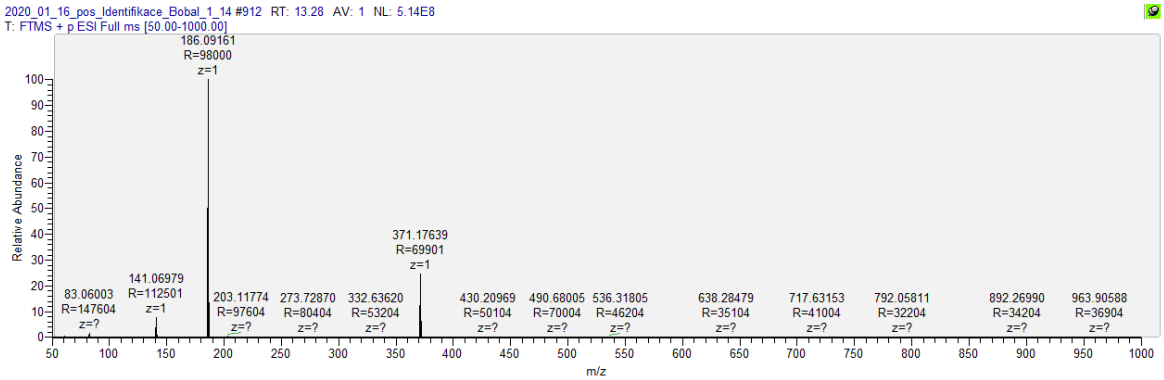

Figure S89. HRMS (ESI-Orbitrap) spectrum of **1g** $[M+H]^+$.

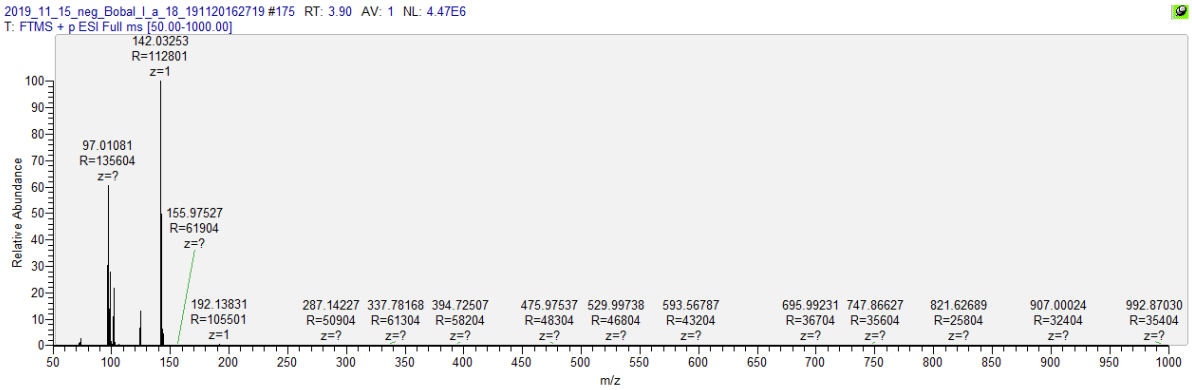

Figure S90. HRMS (ESI-Orbitrap) spectrum of **1h** $[M+H]^+$.

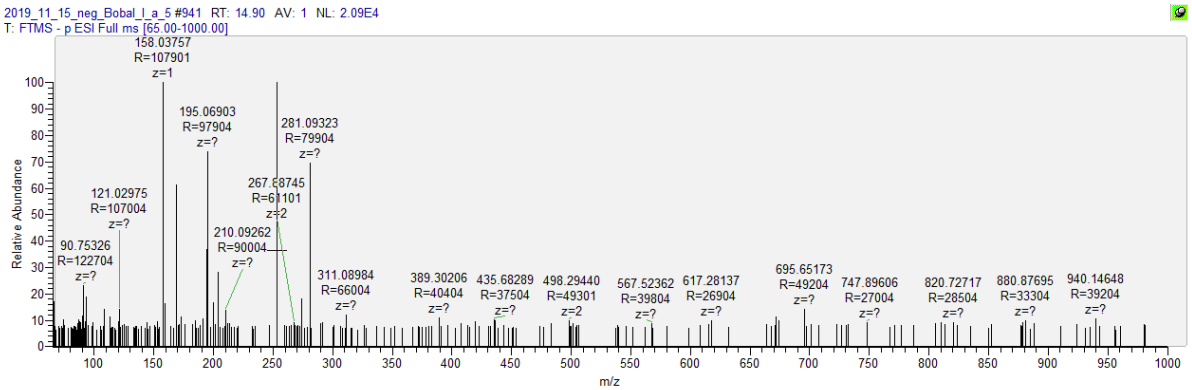

Figure S91. HRMS (ESI-Orbitrap) spectrum of **2a** $[M-H]^-$.

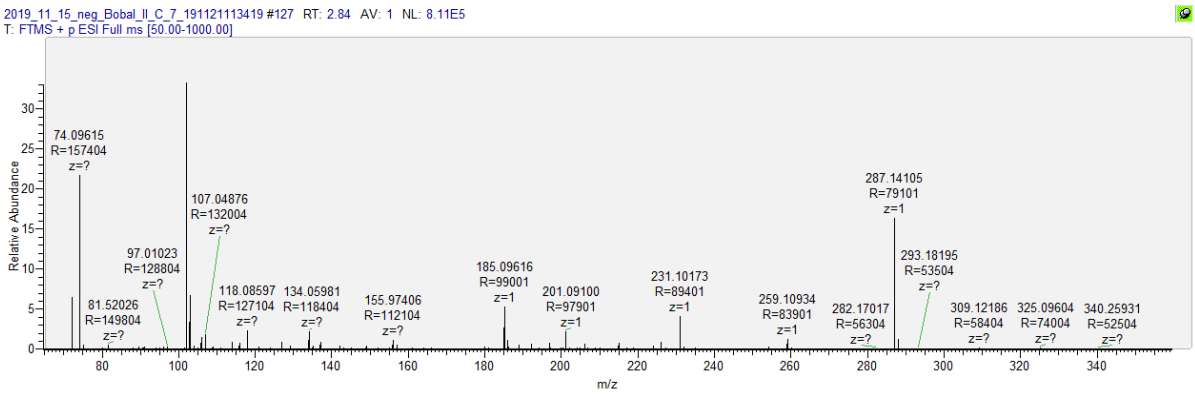

Figure S92. HRMS (ESI-Orbitrap) spectrum of **2ba** $[M+H]^+$.

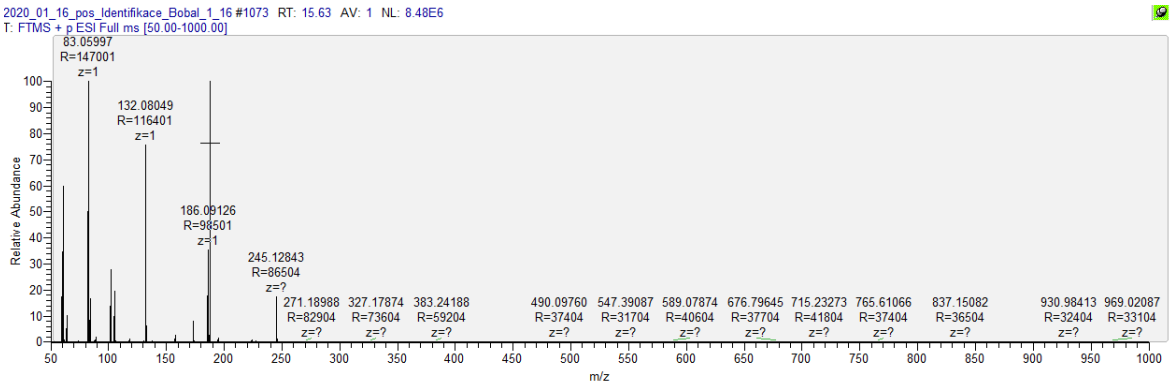

Figure S93. HRMS (ESI-Orbitrap) spectrum of **2c** $[M+H]^+$.

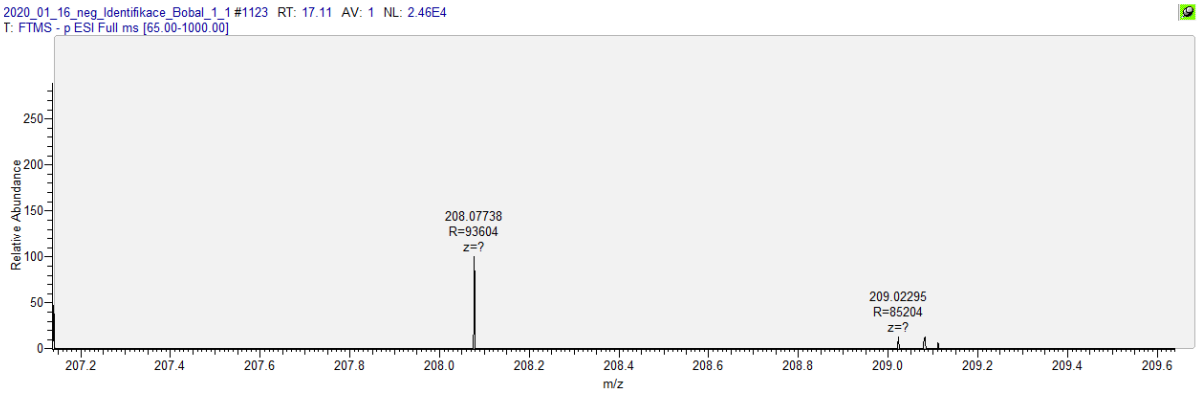

Figure S94. HRMS (ESI-Orbitrap) spectrum of **2da** $[M-H]^-$.

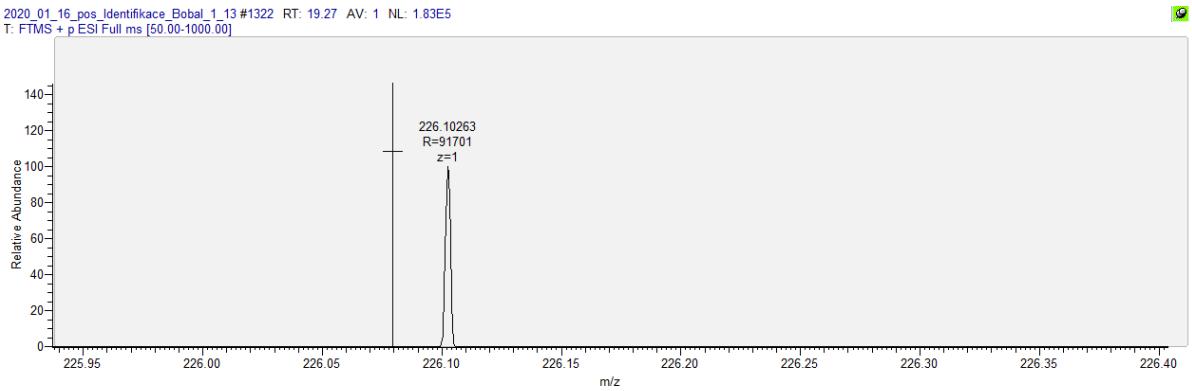

Figure S95. HRMS (ESI-Orbitrap) spectrum of **2e** $[M+H]^+$.

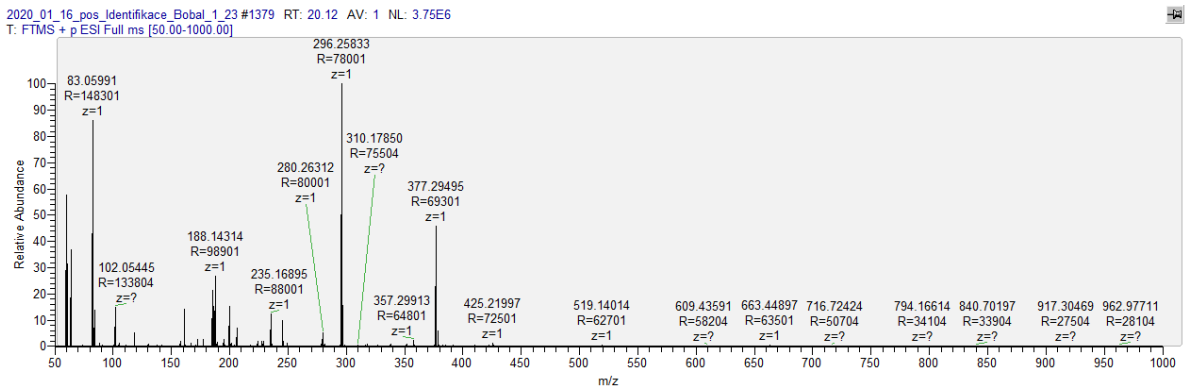

Figure S96. HRMS (ESI-Orbitrap) spectrum of **2f** $[M+H]^+$.

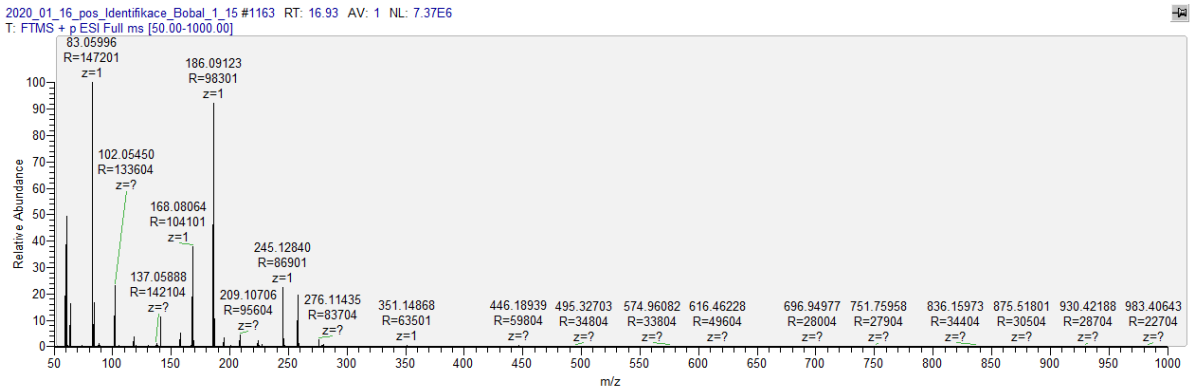

Figure S97. HRMS (ESI-Orbitrap) spectrum of **2g** $[M+H]^+$.

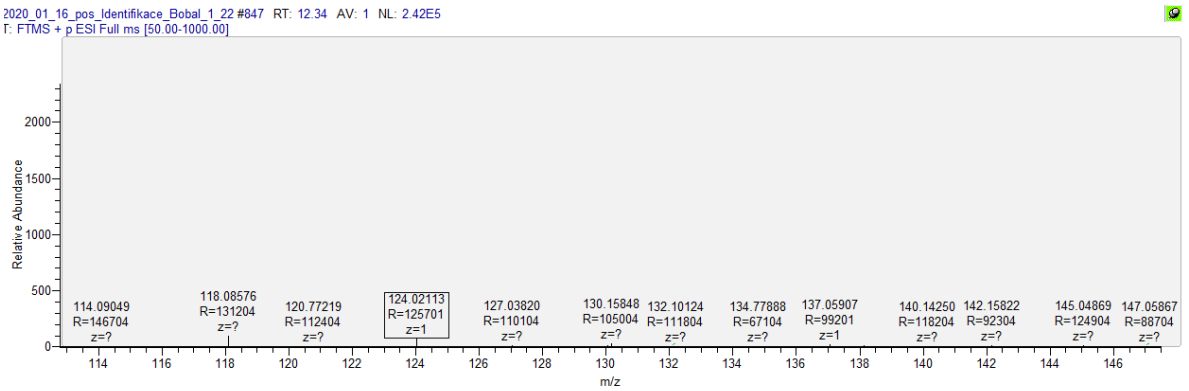

Figure S98. HRMS (ESI-Orbitrap) spectrum of **2h** $[M+H]^+$.

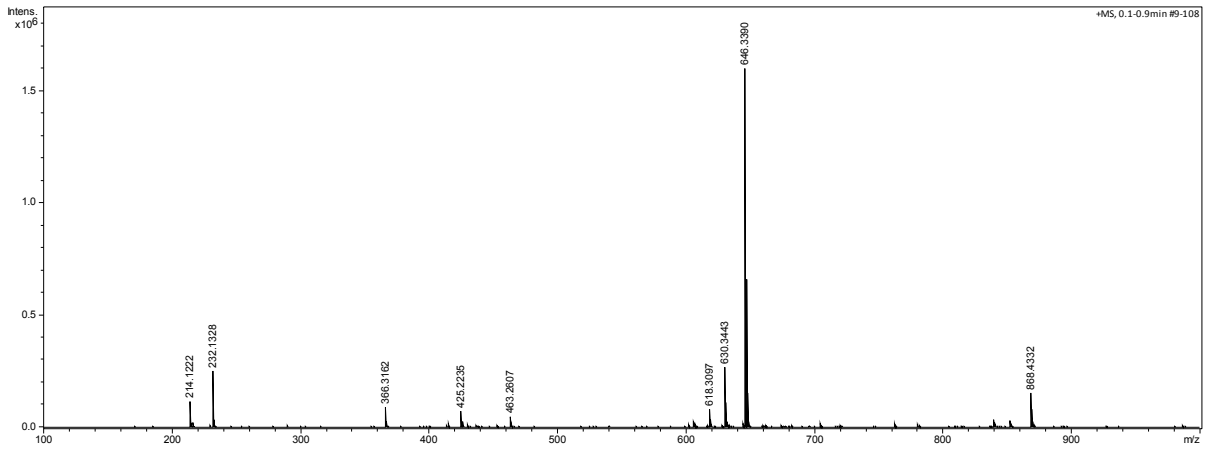

Figure S99. HRMS (ESI–Q-TOF) spectrum of **3a** $[M+H]^+$.

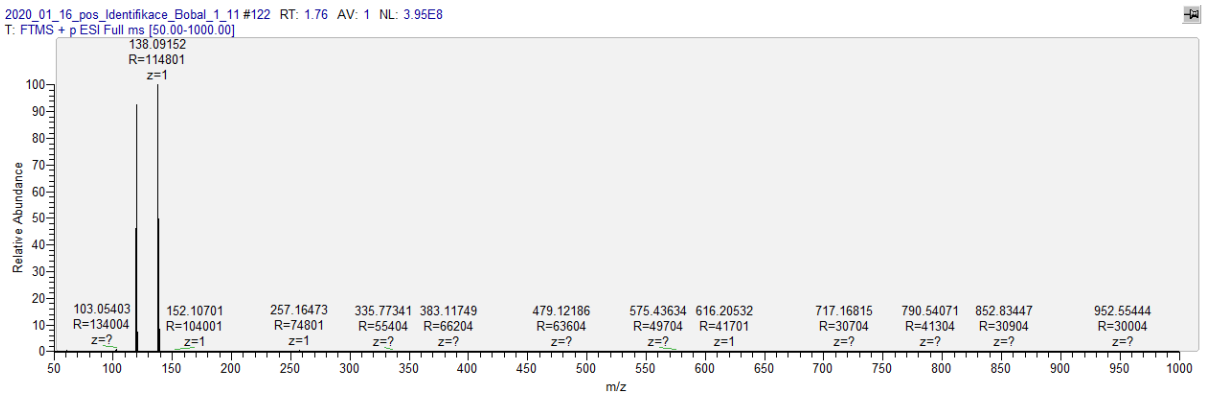

Figure S100. HRMS (ESI-Obritrap) spectrum of **3b** $[M+H]^+$.

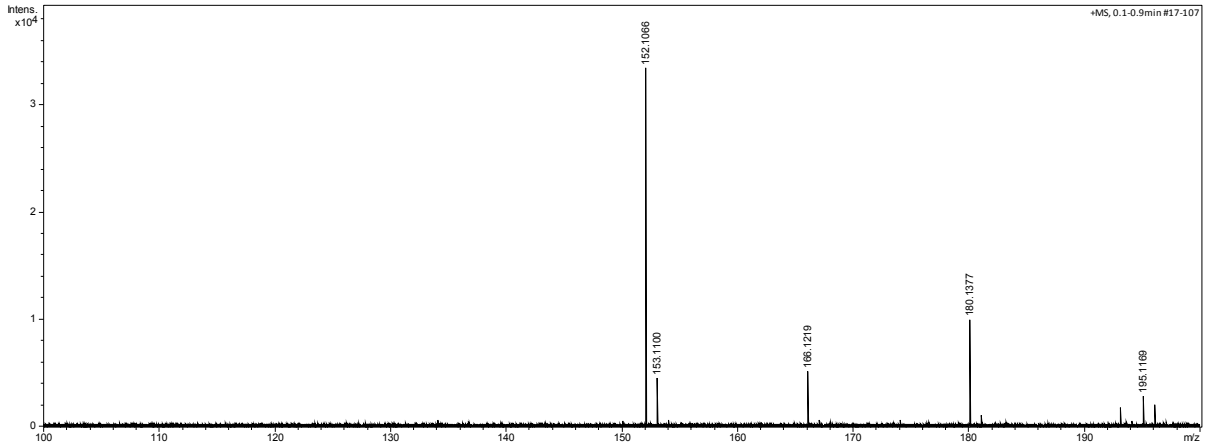

Figure S101. HRMS (ESI–Q-TOF) spectrum of **3c** $[M+H]^+$.

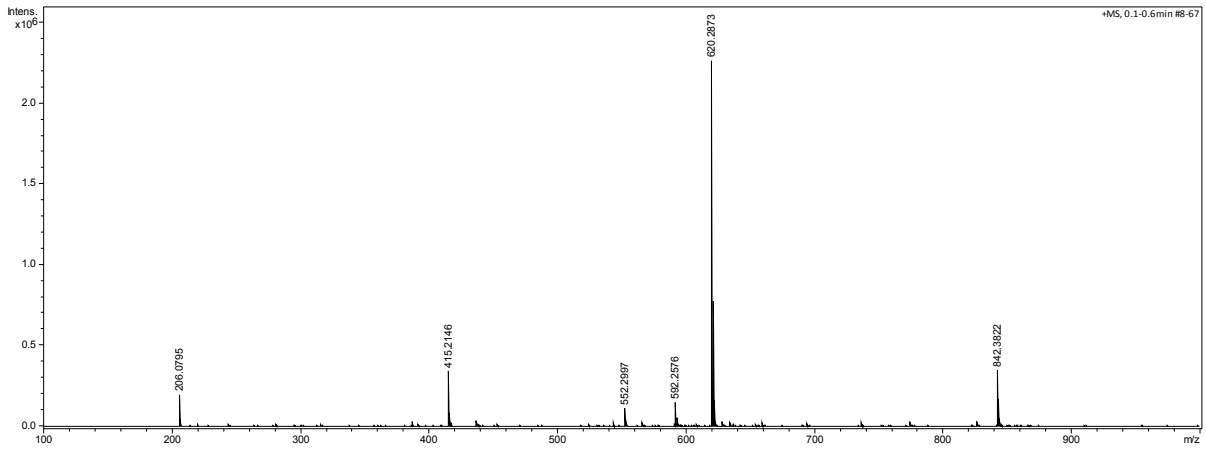

Figure S102. HRMS (ESI–Q-TOF) spectrum of **3ca** $[M+H]^+$.

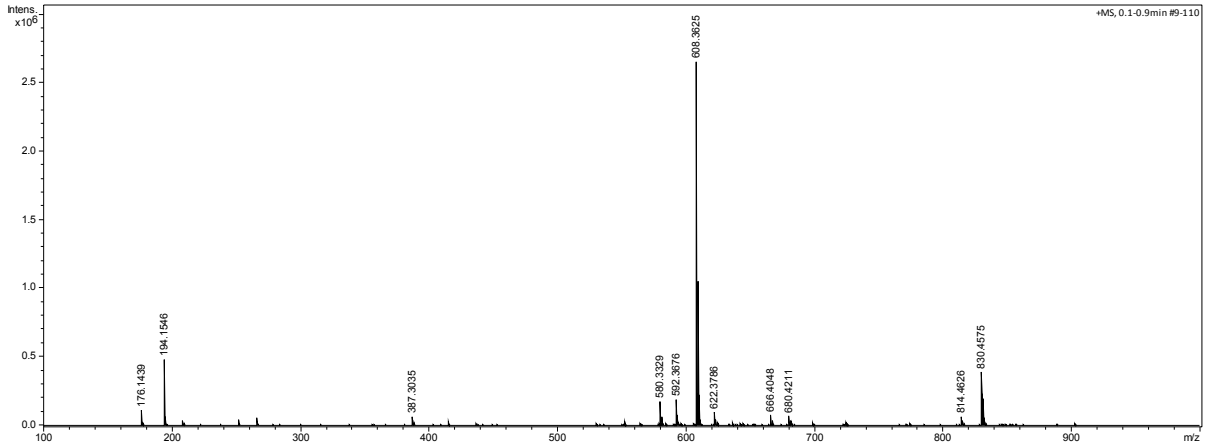

Figure S103. HRMS (ESI–Q-TOF) spectrum of **3cb** $[M+H]^+$.

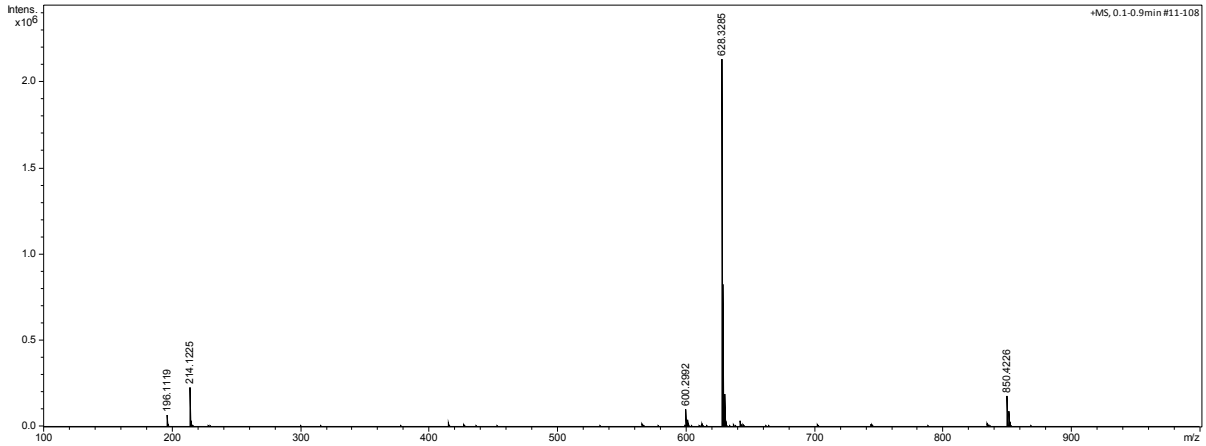

Figure S104. HRMS (ESI–Q-TOF) spectrum of **3d** $[M+H]^+$.

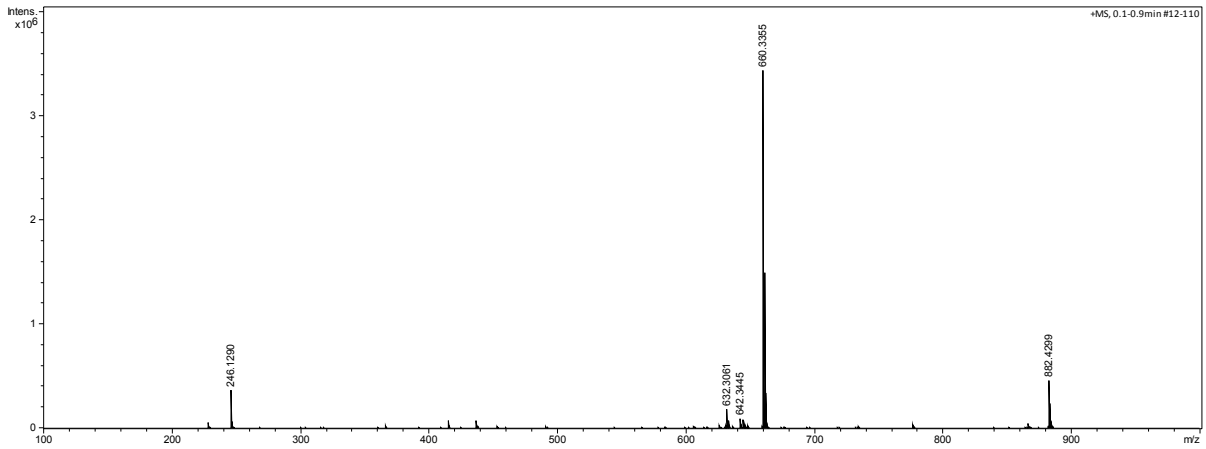

Figure S105. HRMS (ESI–Q-TOF) spectrum of **3e** $[M+H]^+$.

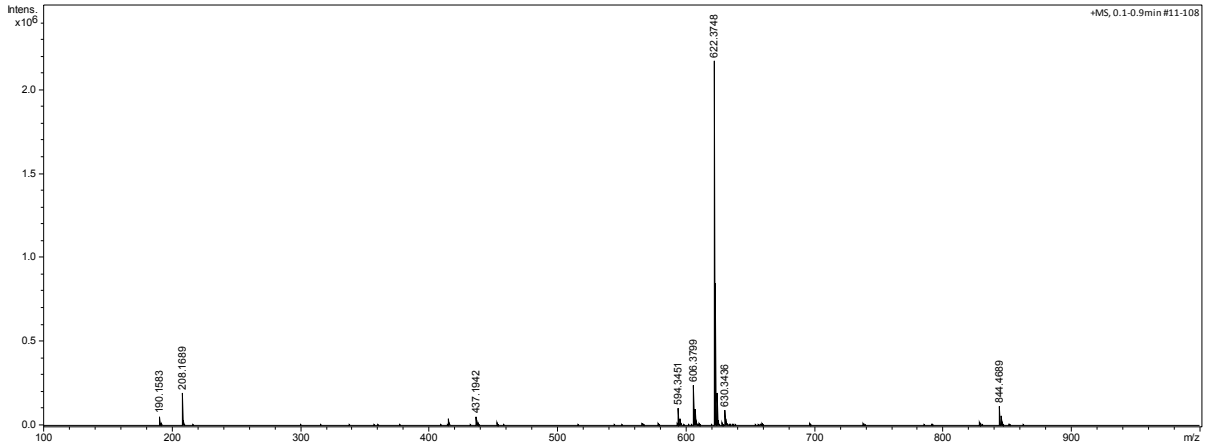

Figure S106. HRMS (ESI–Q-TOF) spectrum of **3f** $[M+H]^+$.

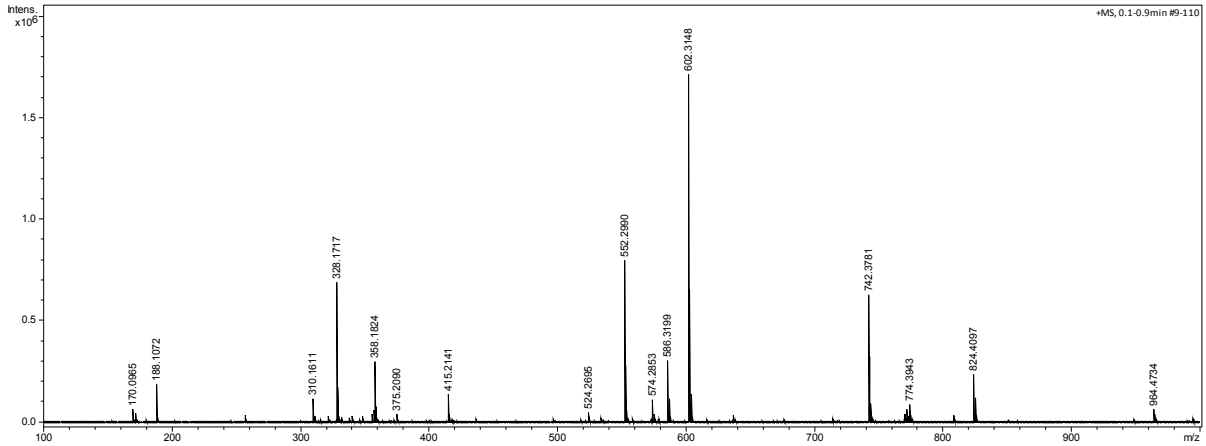

Figure S107. HRMS (ESI–Q-TOF) spectrum of **3g** $[M+H]^+$.

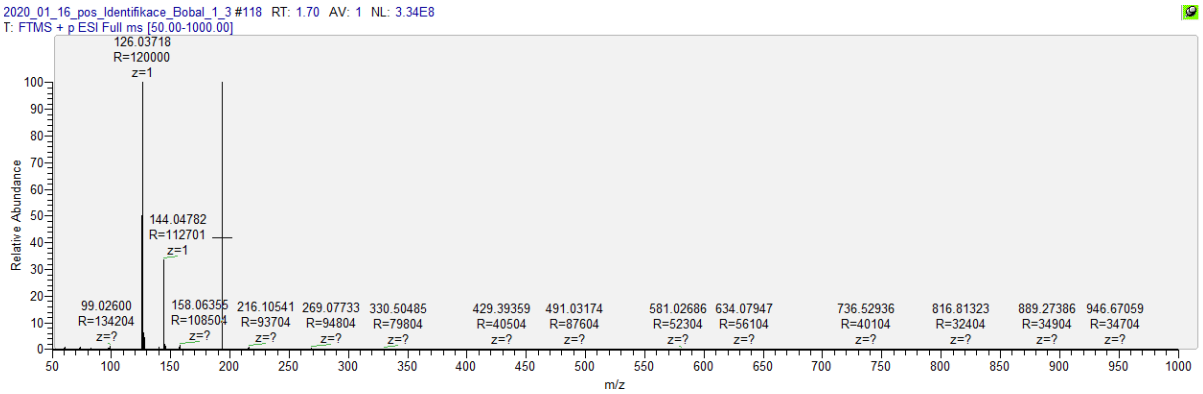

Figure S108. HRMS (ESI-Orbitrap) spectrum of **3h** $[M+H]^+$.

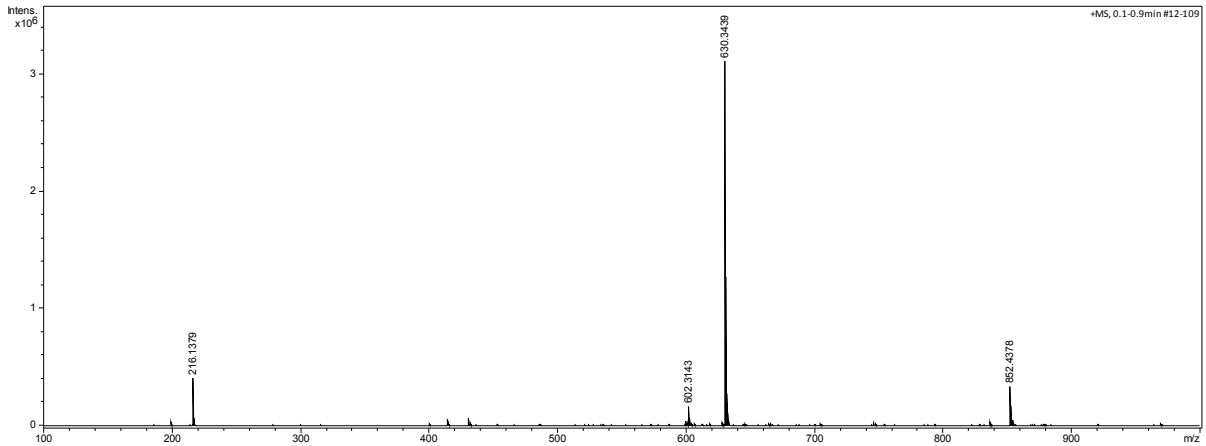

Figure S109. HRMS (ESI–Q-TOF) spectrum of **4a** $[M+H]^+$.

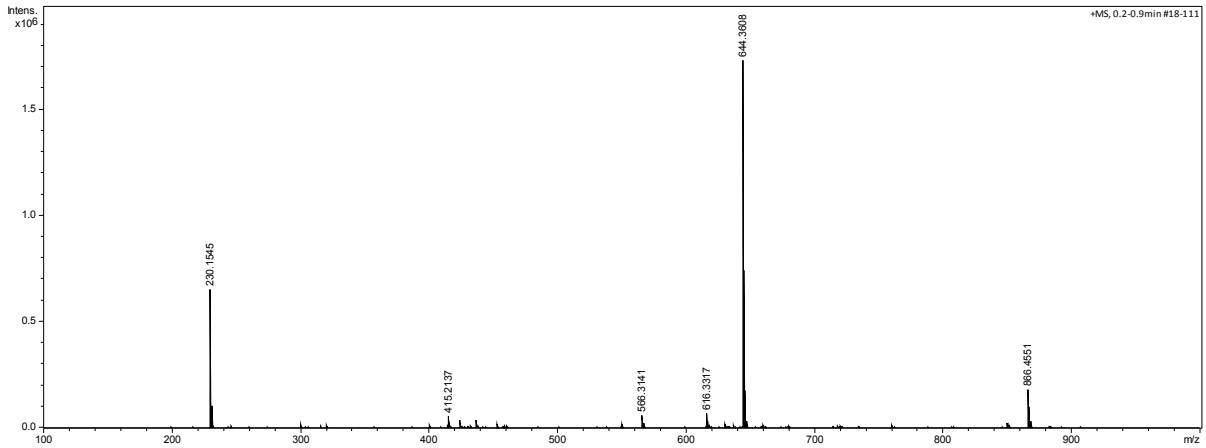

Figure S110. HRMS (ESI–Q-TOF) spectrum of **4aa** $[M+H]^+$.

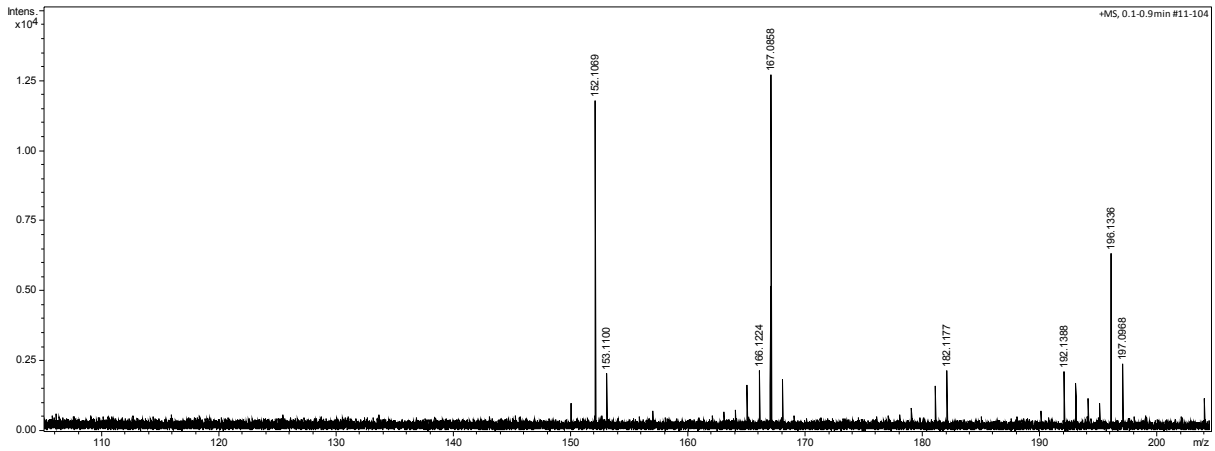

Figure S111. HRMS (ESI–Q-TOF) spectrum of **4ba** $[M+H]^+$.

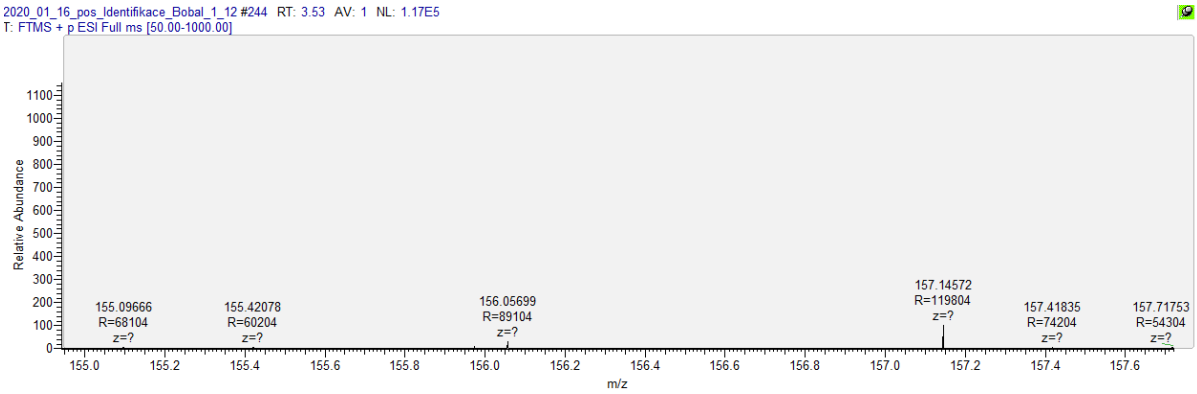

Figure S112. HRMS (ESI-Orbitrap) spectrum of **4bb** $[M+H]^+$.

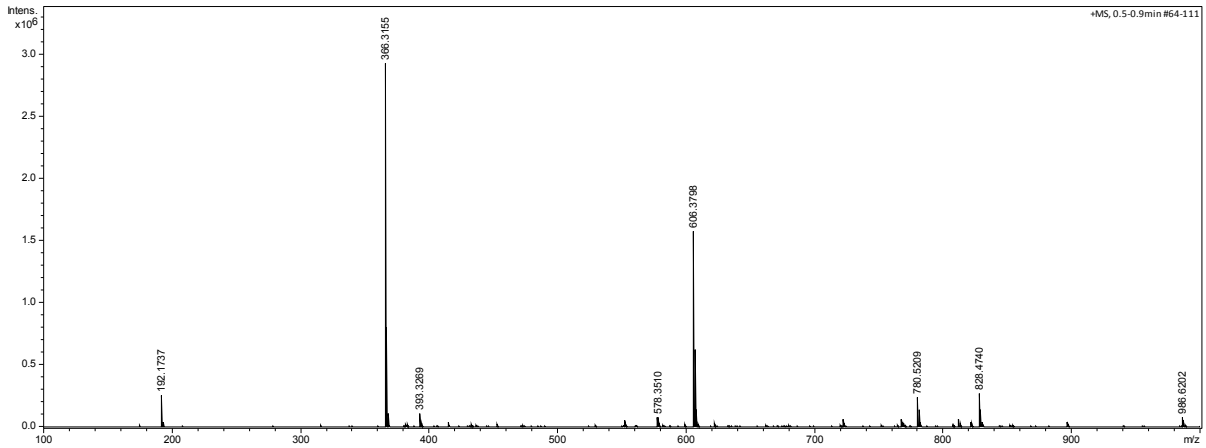

Figure S113. HRMS (ESI–Q-TOF) spectrum of **4f** $[M+H]^+$.

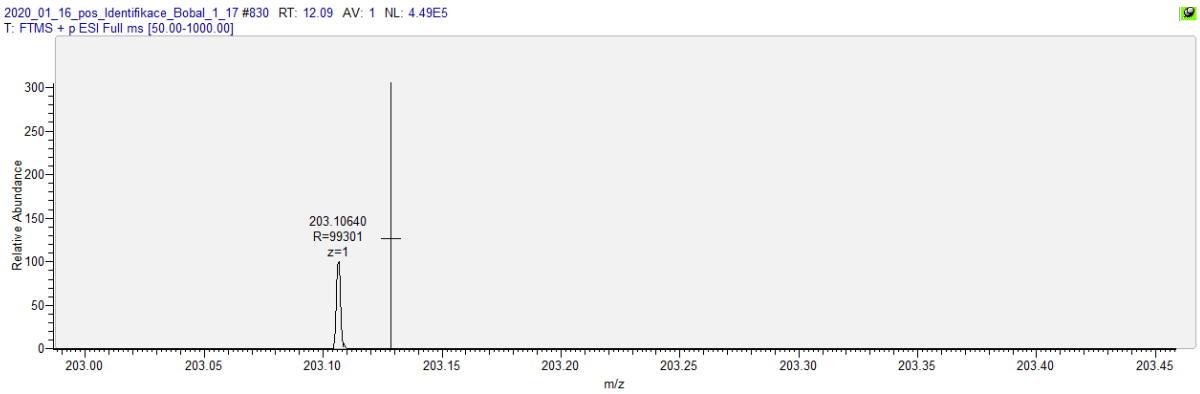

Figure S114. HRMS (ESI-Orbitrap) spectrum of **5a** $[M+H]^+$.

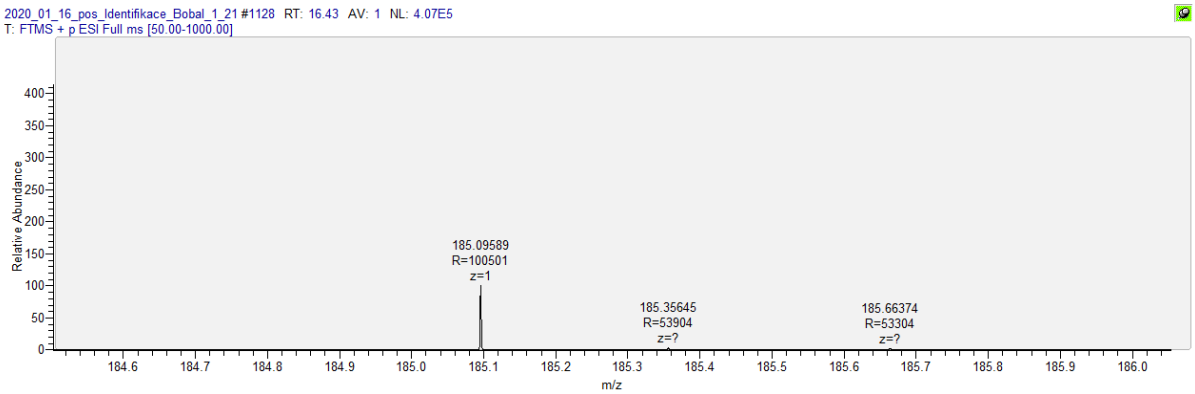

Figure S115. HRMS (ESI-Orbitrap) spectrum of **5c** $[M+H]^+$.

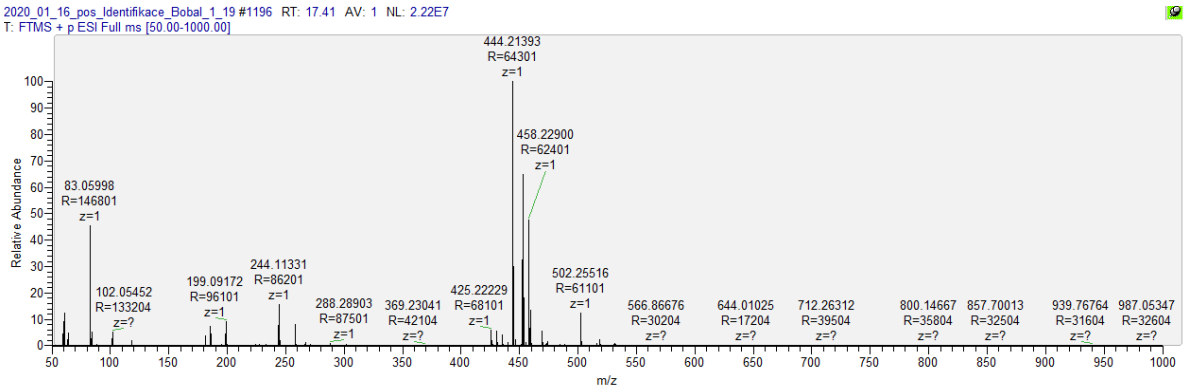

Figure S116. HRMS (ESI-Orbitrap) spectrum of **5d** $[M-H_2O+H]^+$.

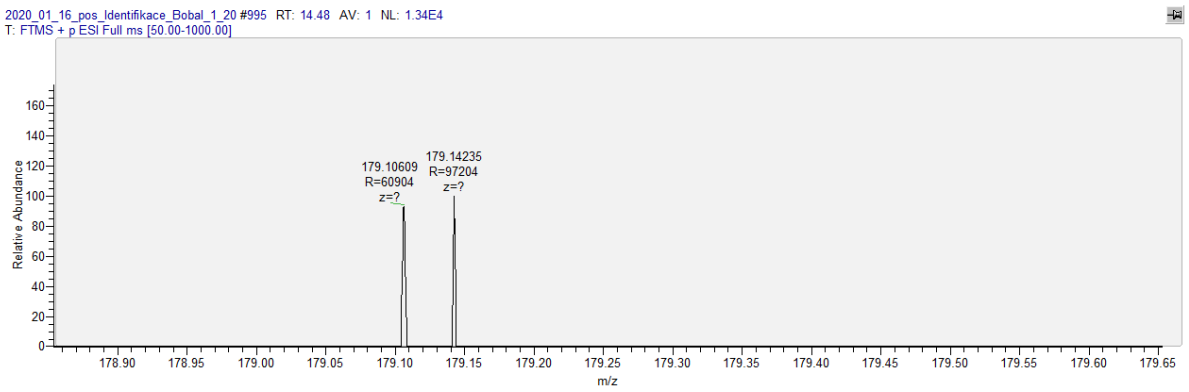

Figure S117. HRMS (ESI-Orbitrap) spectrum of **5e** $[M+H]^+$.

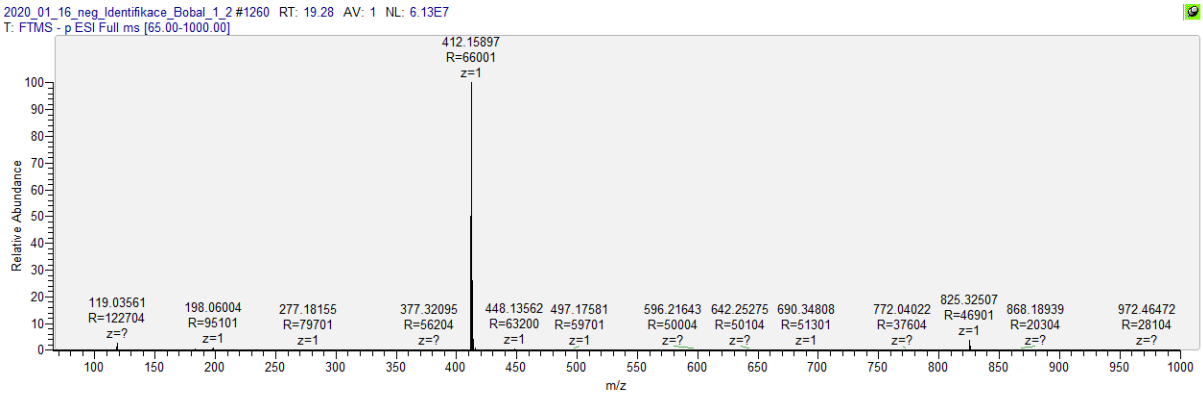

Figure S118. HRMS (ESI-Orbitrap) spectrum of **8a** $[M–H]^-$.

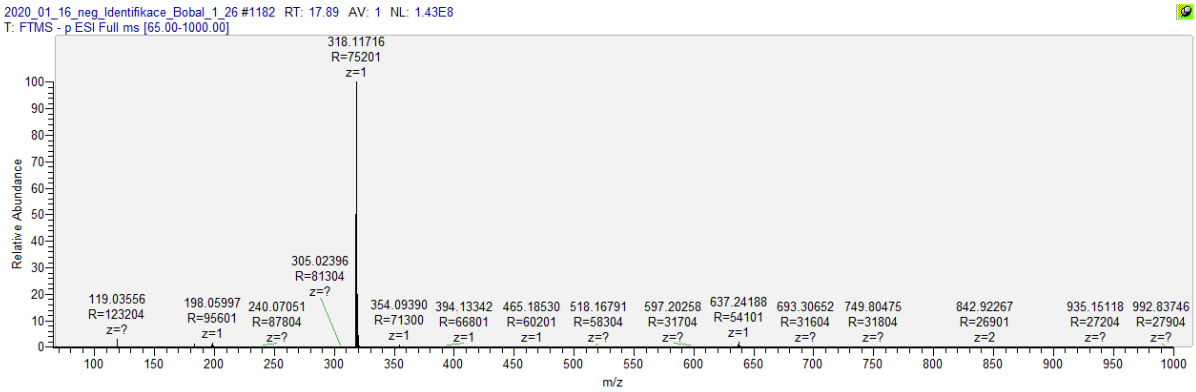

Figure S119. HRMS (ESI-Orbitrap) spectrum of **8b** $[M−H]^-$.

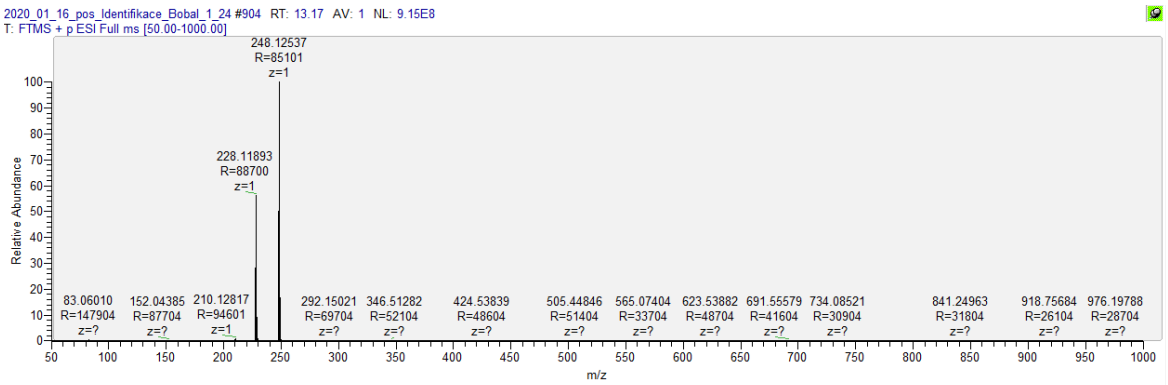

Figure S120. HRMS (ESI-Orbitrap) spectrum of **9** $[M+H]^+$.

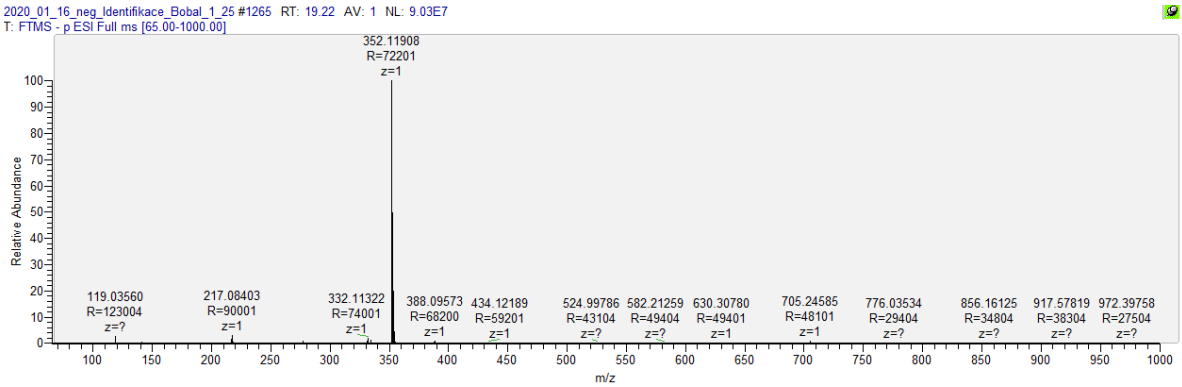

Figure S121. HRMS (ESI-Orbitrap) spectrum of **10** $[M-H]^-$.

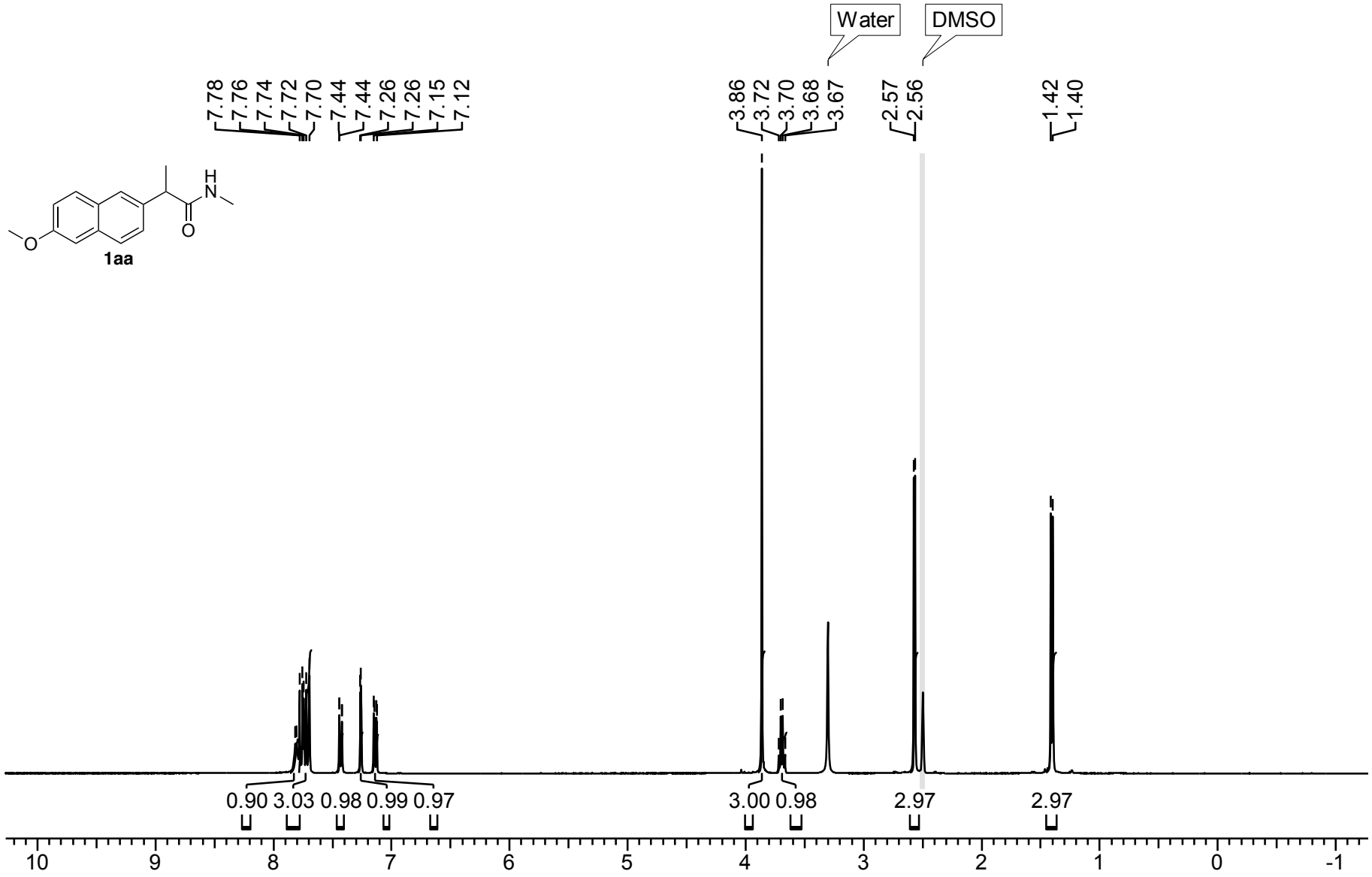

Figure S122. ^{1}H NMR (400 MHz, DMSO-d_6) spectrum of **1aa**.

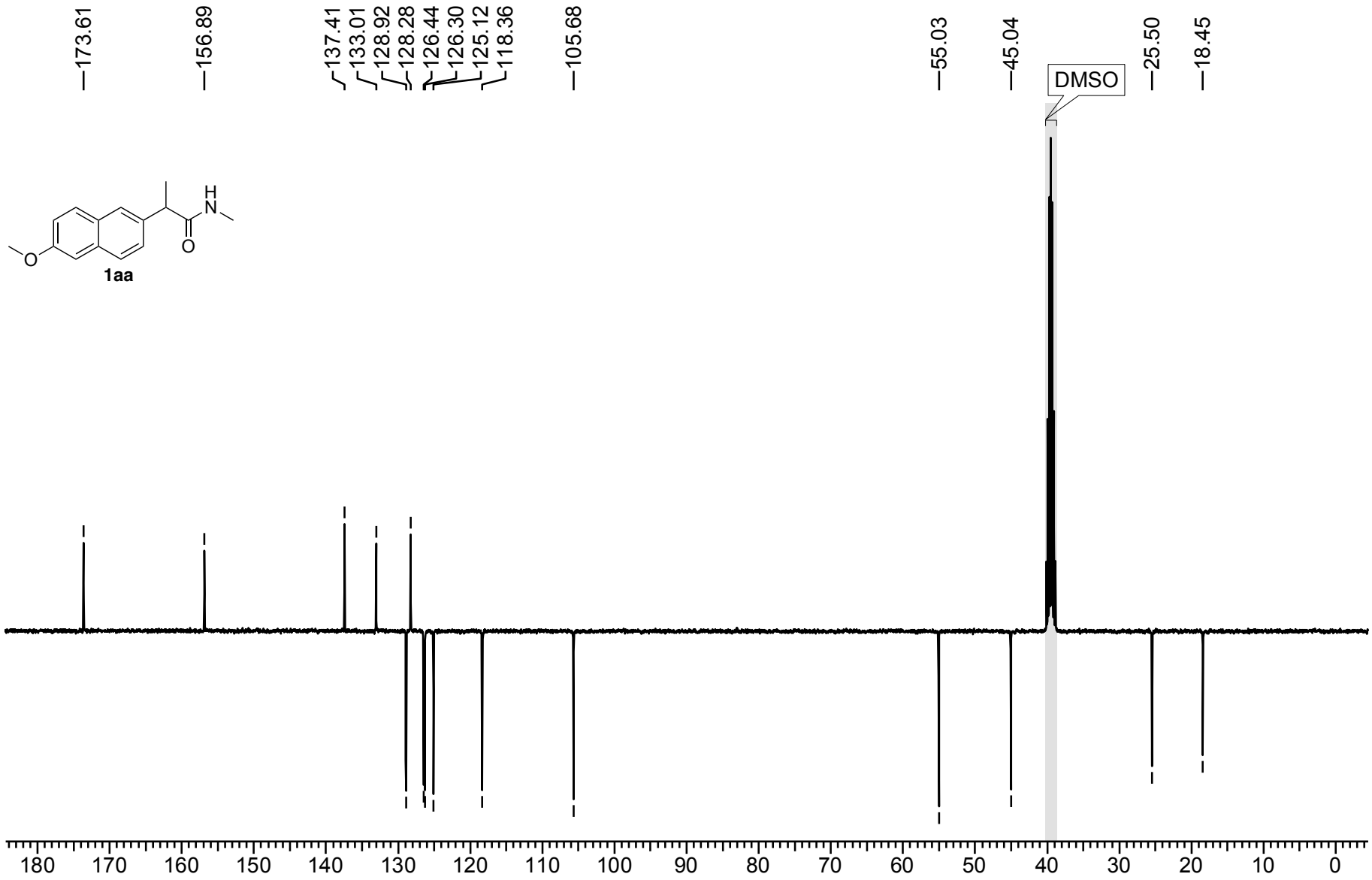

Figure S123. ^{13}C NMR APT (100 MHz, DMSO-d_6) spectrum of **1aa**.

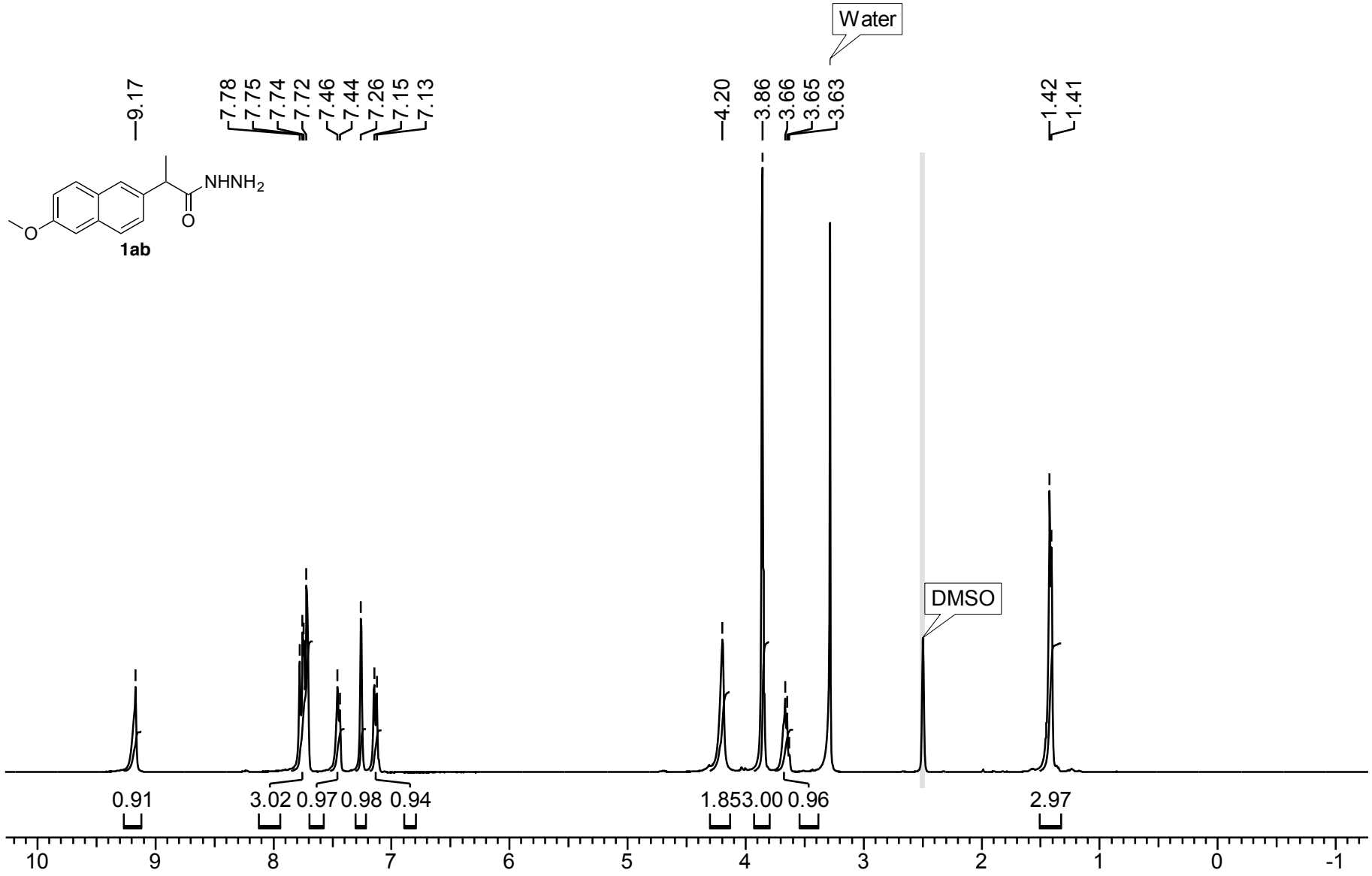

Figure S124. ^{1}H NMR (400 MHz, DMSO-d_6) spectrum of **1ab**.

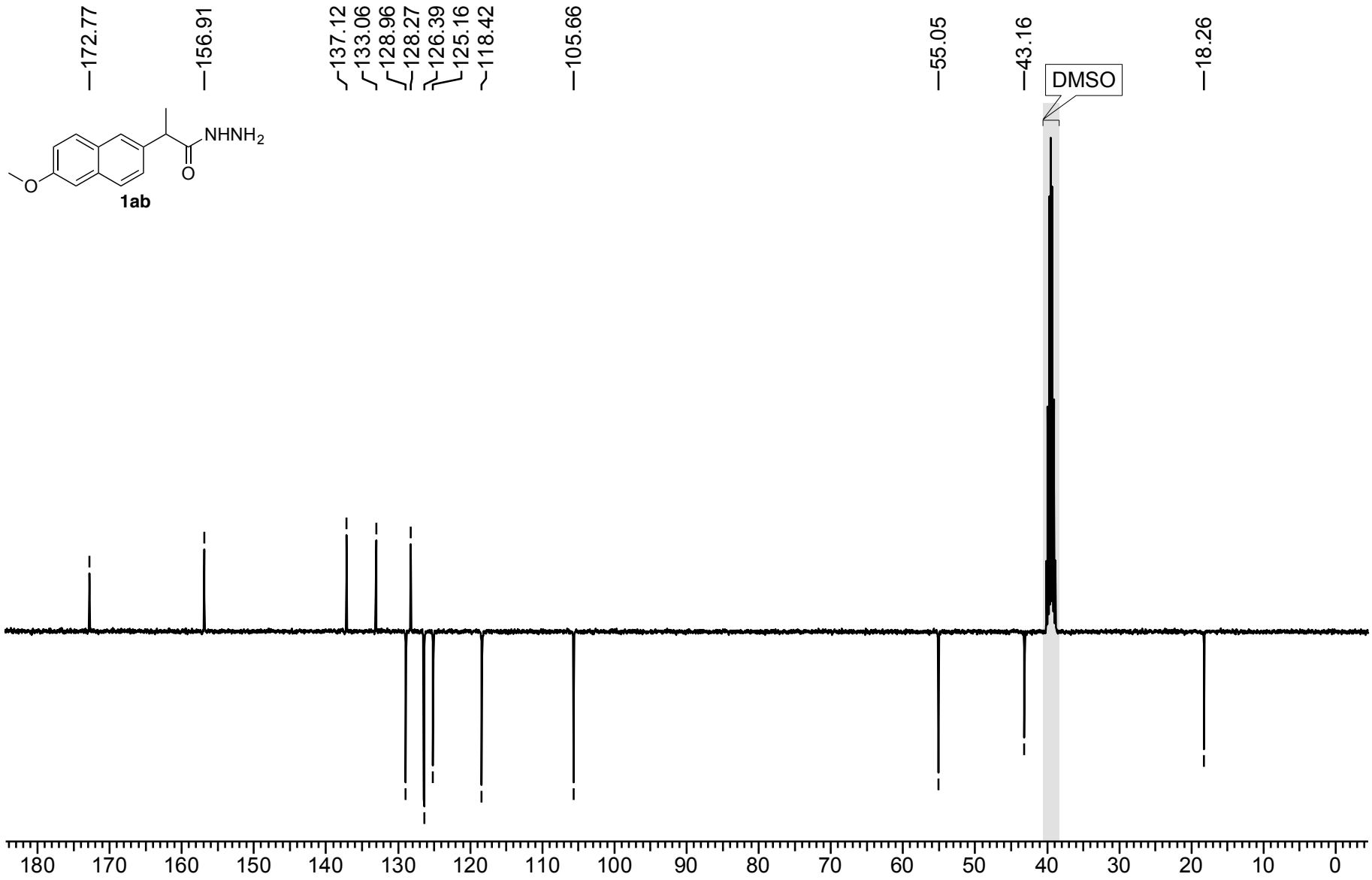

Figure S125. ^{13}C NMR APT (100 MHz, DMSO-d_6) spectrum of **1ab**.

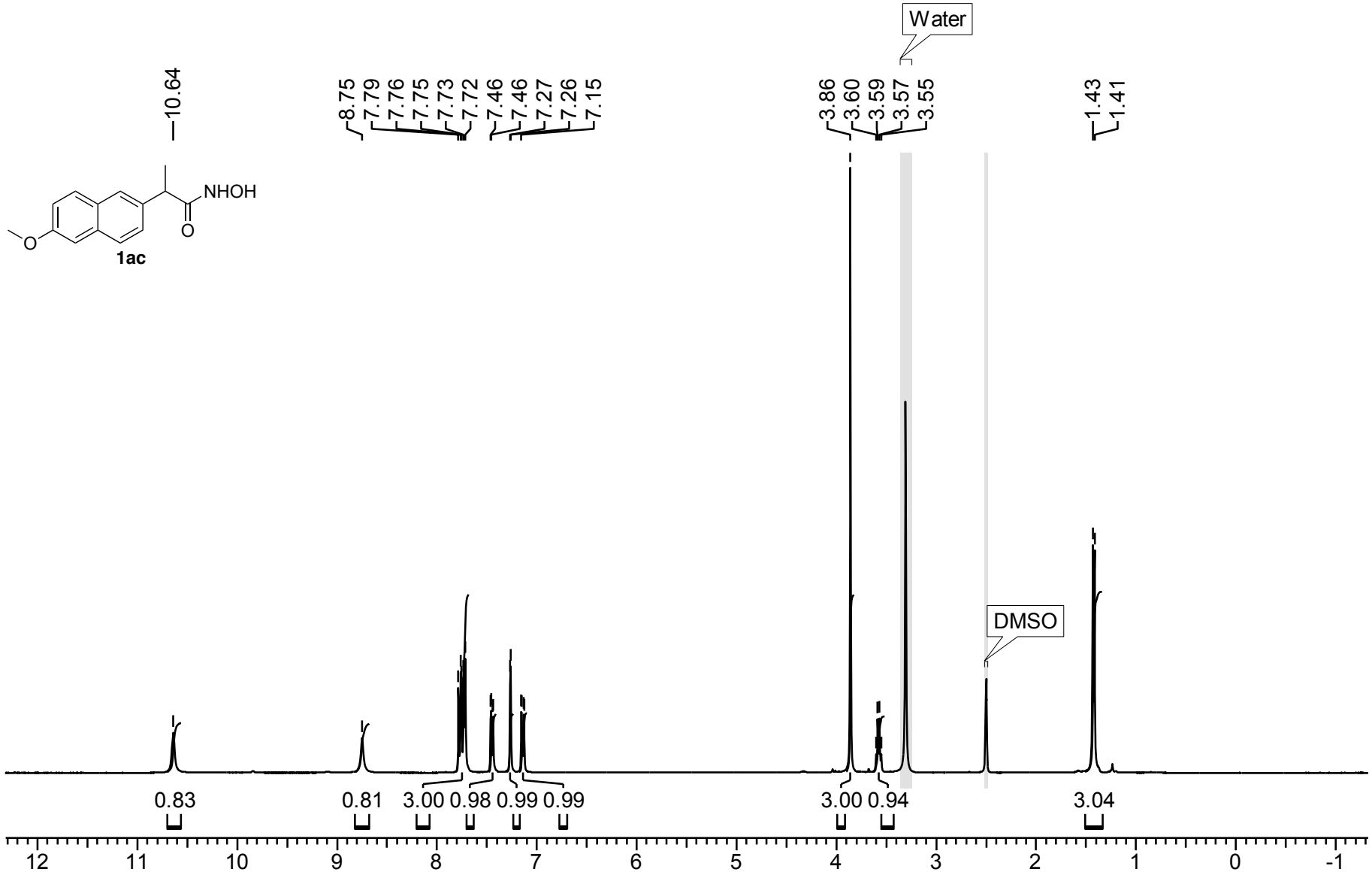

Figure S126. ^{1}H NMR (400 MHz, DMSO-d_6) spectrum of **1ac**.

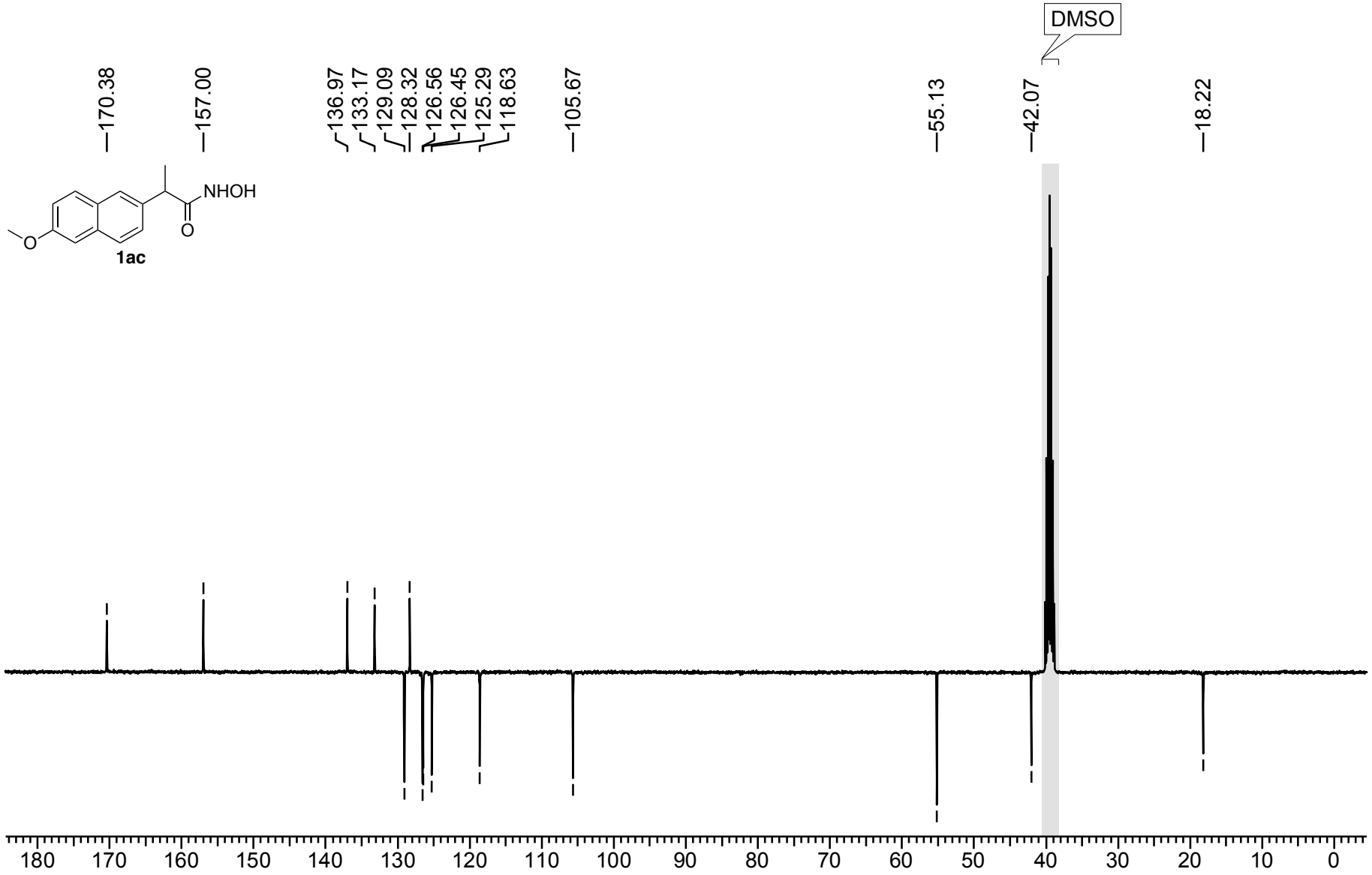

Figure S127. ^{13}C NMR APT (100 MHz, DMSO-d_6) spectrum of **1ac**.

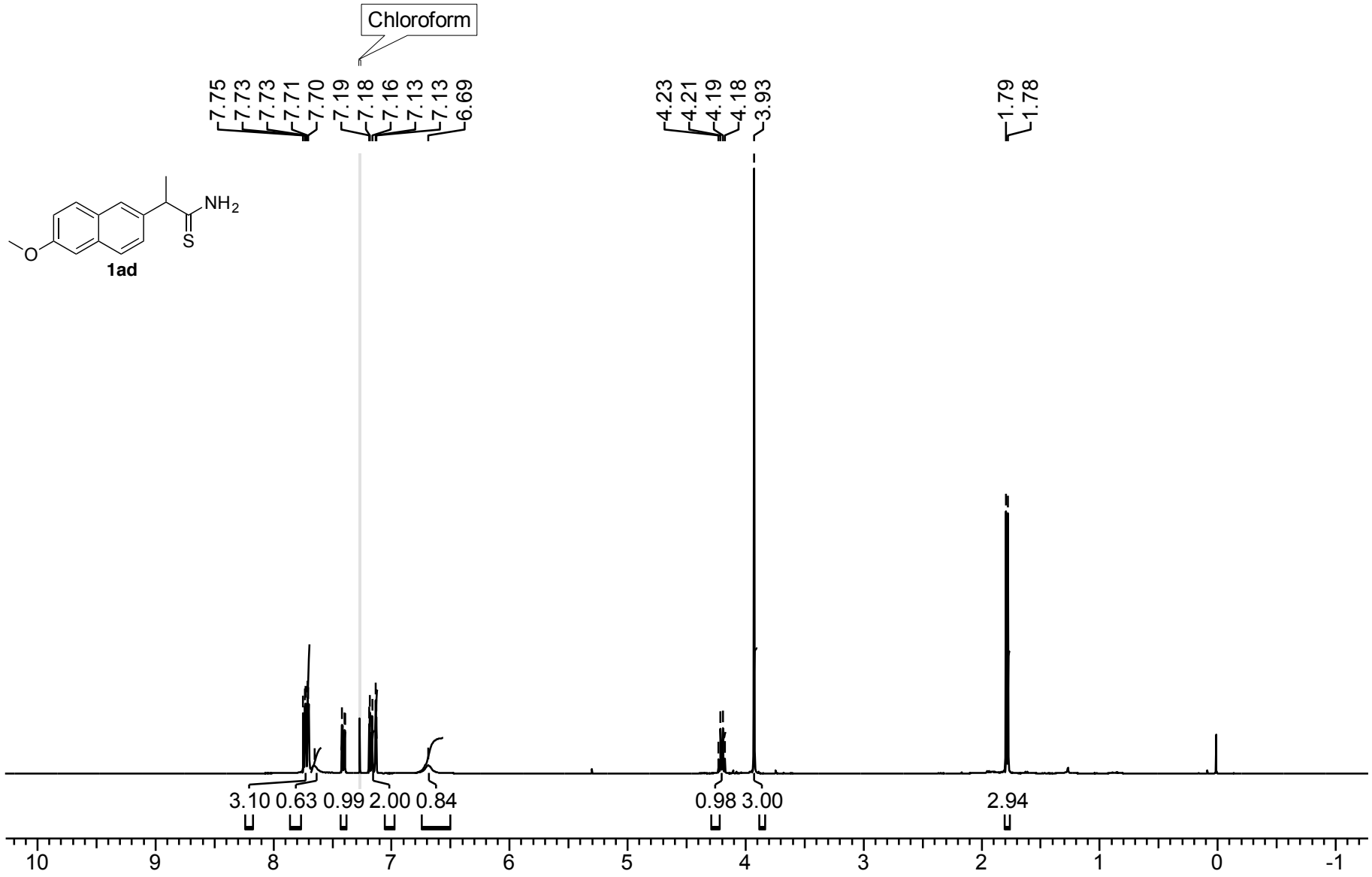

Figure S128. ^{1}H NMR (400 MHz, $CDCl_3$) spectrum of **1ad**.

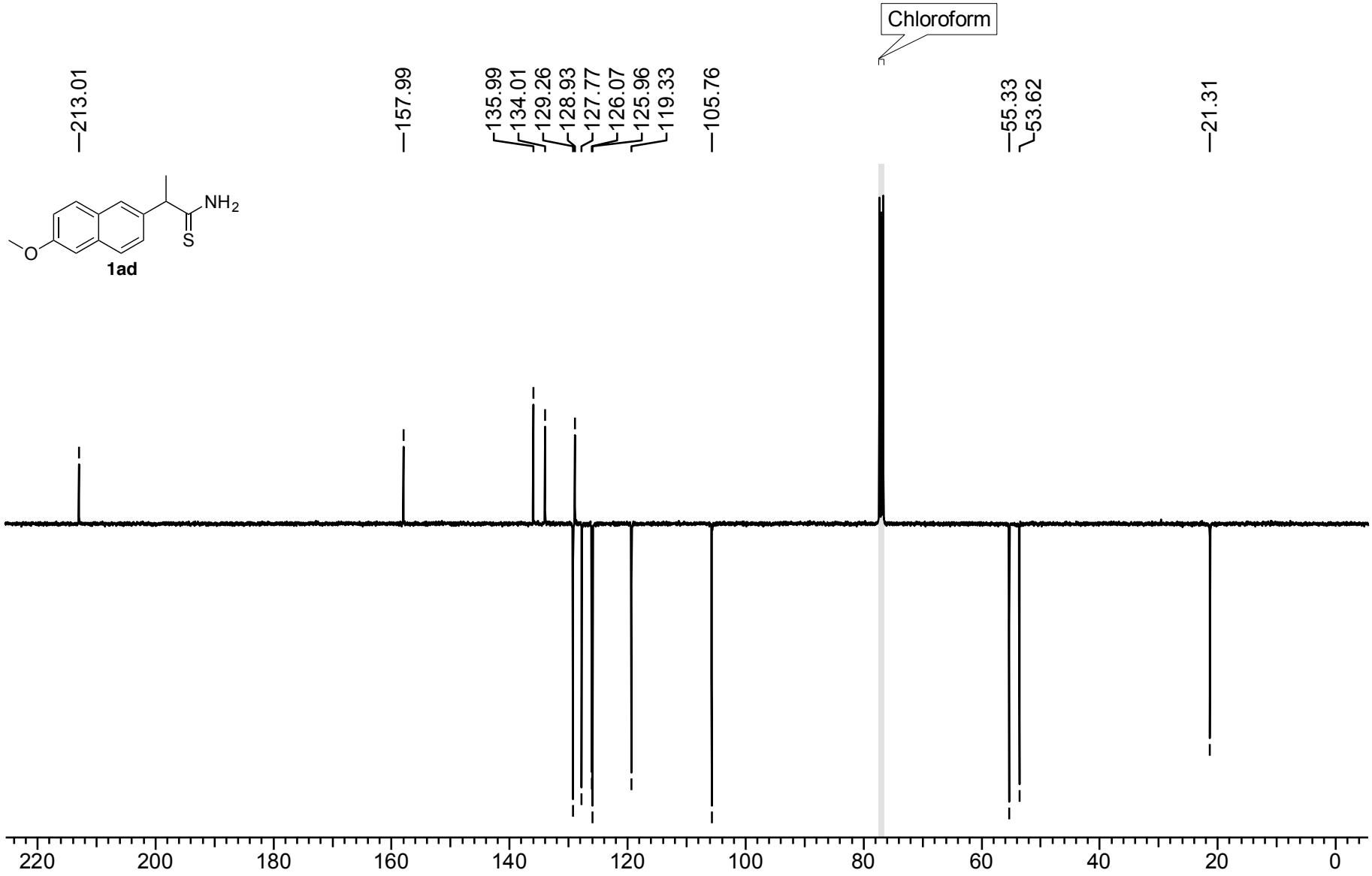

Figure S129. ^{13}C NMR APT (100 MHz, $CDCl_3$) spectrum of **1ad**.

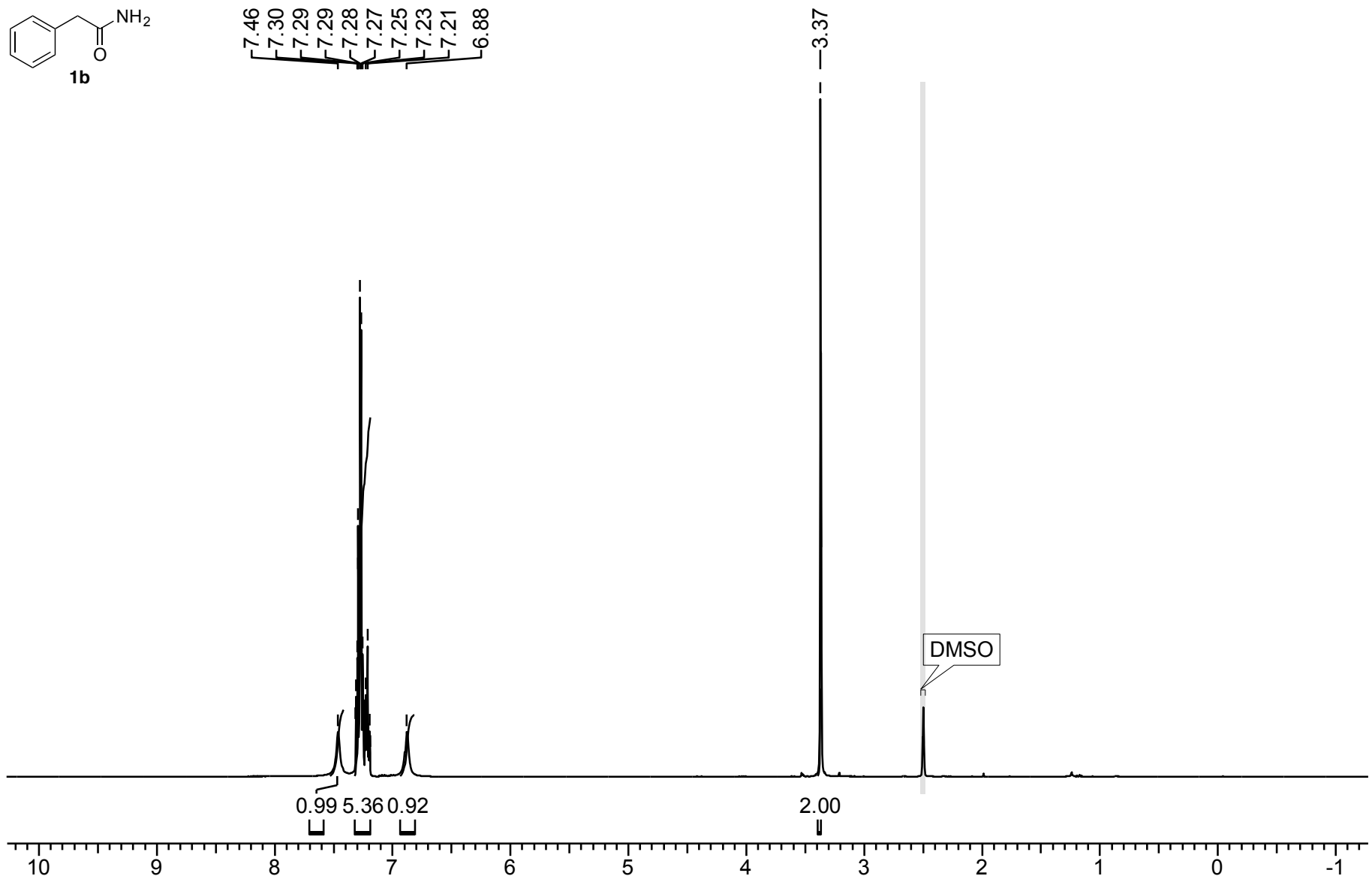

Figure S130. ^{1}H NMR (400 MHz, DMSO-d_6) spectrum of **1b**.

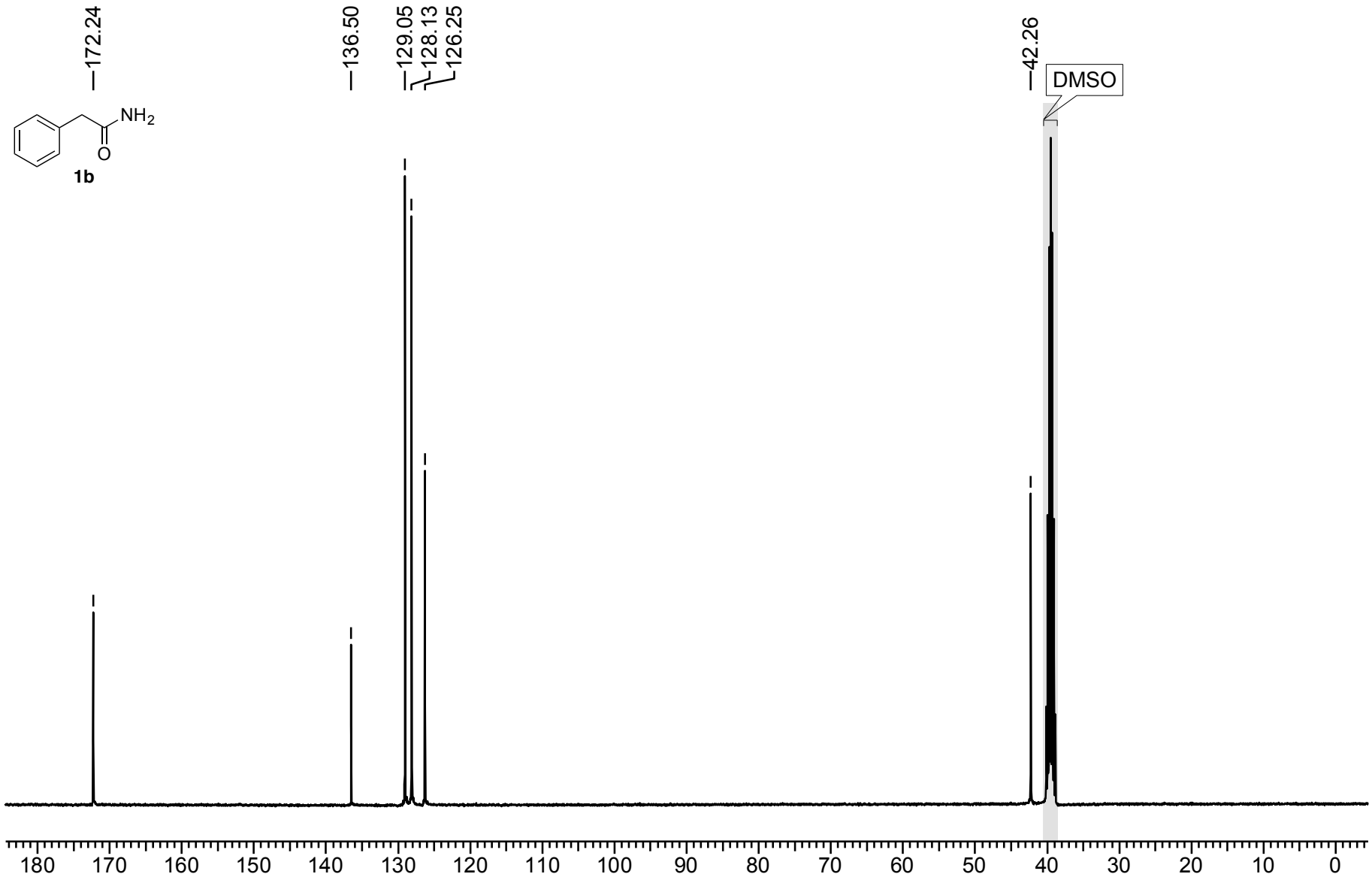

Figure S131. ^{13}C NMR (100 MHz, DMSO-d_6) spectrum of **1b**.

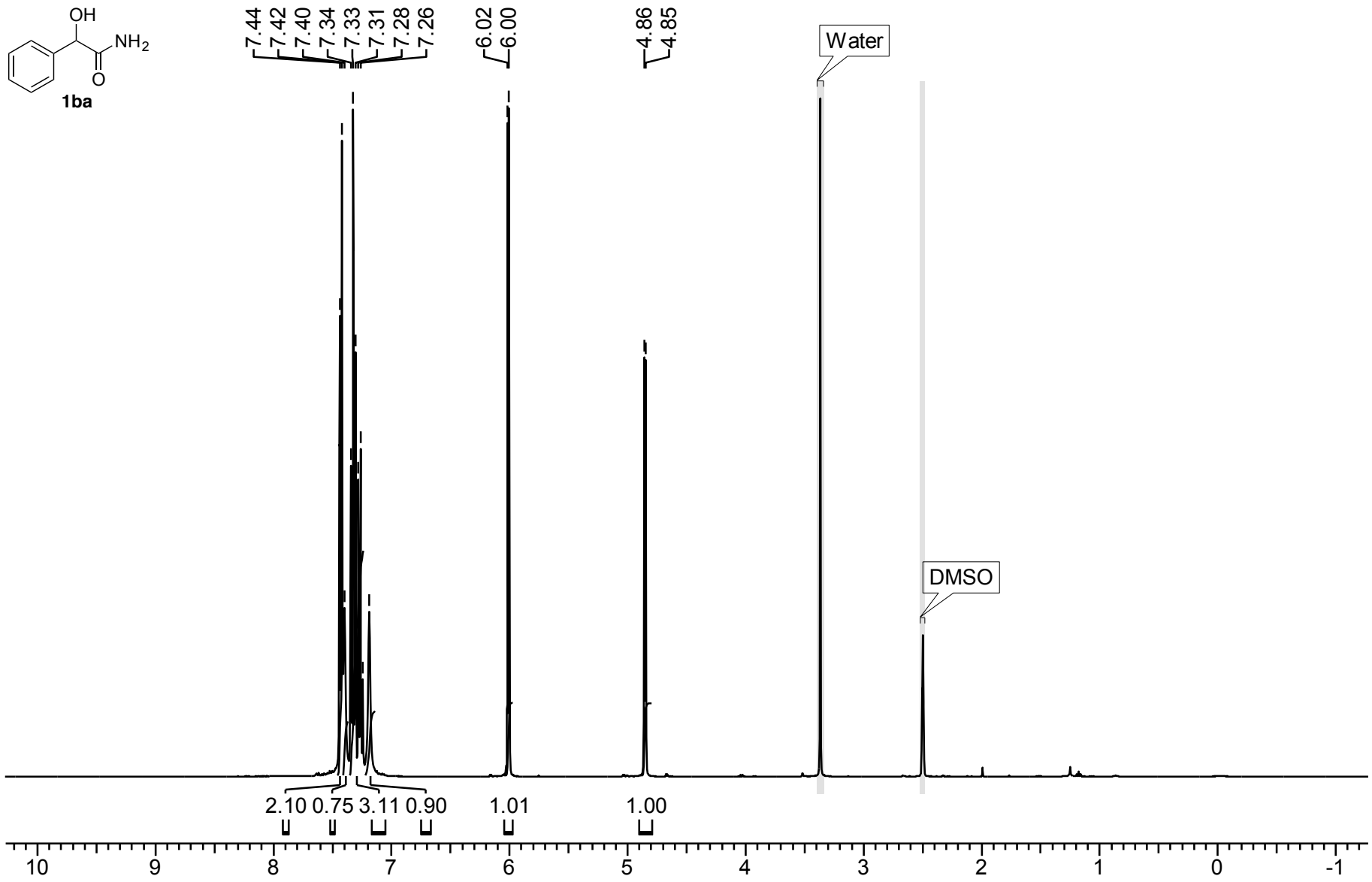

Figure S132. ^{1}H NMR (400 MHz, DMSO-d_6) spectrum of **1ba**.

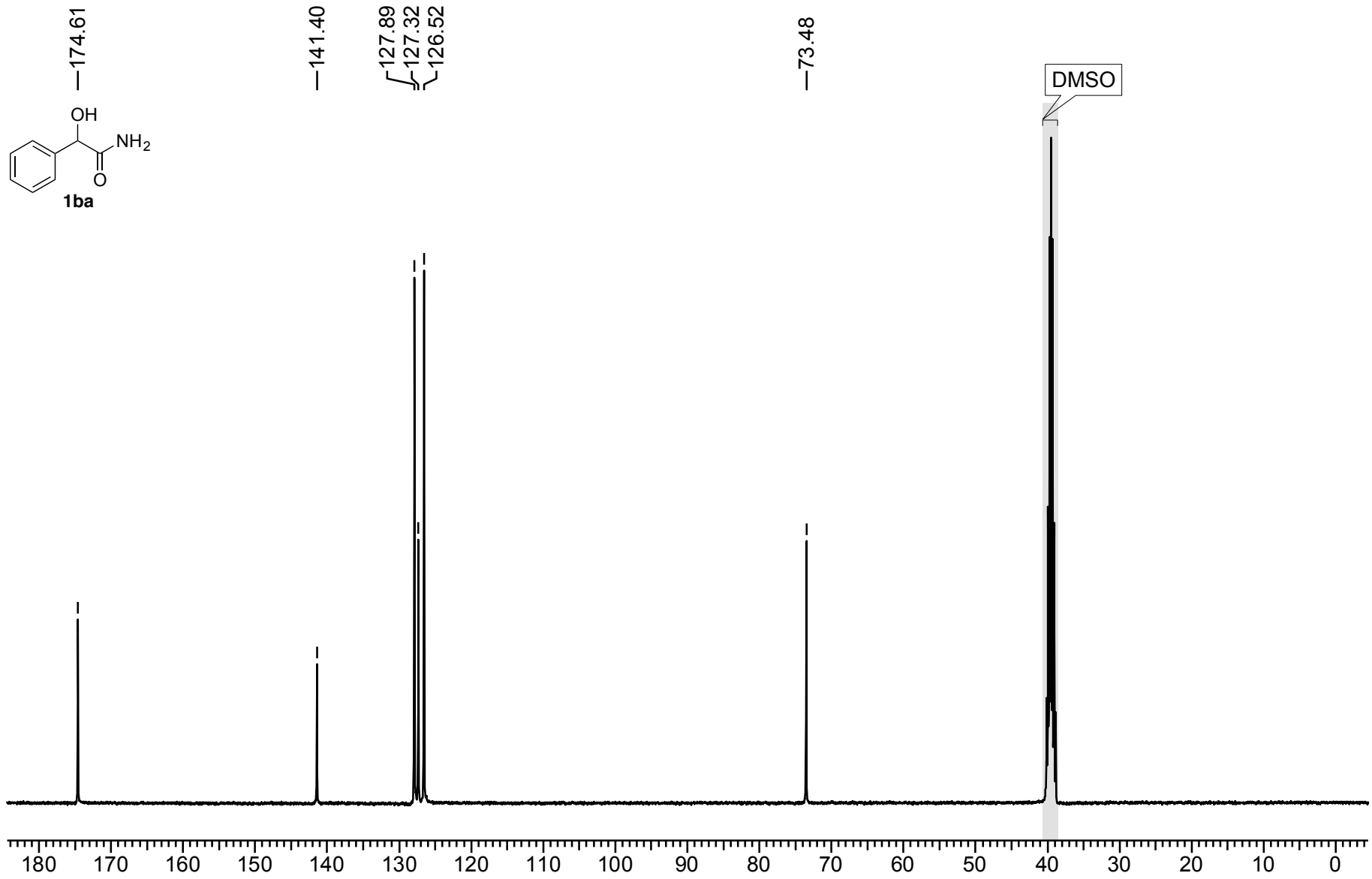

Figure S133. ^{13}C NMR (100 MHz, DMSO-d_6) spectrum of **1ba**.

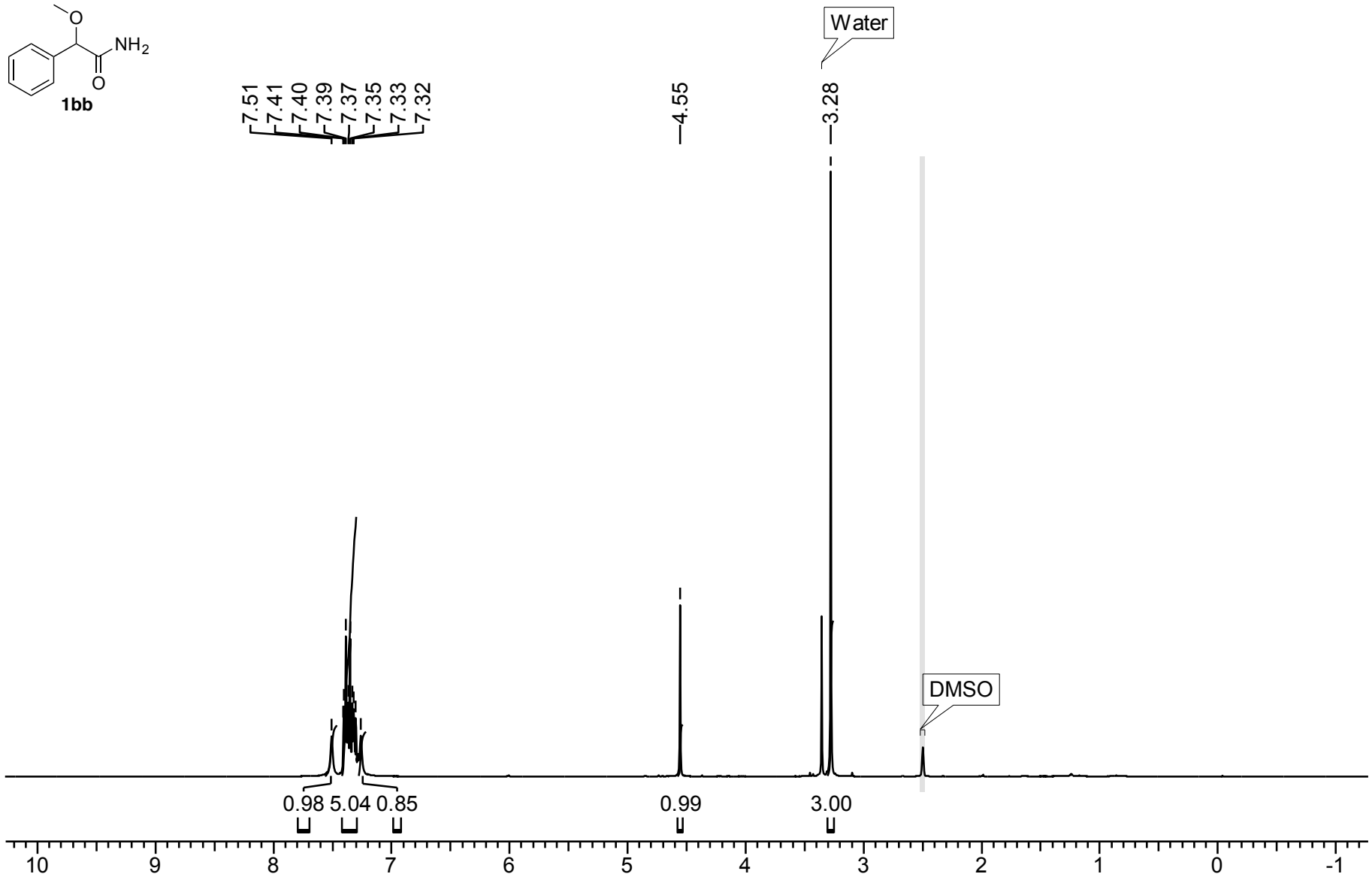

Figure S134. ^{1}H NMR (400 MHz, DMSO-d_6) spectrum of **1bb**.

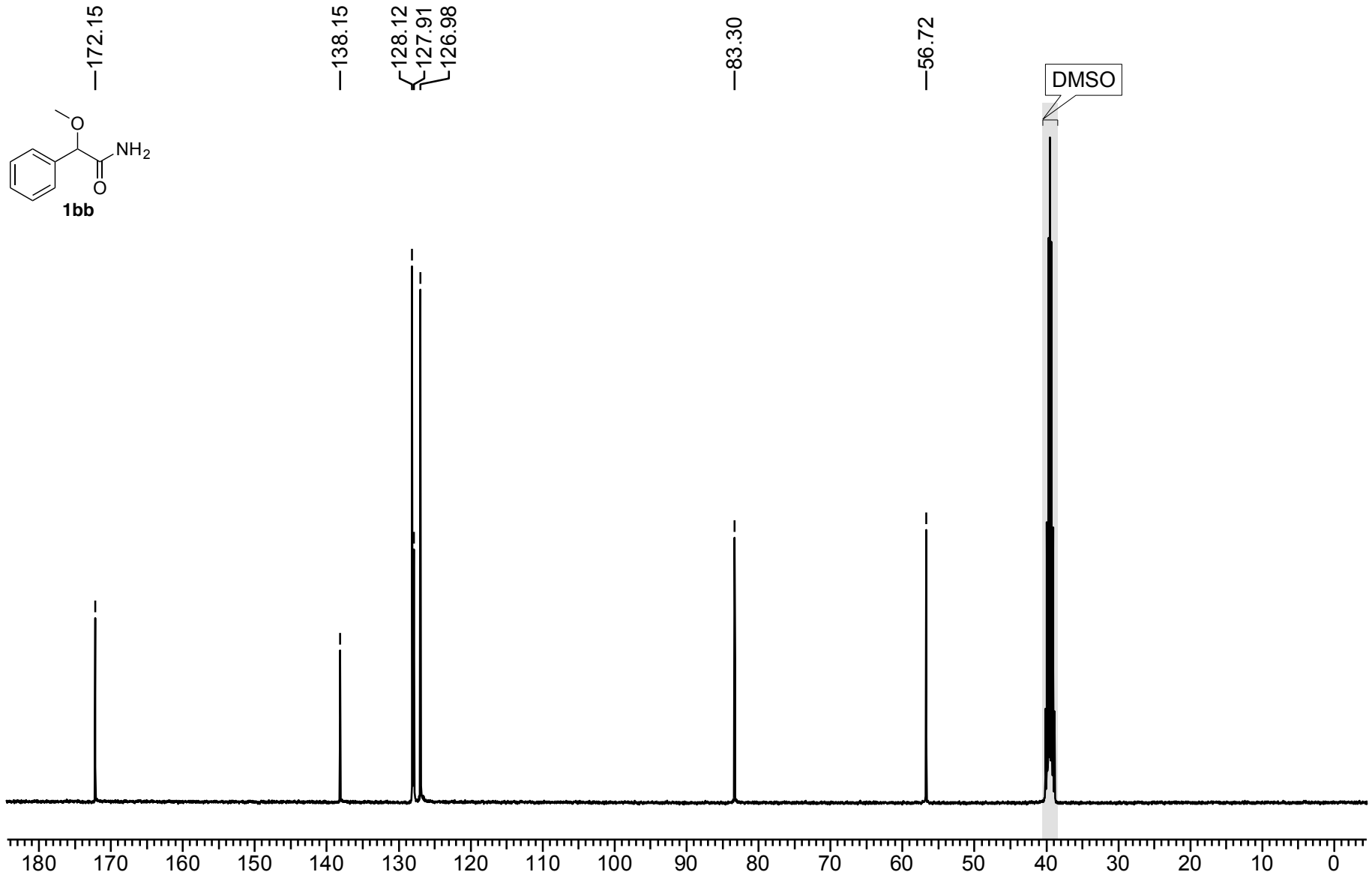

Figure S135. ^{13}C NMR (100 MHz, DMSO-d_6) spectrum of **1bb**.

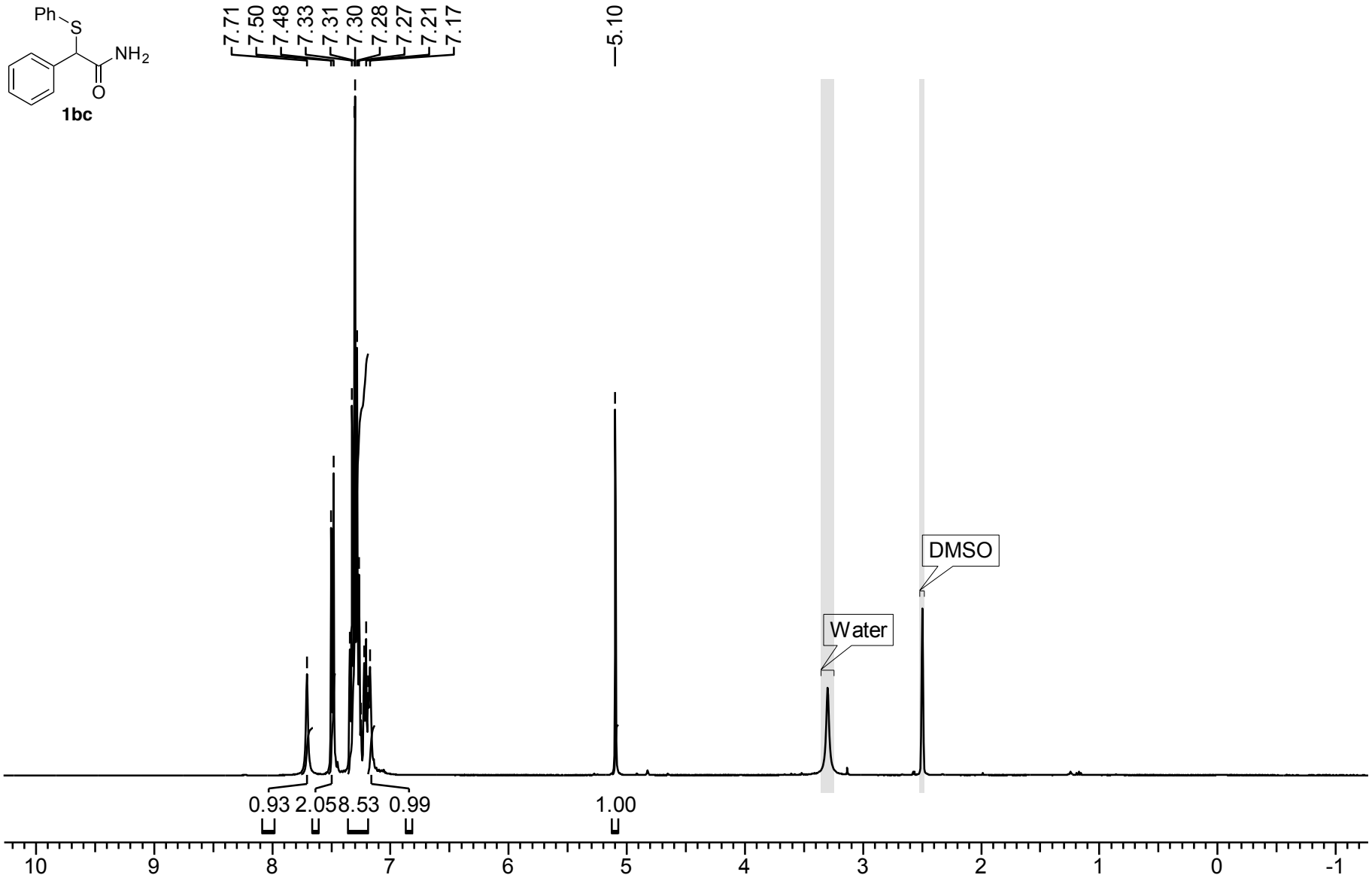

Figure S136. ^{1}H NMR (400 MHz, DMSO-d_6) spectrum of **1bc**.

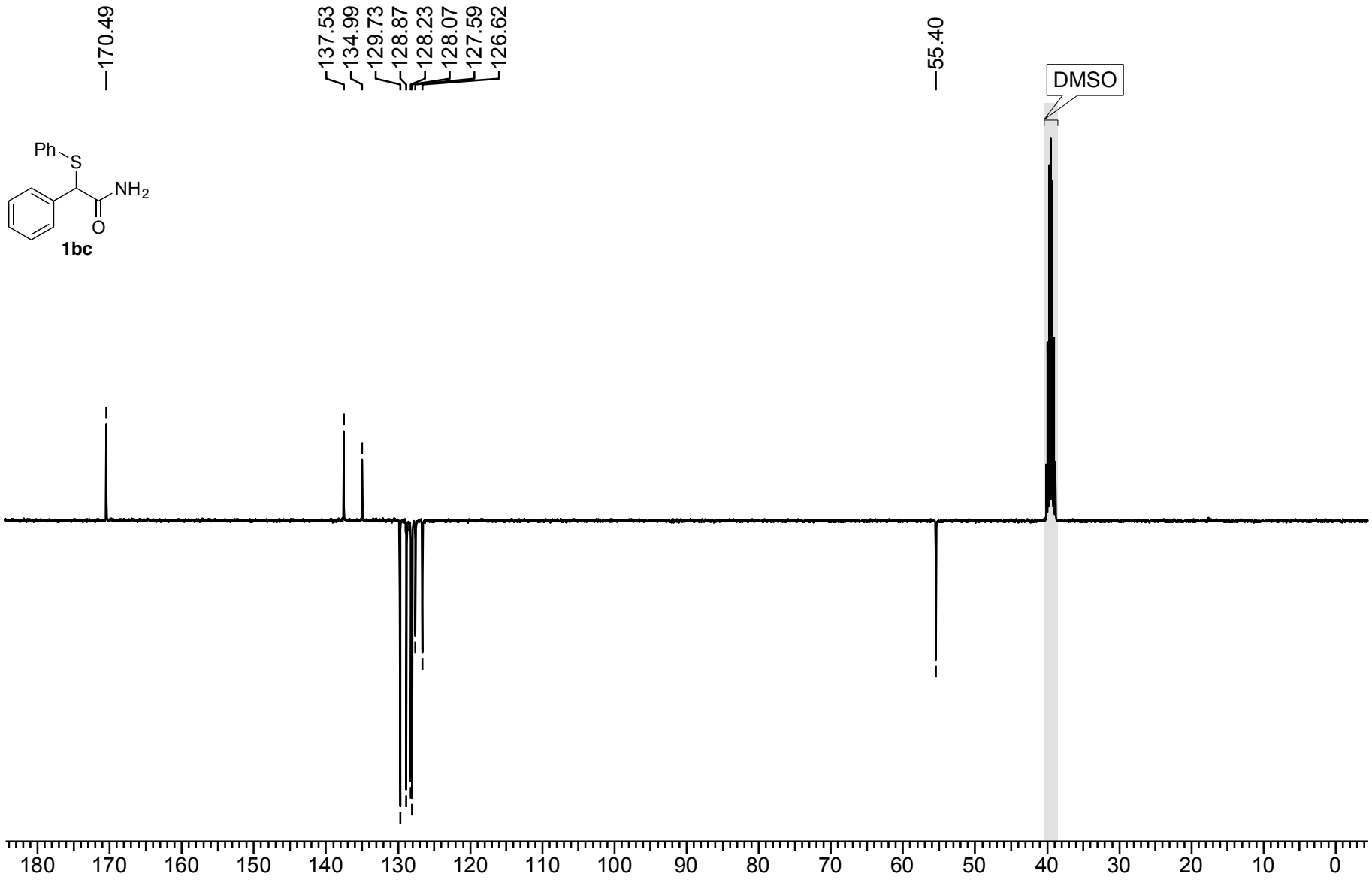

Figure S137. ^{13}C NMR APT (100 MHz, DMSO-d_6) spectrum of **1bc**.

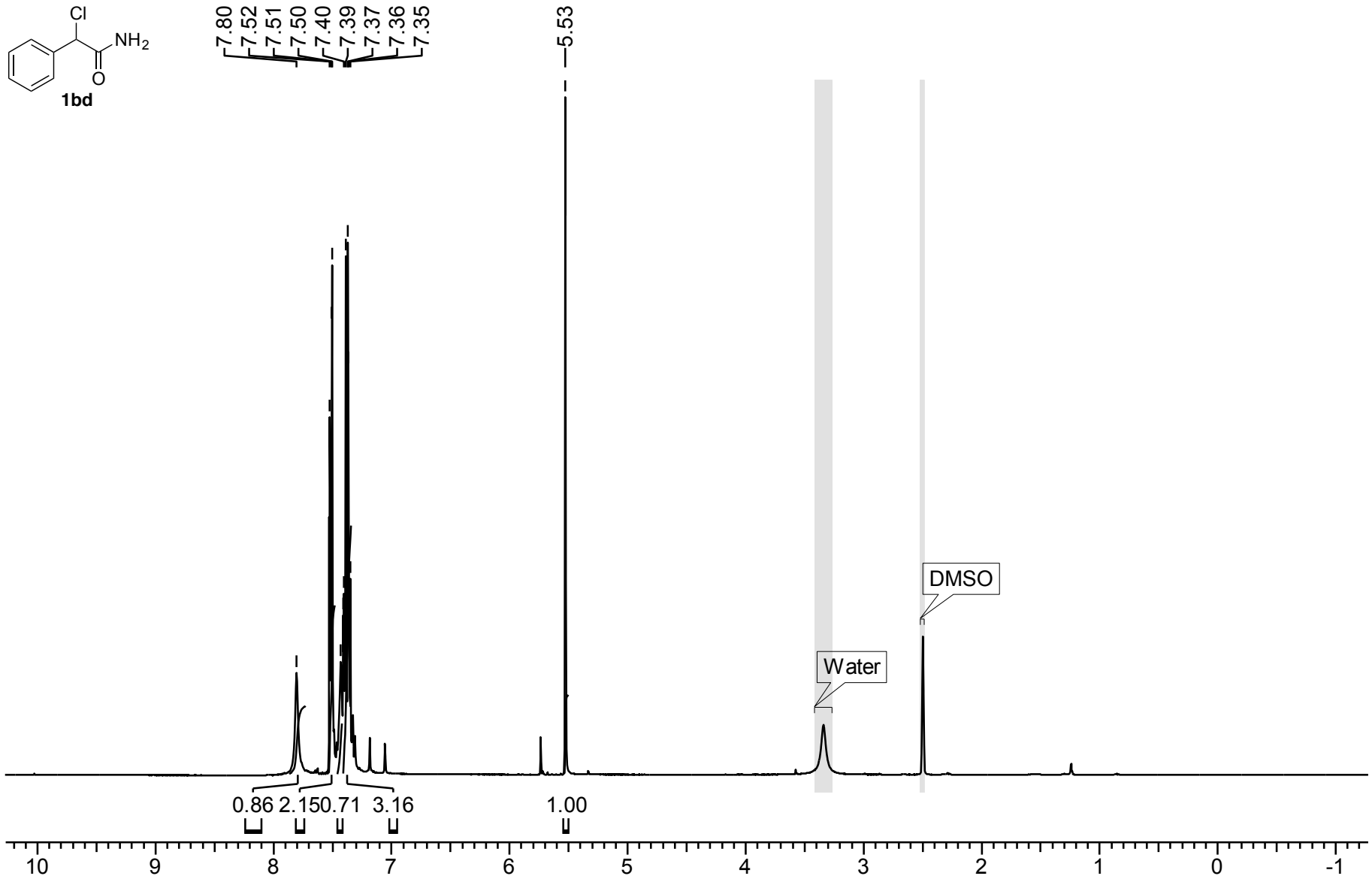

Figure S138. ^{1}H NMR (400 MHz, DMSO-d_6) spectrum of **1bd**.

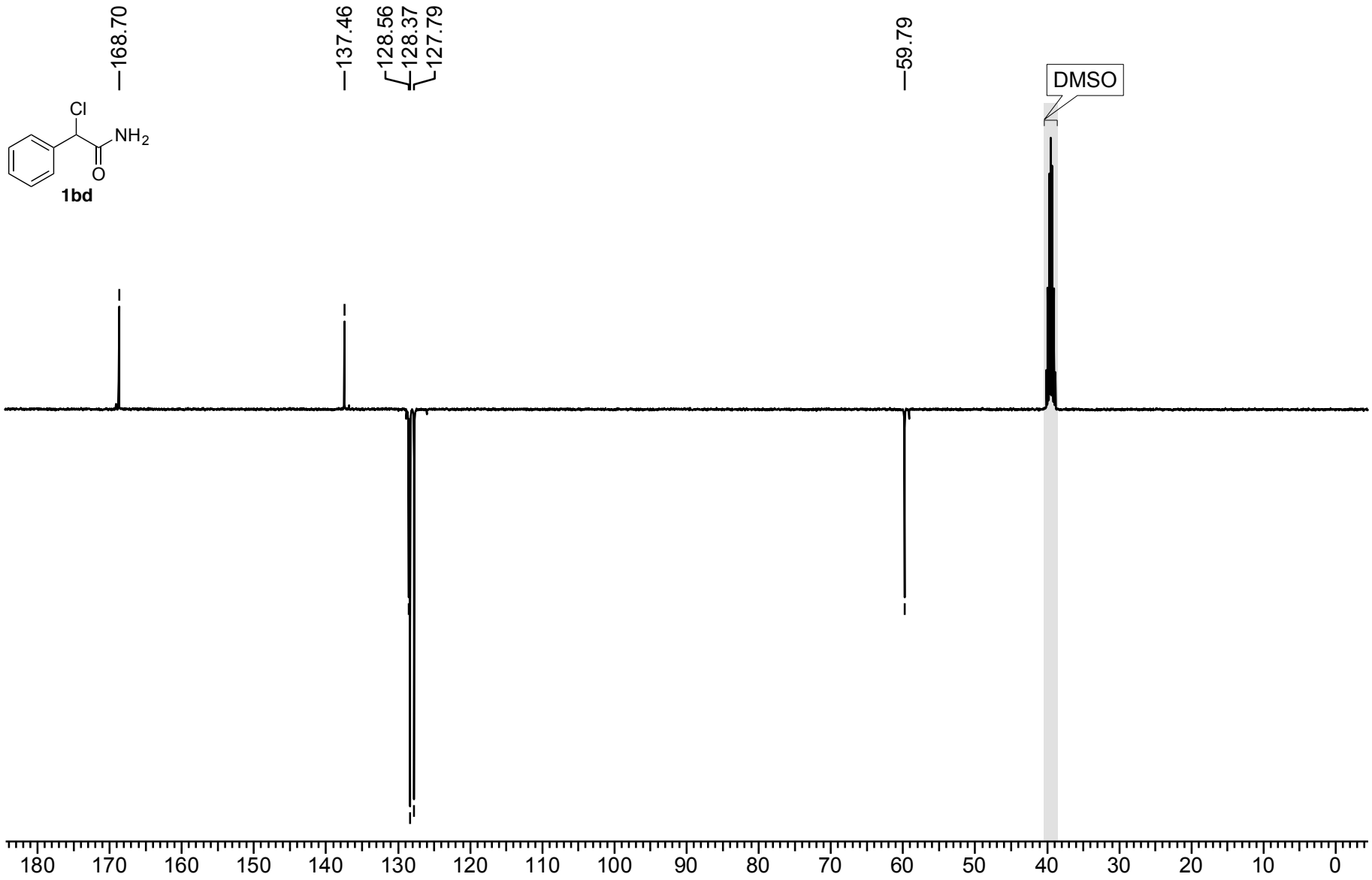

Figure S139. ^{13}C NMR APT (100 MHz, DMSO-d_6) spectrum of **1bd**.

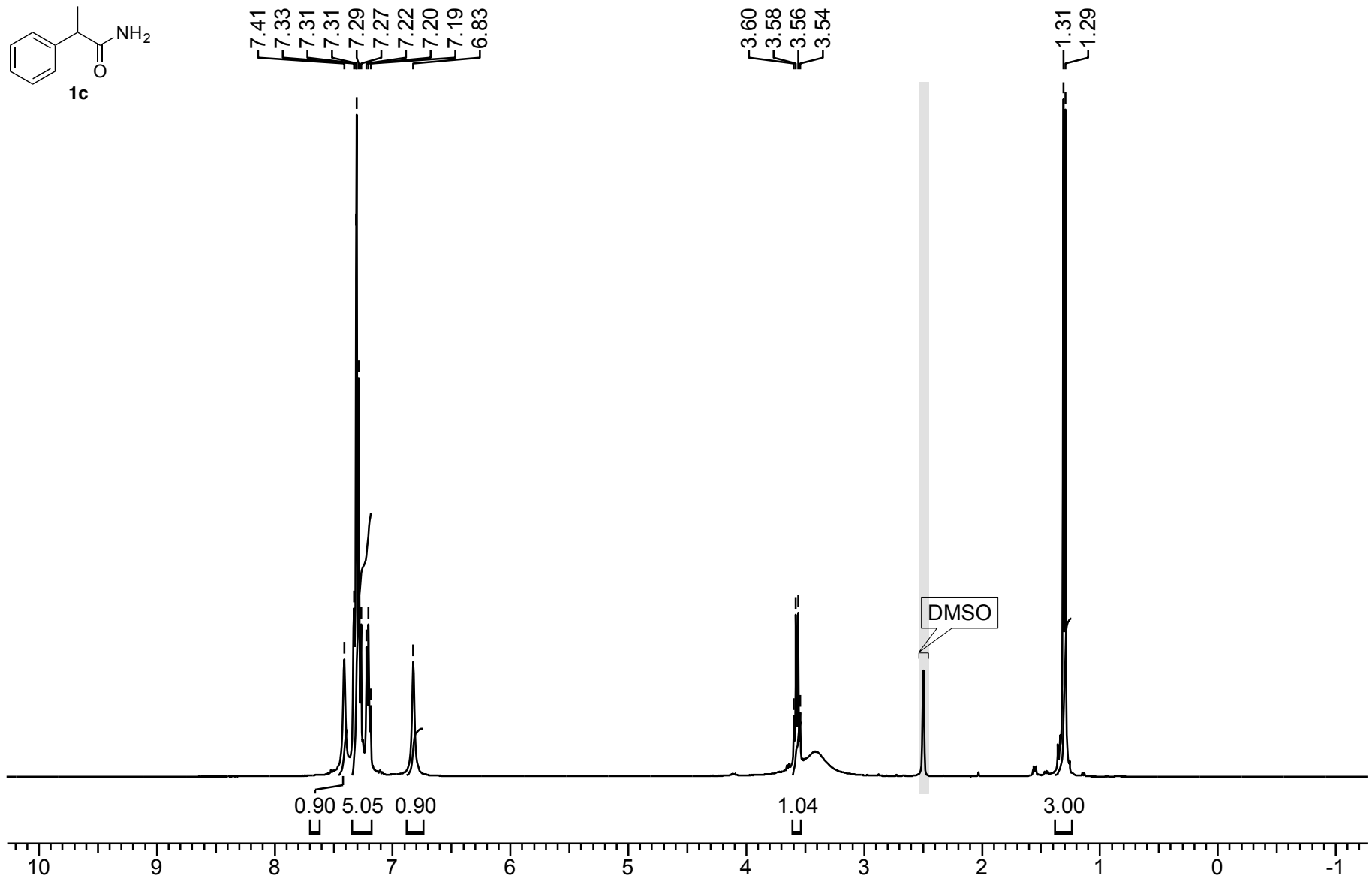

Figure S140. ^{1}H NMR (400 MHz, DMSO-d_6) spectrum of **1c**.

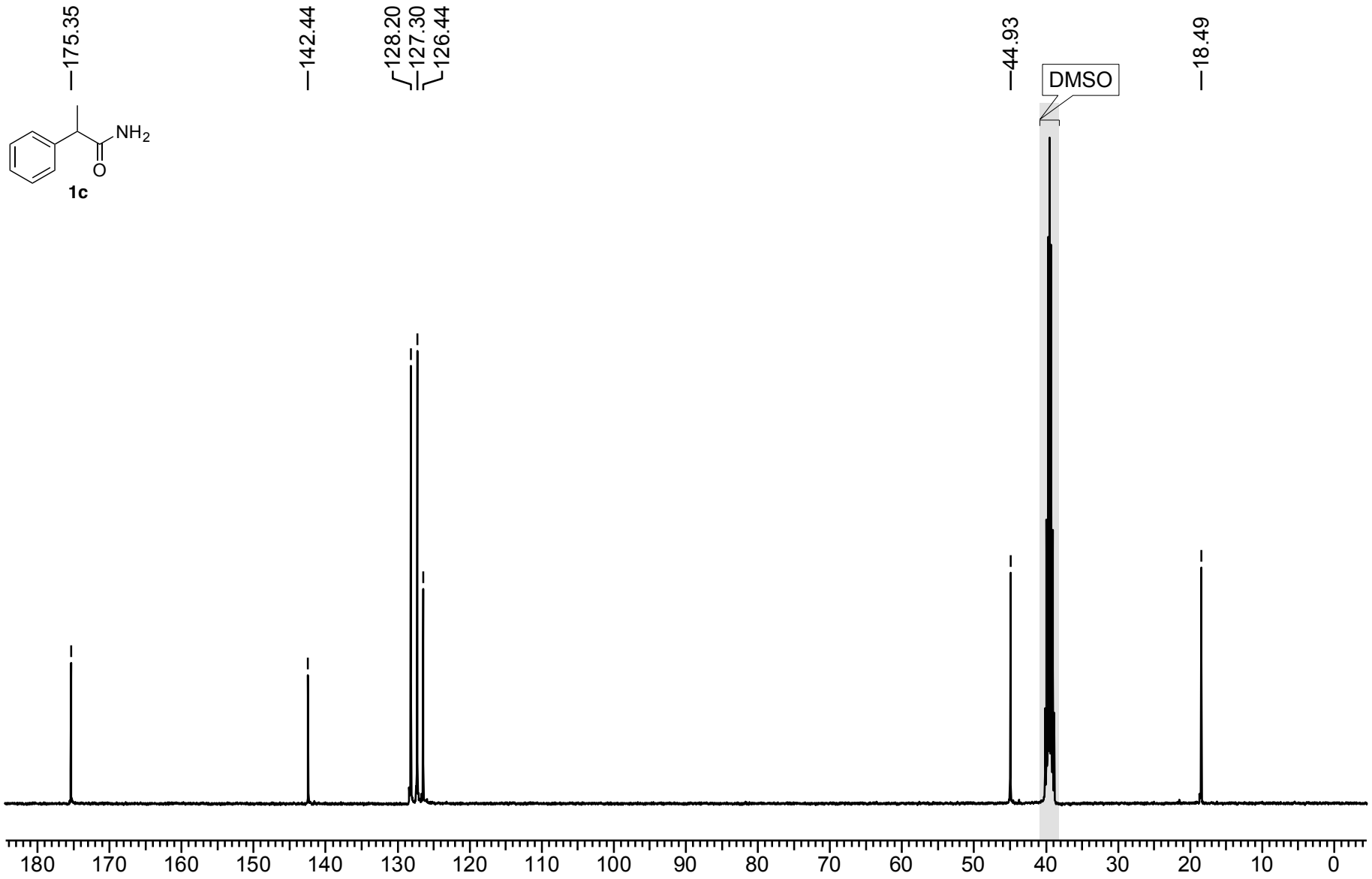

Figure S141. ^{13}C NMR (100 MHz, DMSO-d_6) spectrum of **1c**.

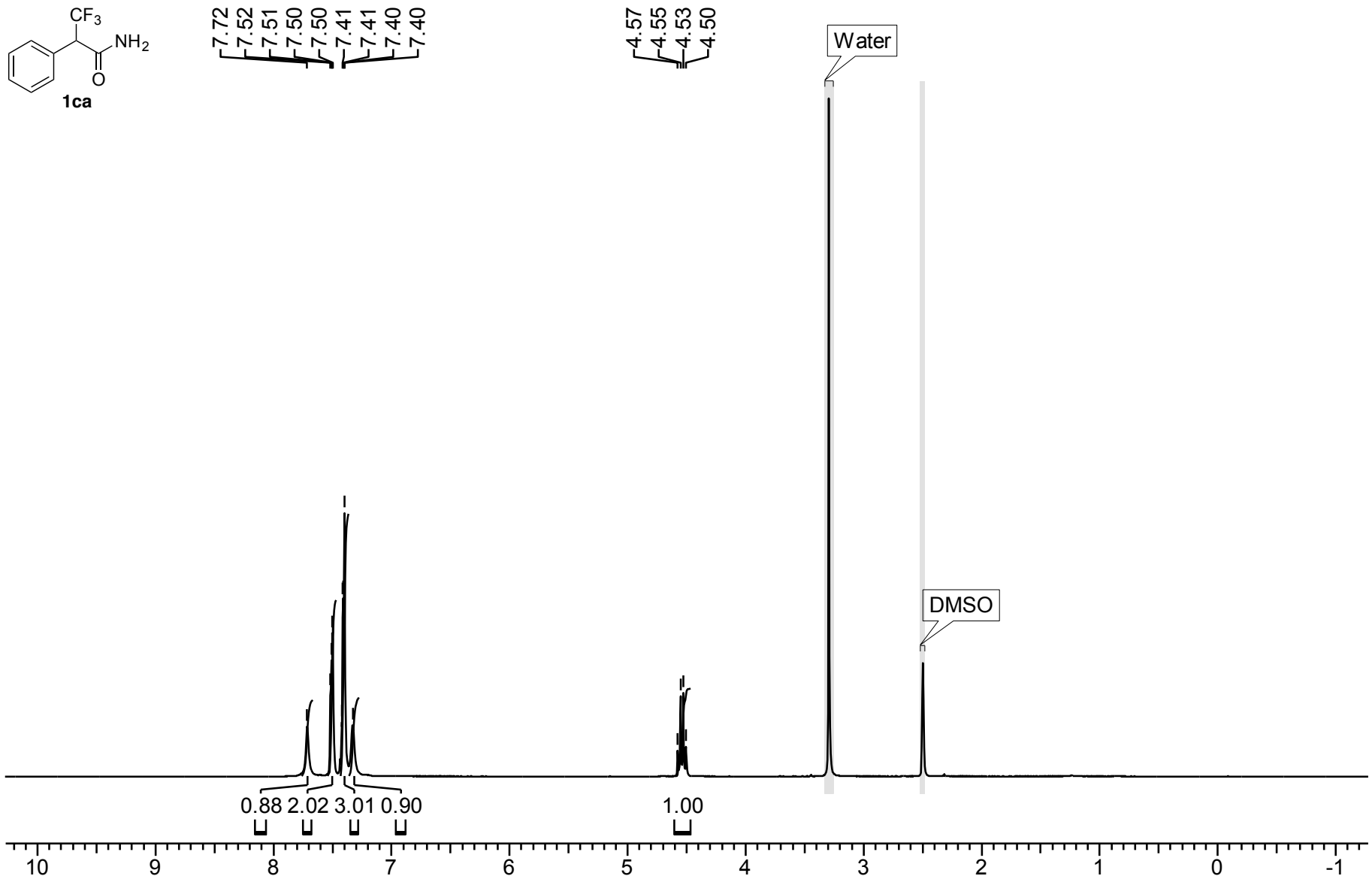

Figure S142. ^{1}H NMR (400 MHz, DMSO-d_6) spectrum of **1ca**.

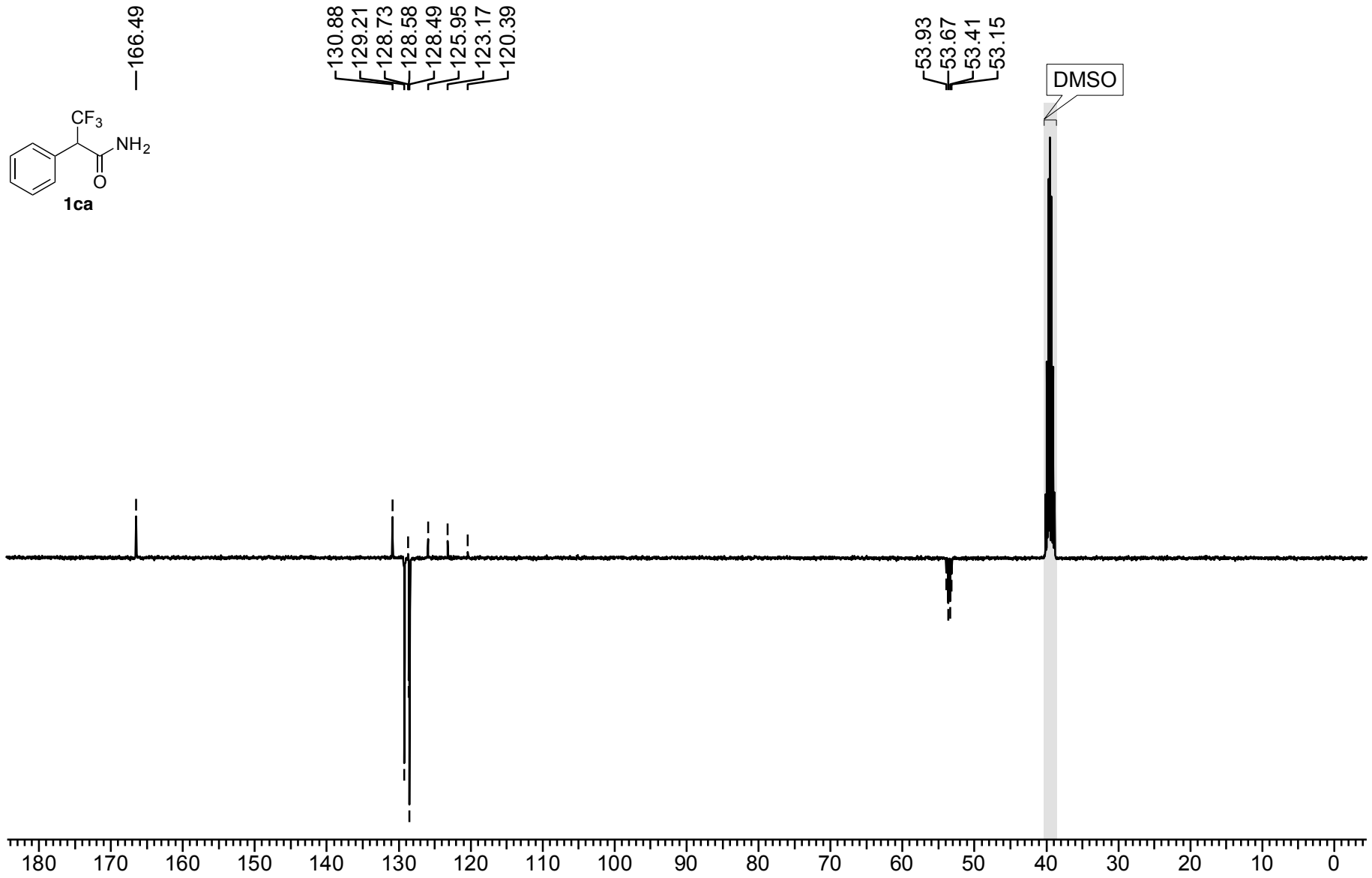

Figure S143. ^{13}C NMR APT (100 MHz, DMSO-d_6) spectrum of **1ca**.

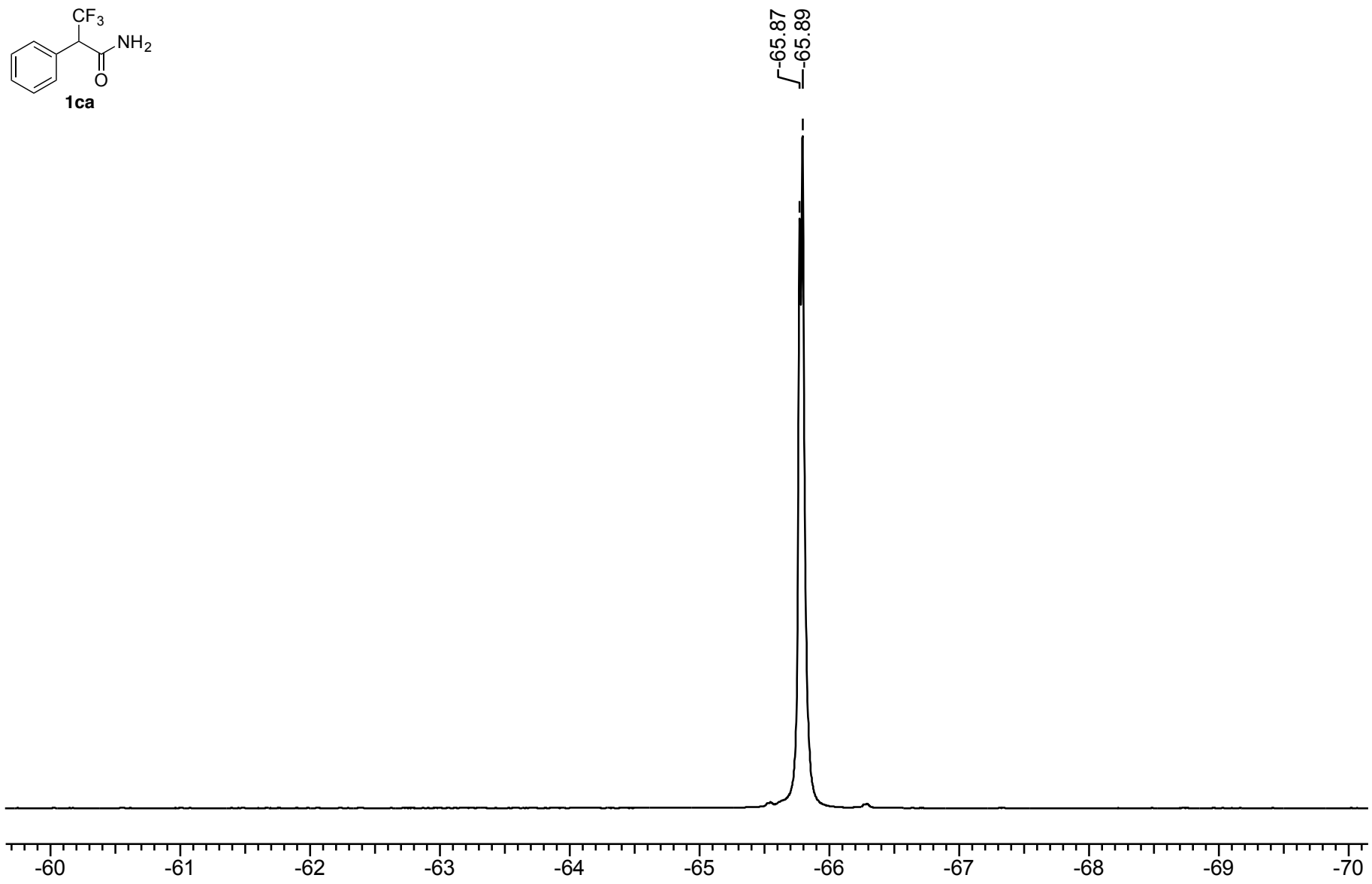

Figure S144. ^{19}F NMR (376 MHz, DMSO-d_6) spectrum of **1ca**.

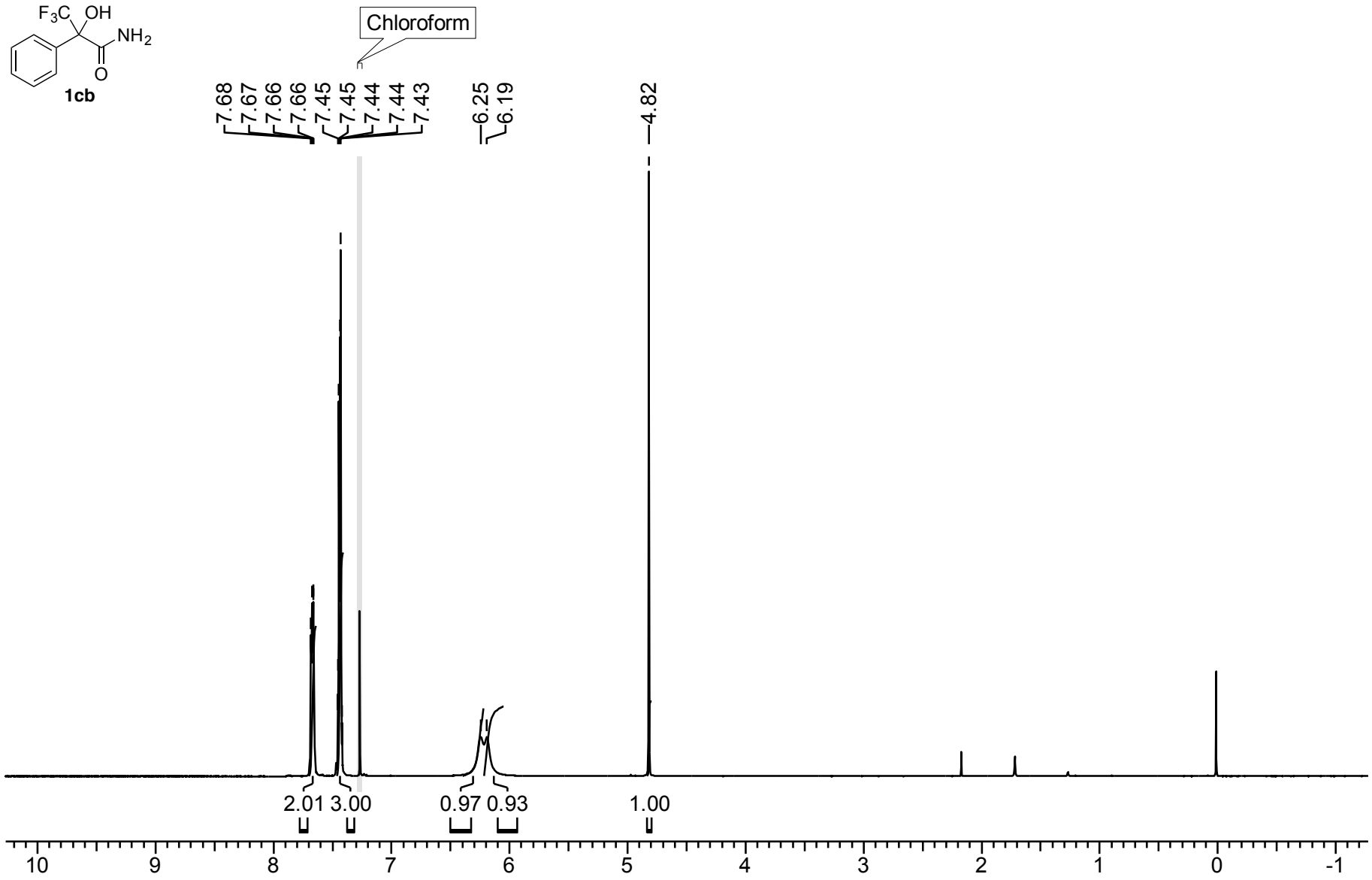

Figure S145. ^{1}H NMR (400 MHz, $CDCl_3$) spectrum of **1cb**.

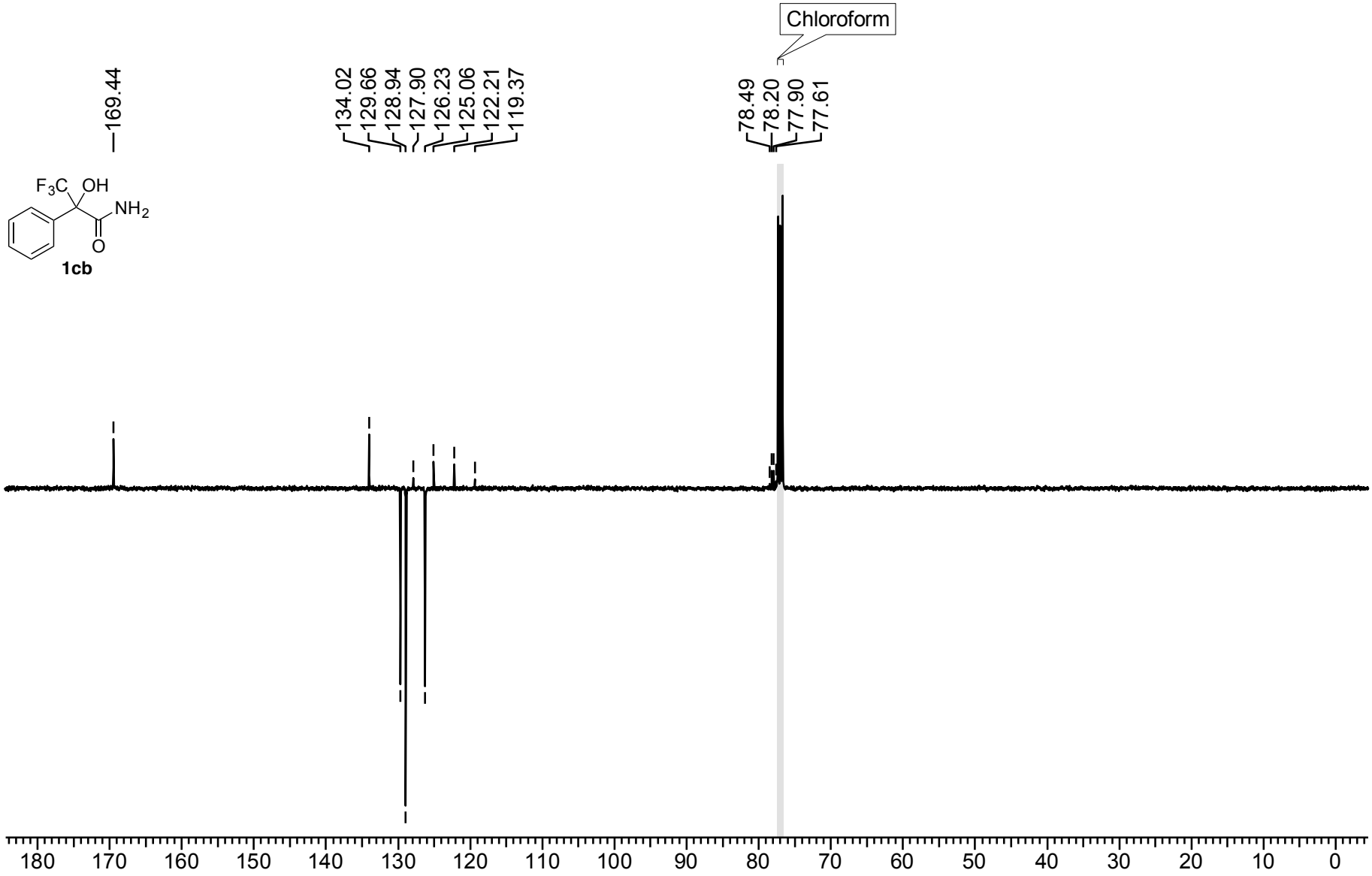

Figure S146. ^{13}C NMR APT (100 MHz, $CDCl_3$) spectrum of **1cb**.

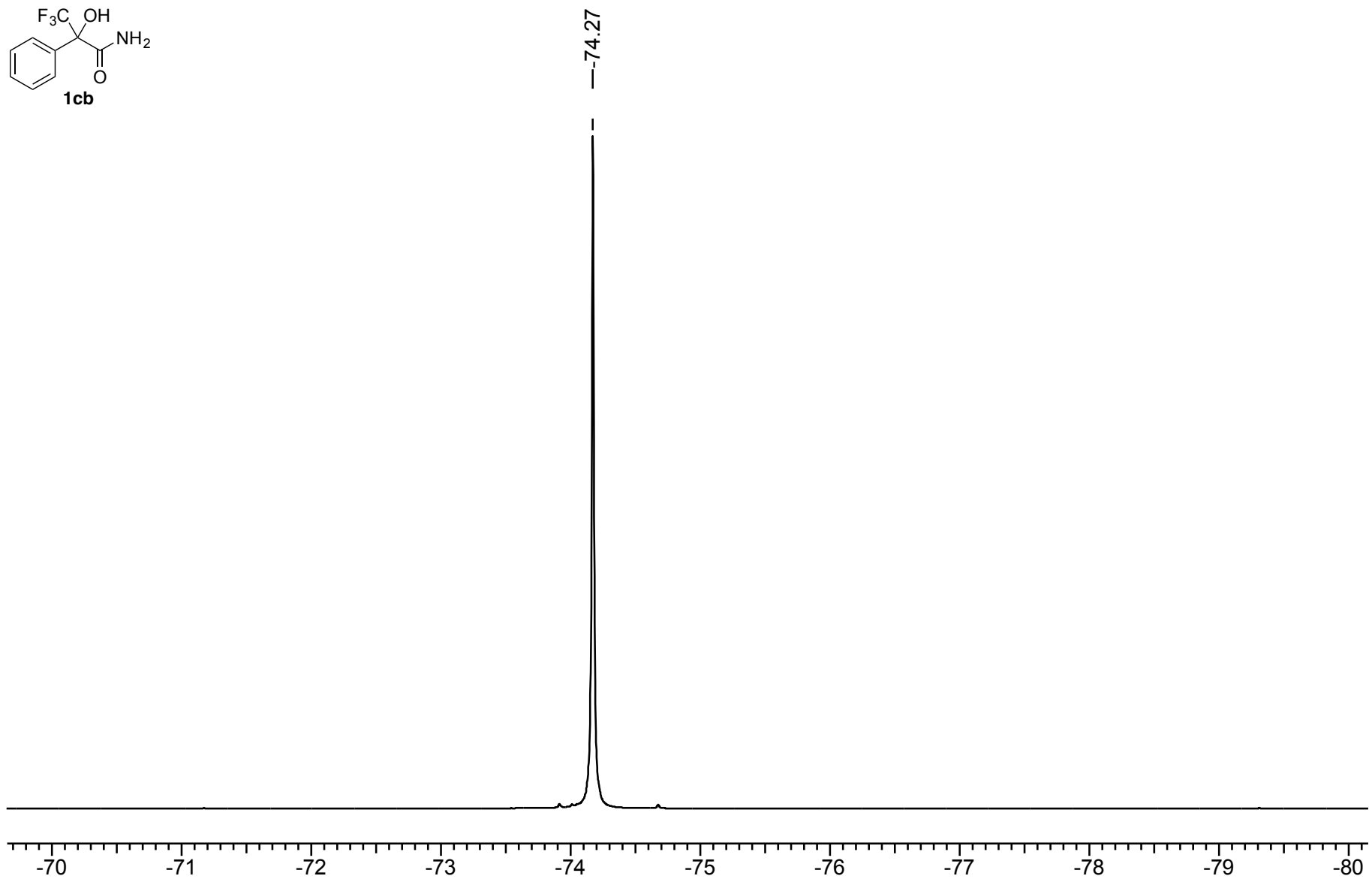

Figure S147. ^{19}F NMR (376 MHz, $CDCl_3$) spectrum of **1cb**.

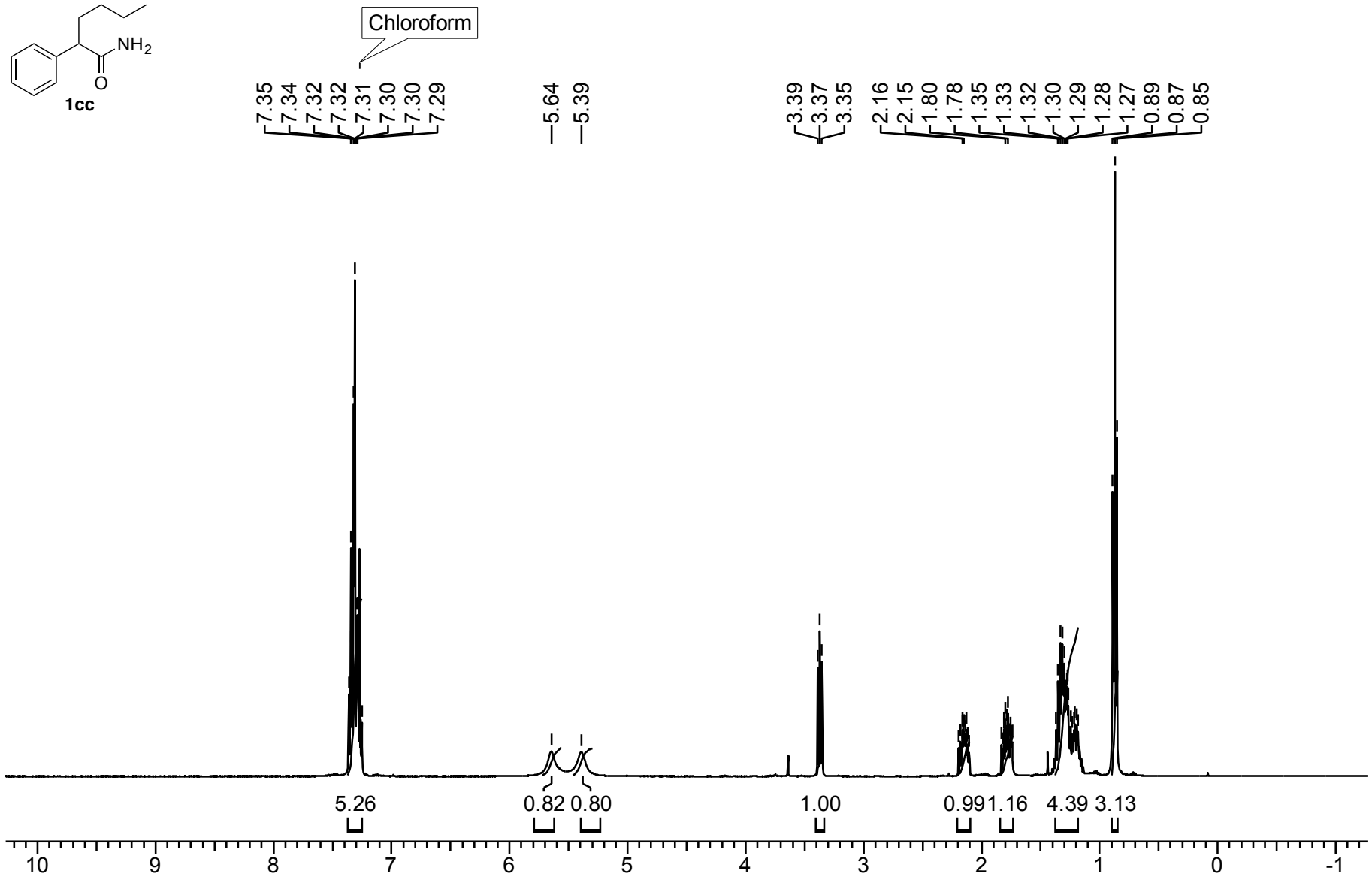

Figure S148. ^{1}H NMR (400 MHz, $CDCl_3$) spectrum of **1cc**.

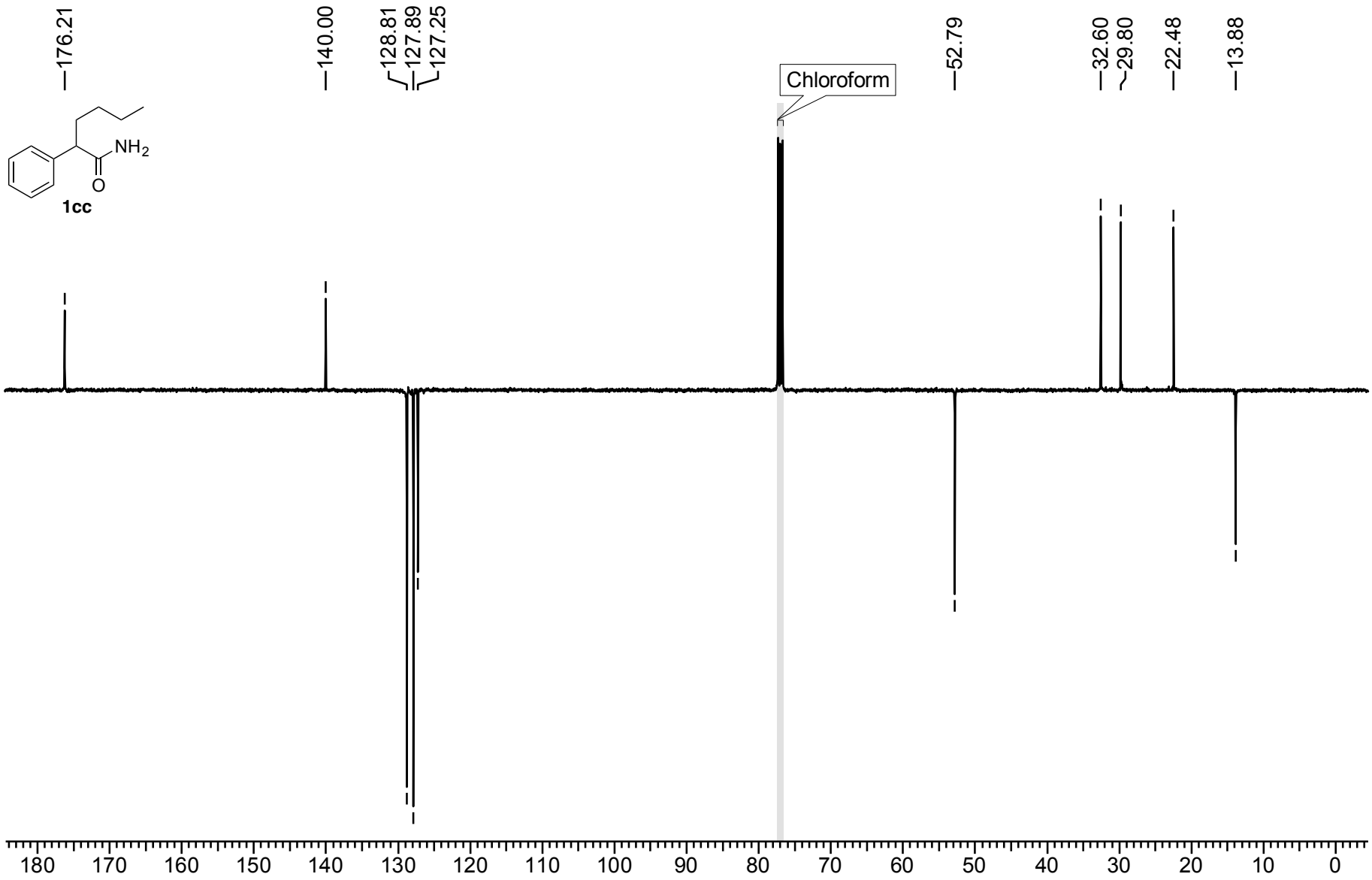

Figure S149. ^{13}C APT NMR (100 MHz, $CDCl_3$) spectrum of **1cc**.

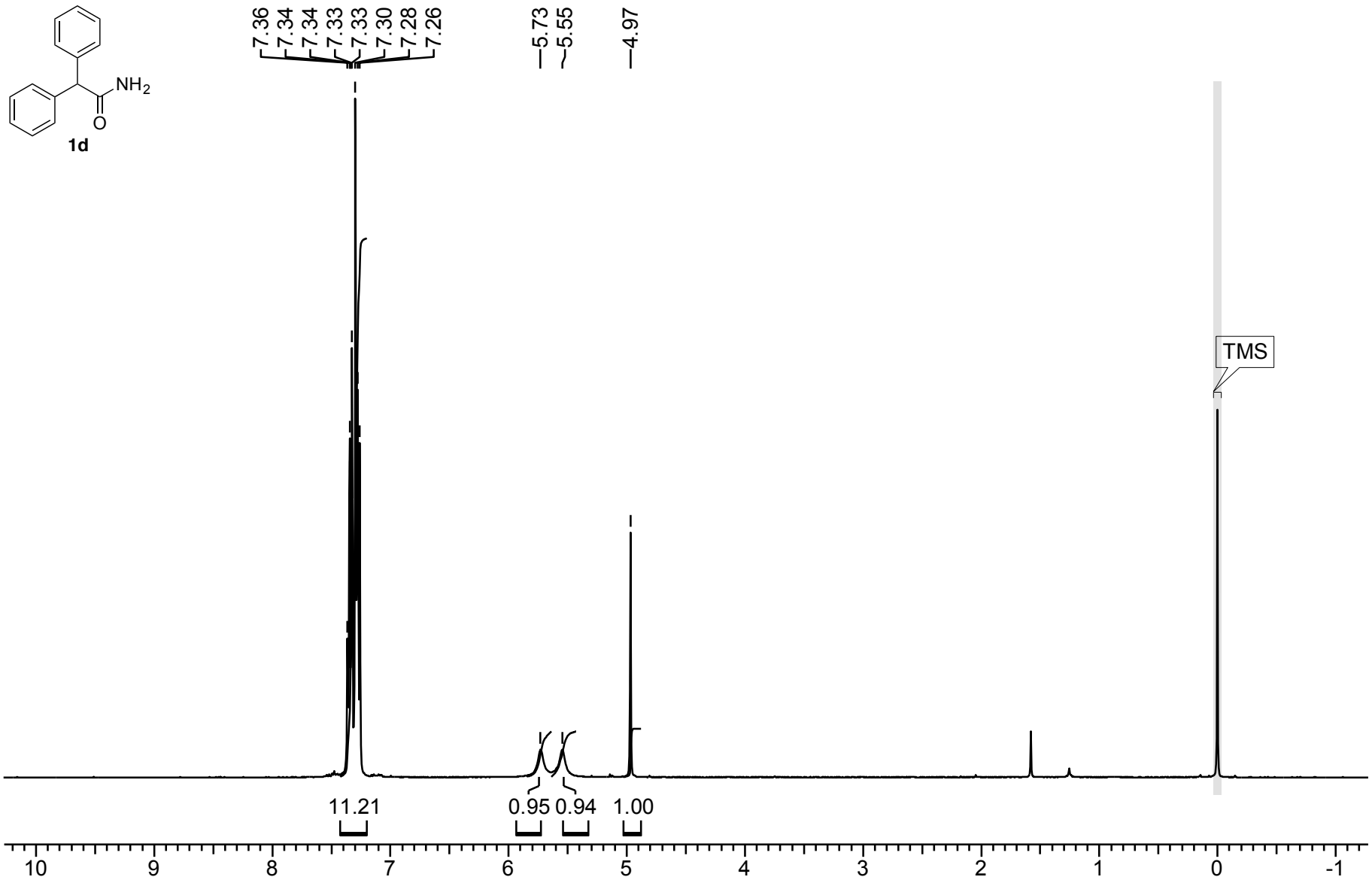

Figure S150. ^{1}H NMR (400 MHz, $CDCl_3$) spectrum of **1d**.

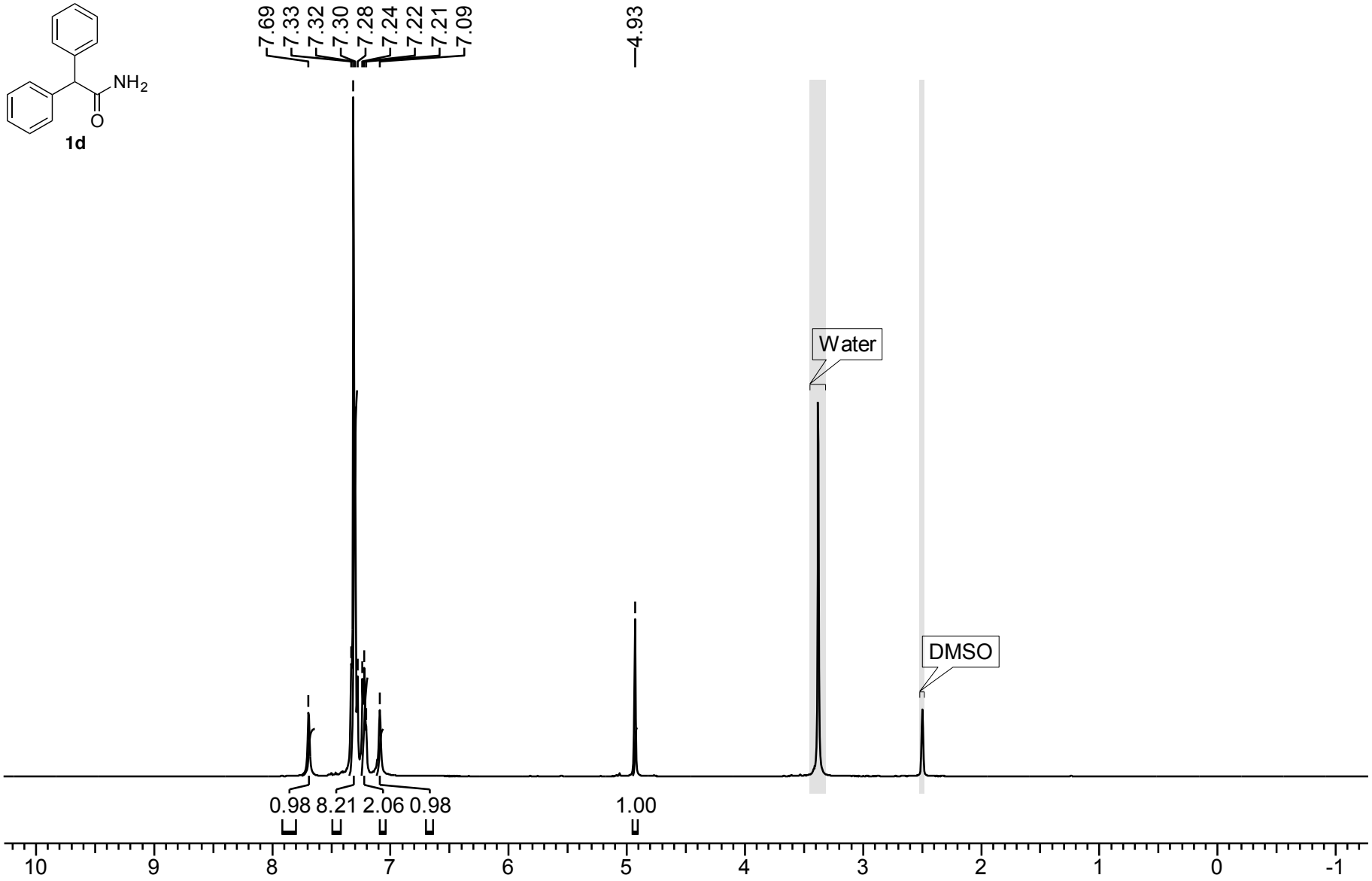

Figure S151. ^{1}H NMR (400 MHz, DMSO-d_6) spectrum of **1d**.

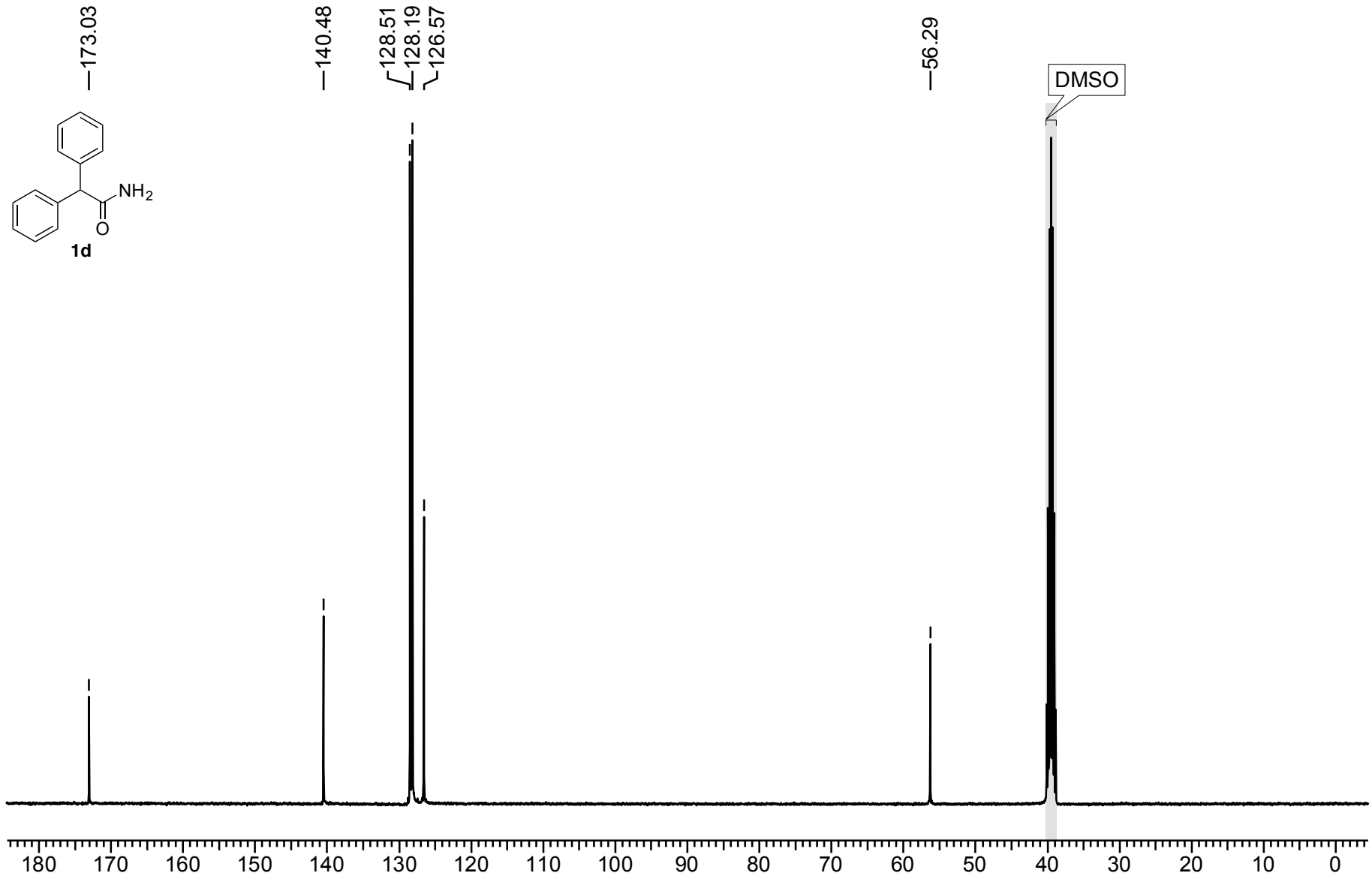

Figure S152. ^{13}C NMR (100 MHz, DMSO-d_6) spectrum of **1d**.

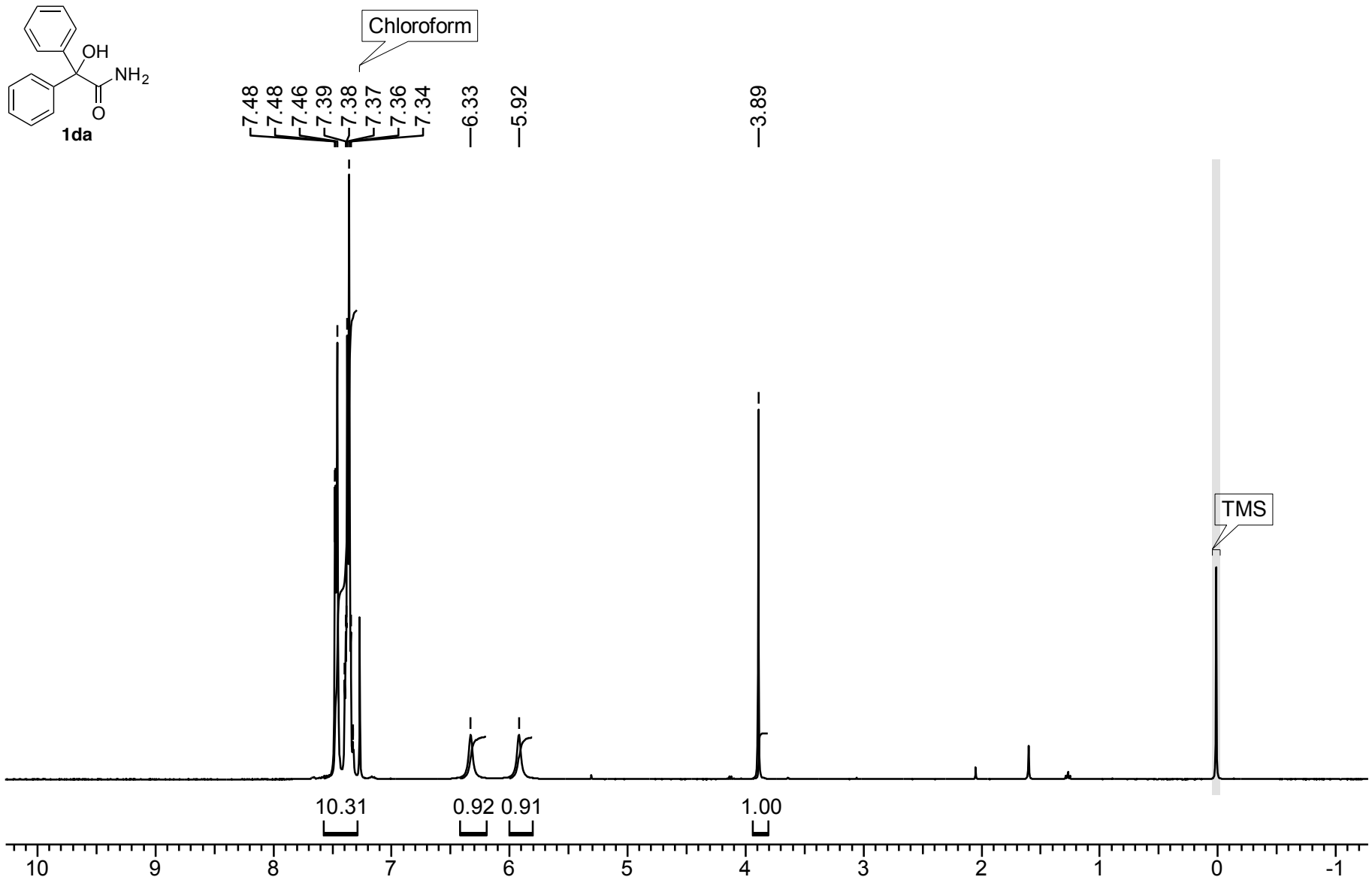

Figure S153. ^{1}H NMR (400 MHz, $CDCl_3$) spectrum of **1da**.

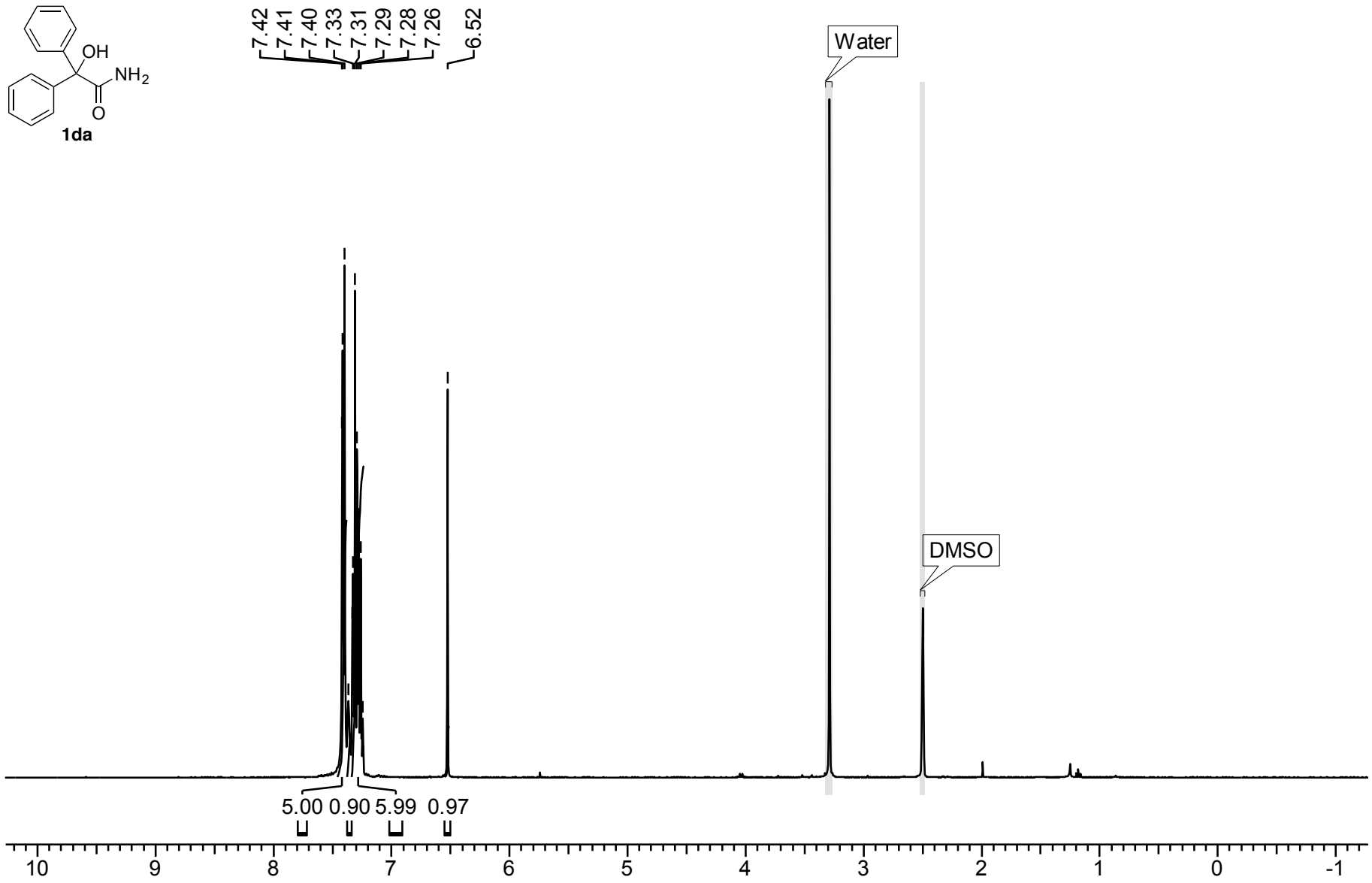

Figure S154. ^{1}H NMR (400 MHz, DMSO-d_6) spectrum of **1da**.

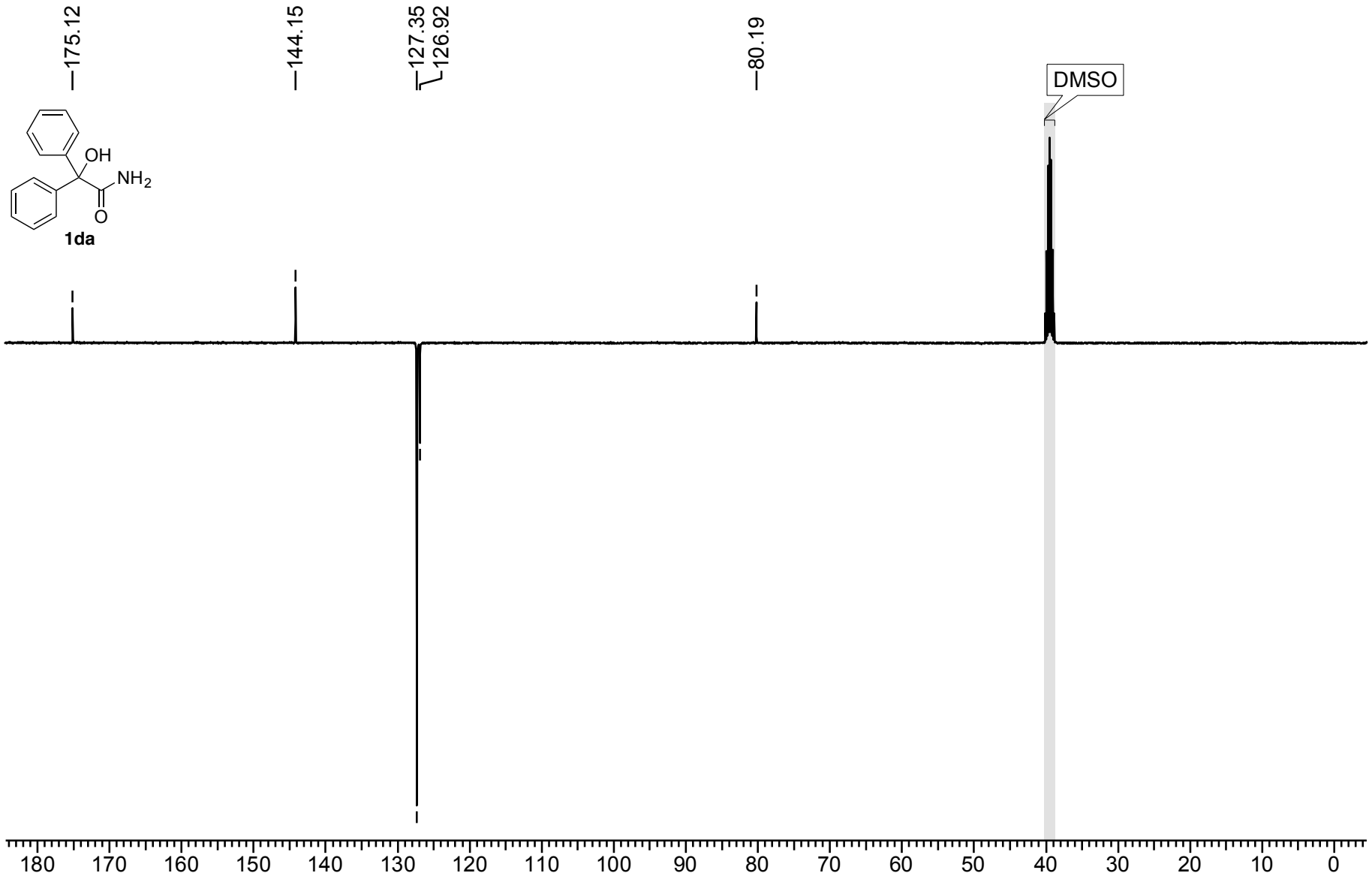

Figure S155. ^{13}C NMR APT (100 MHz, DMSO-d_6) spectrum of **1da**.

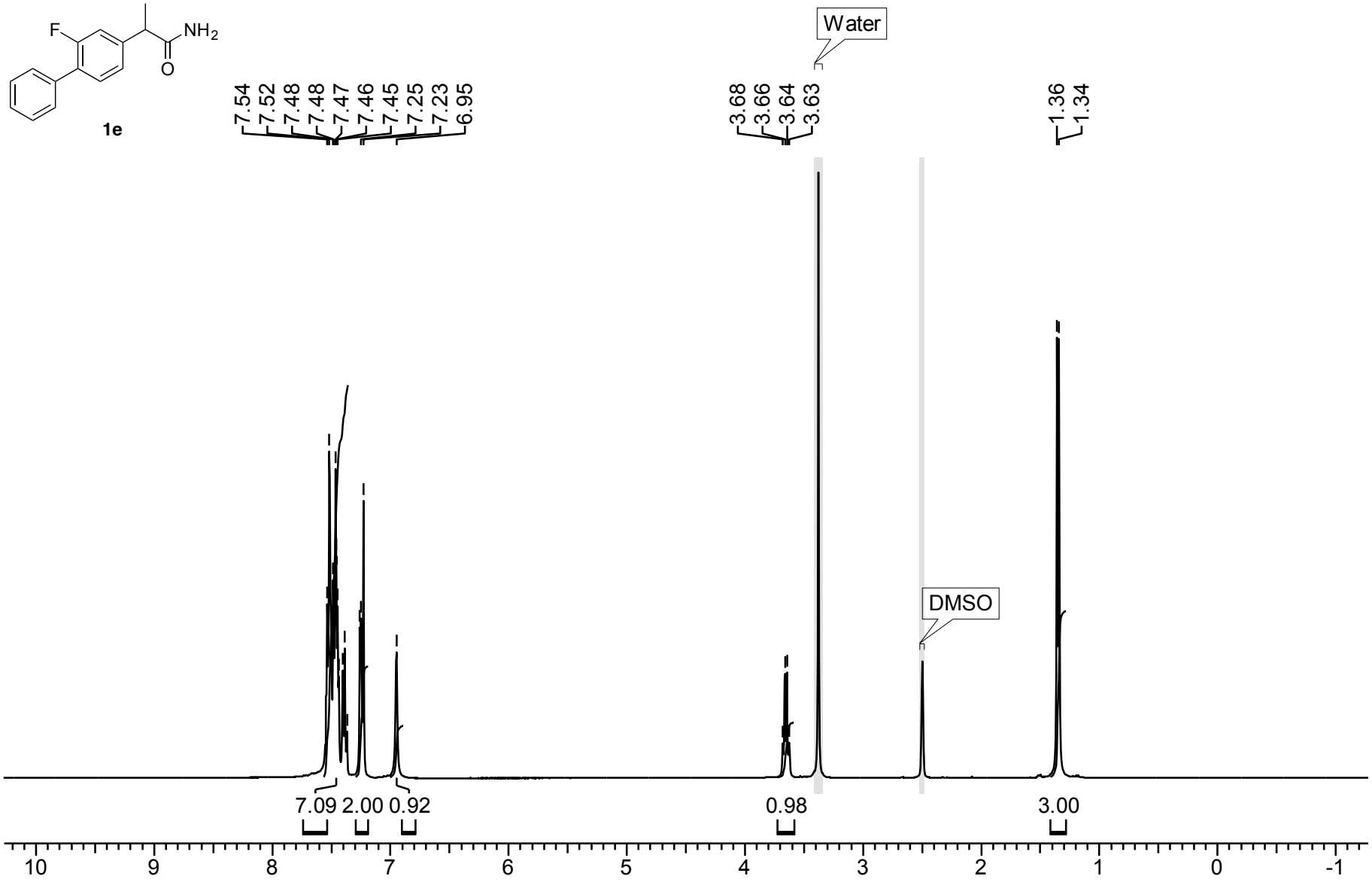

Figure S156. ^{1}H NMR (400 MHz, DMSO-d_6) spectrum of **1e**.

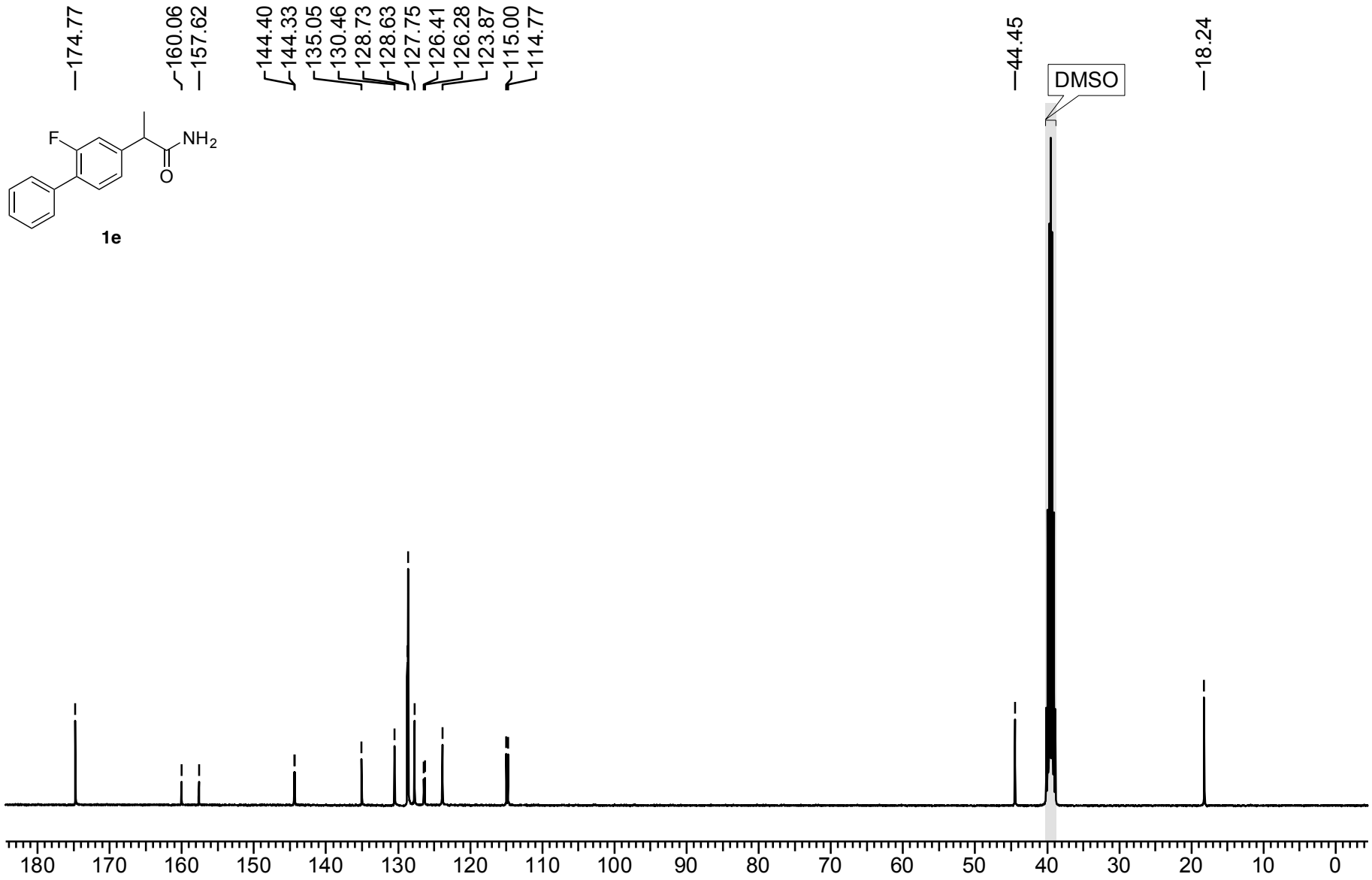

Figure S157. ^{13}C NMR (100 MHz, DMSO-d_6) spectrum of **1e**.

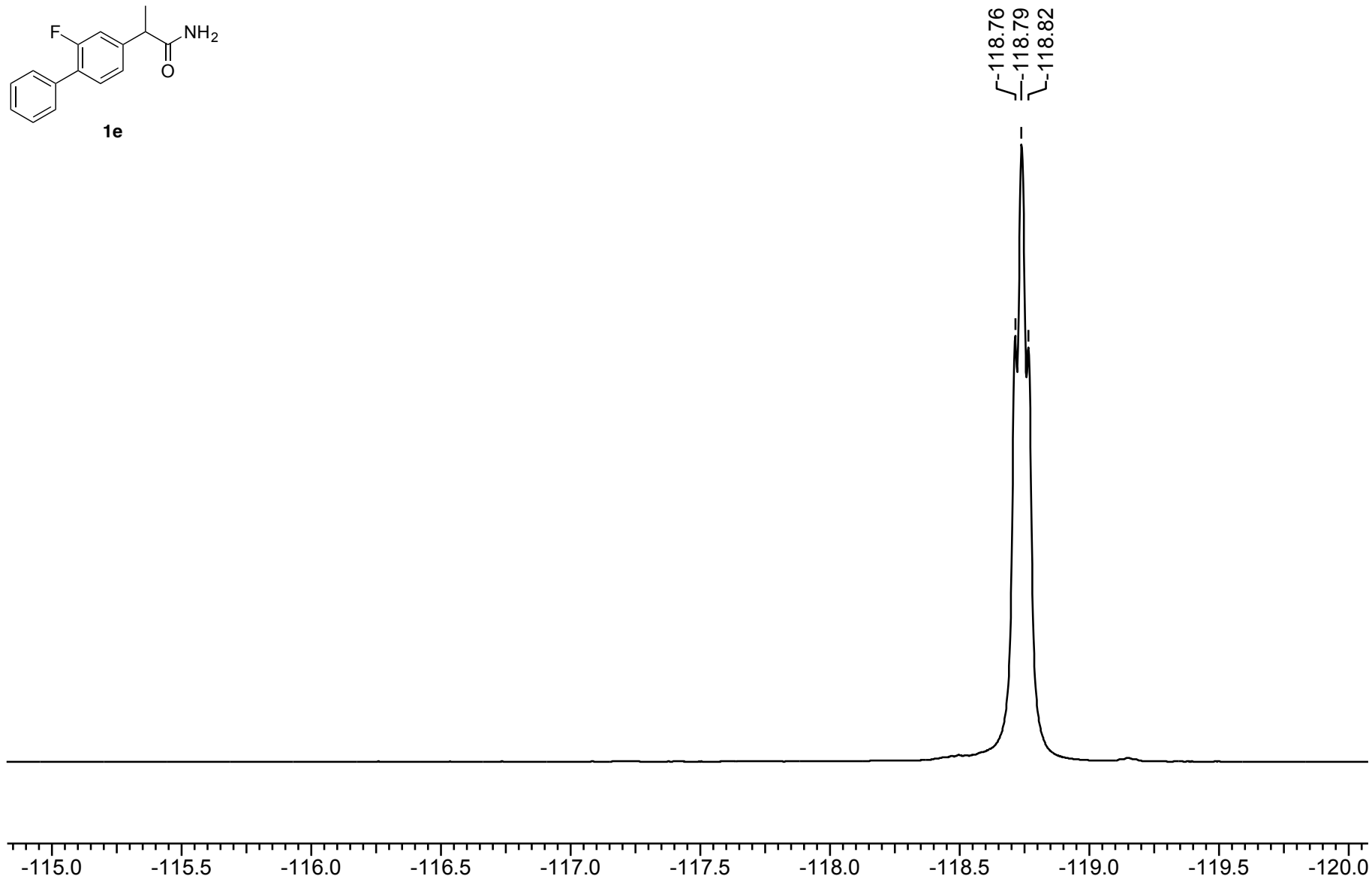

Figure S158. ^{19}F NMR (376 MHz, DMSO-d_6) spectrum of **1e**.

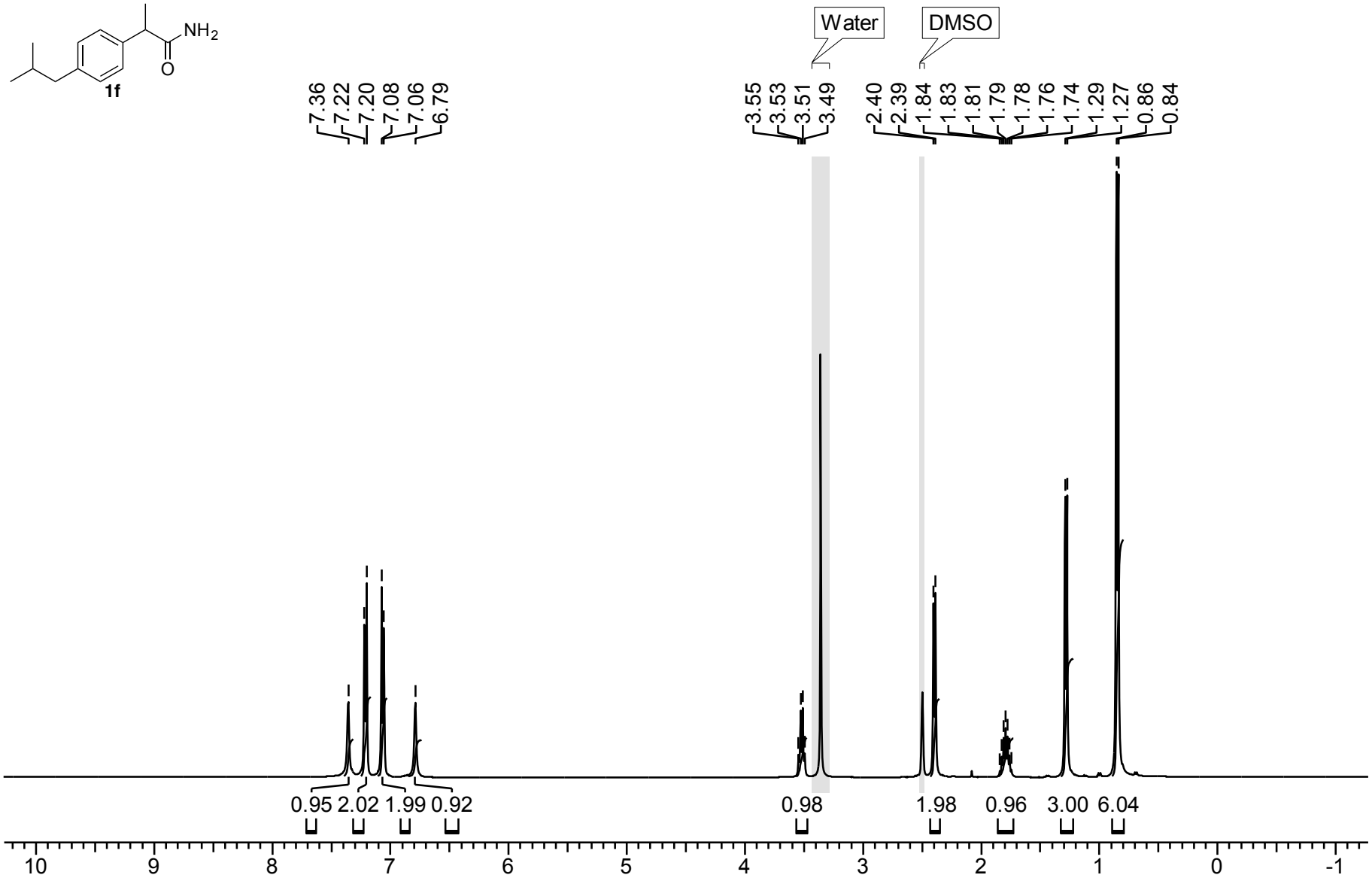

Figure S159. ^{1}H NMR (400 MHz, DMSO-d_6) spectrum of **1f**.

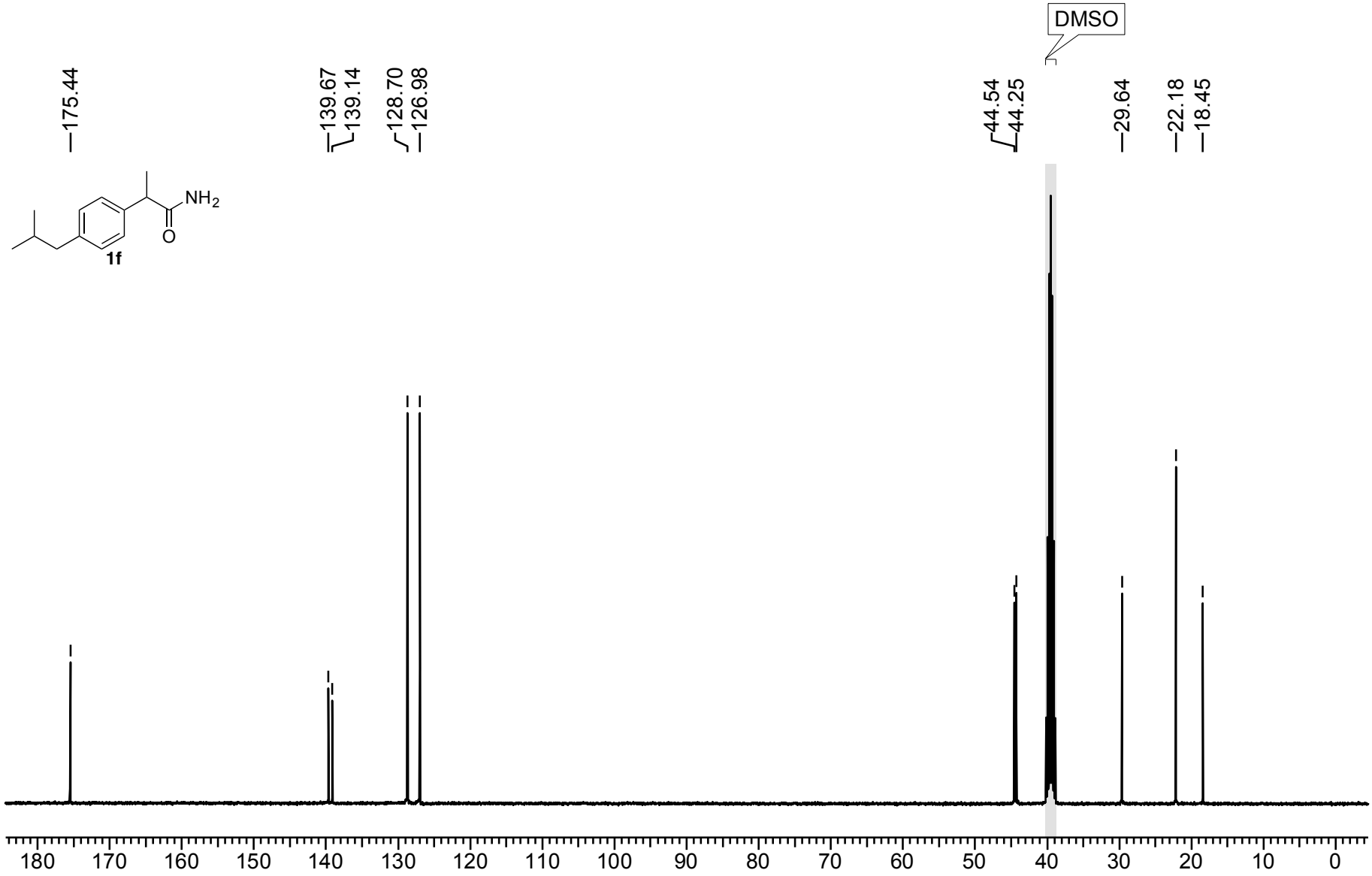

Figure S160. ^{13}C NMR (100 MHz, DMSO-d_6) spectrum of **1f**.

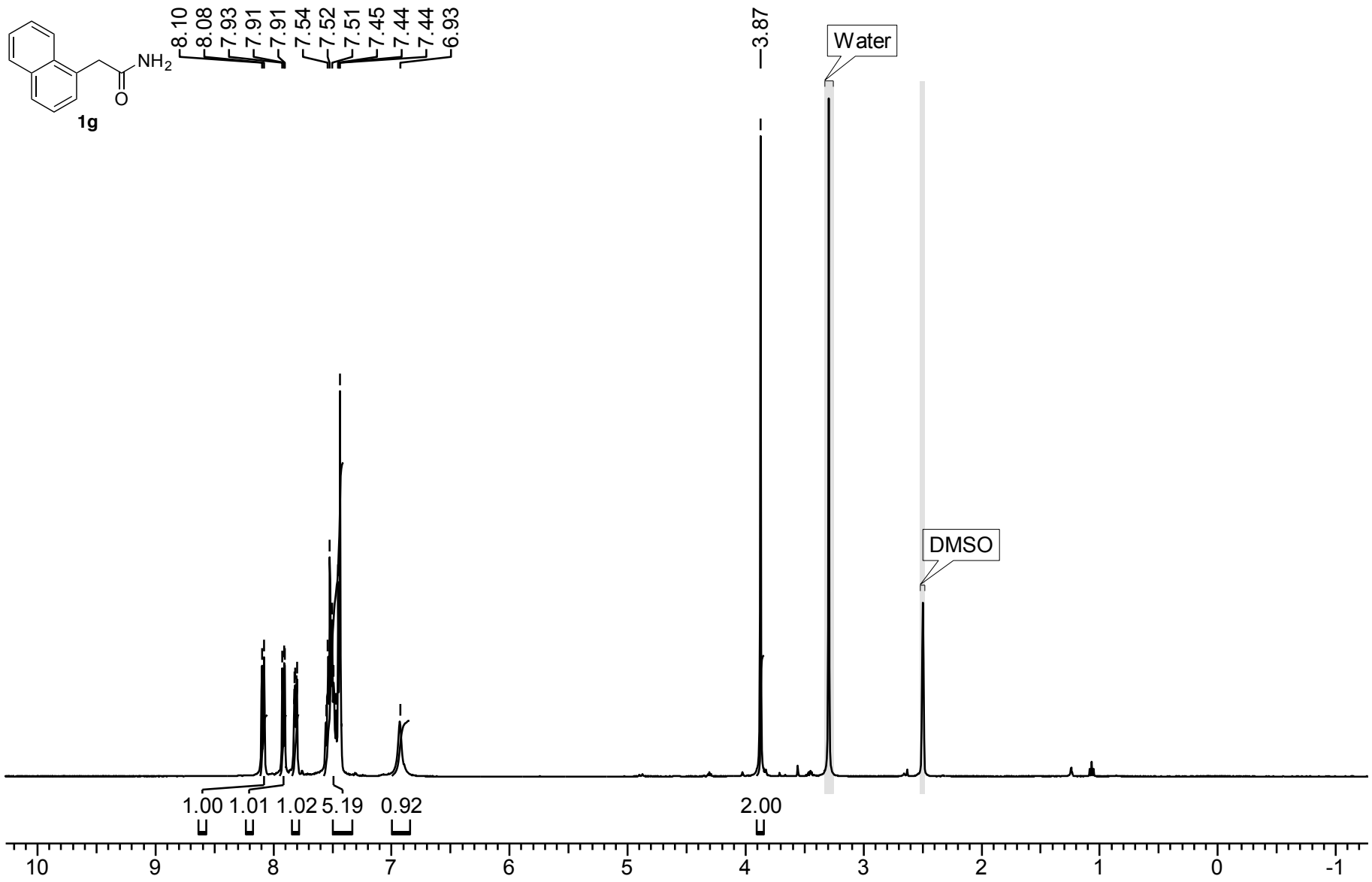

Figure S161. ^{1}H NMR (400 MHz, DMSO-d_6) spectrum of **1g**.

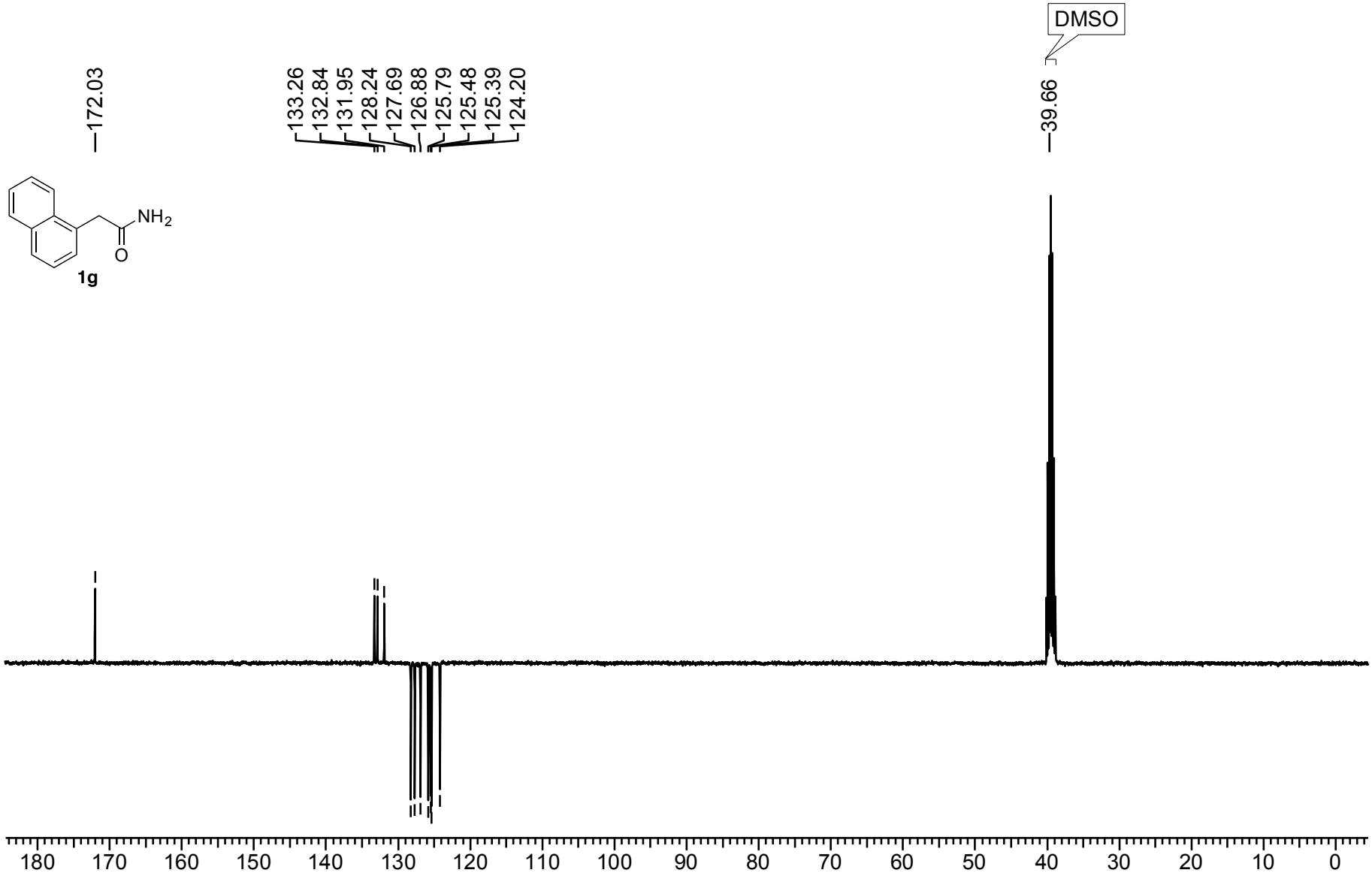

Figure S162. ^{13}C NMR APT (100 MHz, DMSO-d_6) spectrum of **1g**.

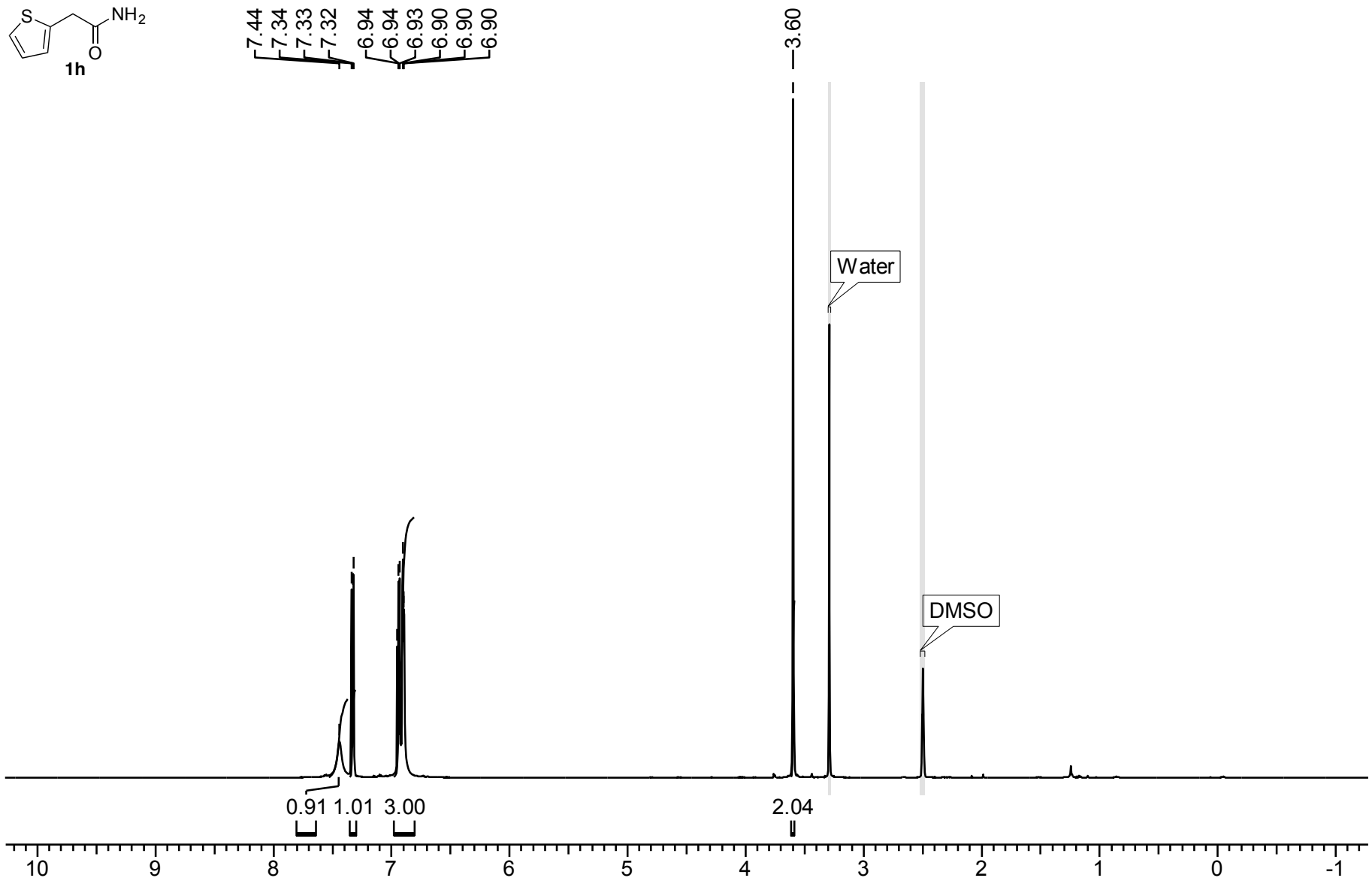

Figure S163. ^{1}H NMR (400 MHz, DMSO-d_6) spectrum of **1h**.

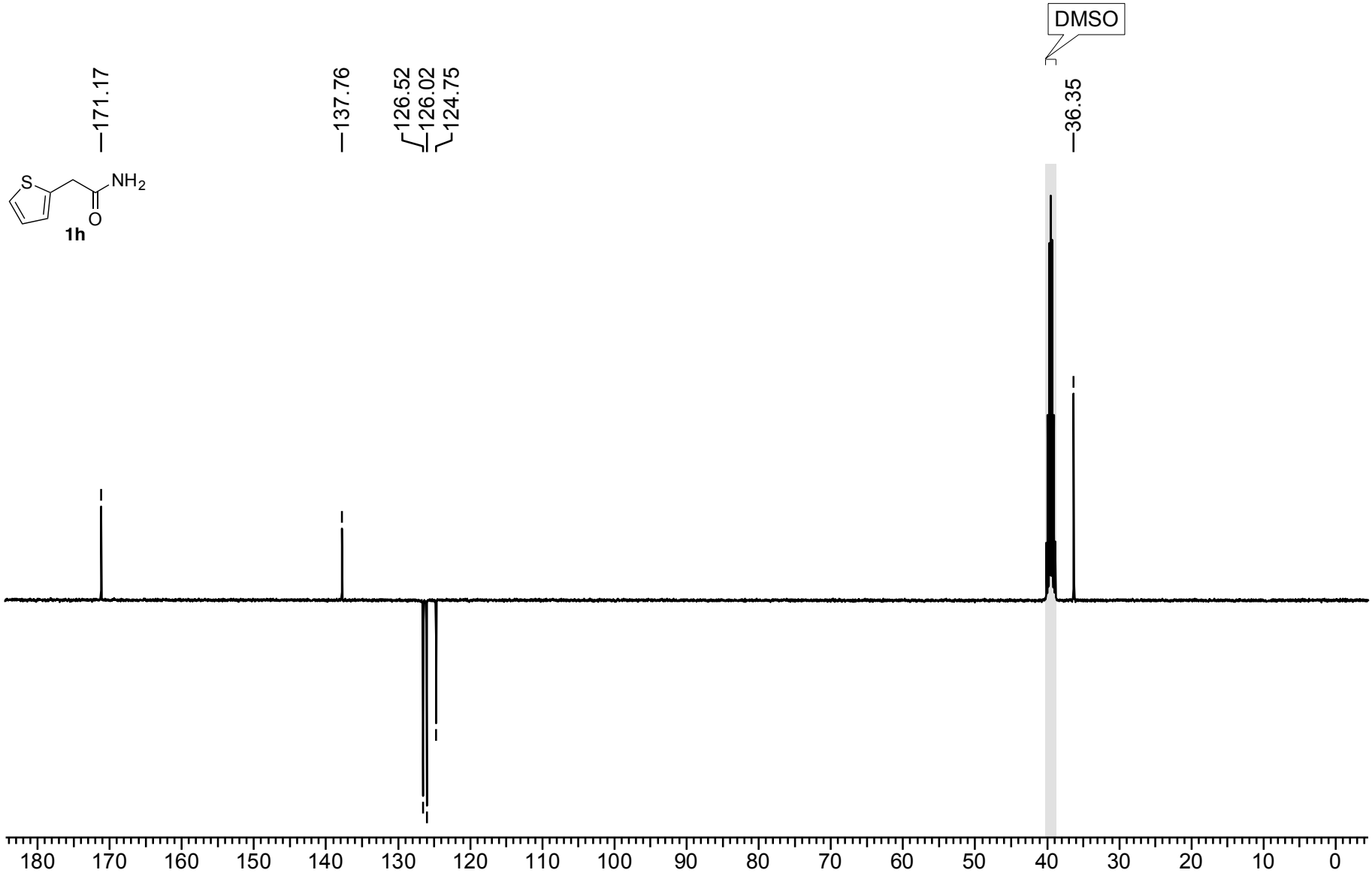

Figure S164. ^{13}C NMR APT (100 MHz, DMSO-d_6) spectrum of **1h**.

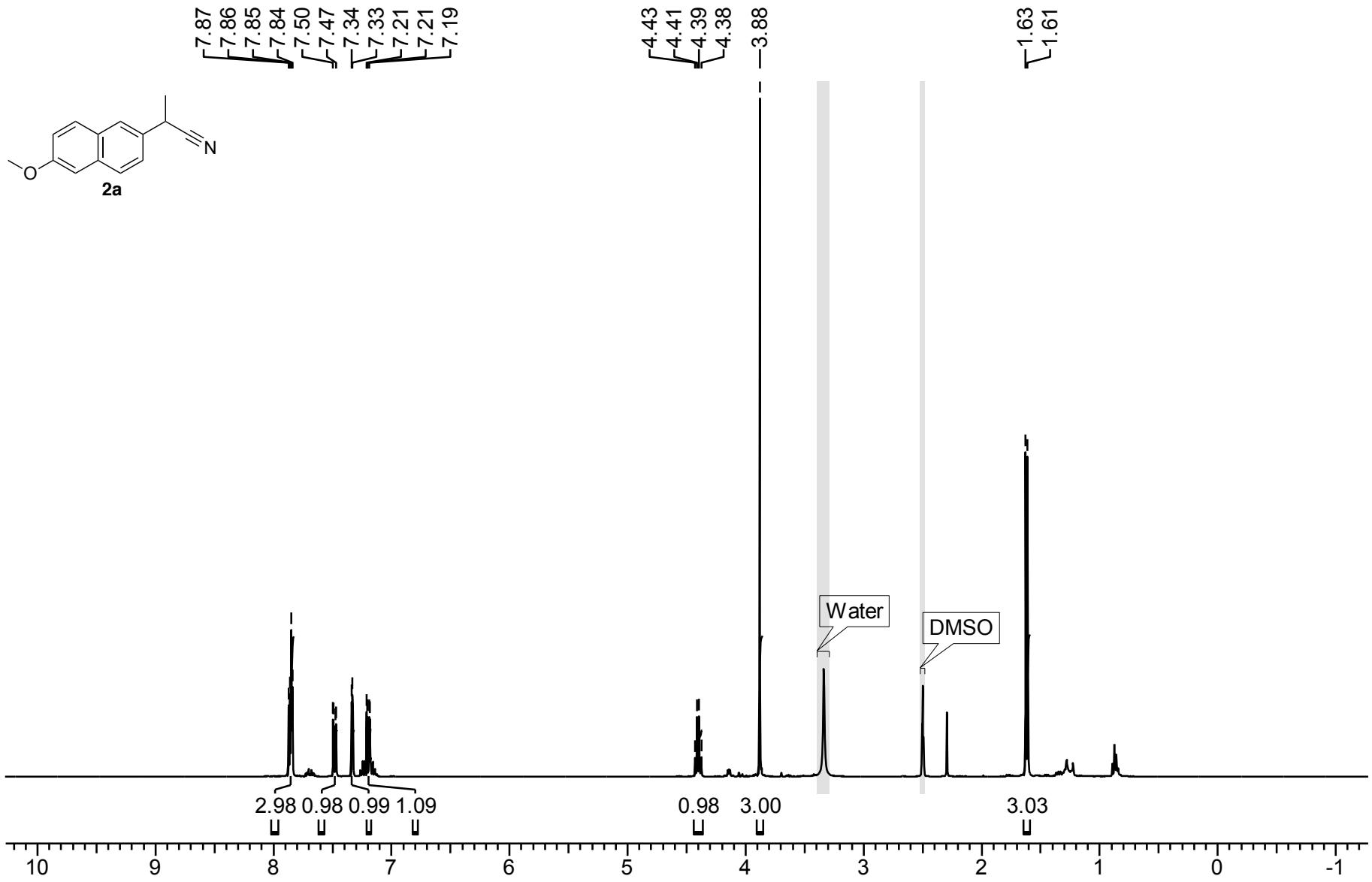

Figure S165. ^{1}H NMR (400 MHz, DMSO-d_6) spectrum of **2a**.

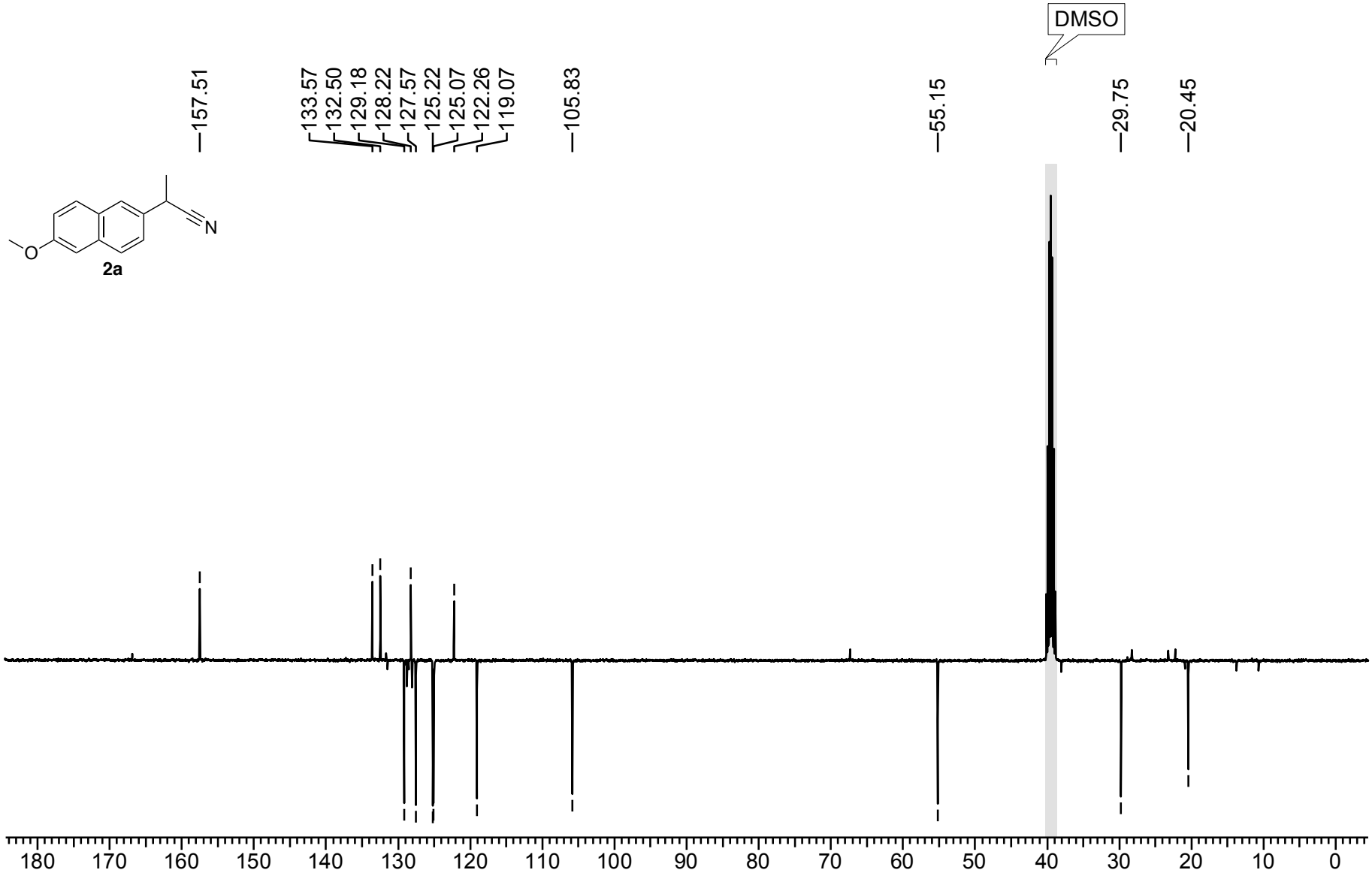

Figure S166. ^{13}C NMR APT (100 MHz, DMSO-d_6) spectrum of **2a**.

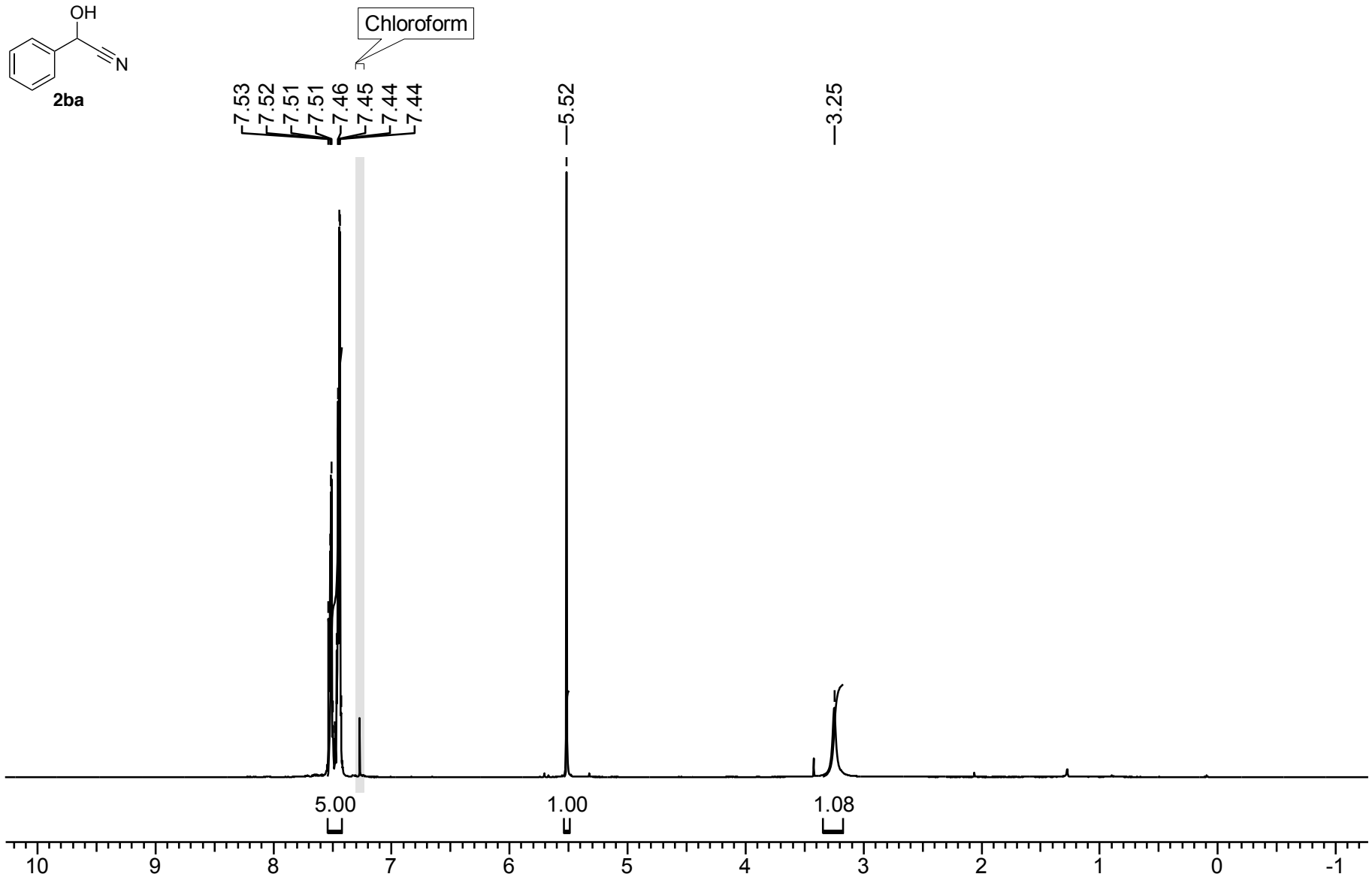

Figure S167. ^{1}H NMR (400 MHz, $CDCl_3$) spectrum of **2ba**.

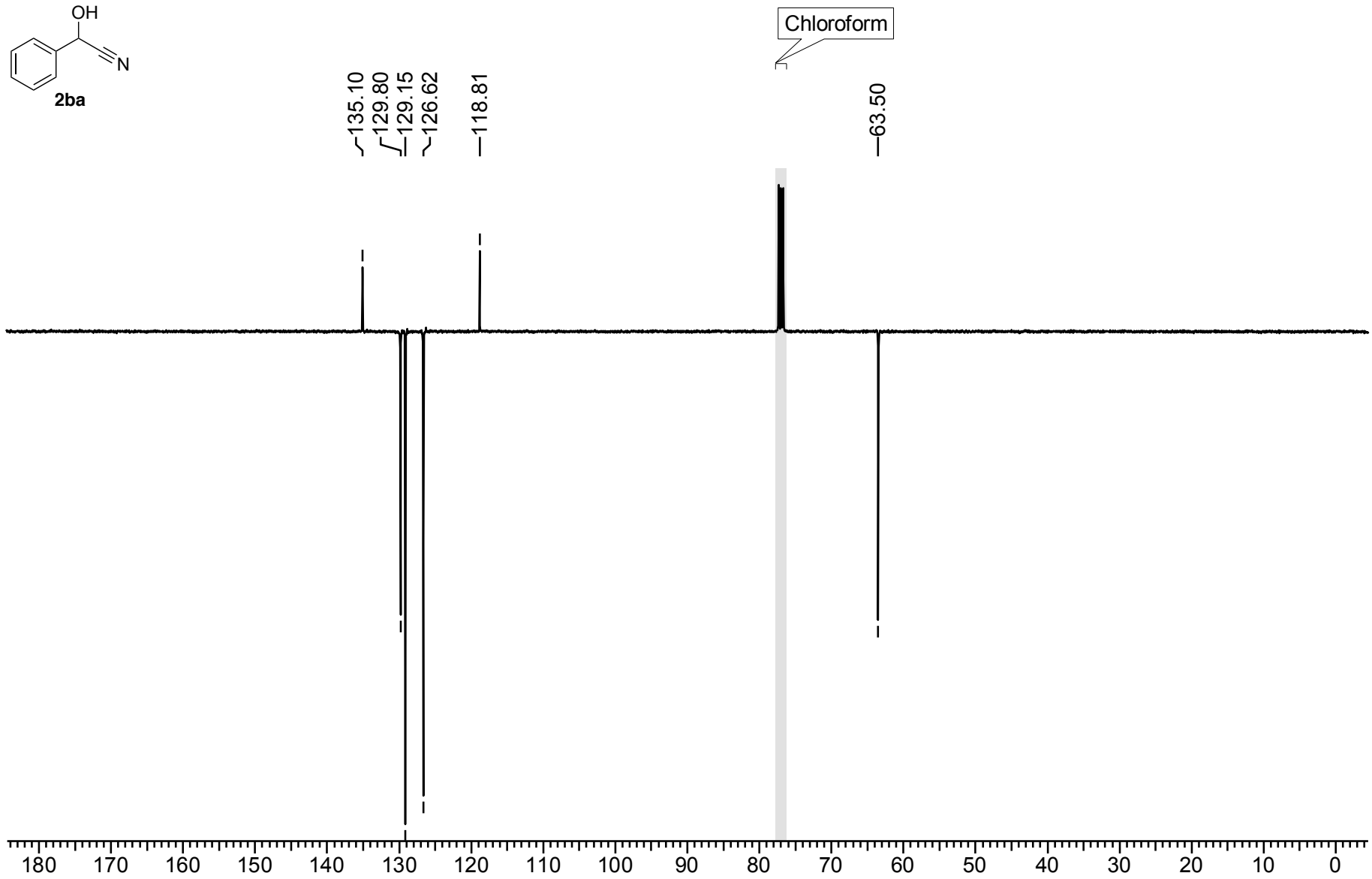

Figure S168. ^{13}C APT NMR (100 MHz, $CDCl_3$) spectrum of **2ba**.

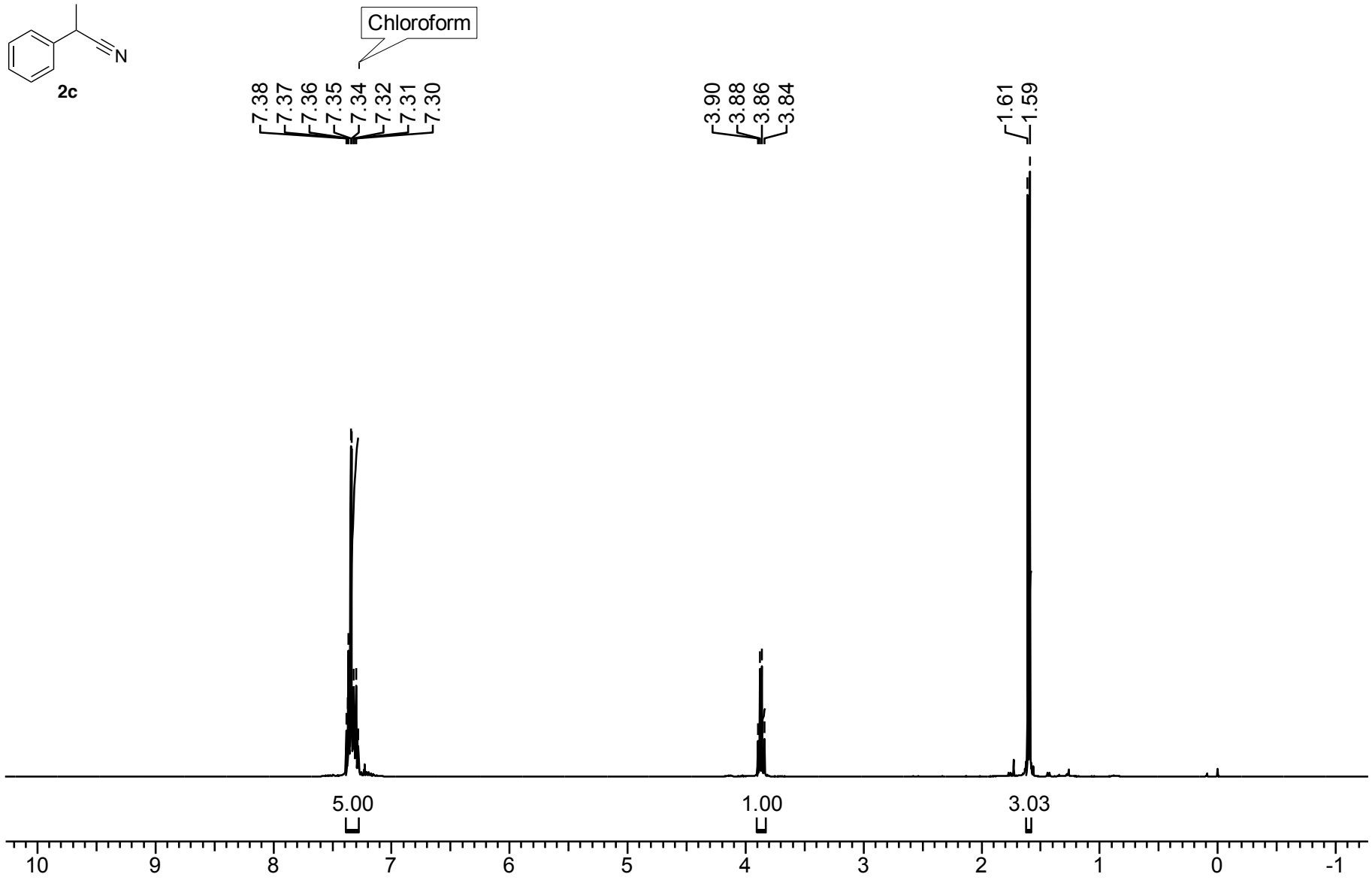

Figure S169. ^{1}H NMR (400 MHz, $CDCl_3$) spectrum of **2c**.

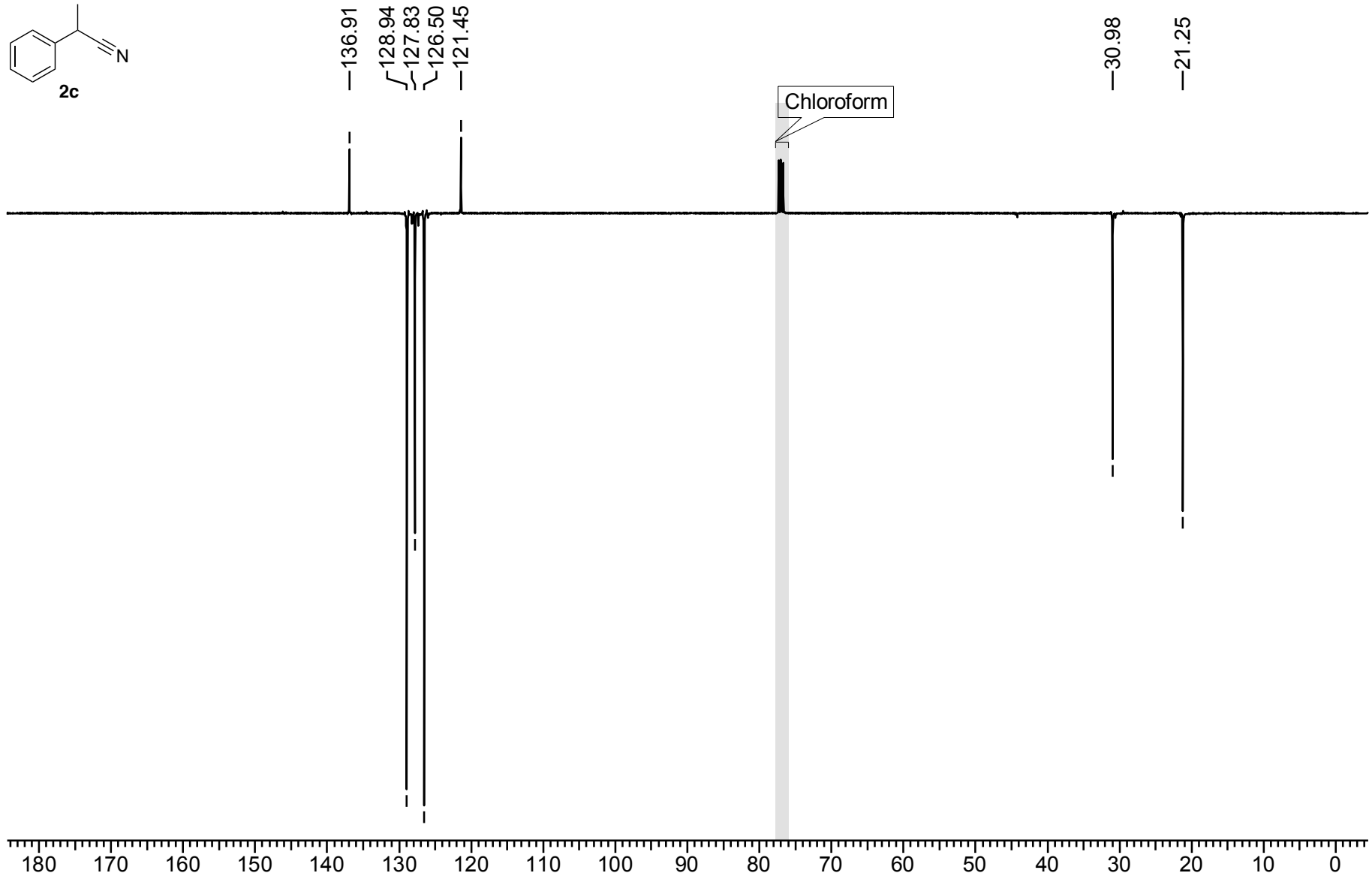

Figure S170. ^{13}C NMR APT (100 MHz, $CDCl_3$) spectrum of **2c**.

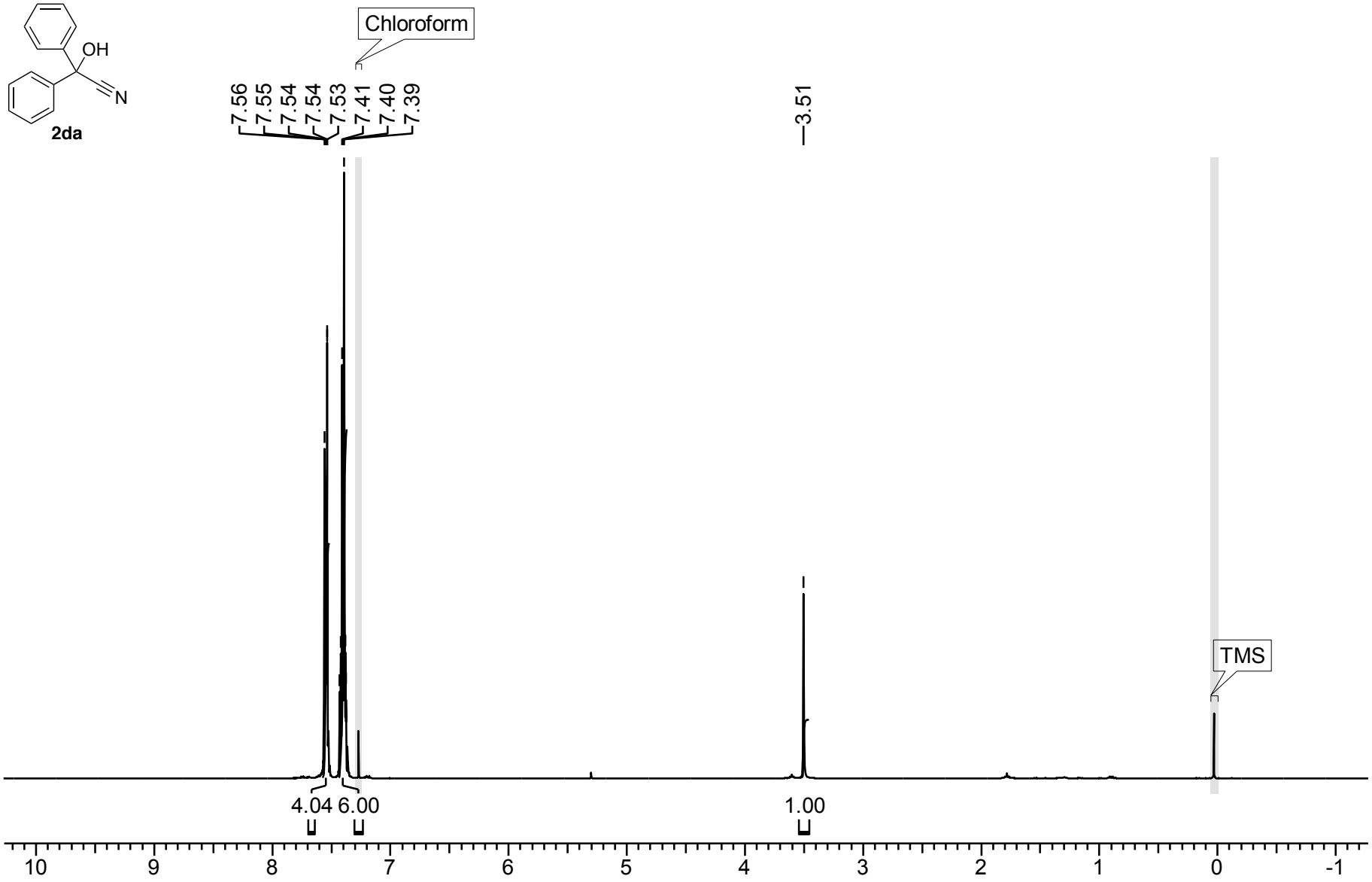

Figure S171. ^{1}H NMR (400 MHz, $CDCl_3$) spectrum of **2da**.

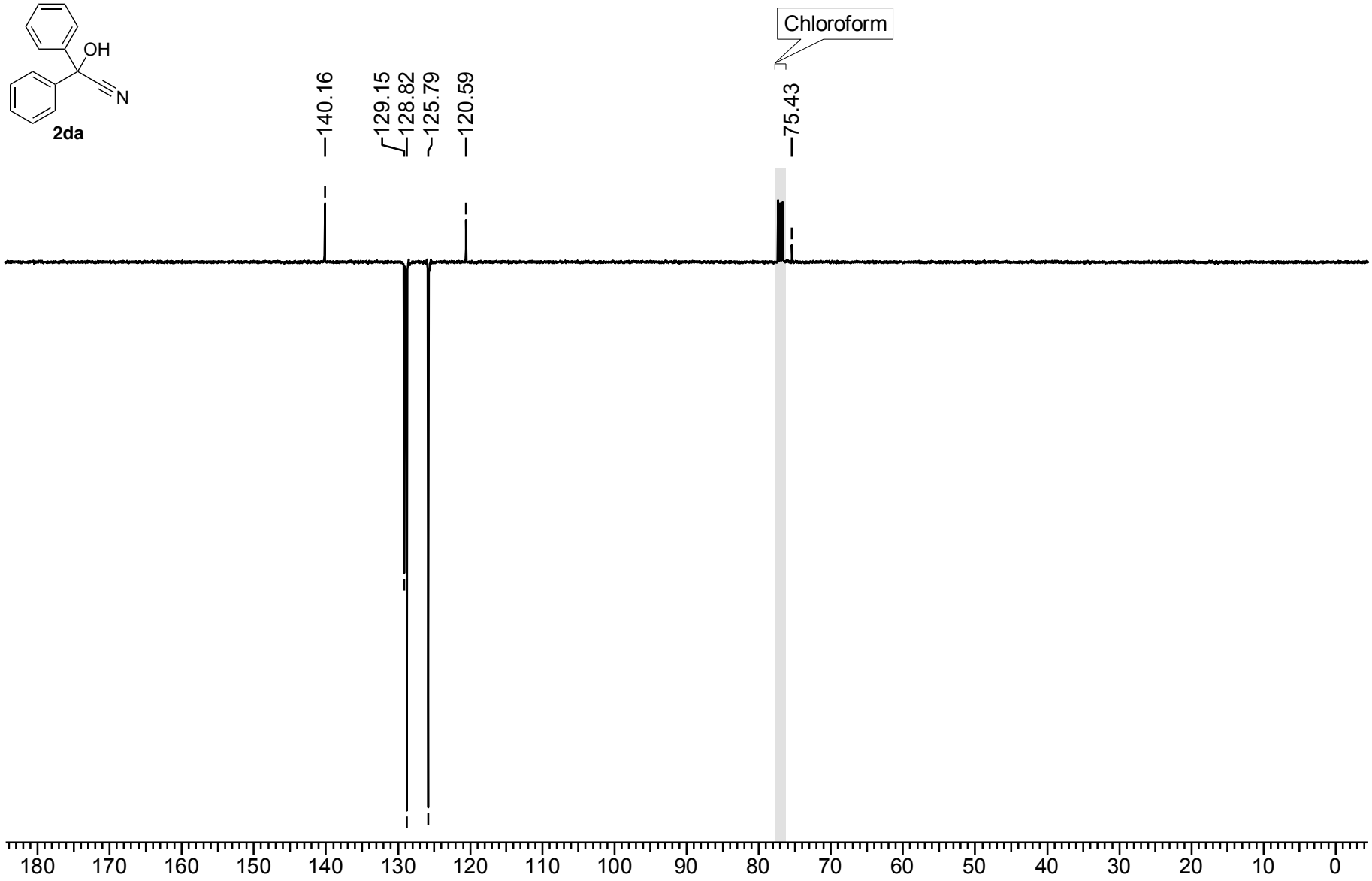

Figure S172. ^{13}C NMR APT (100 MHz, $CDCl_3$) spectrum of **2da**.

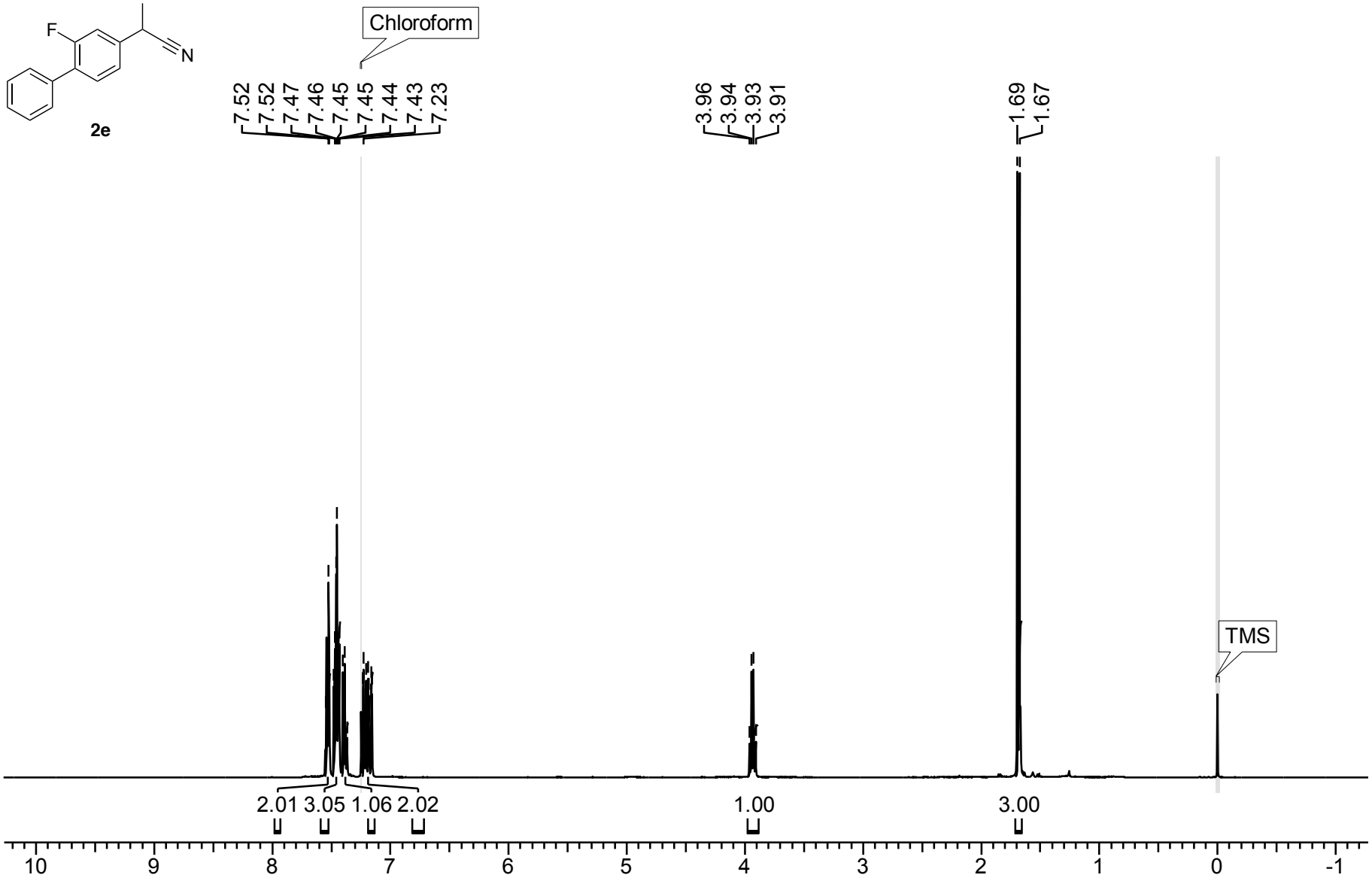

Figure S173. ^{1}H NMR (400 MHz, $CDCl_3$) spectrum of **2e**.

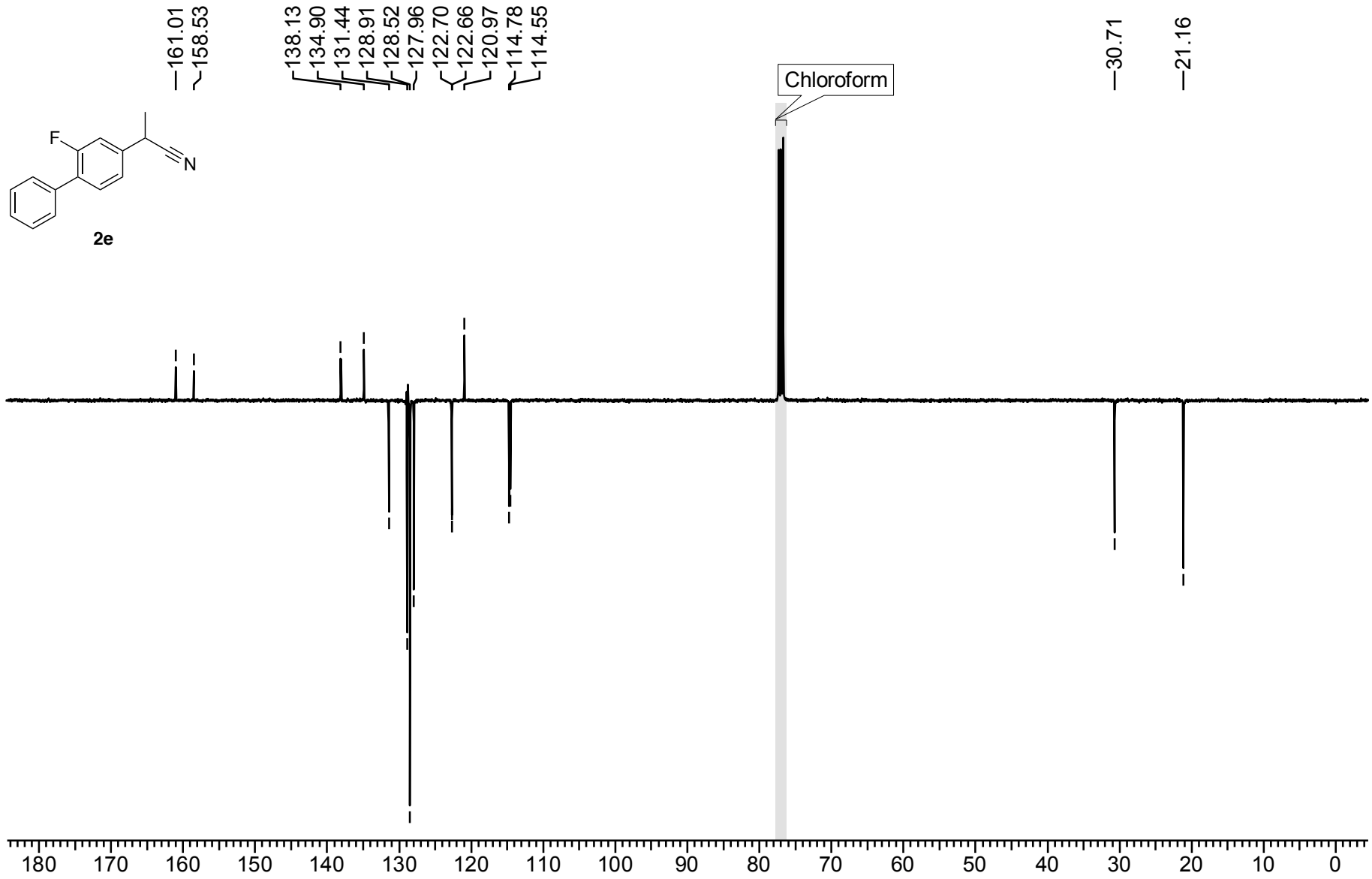

Figure S174. ^{13}C APT NMR (100 MHz, $CDCl_3$) spectrum of **2e**.

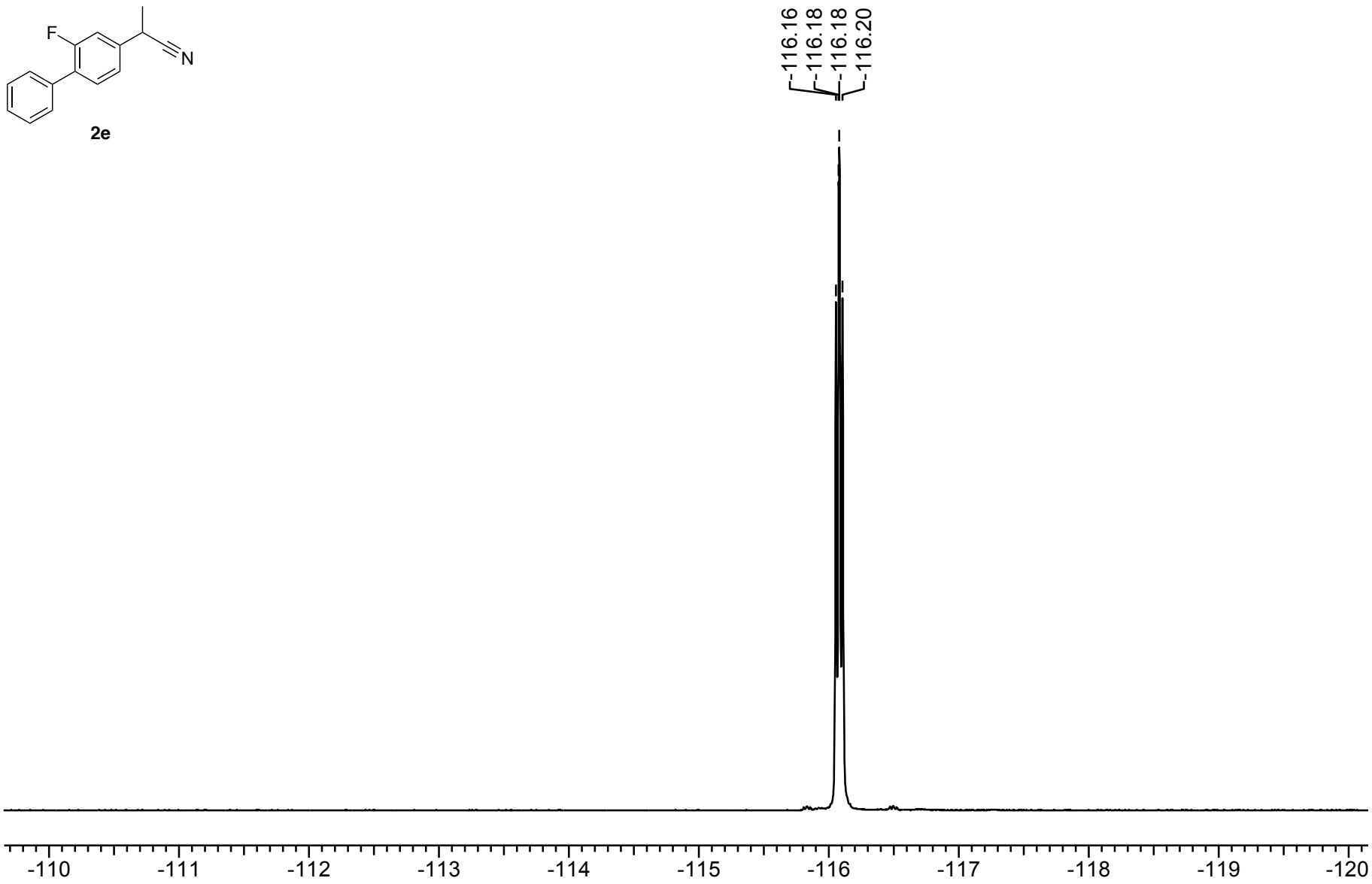

Figure S175. ^{19}F NMR (376 MHz, $CDCl_3$) spectrum of **2e**.

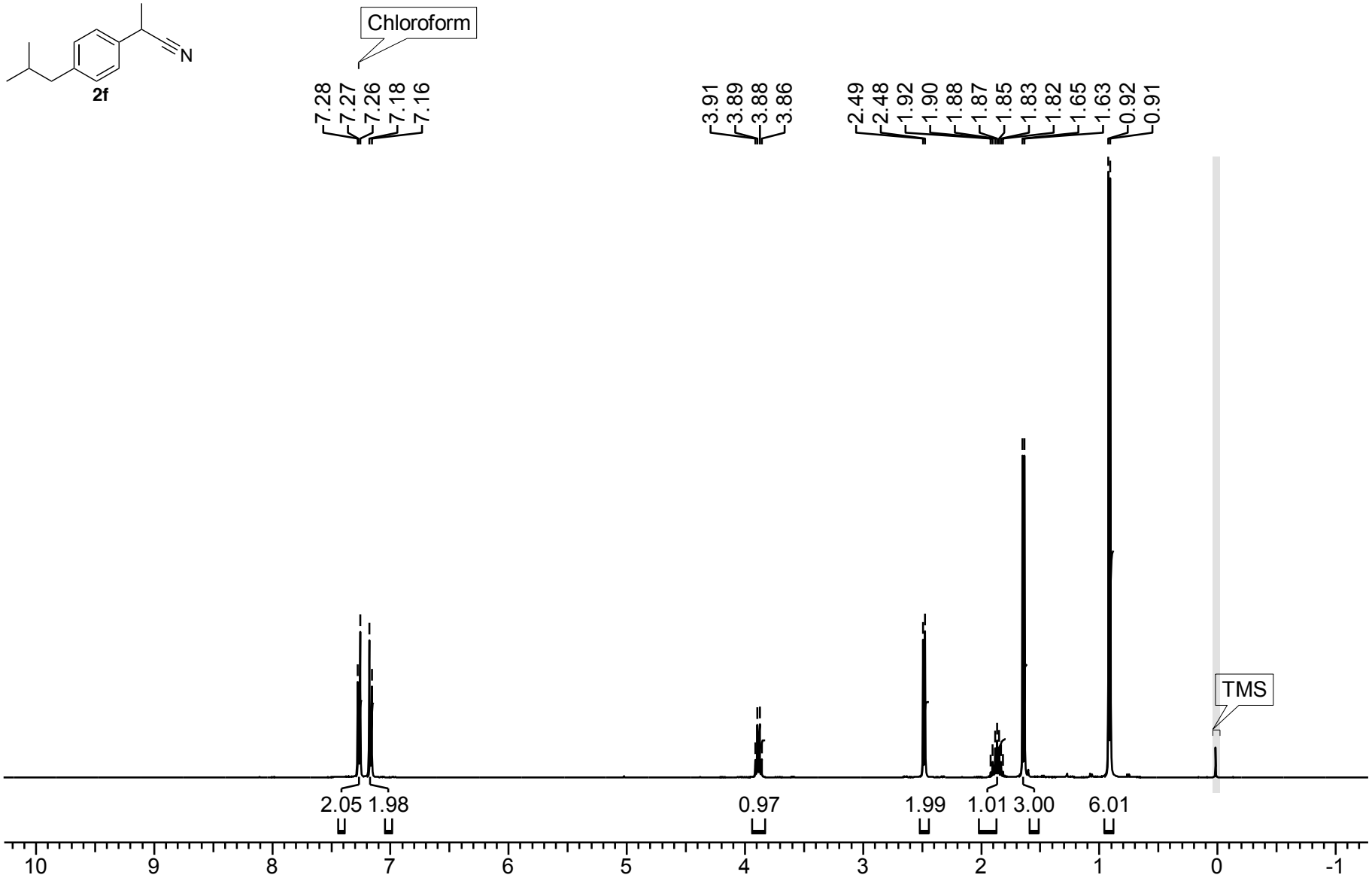

Figure S176. ^{1}H NMR (400 MHz, $CDCl_3$) spectrum of **2f**.

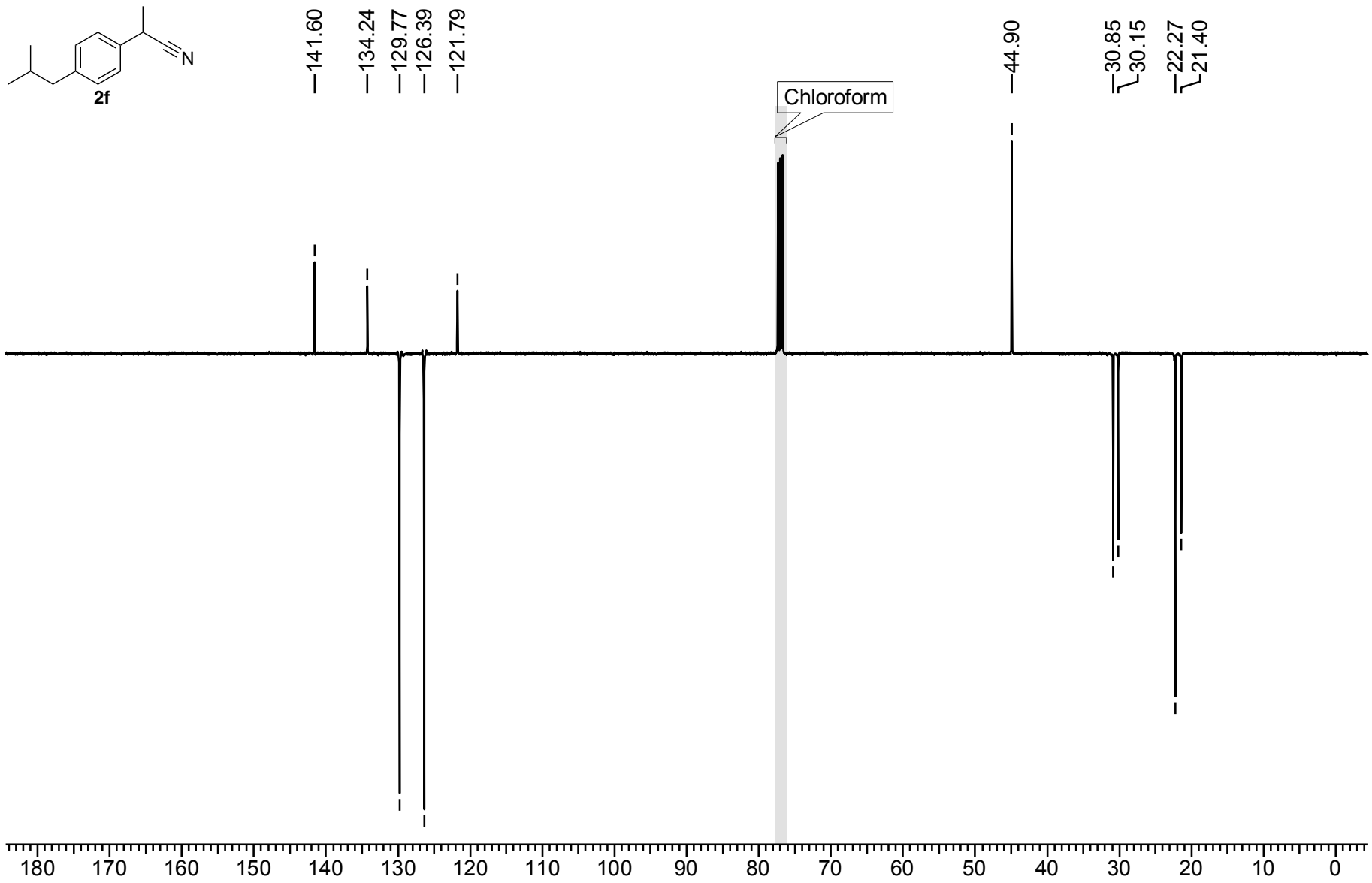

Figure S177. ^{13}C APT NMR (100 MHz, $CDCl_3$) spectrum of **2f**.

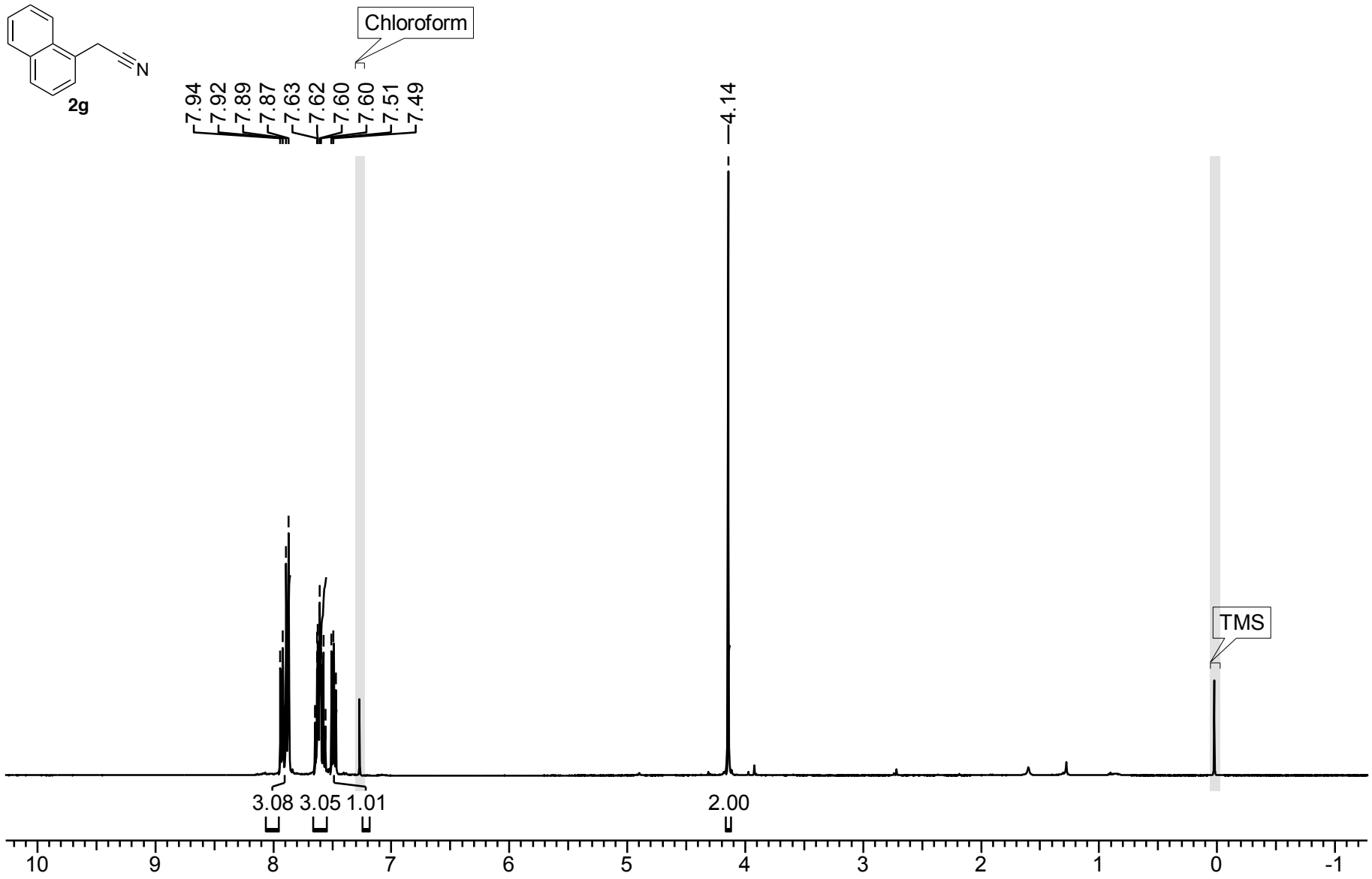

Figure S178. ^{1}H NMR (400 MHz, $CDCl_3$) spectrum of **2g**.

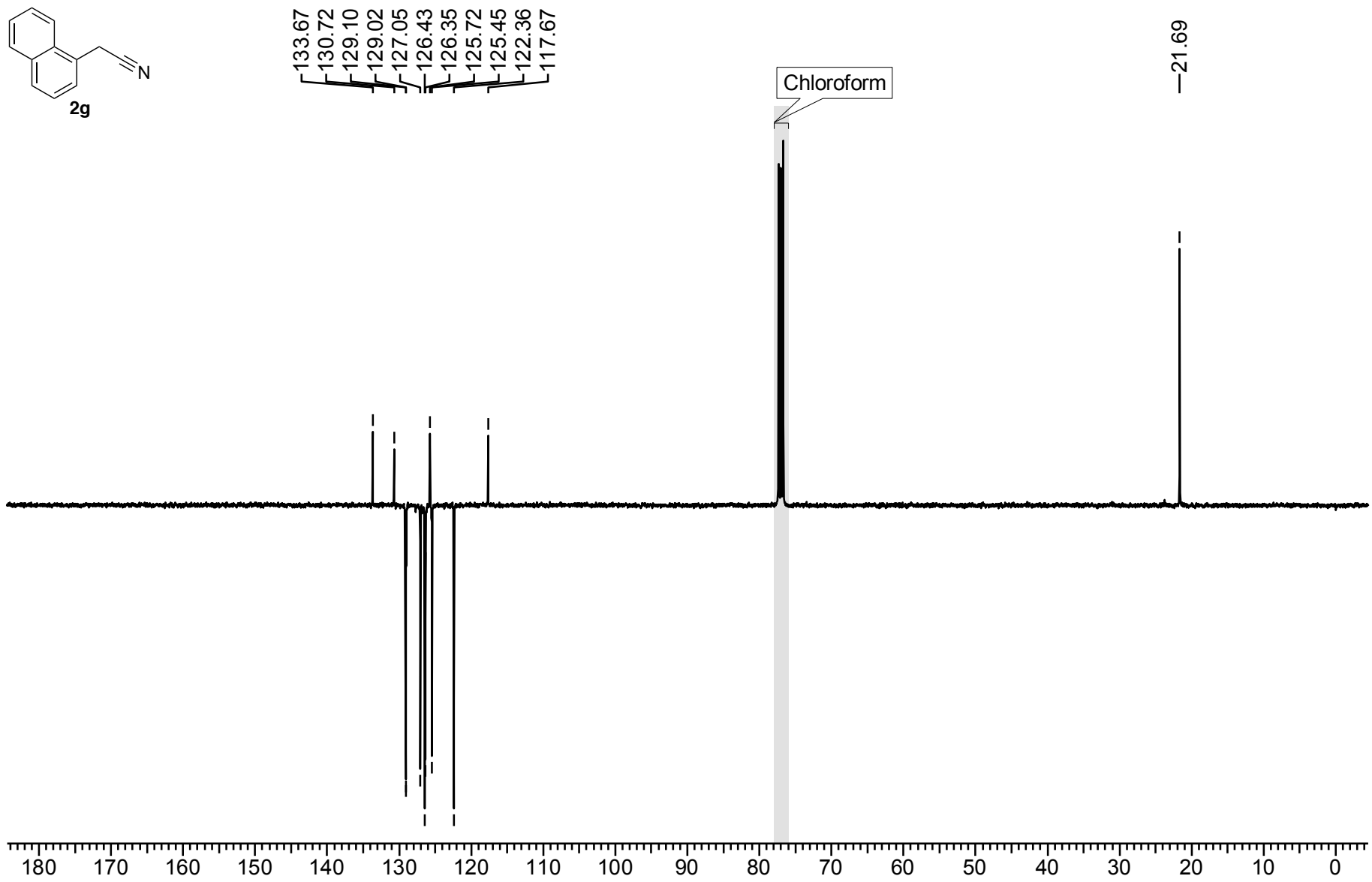

Figure S179. ^{13}C APT NMR (100 MHz, $CDCl_3$) spectrum of **2g**.

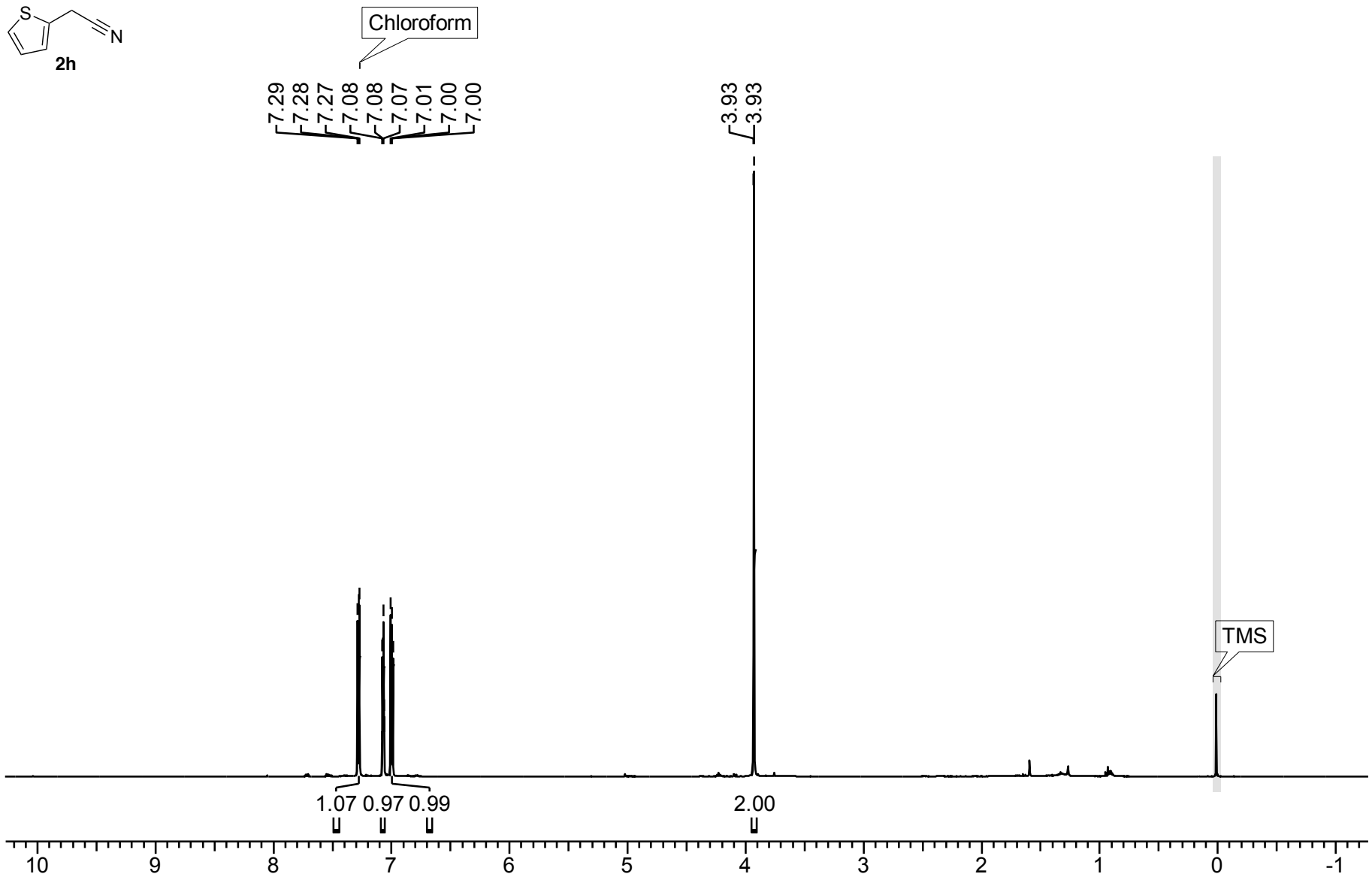

Figure S180. ^{1}H NMR (400 MHz, $CDCl_3$) spectrum of **2h**.

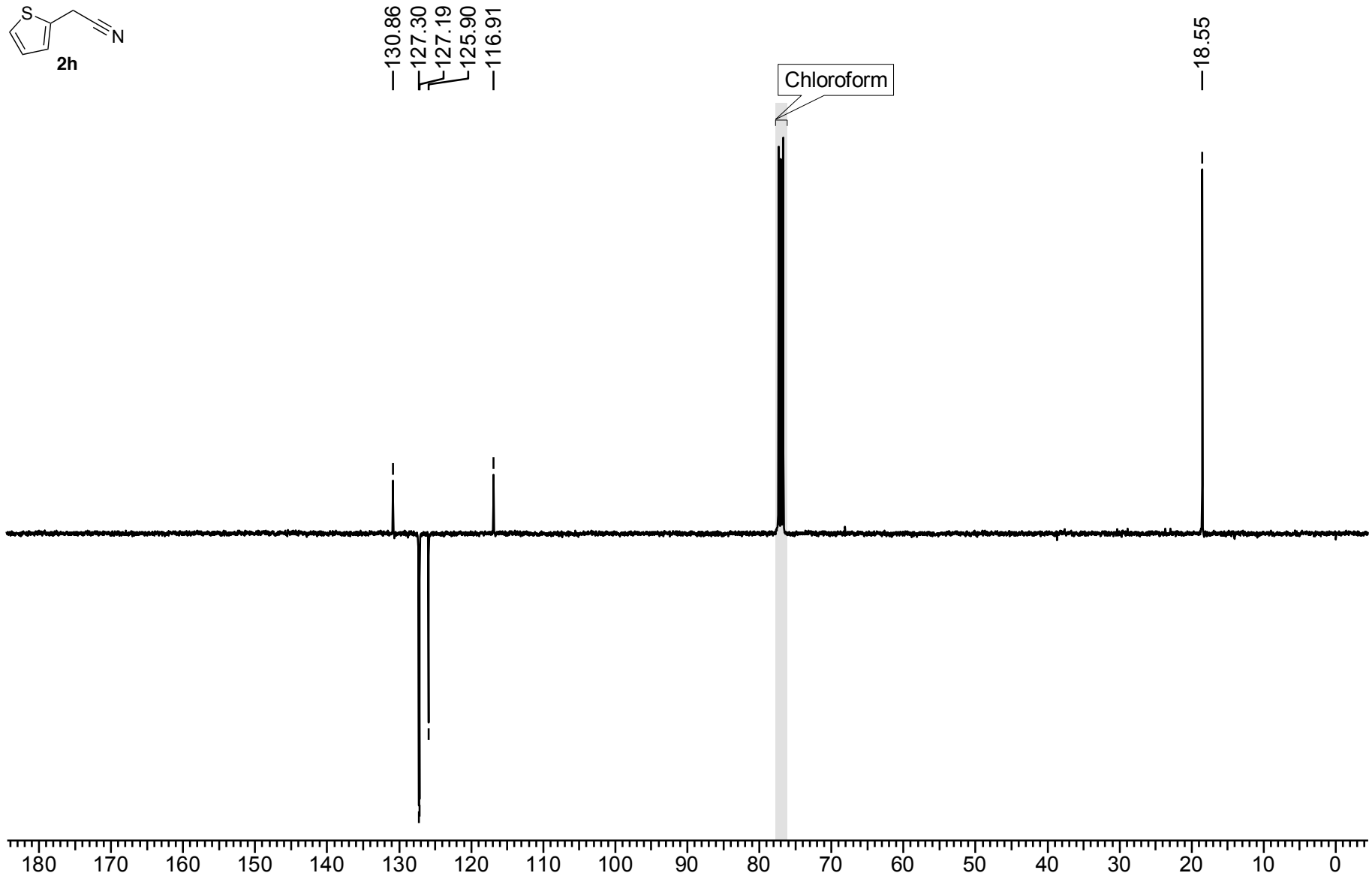

Figure S181. ^{13}C APT NMR (100 MHz, $CDCl_3$) spectrum of **2h**.

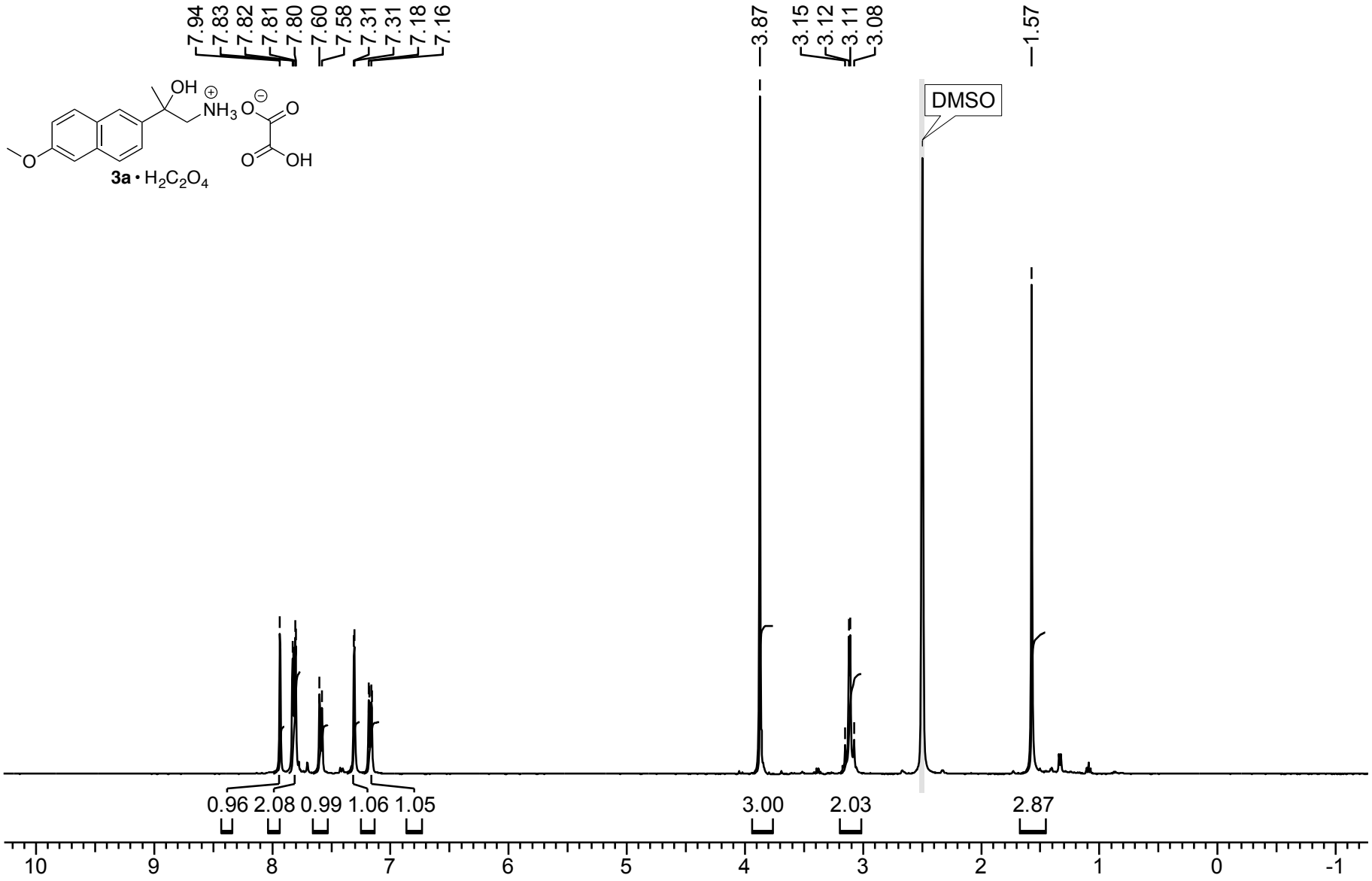

Figure S182. ^{1}H NMR (400 MHz, DMSO-d_6) spectrum of **3a** • $H_2C_2O_4$.

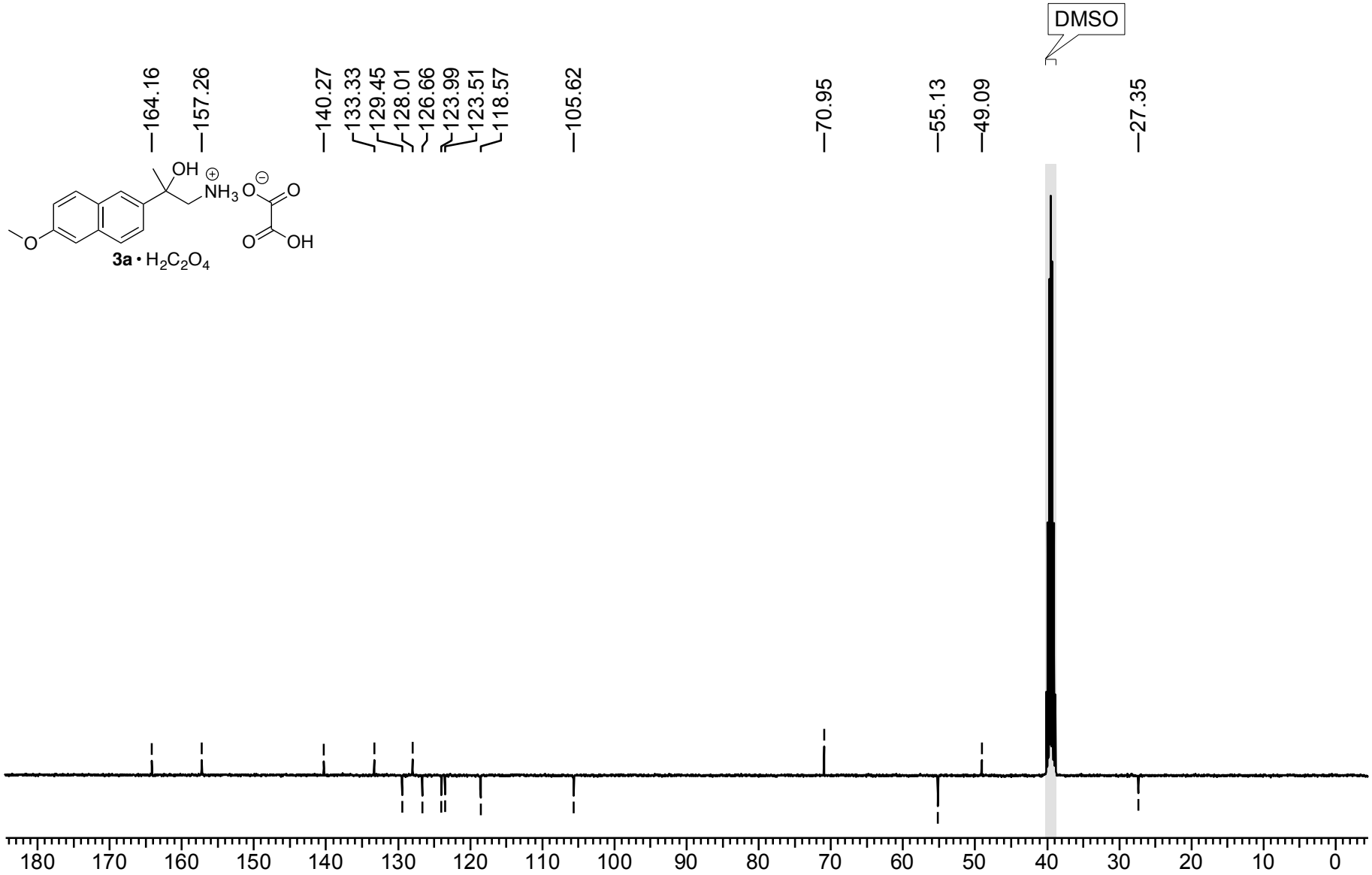

Figure S183. ^{13}C NMR APT (100 MHz, DMSO-d_6) spectrum of **3a** • $H_2C_2O_4$.

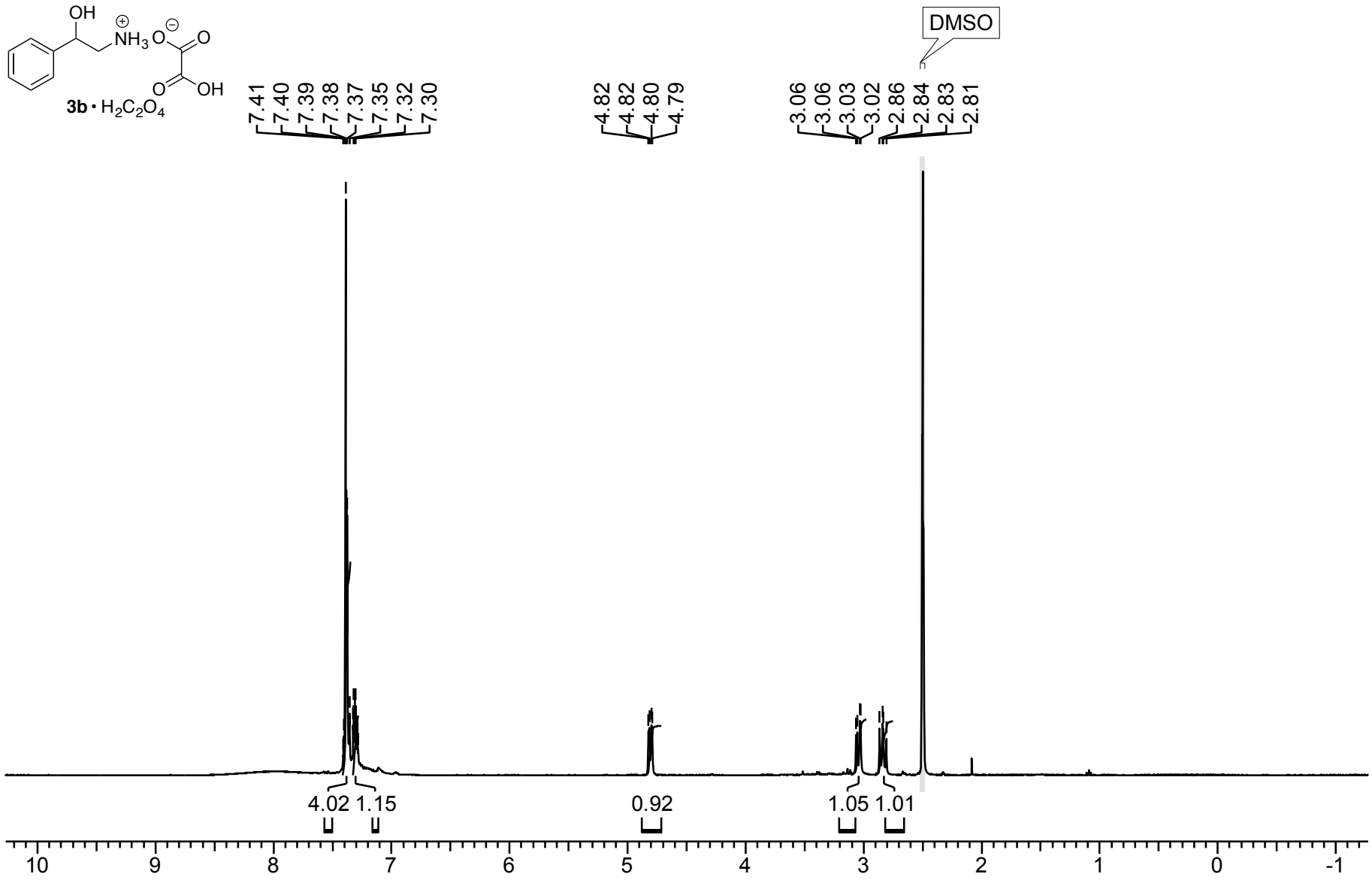

Figure S184. ^{1}H NMR (400 MHz, DMSO-d_6) spectrum of **3b** • $H_2C_2O_4$.

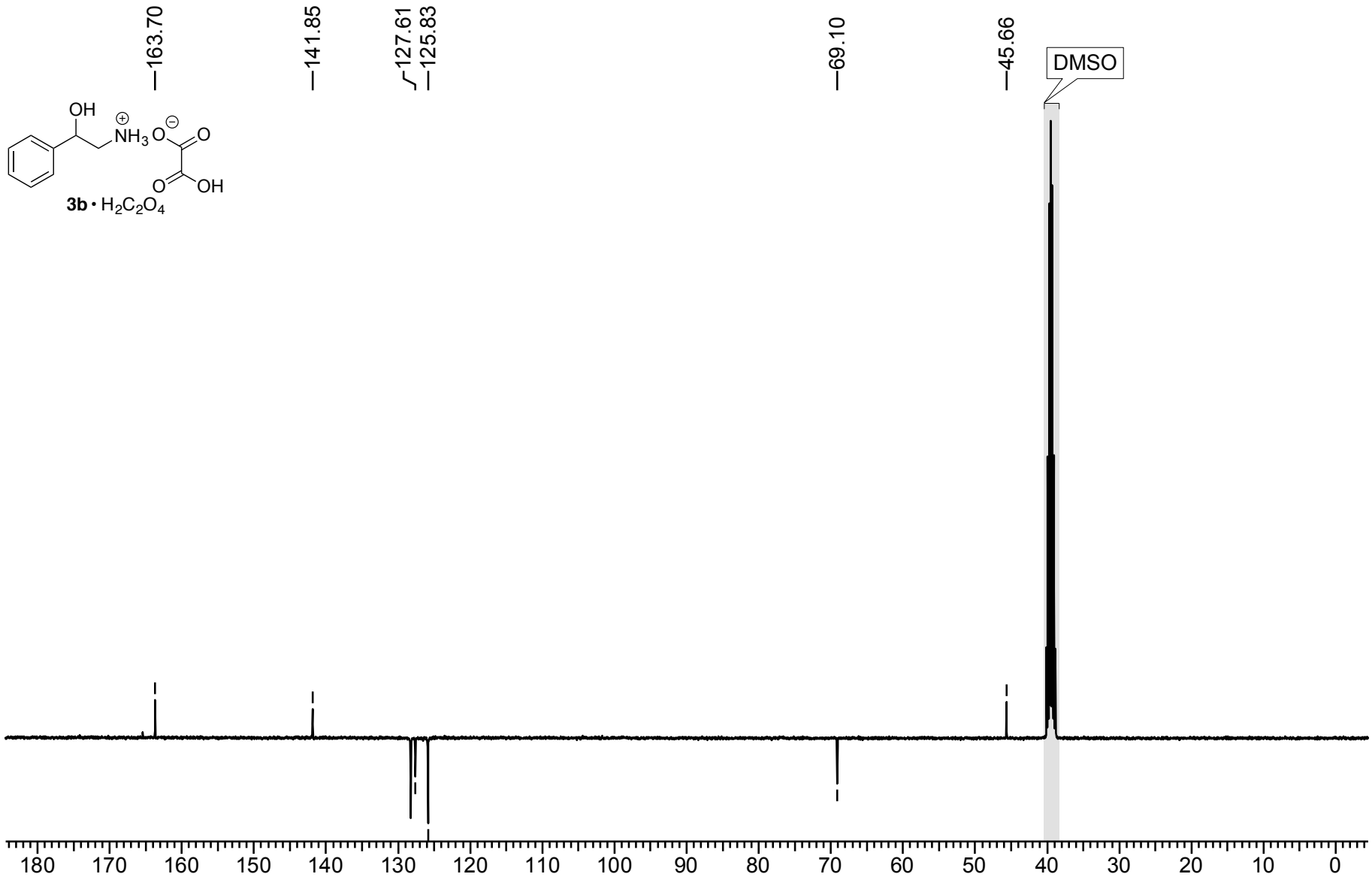

Figure S185. ^{13}C NMR APT (100 MHz, DMSO-d_6) spectrum of **3b** · $H_2C_2O_4$.

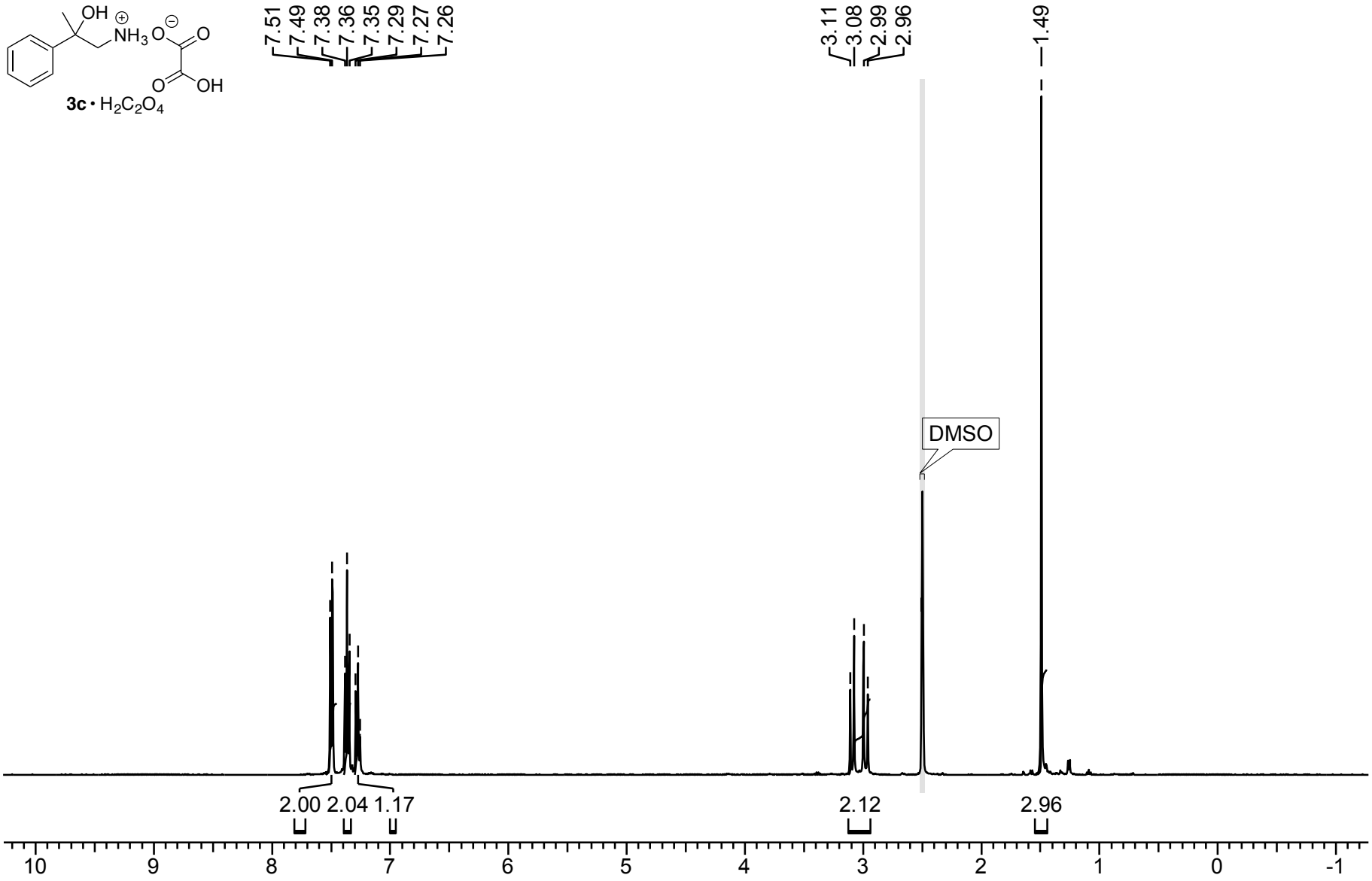

Figure S186. ^{1}H NMR (400 MHz, DMSO-d_6) spectrum of **3c** • $H_2C_2O_4$.

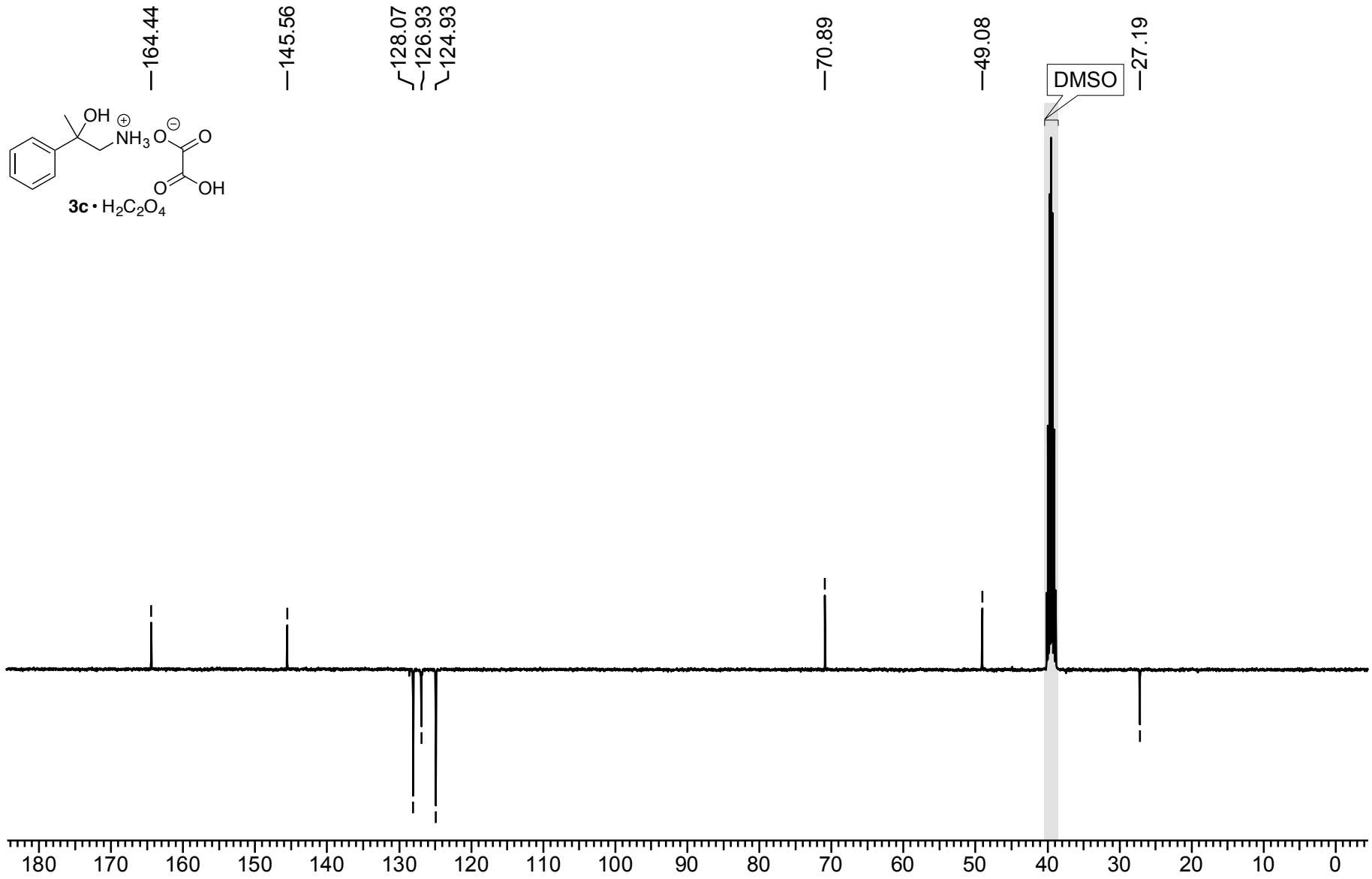

Figure S187. ^{13}C NMR APT (100 MHz, DMSO-d_6) spectrum of **3c** • $H_2C_2O_4$.

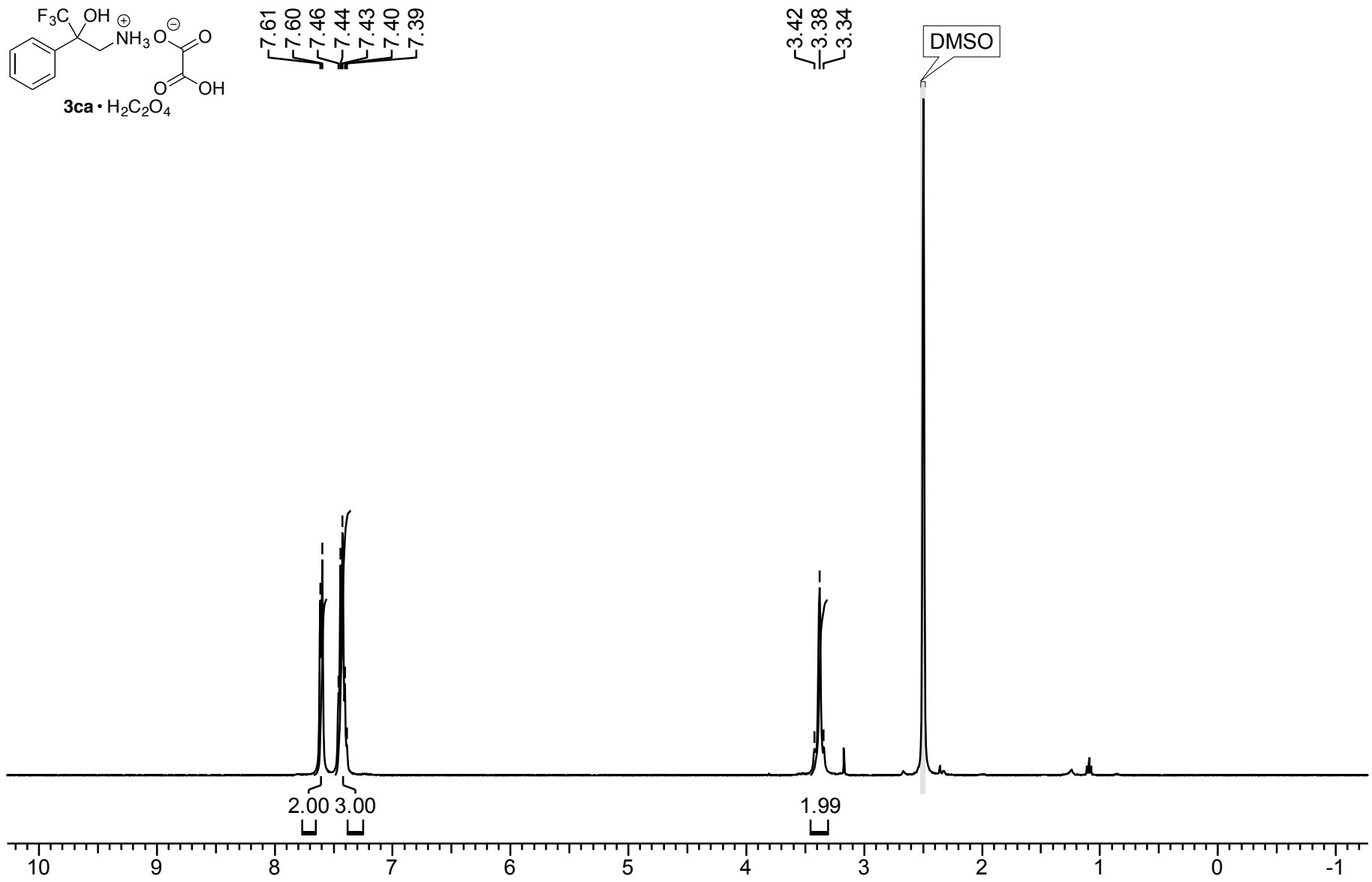

Figure S188. ^{1}H NMR (400 MHz, DMSO-d_6) spectrum of **3ca** · $H_2C_2O_4$.

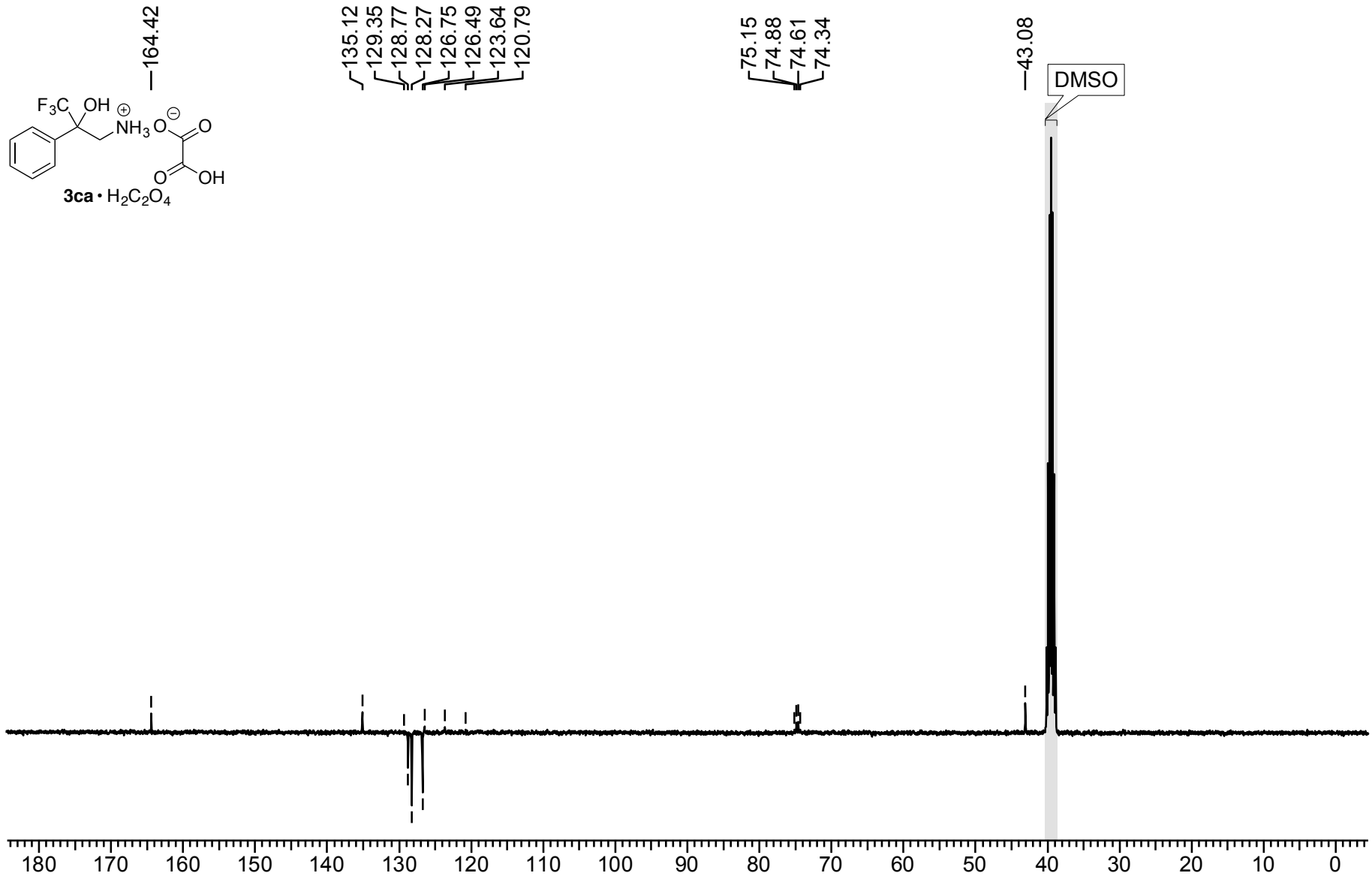

Figure S189. ^{13}C NMR APT (100 MHz, DMSO-d_6) spectrum of **3ca** · $H_2C_2O_4$.

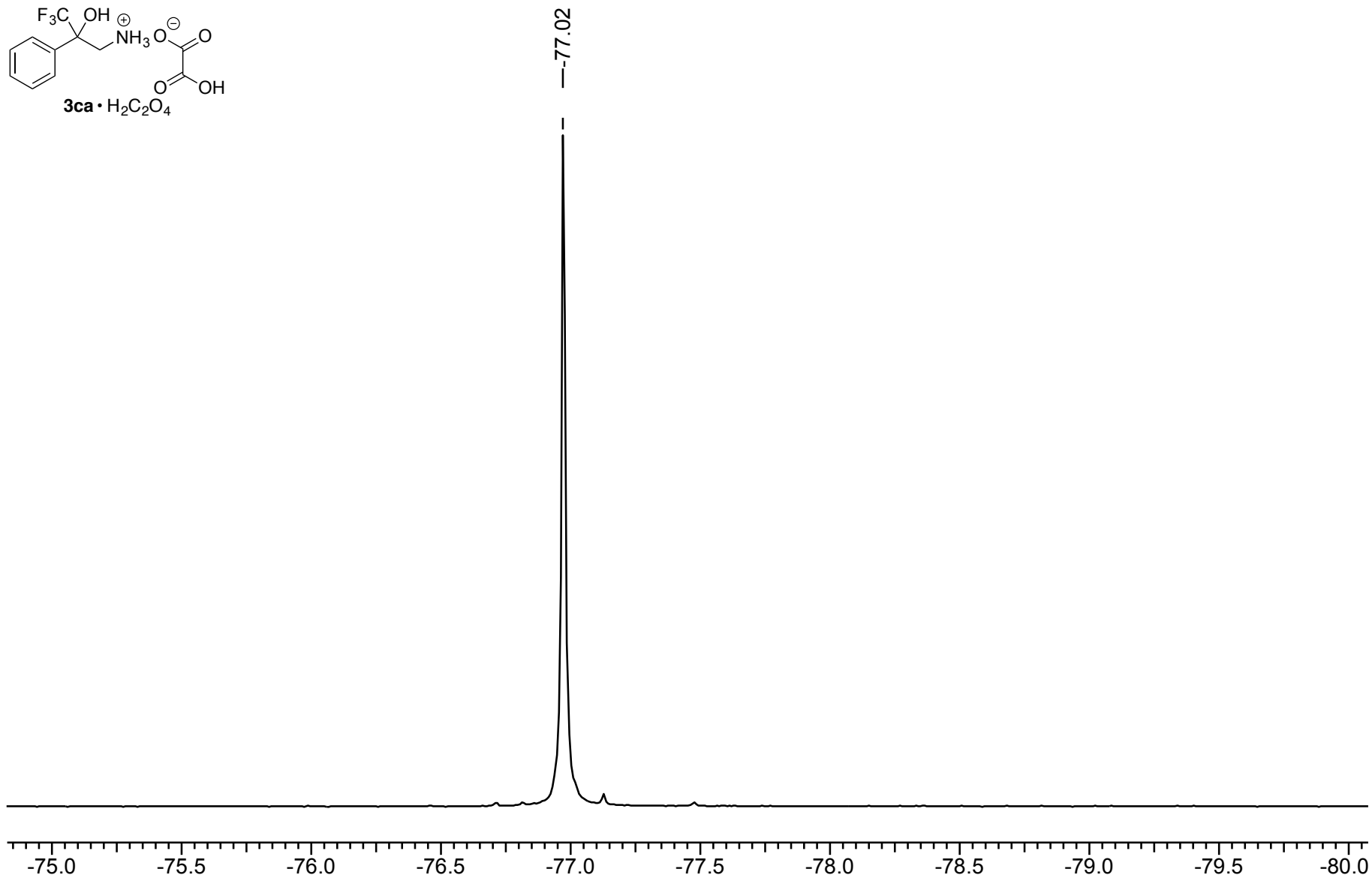

Figure S190. ^{19}F NMR (376 MHz, DMSO-d_6) spectrum of **3ca** · $H_2C_2O_4$.

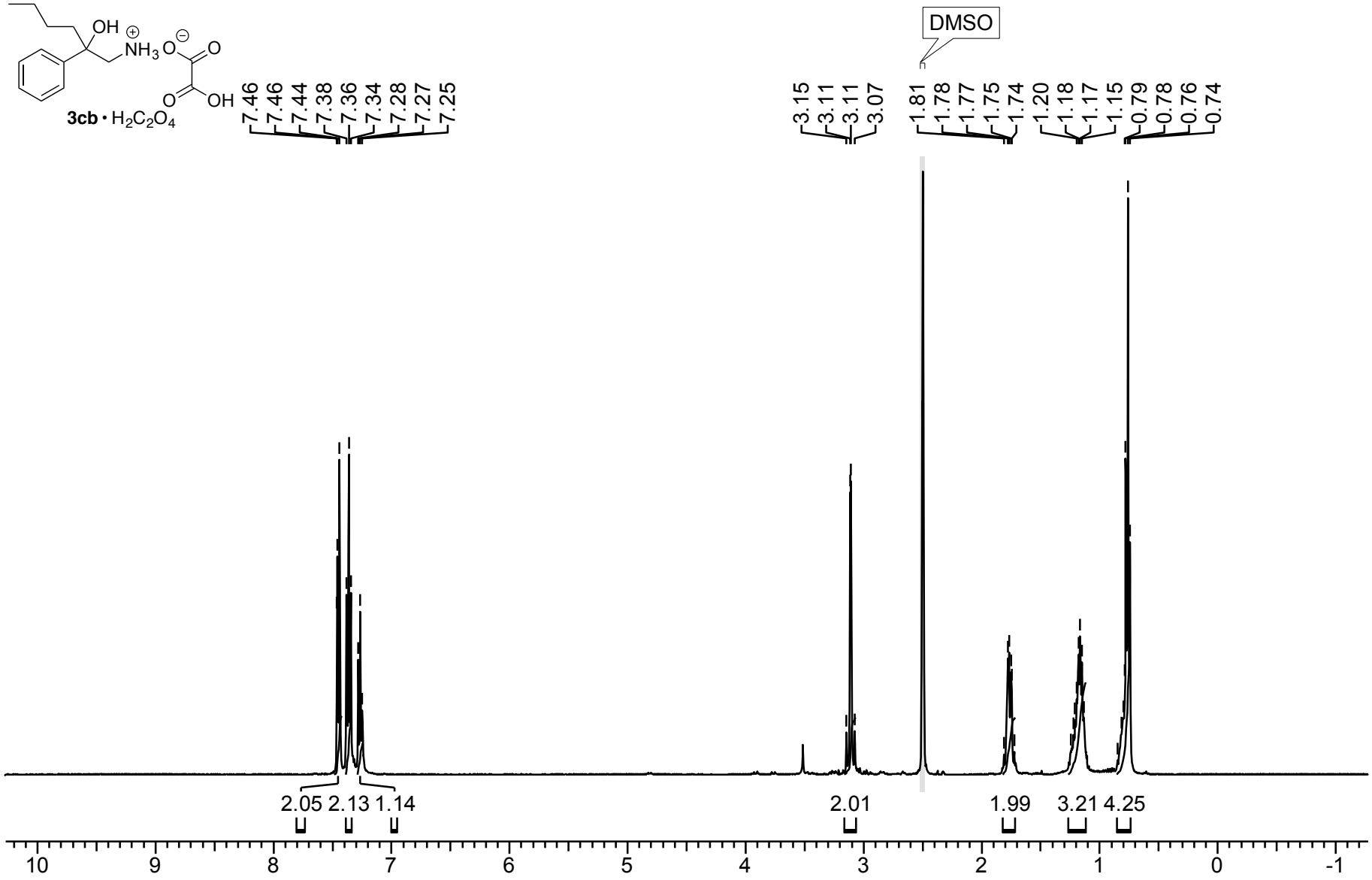

Figure S191. ^{1}H NMR (400 MHz, DMSO-d_6) spectrum of **3cb** • $H_2C_2O_4$.

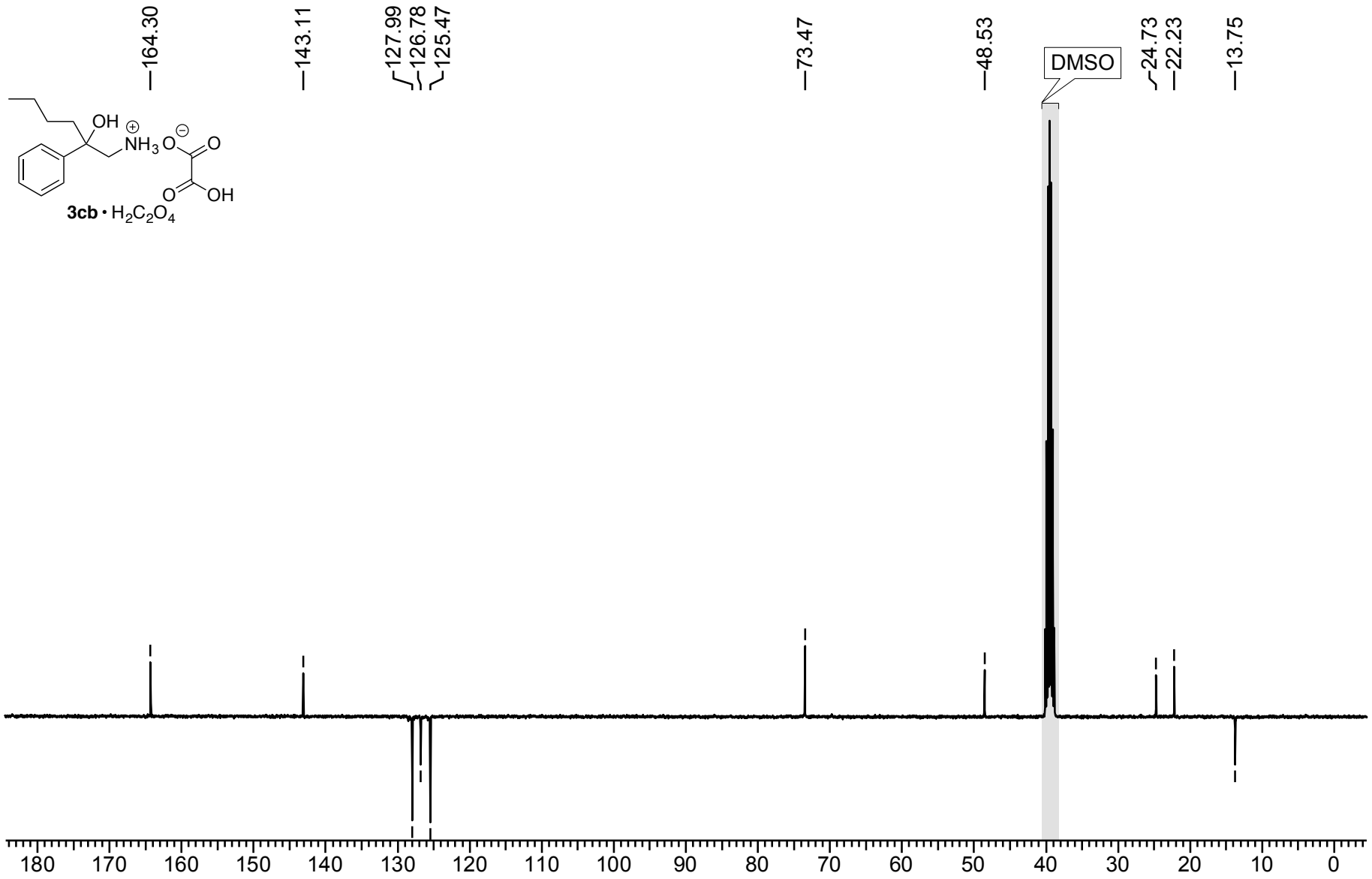

Figure S192. ^{13}C NMR APT (100 MHz, DMSO-d_6) spectrum of **3cb** · $H_2C_2O_4$.

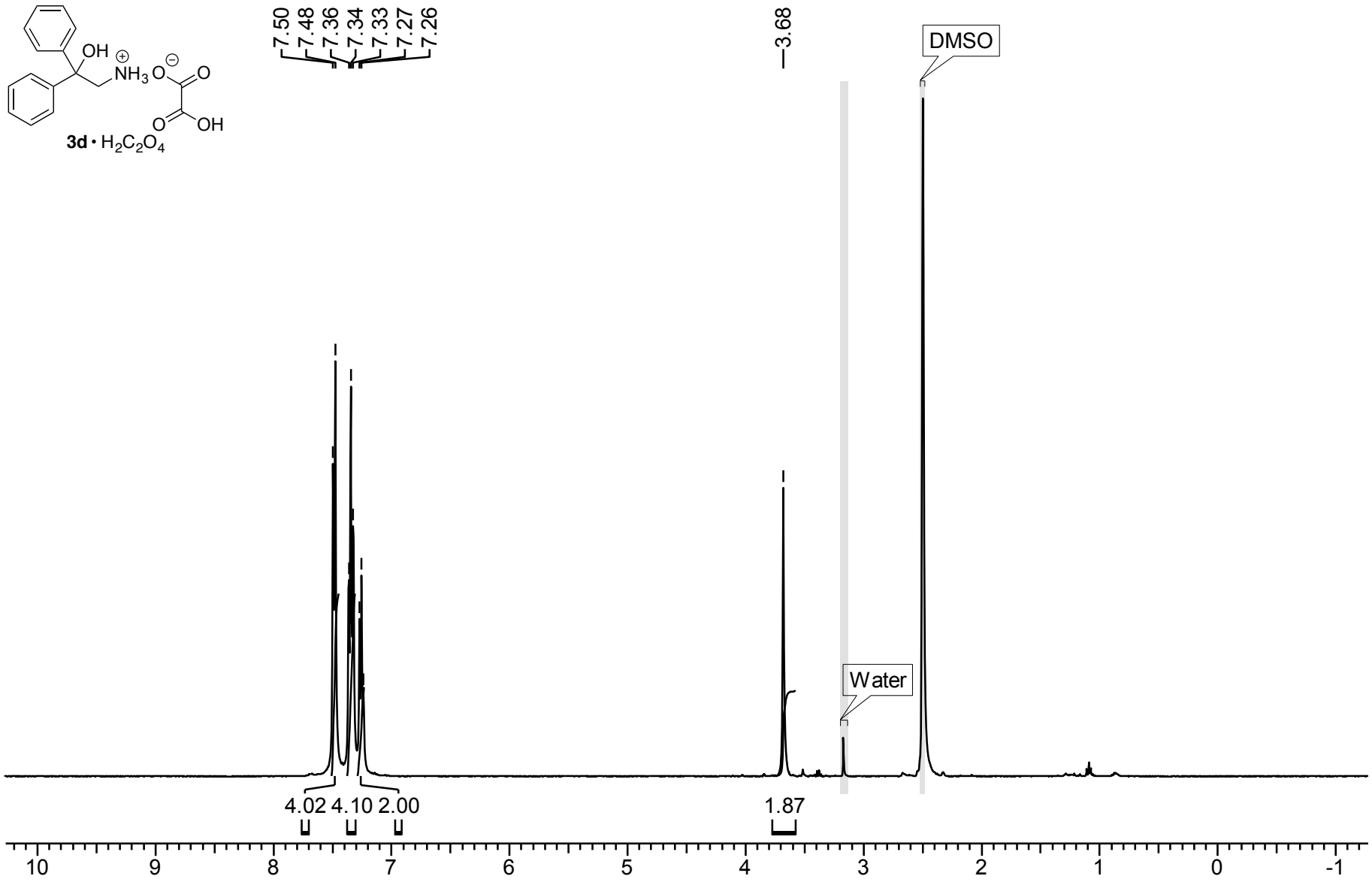

Figure S193. ^{1}H NMR (400 MHz, DMSO-d_6) spectrum of **3d** · $H_2C_2O_4$.

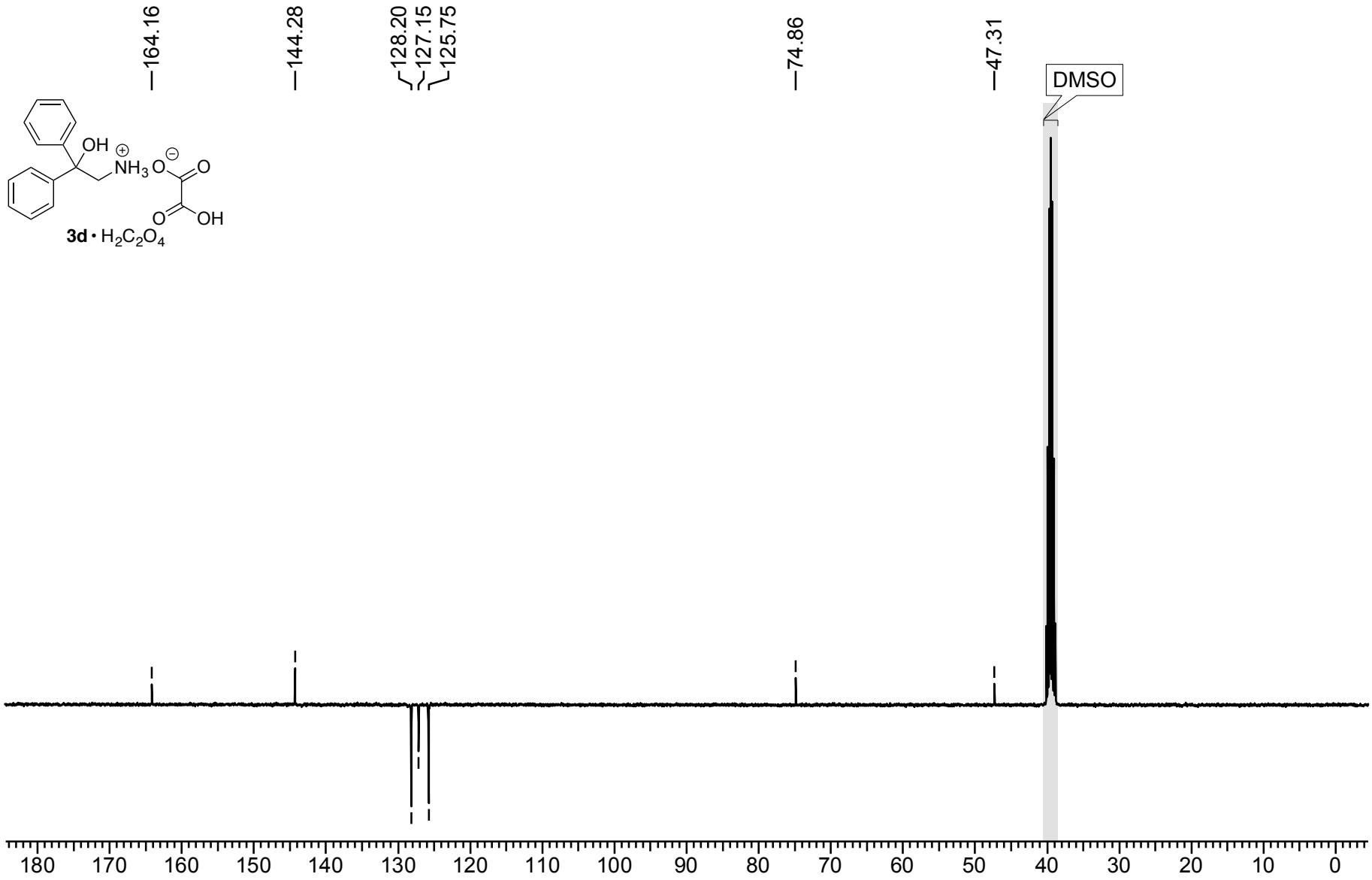

Figure S194. ^{13}C NMR APT (100 MHz, DMSO-d_6) spectrum of **3d** · $H_2C_2O_4$.

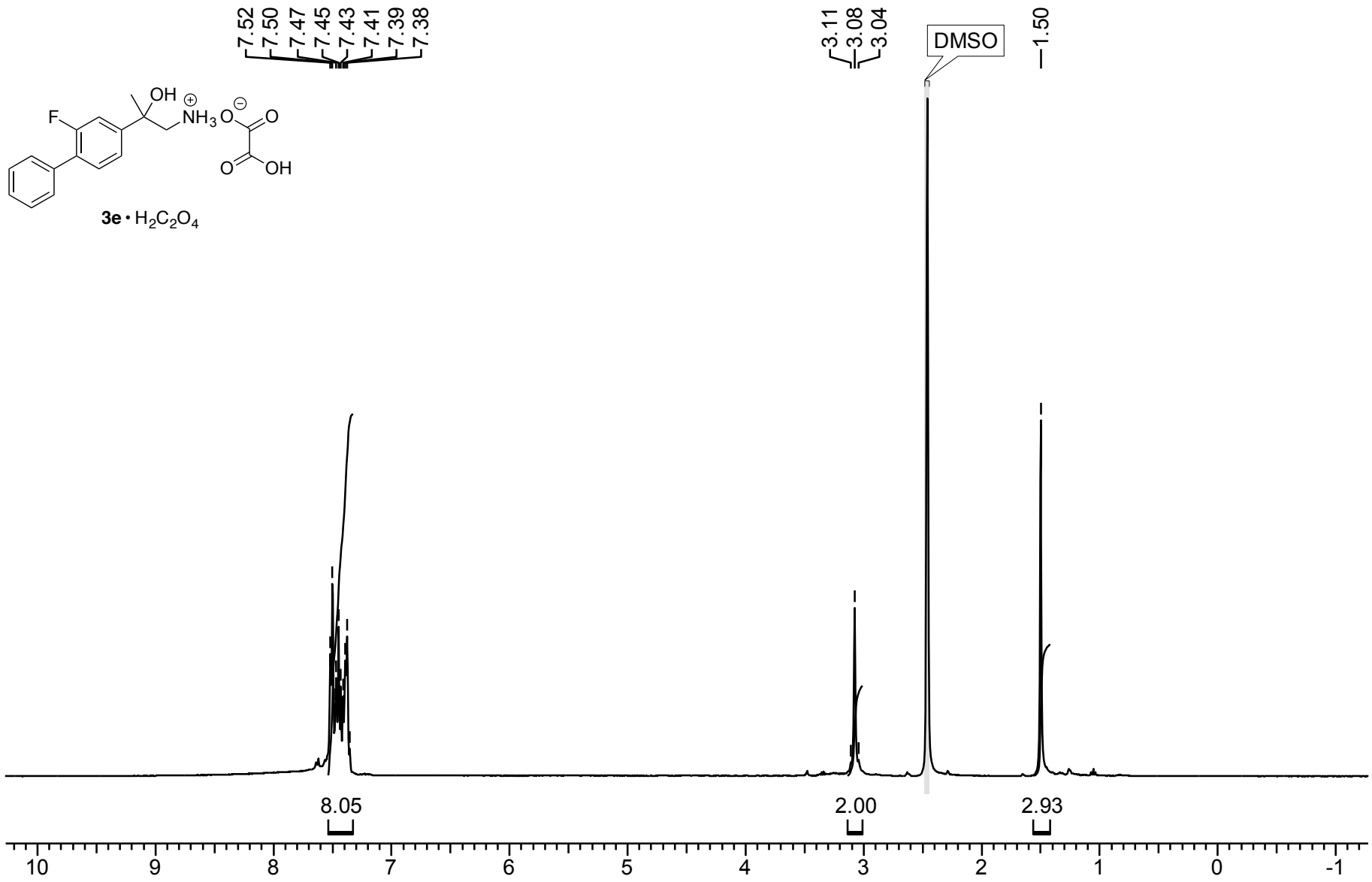

Figure S195. ^{1}H NMR (400 MHz, DMSO-d_6) spectrum of **3e**• $H_2C_2O_4$.

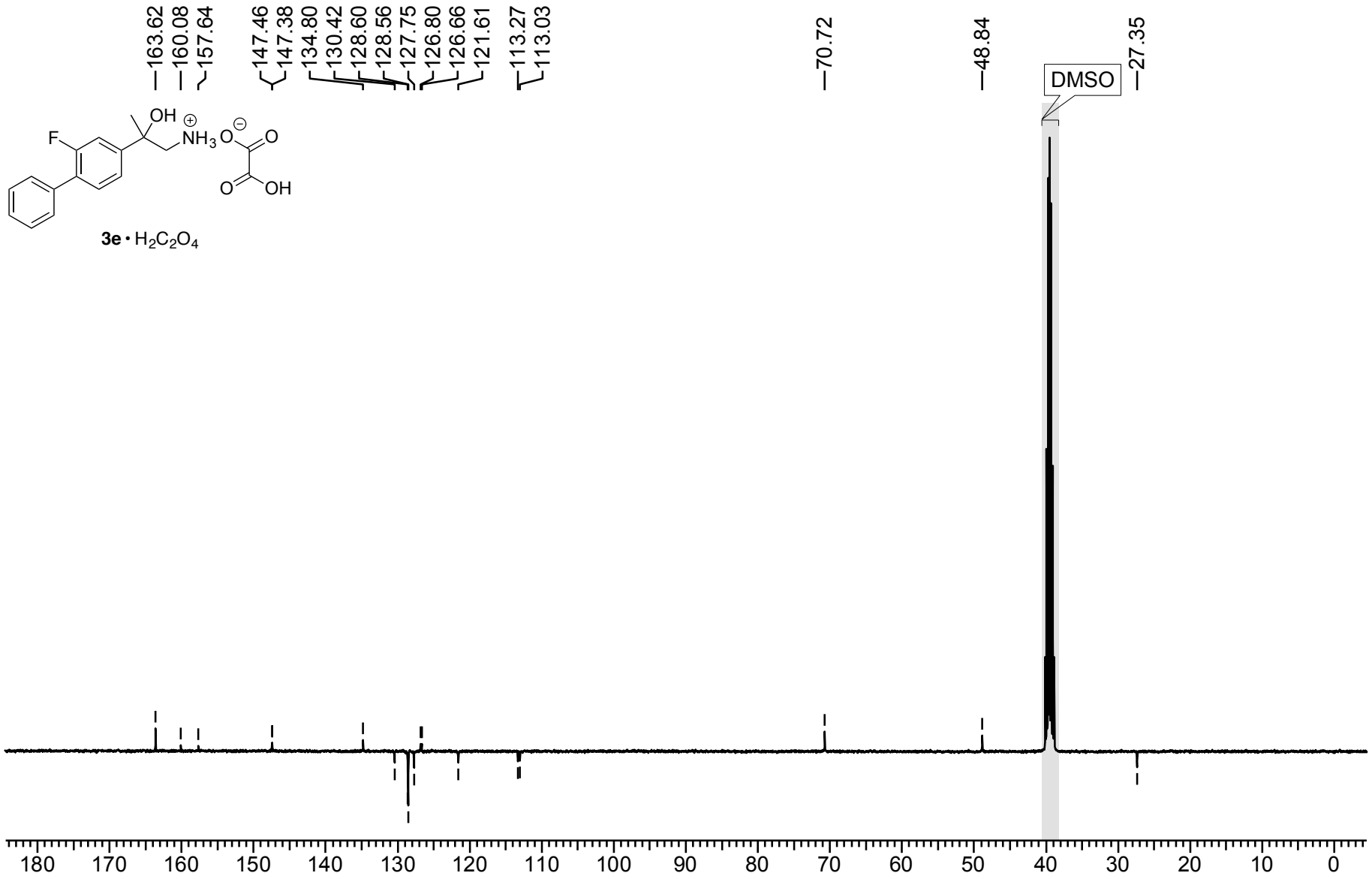

Figure S196. ^{13}C NMR APT (100 MHz, DMSO-d_6) spectrum of **3e** • $H_2C_2O_4$.

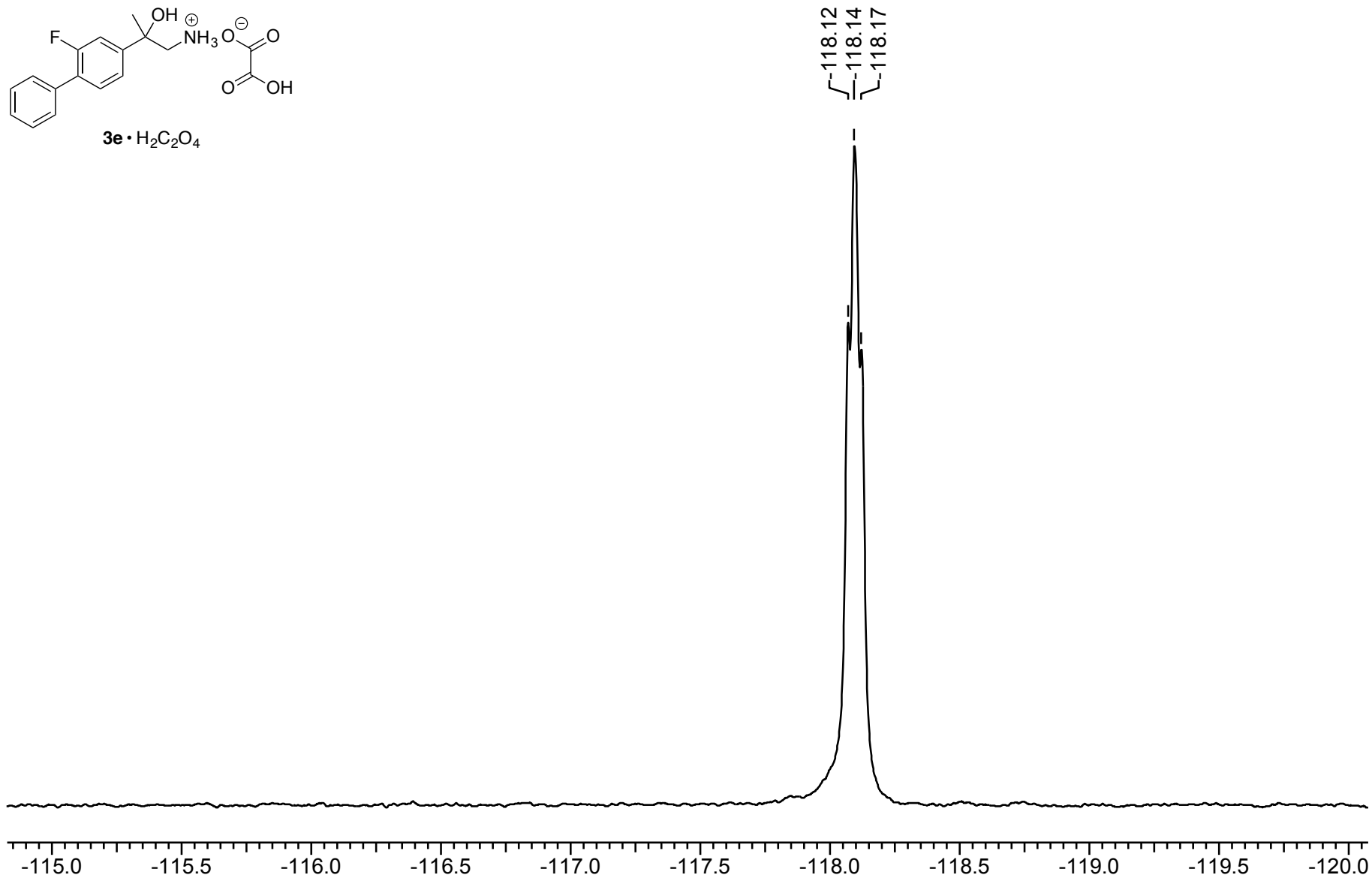

Figure S197. ^{19}F NMR (376 MHz, DMSO-d_6) spectrum of **3e** • $H_2C_2O_4$.

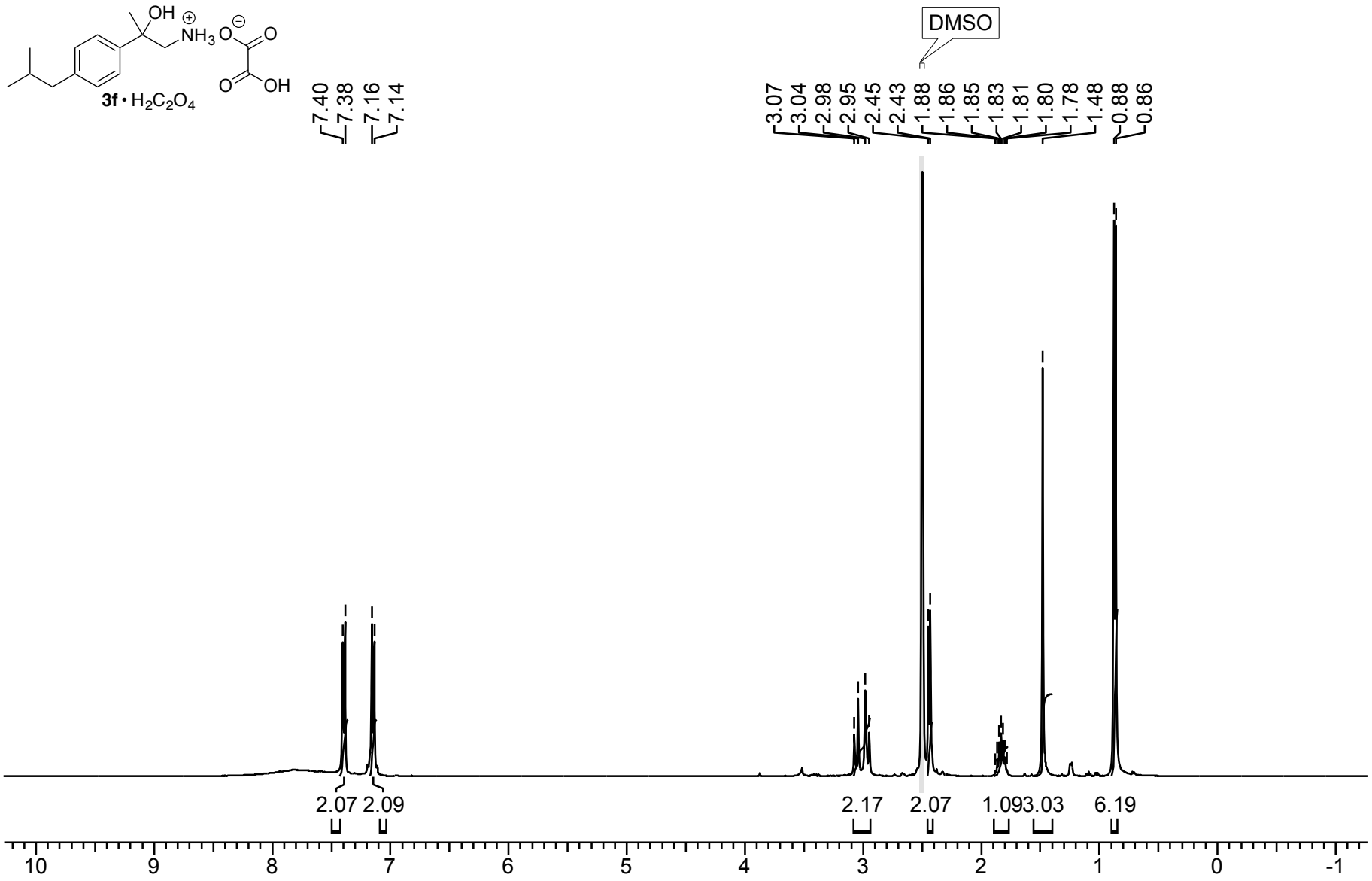

Figure S198. ^{1}H NMR (400 MHz, DMSO-d_6) spectrum of **3f**• $H_2C_2O_4$.

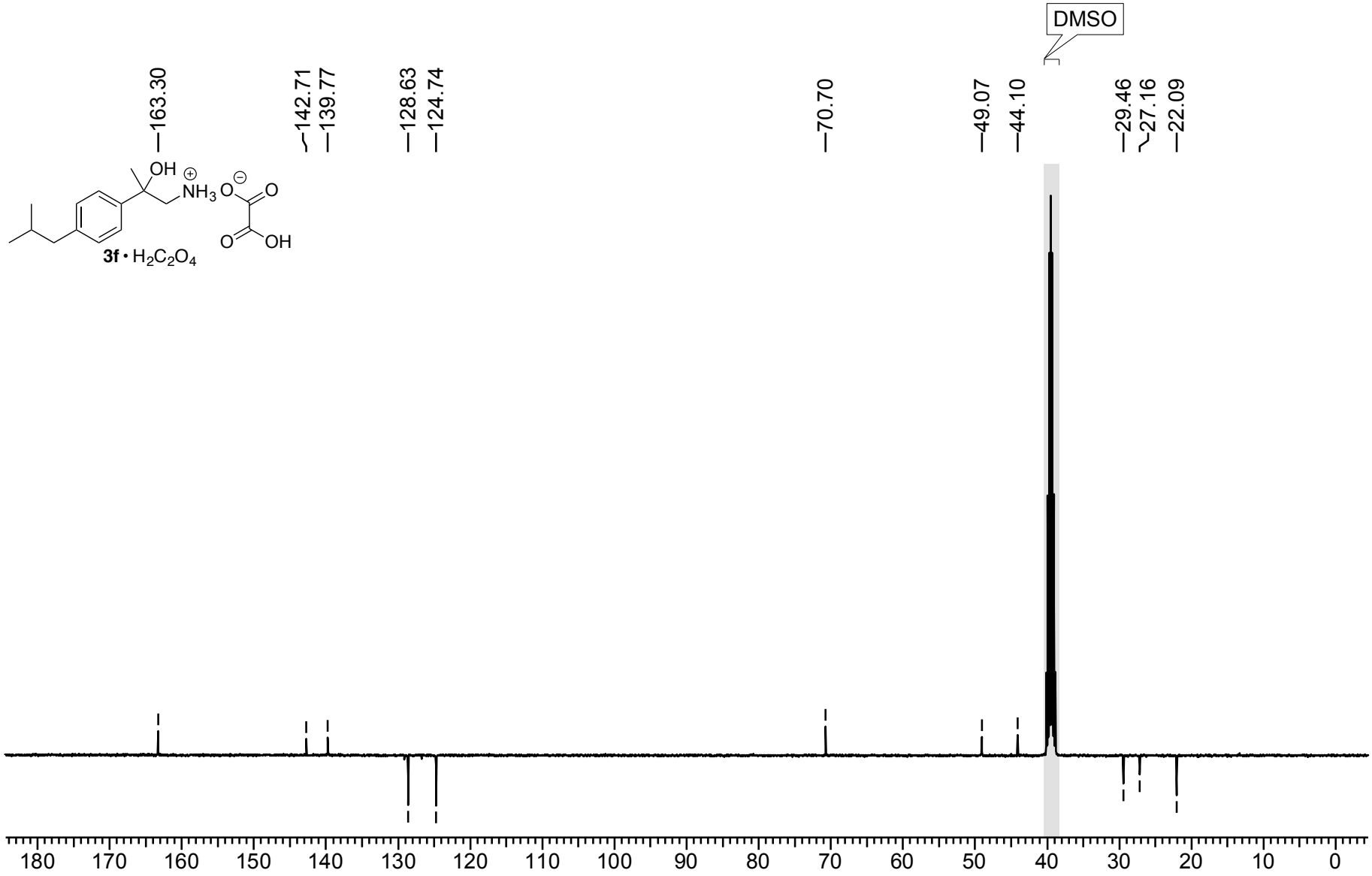

Figure S199. ^{13}C NMR APT (100 MHz, DMSO-d_6) spectrum of **3f**• $H_2C_2O_4$.

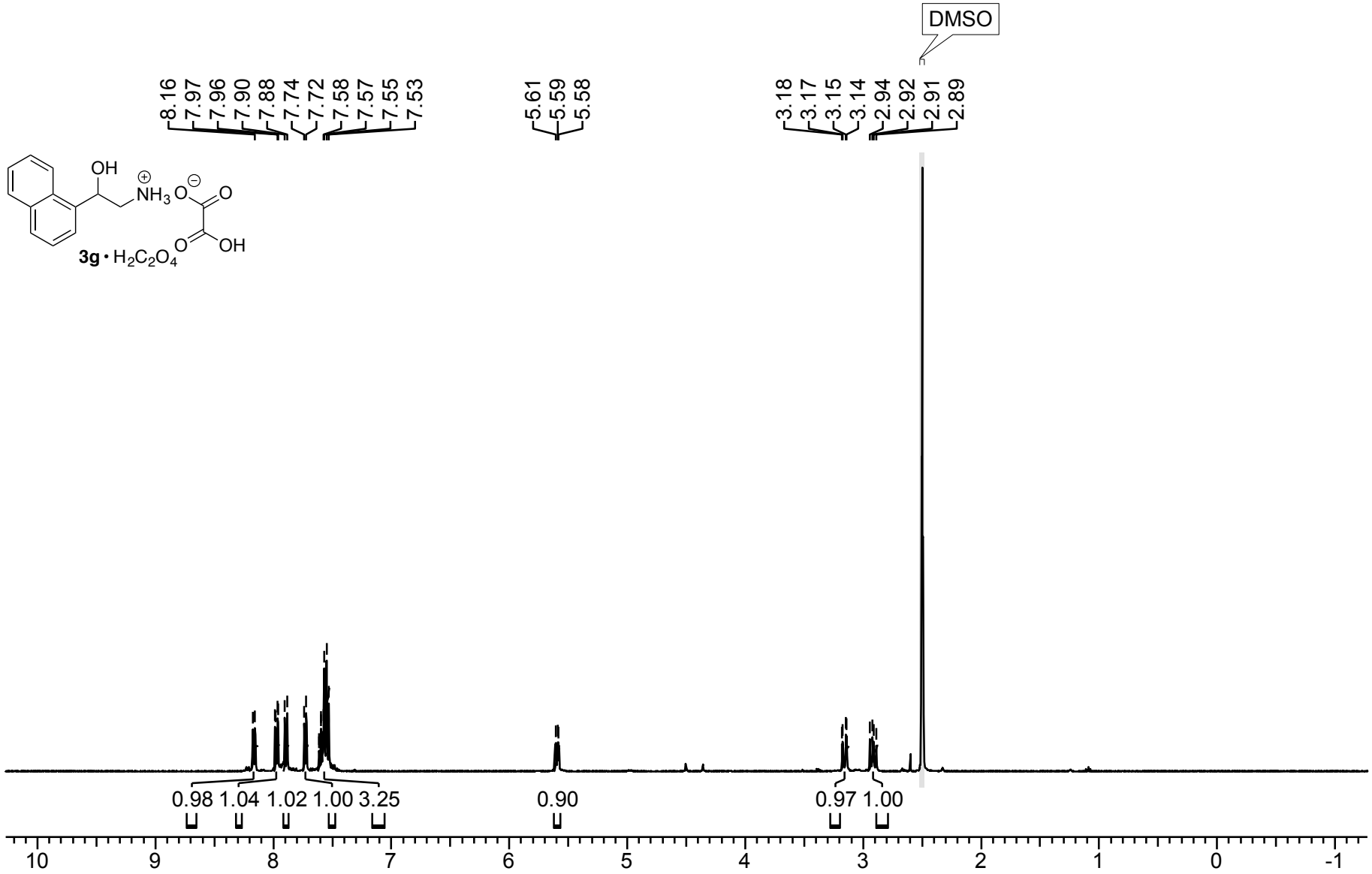

Figure S200. ^{1}H NMR (400 MHz, DMSO-d_6) spectrum of **3g** • $H_2C_2O_4$.

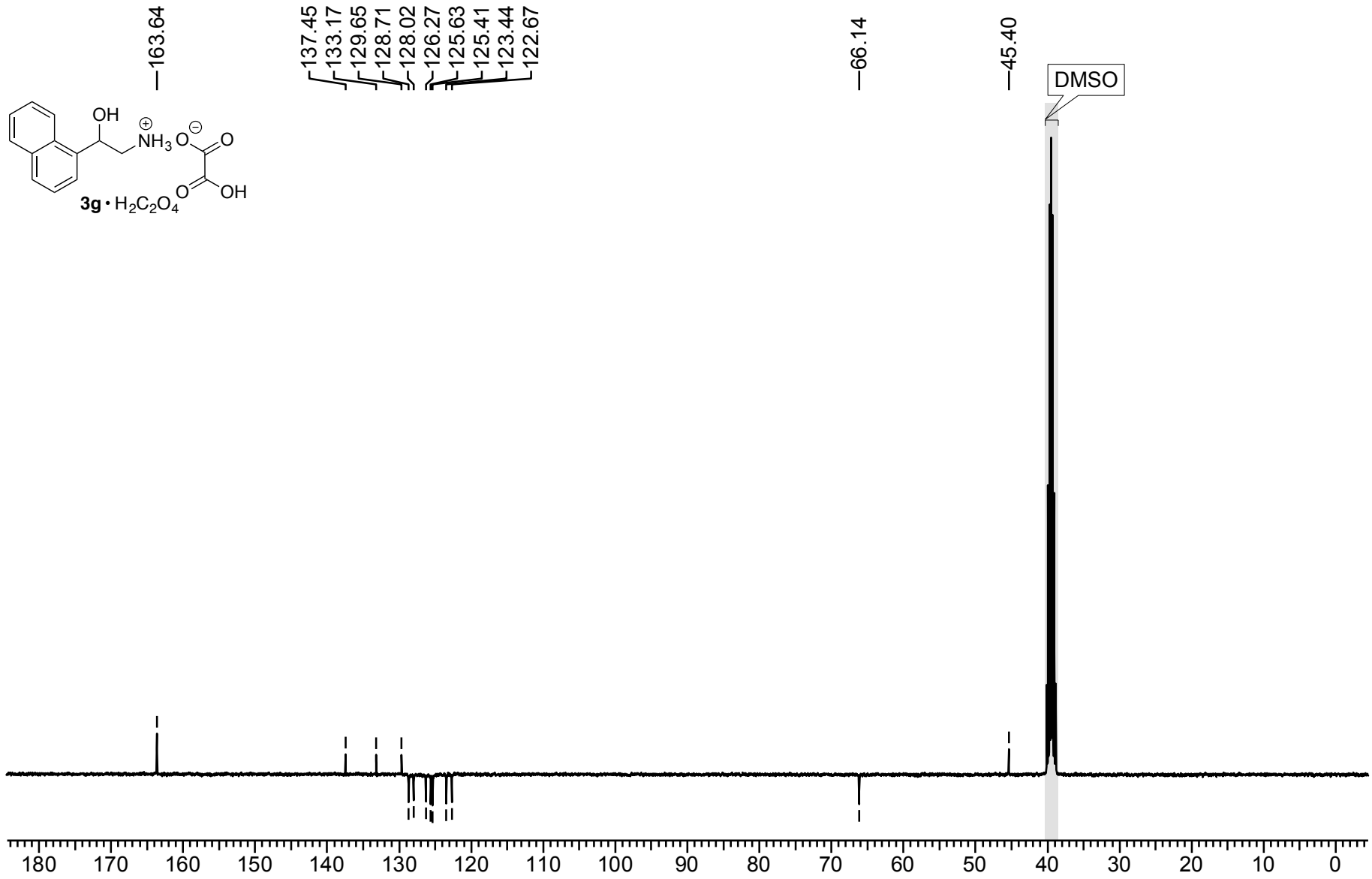

Figure S201. ^{13}C NMR APT (100 MHz, DMSO-d_6) spectrum of **3g**·$H_2C_2O_4$.

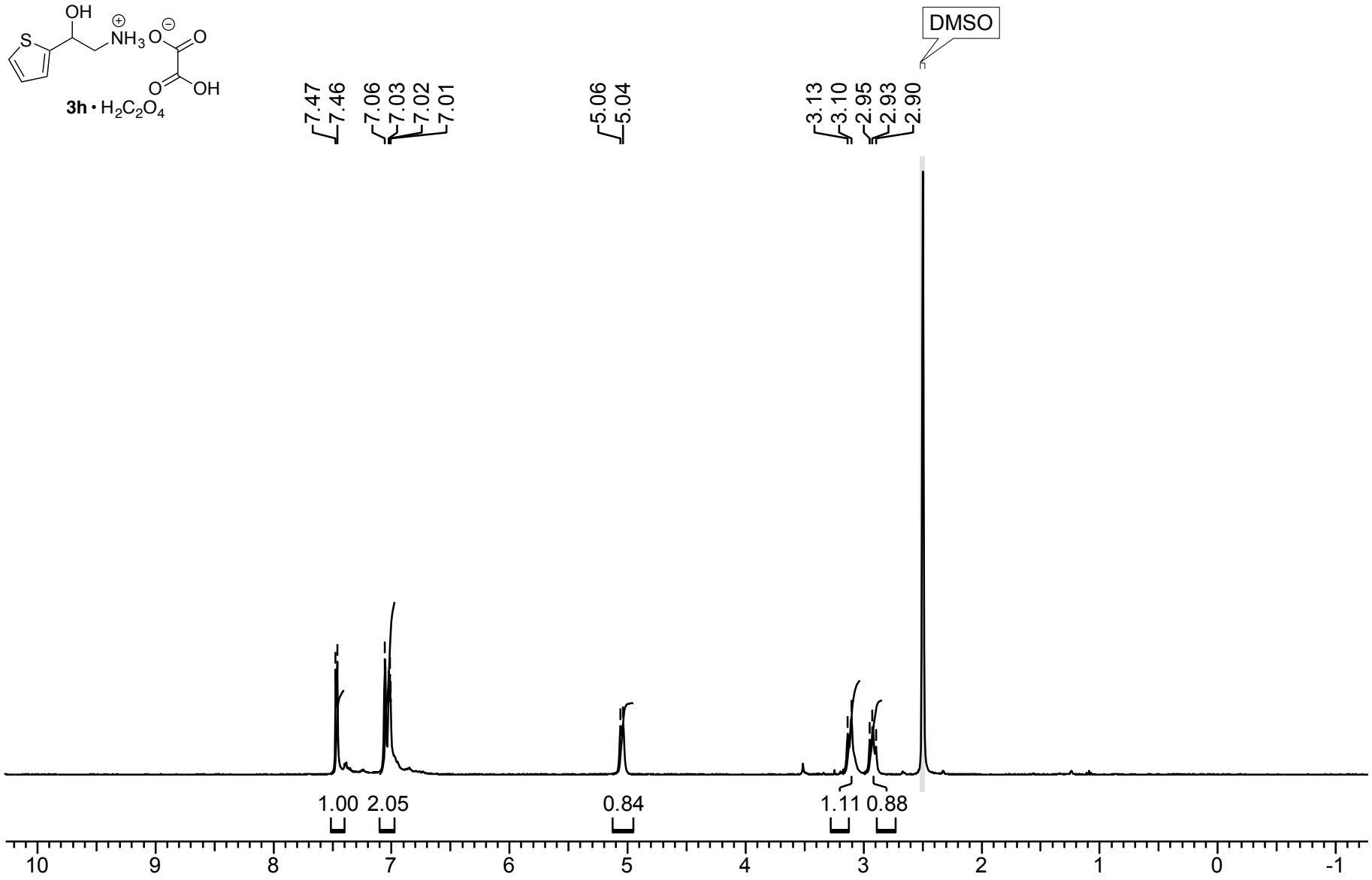

Figure S202. ^{1}H NMR (400 MHz, DMSO-d_6) spectrum of **3h** • $H_2C_2O_4$.

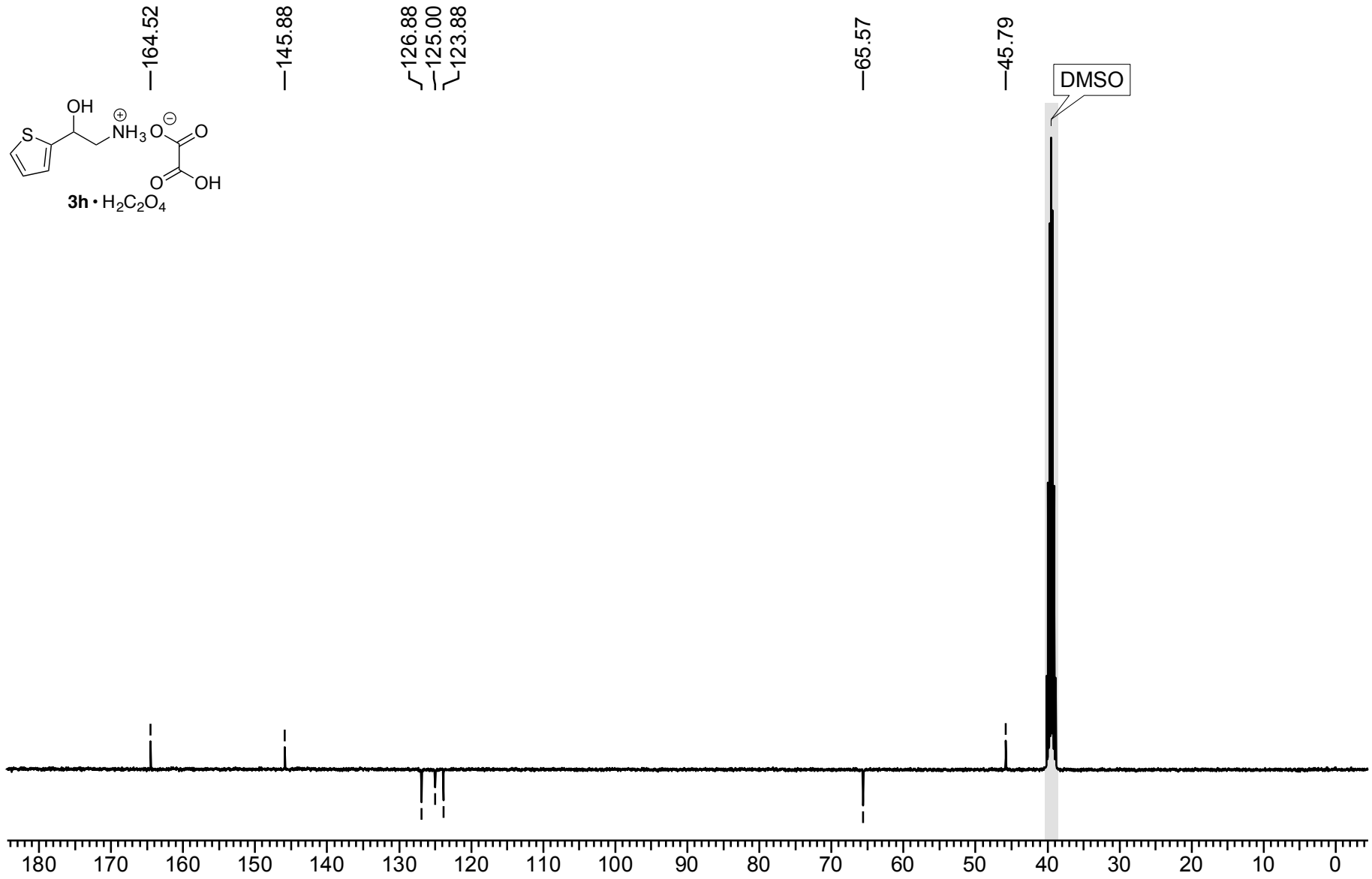

Figure S203. ^{13}C NMR APT (100 MHz, DMSO-d_6) spectrum of **3h** · $H_2C_2O_4$.

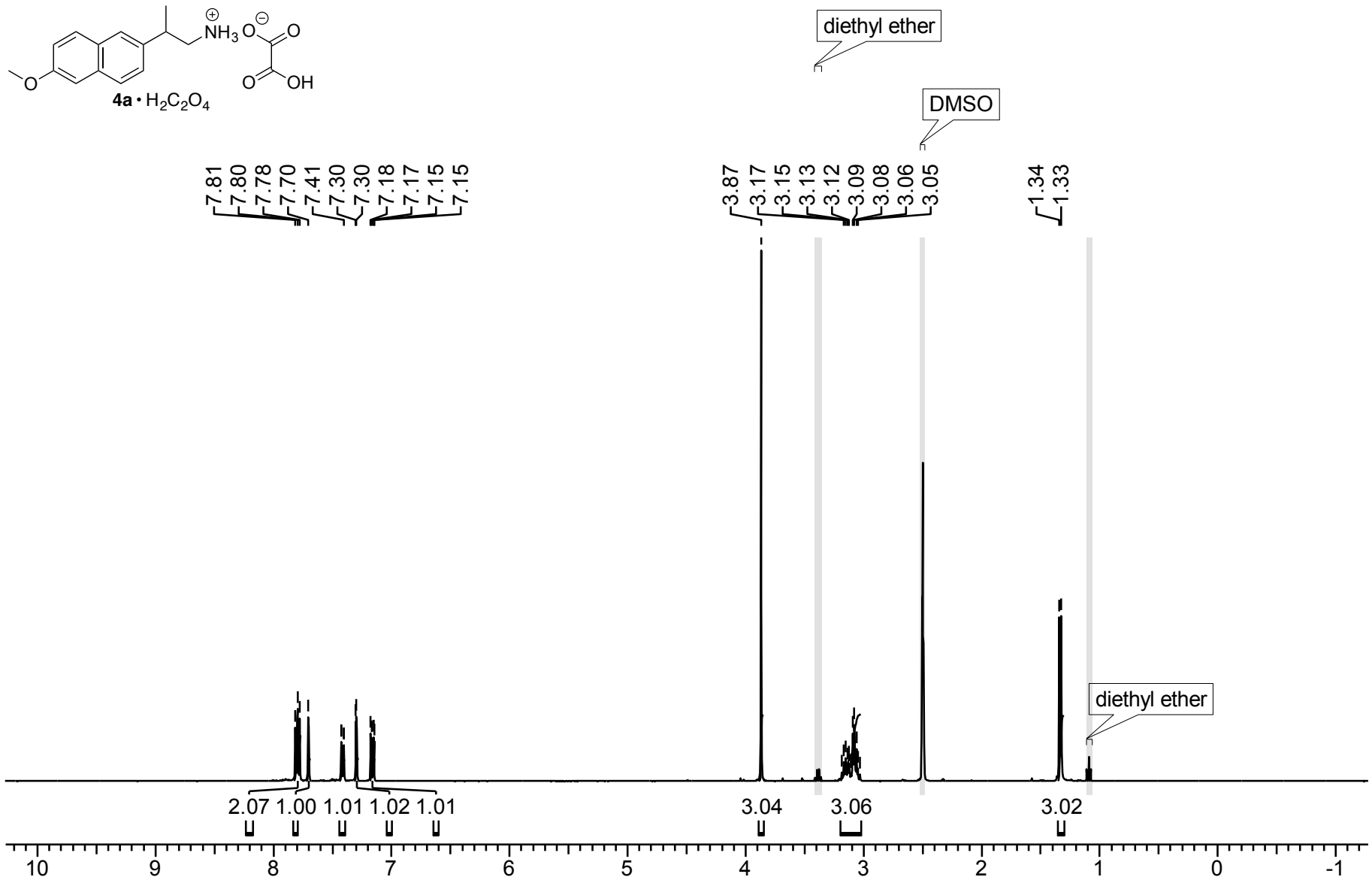

Figure S204. ^{1}H NMR (400 MHz, DMSO-d_6) spectrum of **4a** • $H_2C_2O_4$.

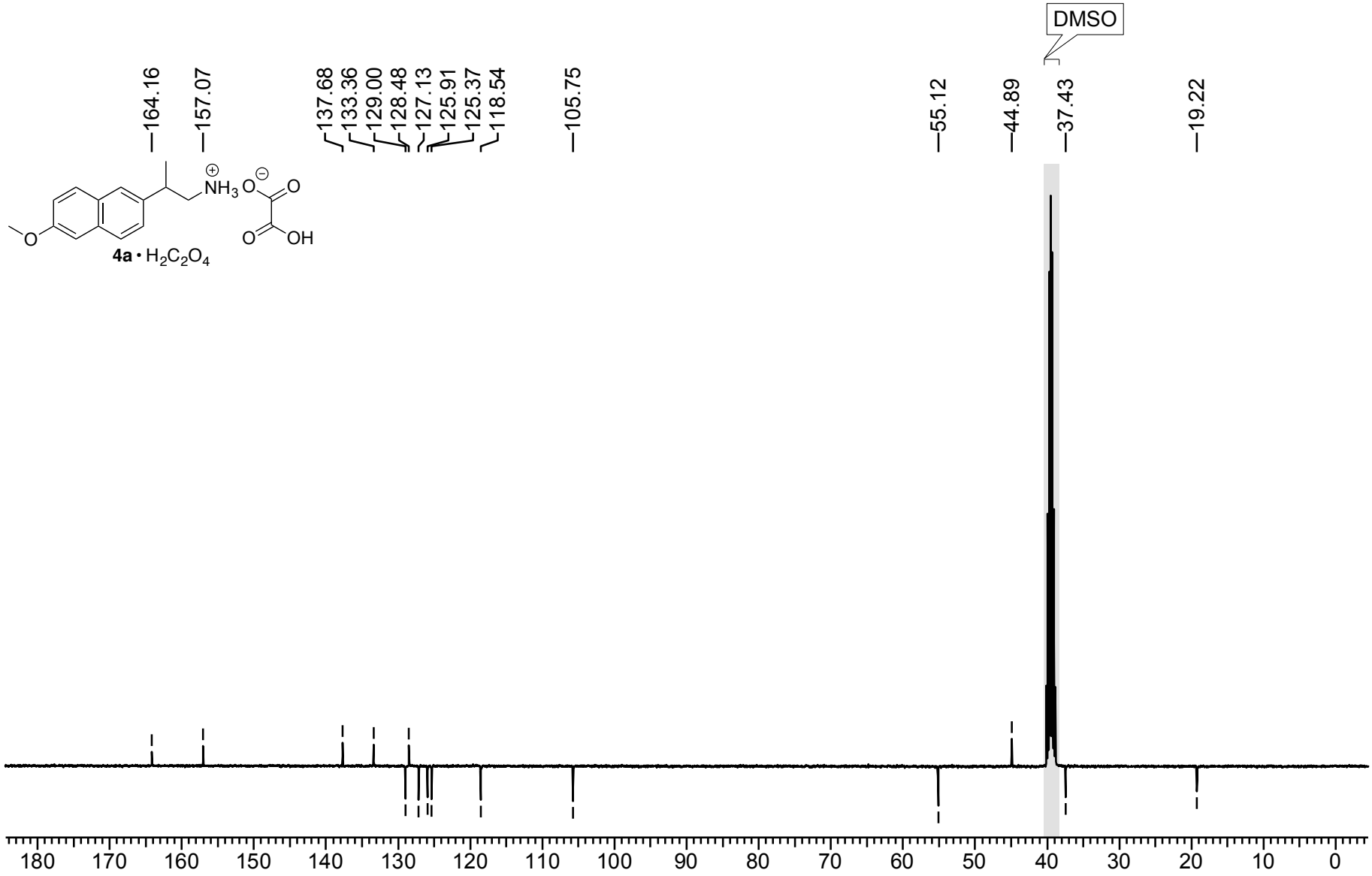

Figure S205. ^{13}C NMR APT (100 MHz, DMSO-d_6) spectrum of **4a** • $H_2C_2O_4$.

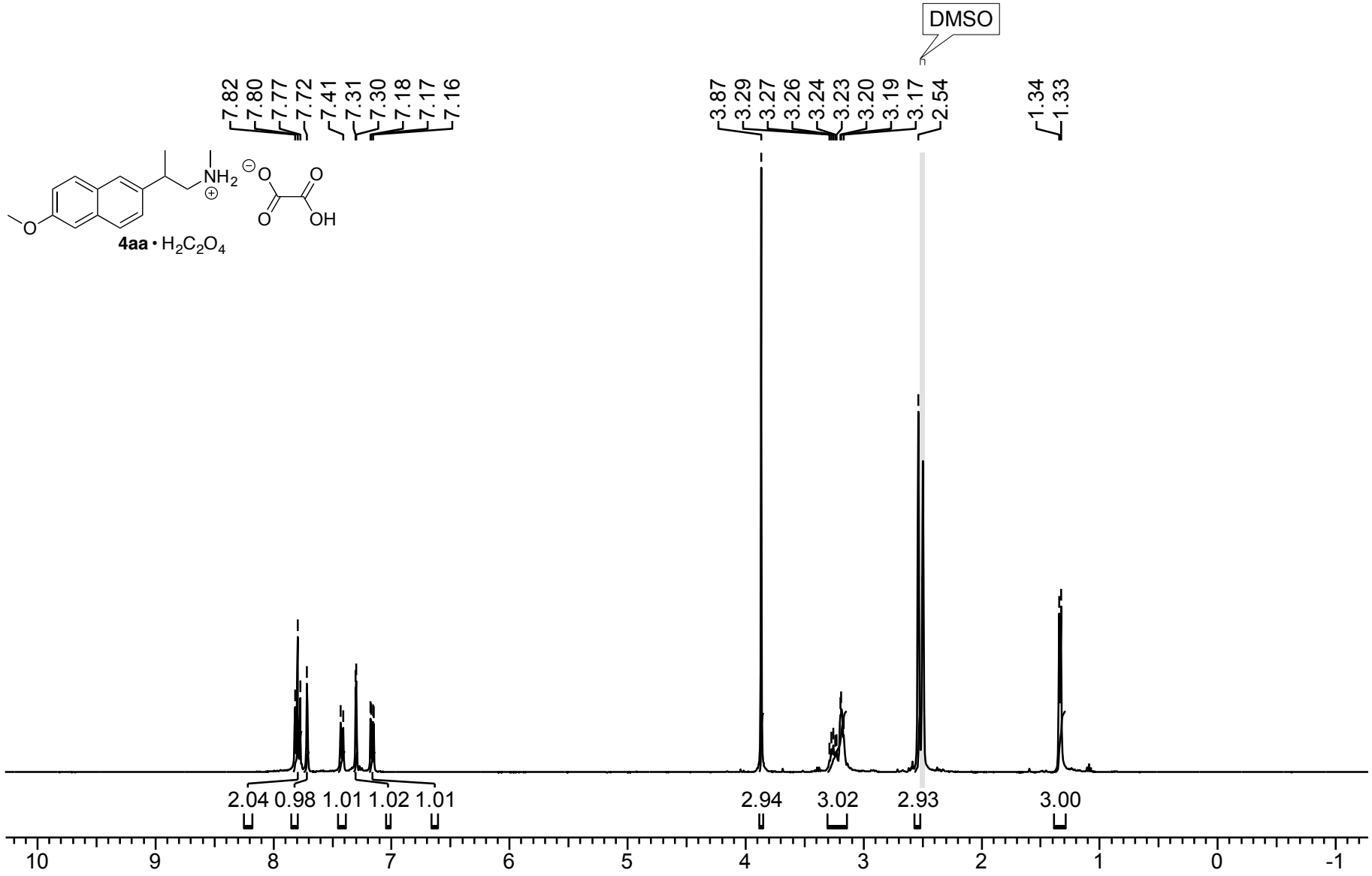

Figure S206. ^{1}H NMR (400 MHz, DMSO-d_6) spectrum of **4aa** • $H_2C_2O_4$.

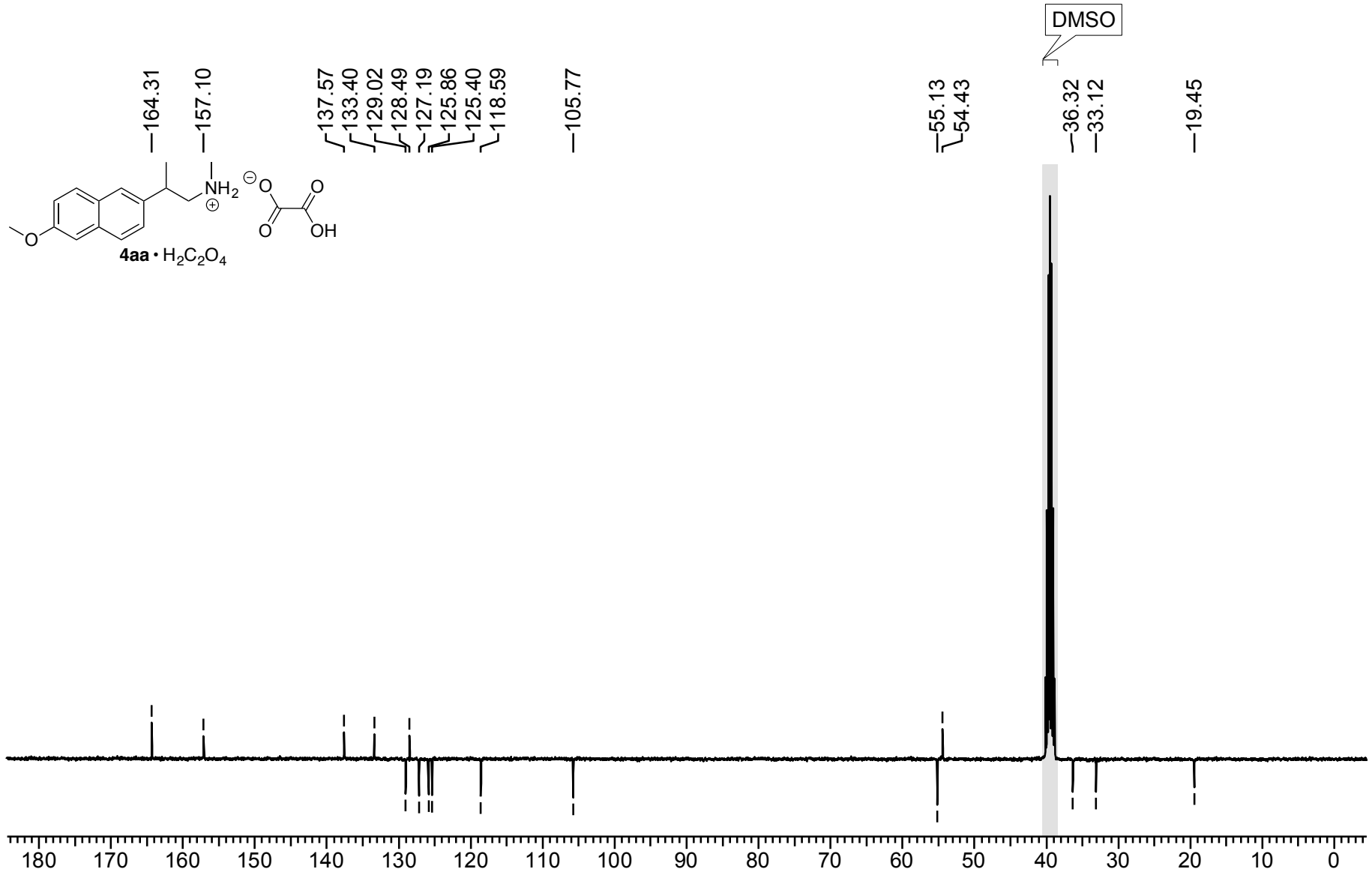

Figure S207. ^{13}C NMR APT (100 MHz, DMSO-d_6) spectrum of **4aa** · $H_2C_2O_4$.

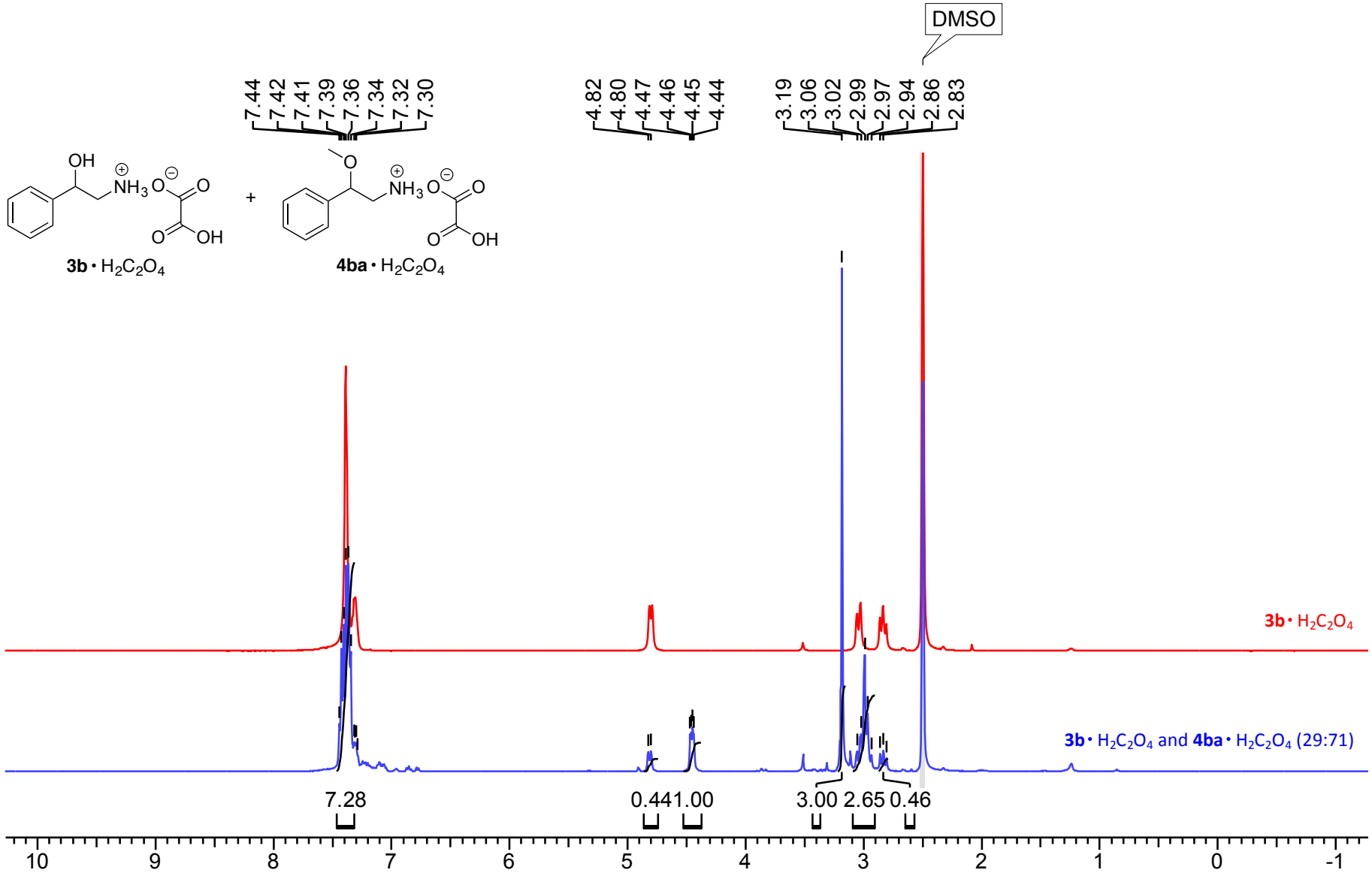

Figure S208. Comparison of ^{1}H NMR (400 MHz, DMSO-d_6) spectra of the pure **3b**• $H_2C_2O_4$ and the mixture of **3b**• $H_2C_2O_4$ and **4ba**• $H_2C_2O_4$ (29:71).

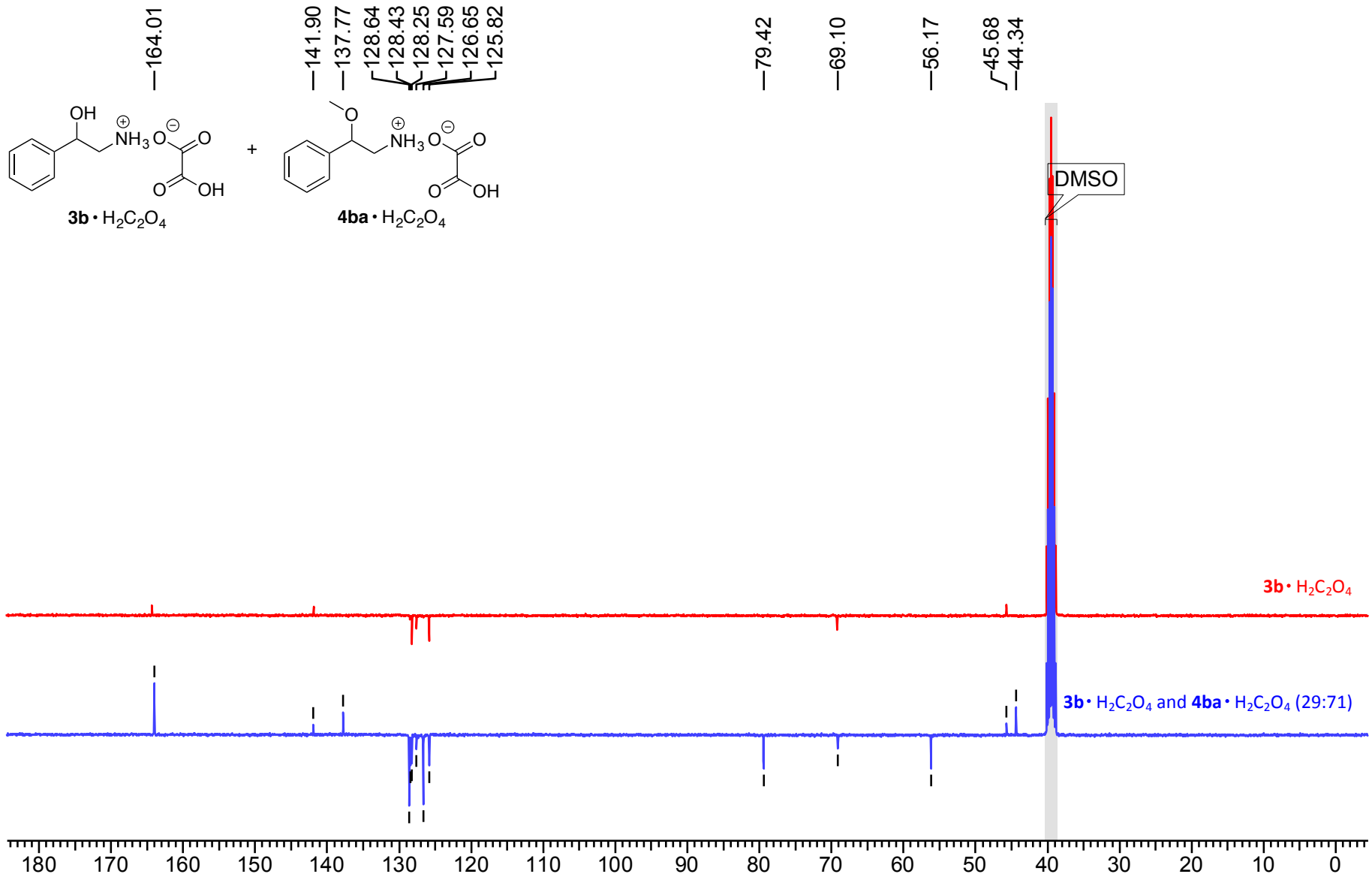

Figure S209. Comparison of ^{13}C NMR (100 MHz, DMSO-d_6) spectra of the pure **3b**· $H_2C_2O_4$ and the mixture of **3b**· $H_2C_2O_4$ and **4ba**· $H_2C_2O_4$ (29:71).

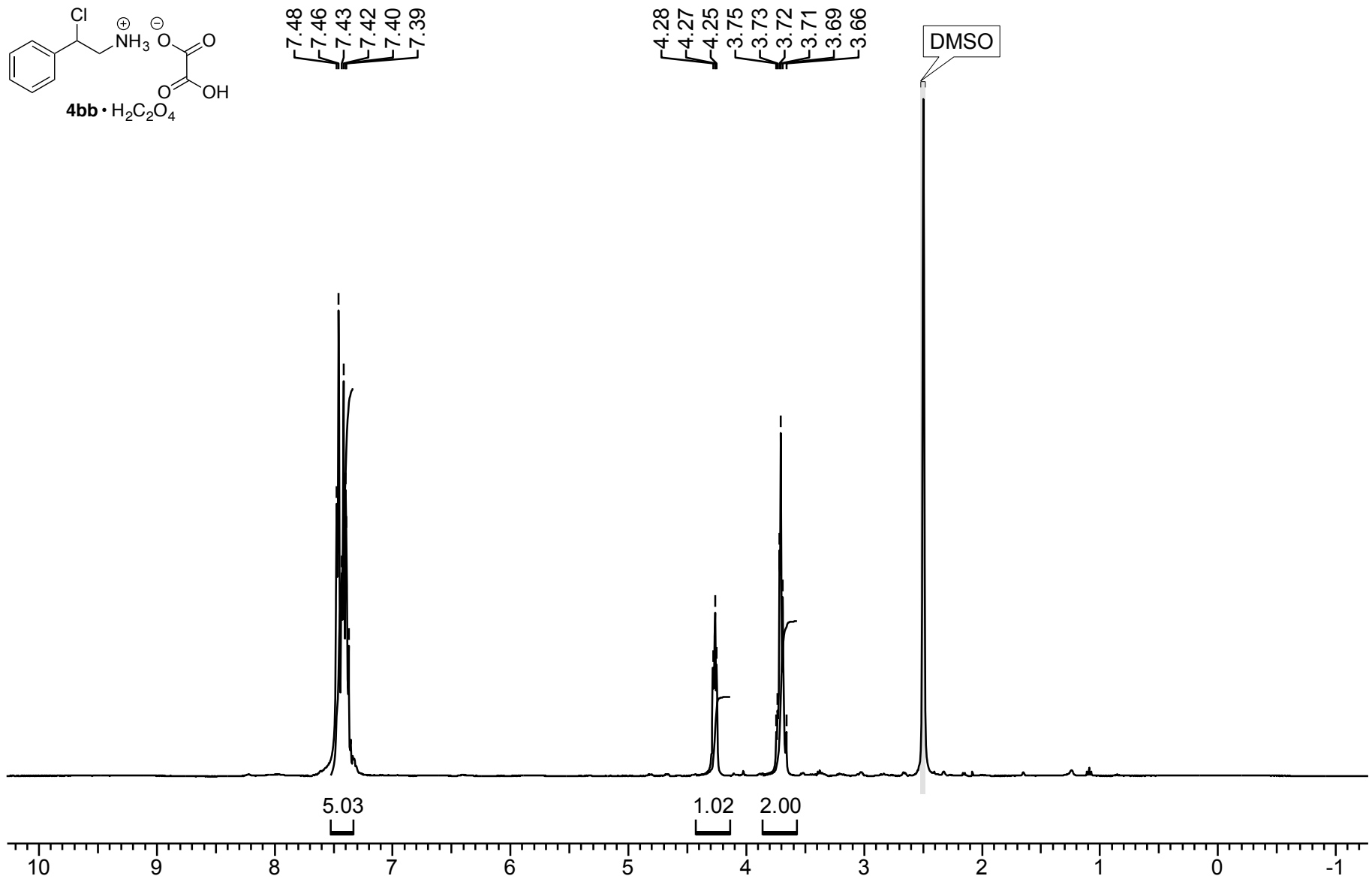

Figure S210. ^{1}H NMR (400 MHz, DMSO-d_6) spectrum of **4bb** · $H_2C_2O_4$.

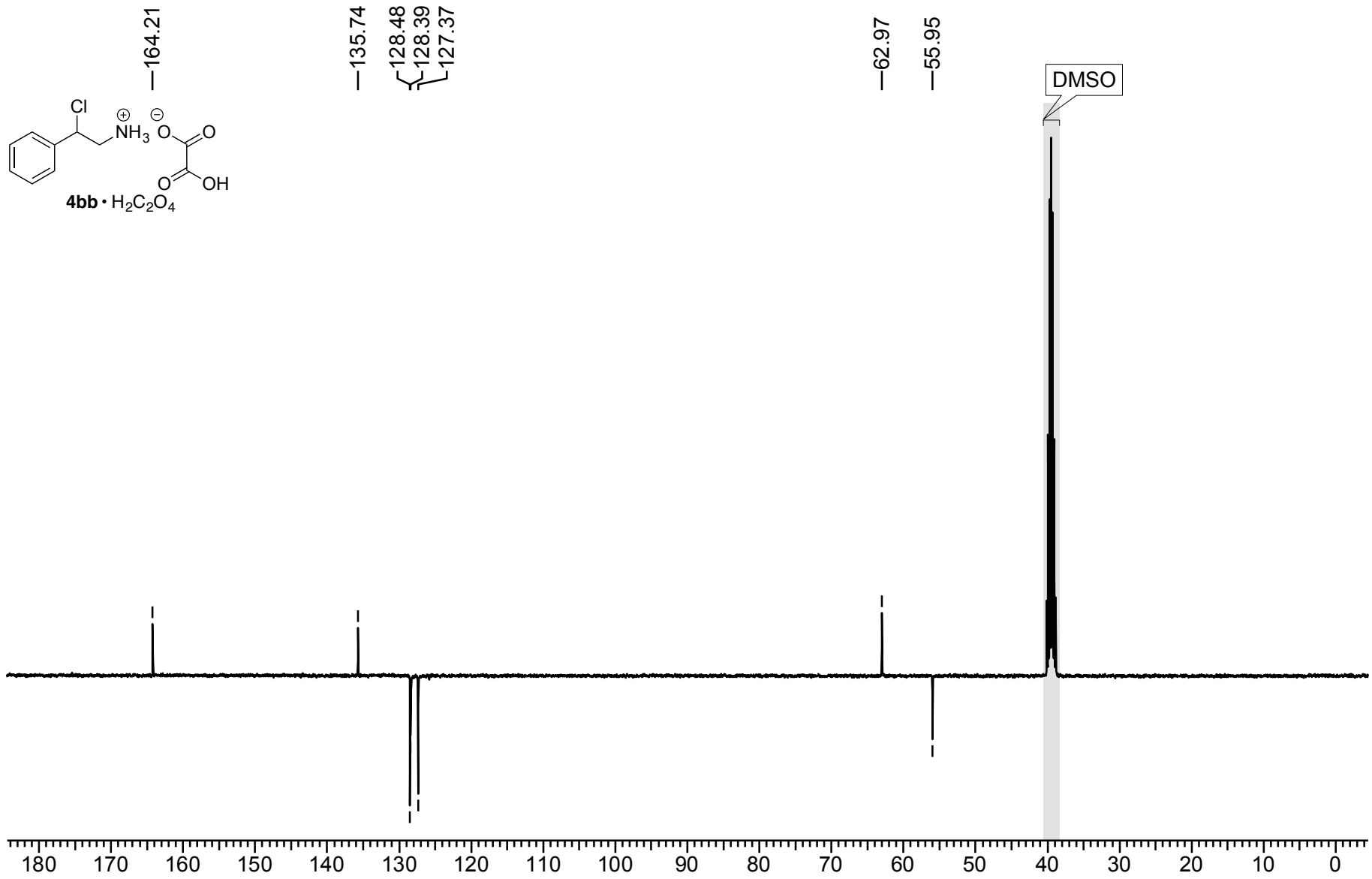

Figure S211. ^{13}C NMR APT (100 MHz, DMSO-d_6) spectrum of **4bb** · $H_2C_2O_4$.

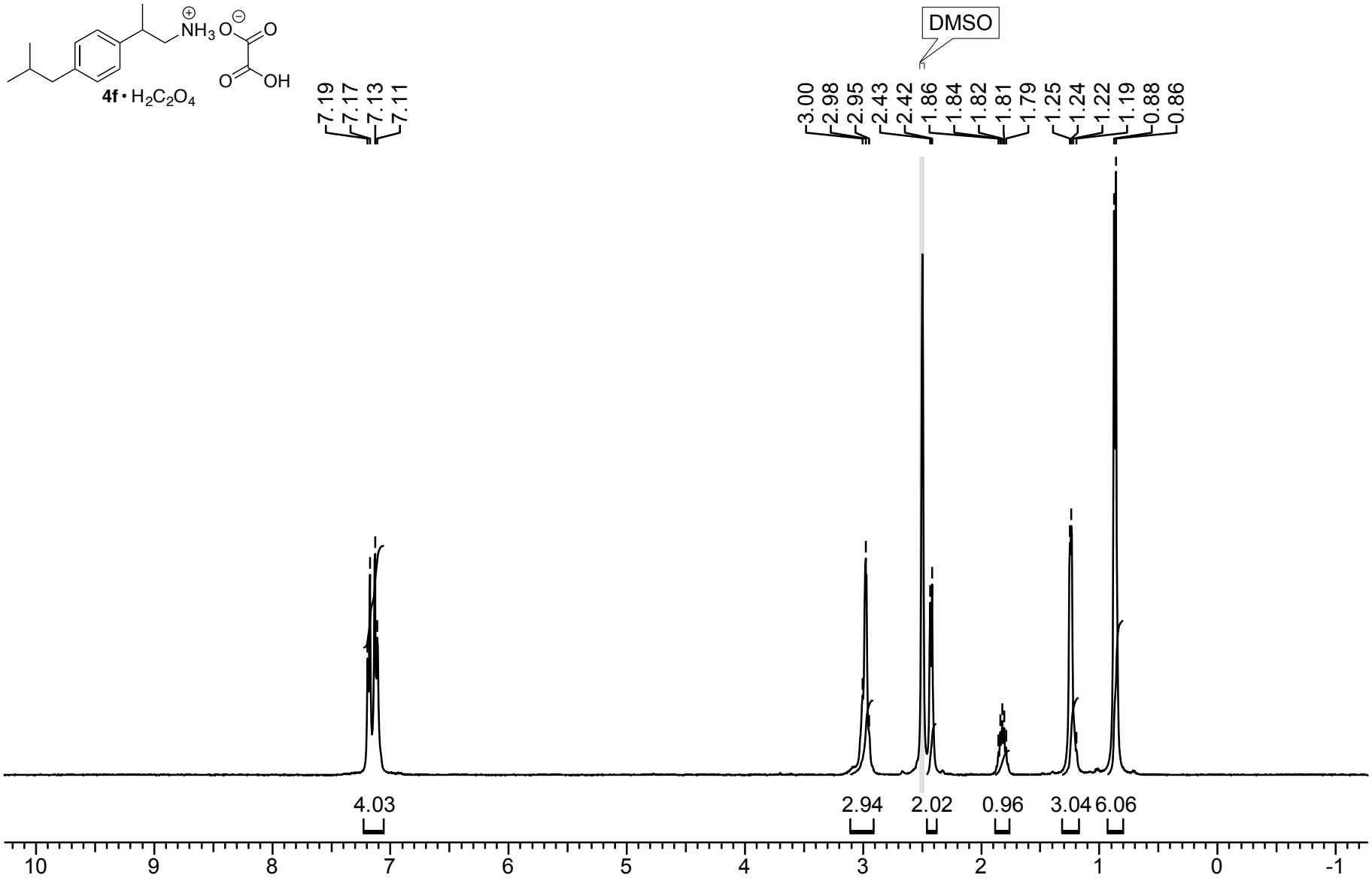

Figure S212. ^{1}H NMR (400 MHz, DMSO-d_6) spectrum of **4f**• $H_2C_2O_4$.

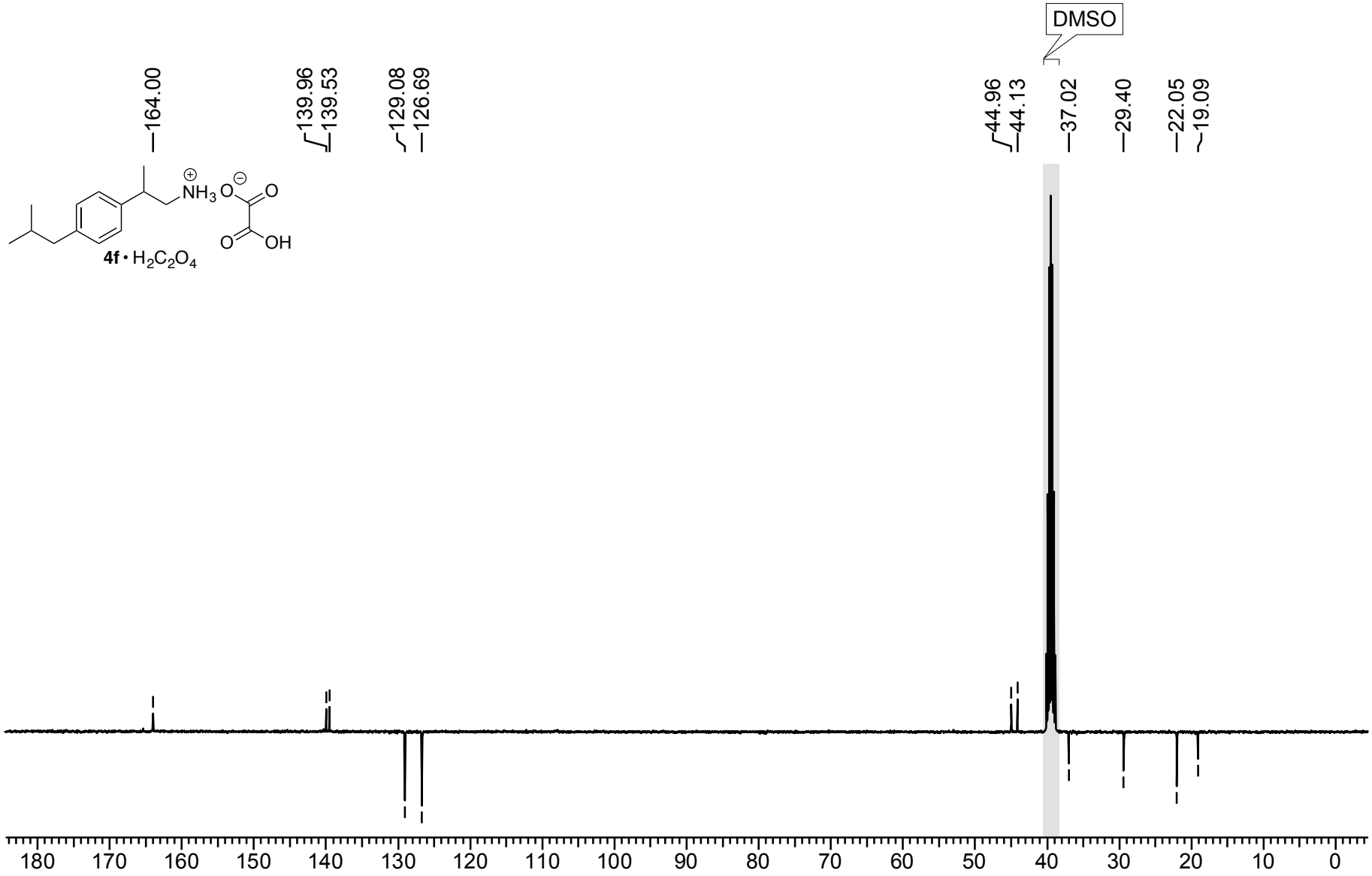

Figure S213. ^{13}C NMR APT (100 MHz, DMSO-d_6) spectrum of **4f**• $H_2C_2O_4$.

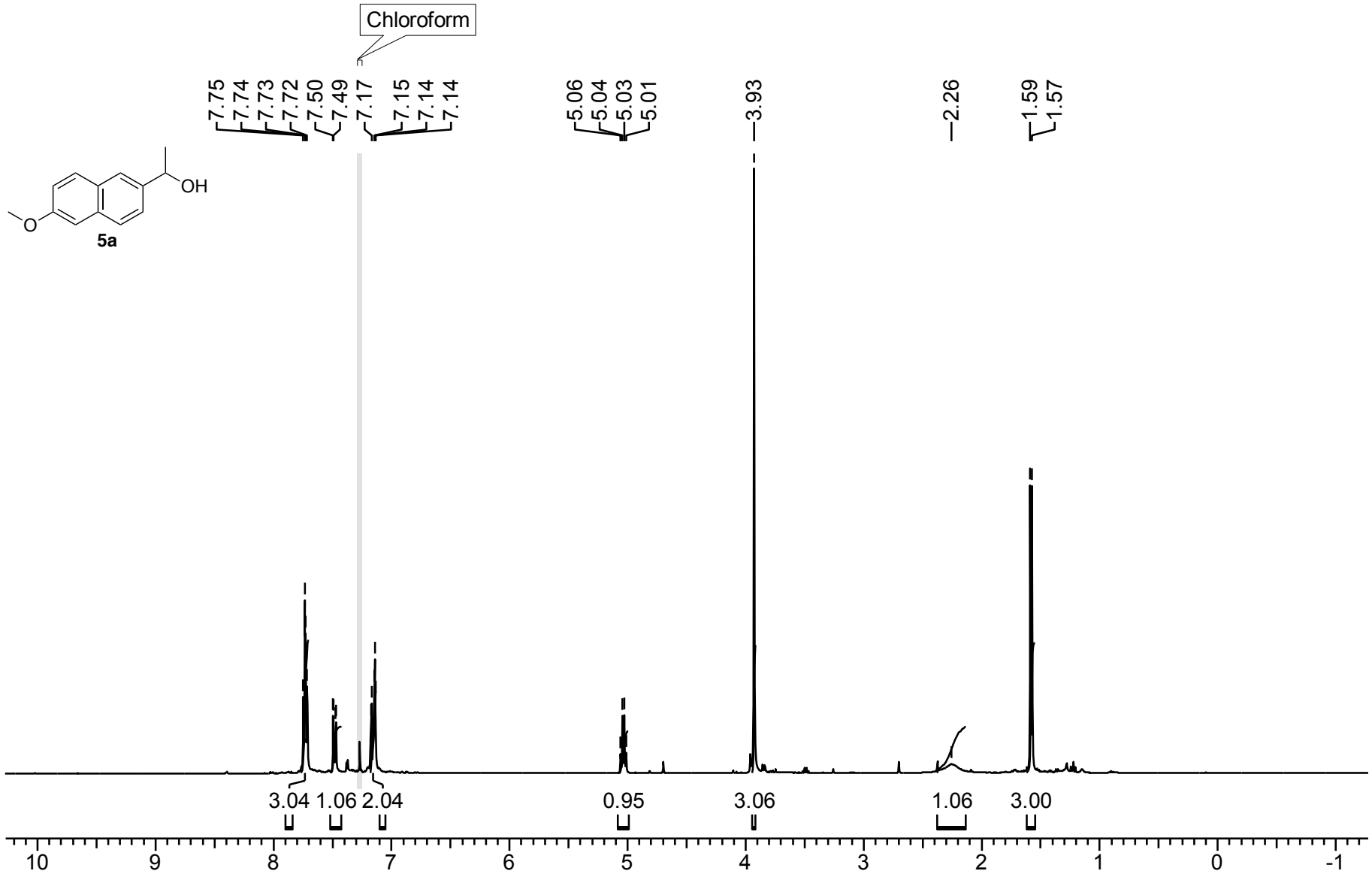

Figure S214. ^{1}H NMR (400 MHz, $CDCl_3$) spectrum of **5a**.

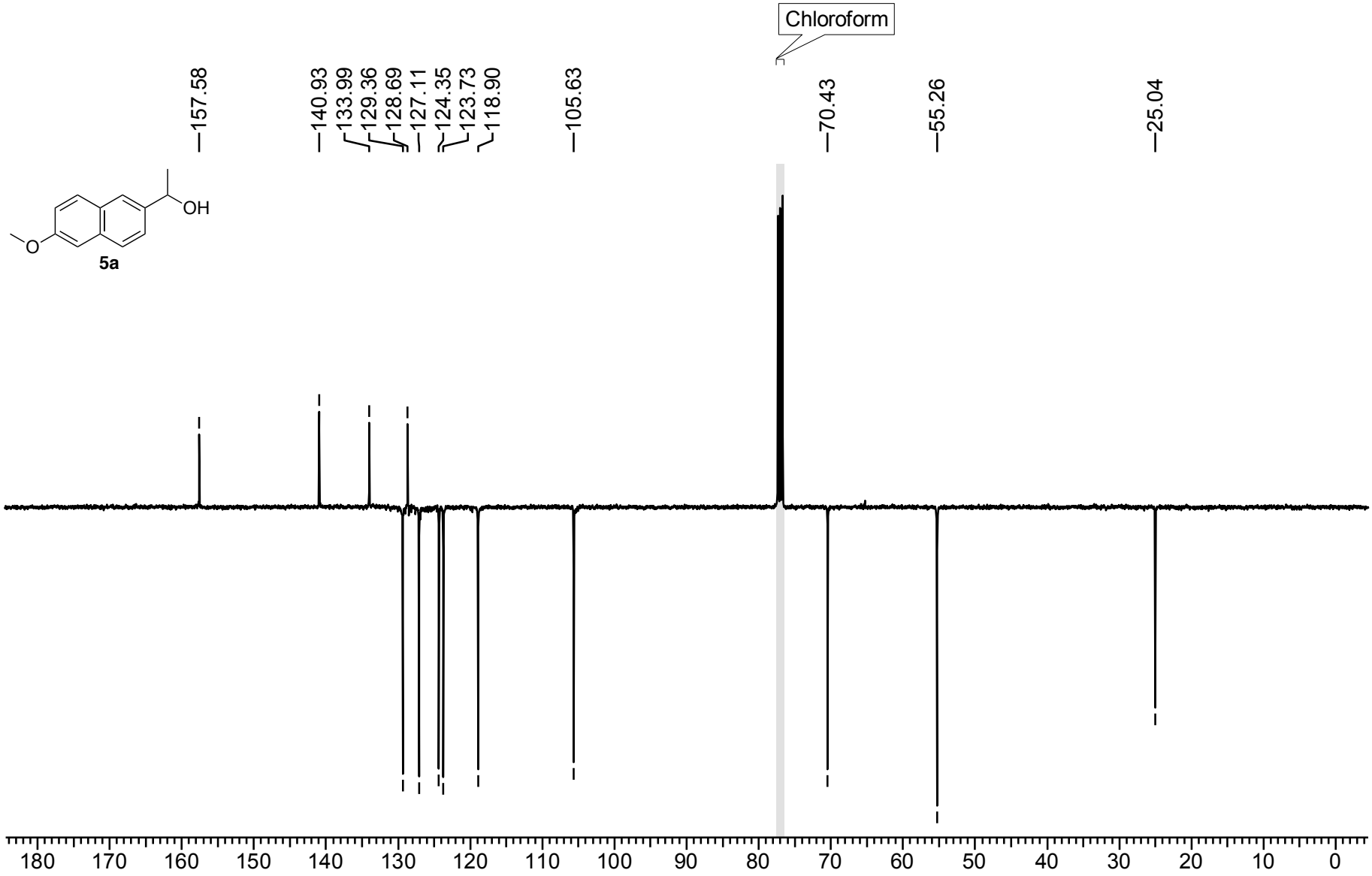

Figure S215. ^{13}C NMR APT (100 MHz, $CDCl_3$) spectrum of **5a**.

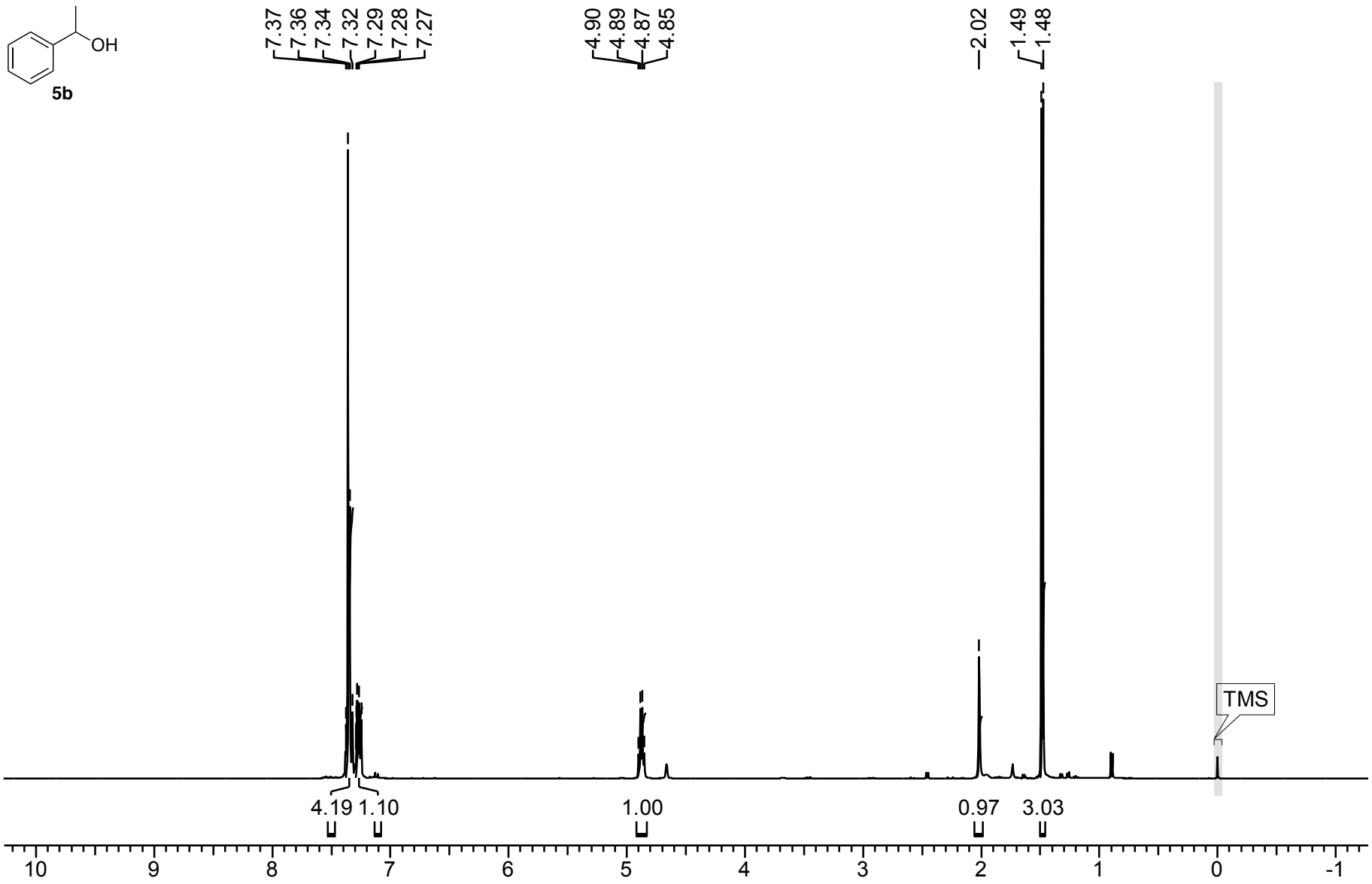

Figure S216. ^{1}H NMR (400 MHz, $CDCl_3$) spectrum of **5b**.

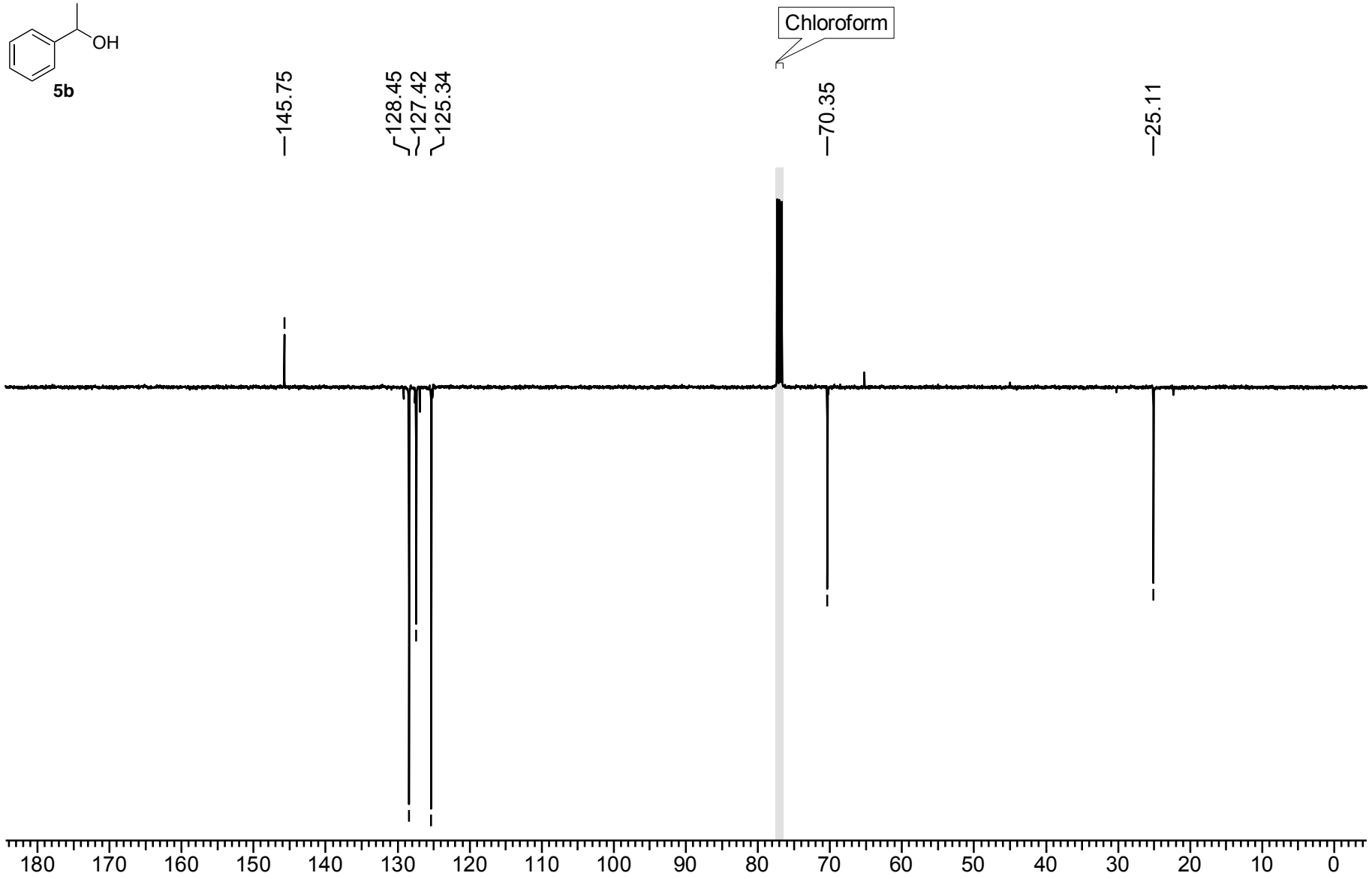

Figure S217. ^{13}C NMR APT (100 MHz, $CDCl_3$) spectrum of **5b**.

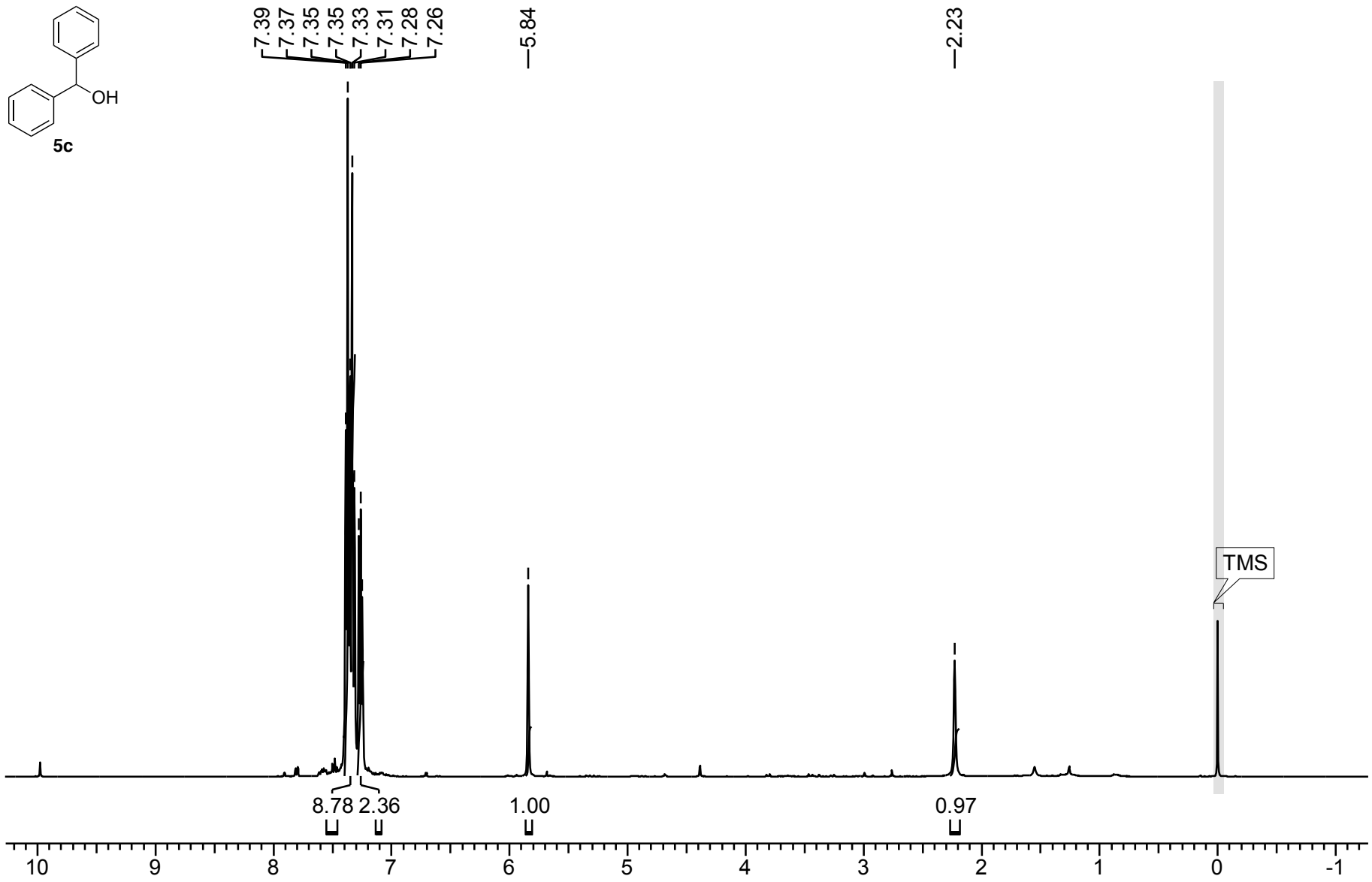

Figure S218. ^{1}H NMR (400 MHz, $CDCl_3$) spectrum of **5c**.

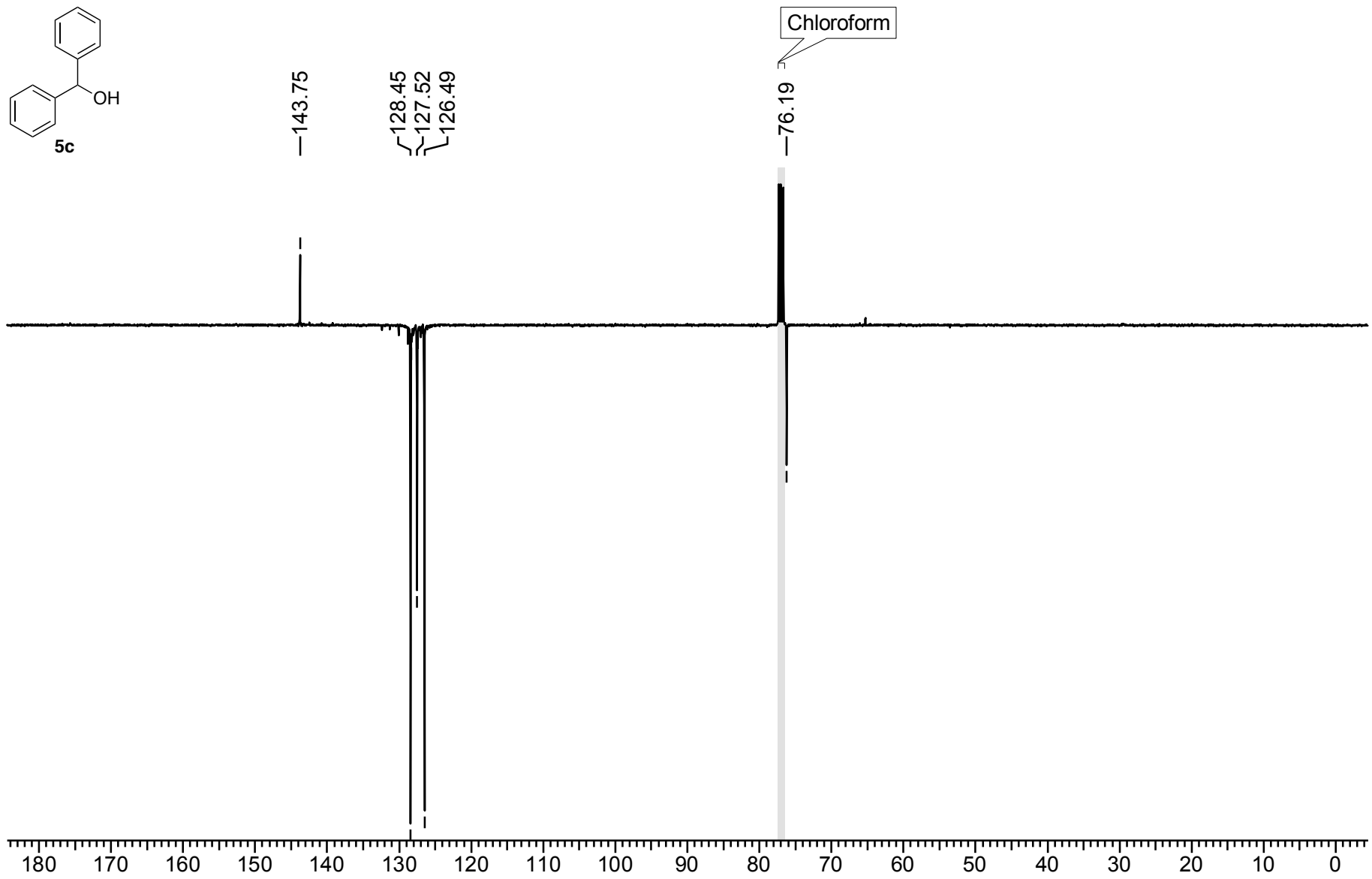

Figure S219. ^{13}C NMR APT (100 MHz, $CDCl_3$) spectrum of **5c**.

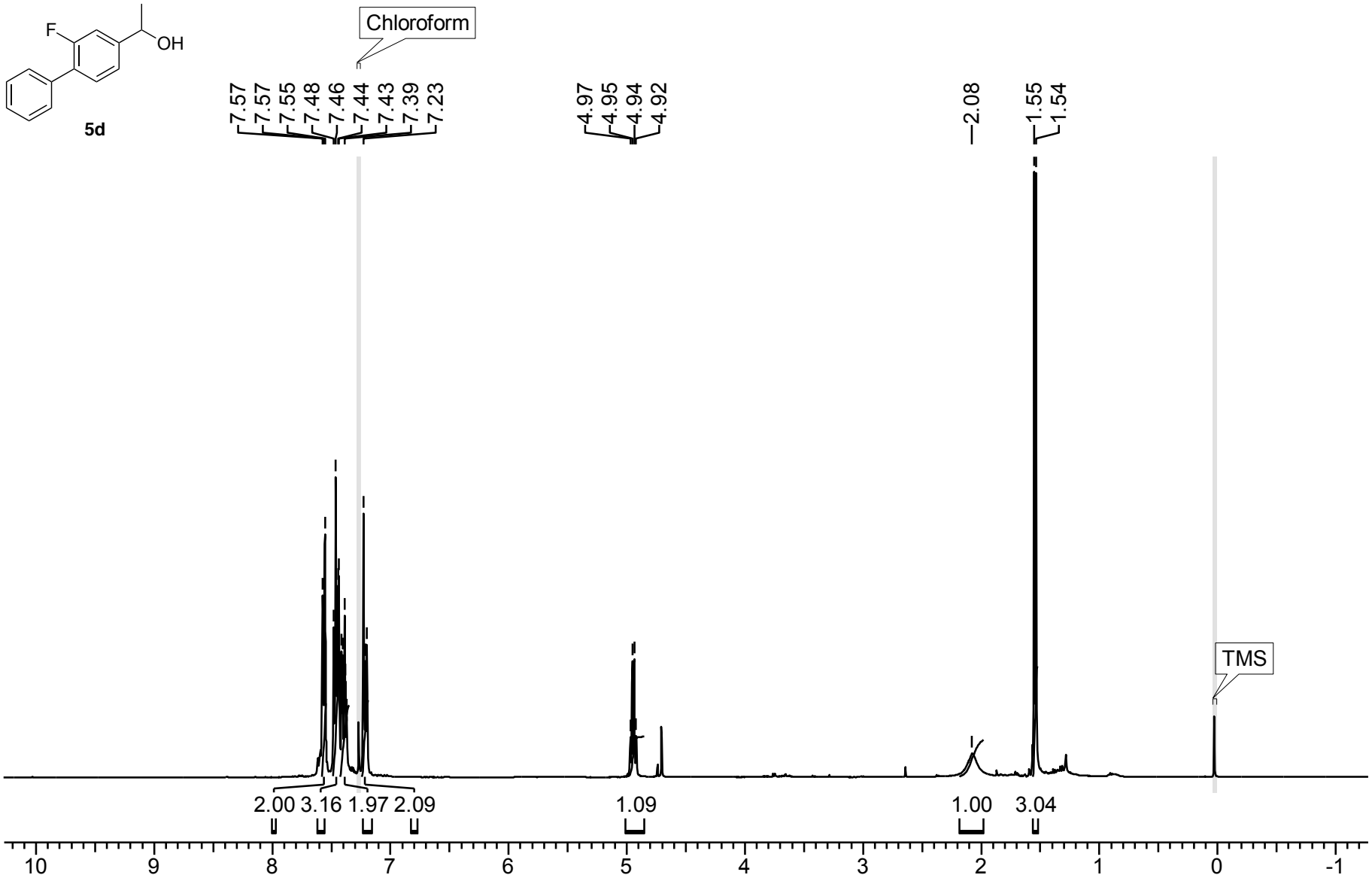

Figure S220. ^{1}H NMR (400 MHz, $CDCl_3$) spectrum of **5d**.

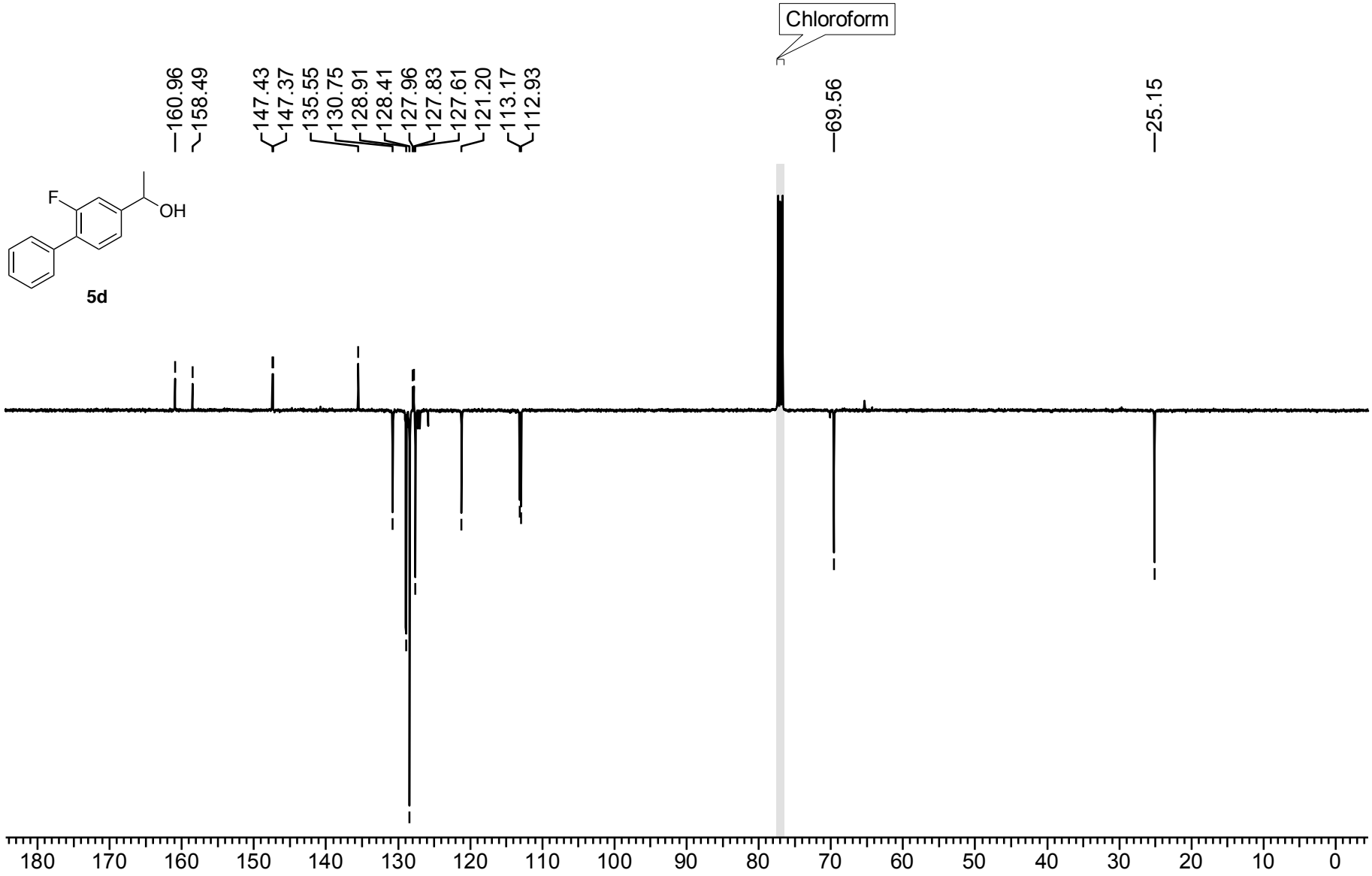

Figure S221. ^{13}C NMR APT (100 MHz, $CDCl_3$) spectrum of **5d**.

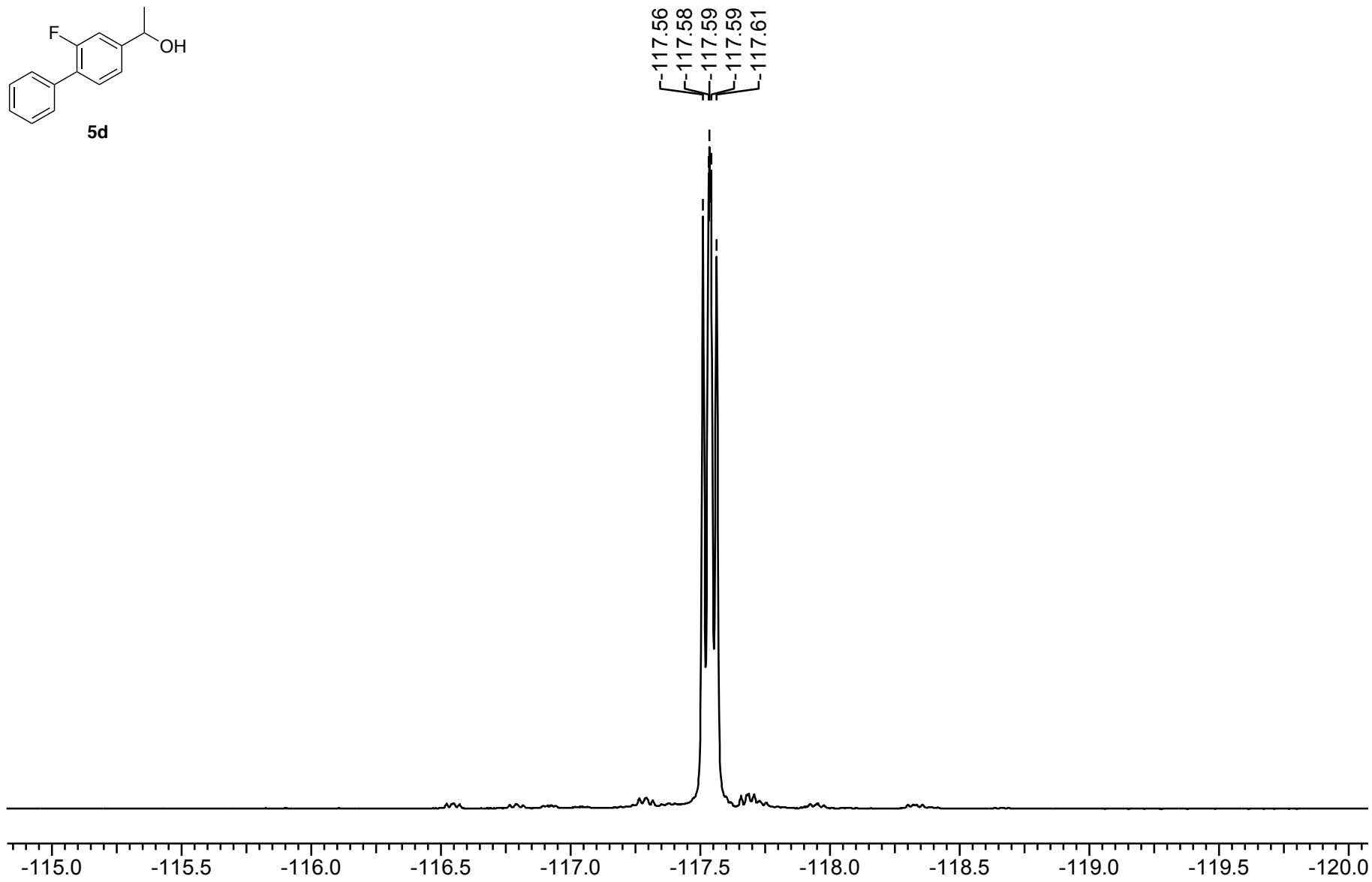

Figure S222. ^{19}F NMR (376 MHz, $CDCl_3$) spectrum of **5d**.

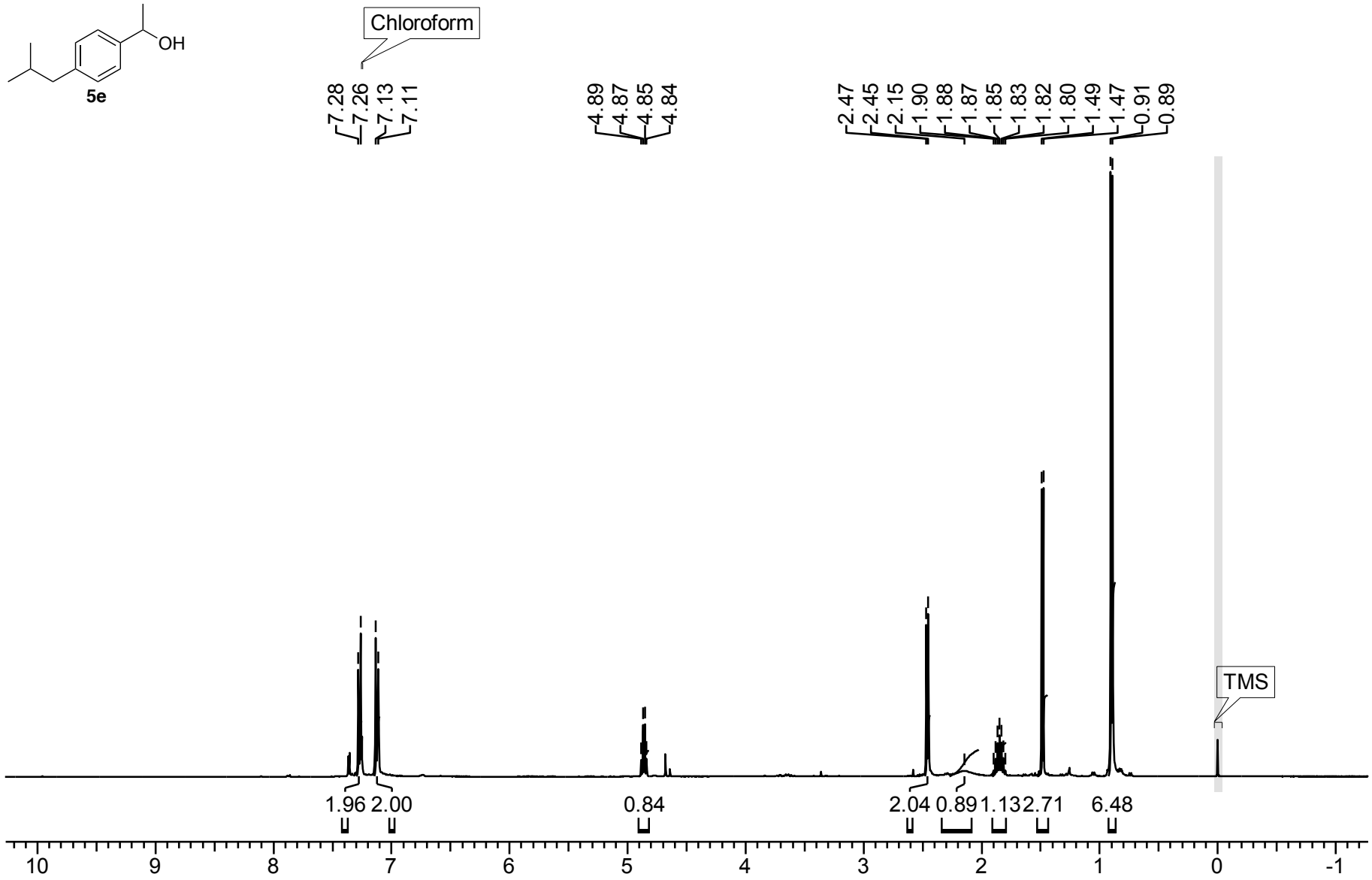

Figure S223. ^{1}H NMR (400 MHz, $CDCl_3$) spectrum of **5e**.

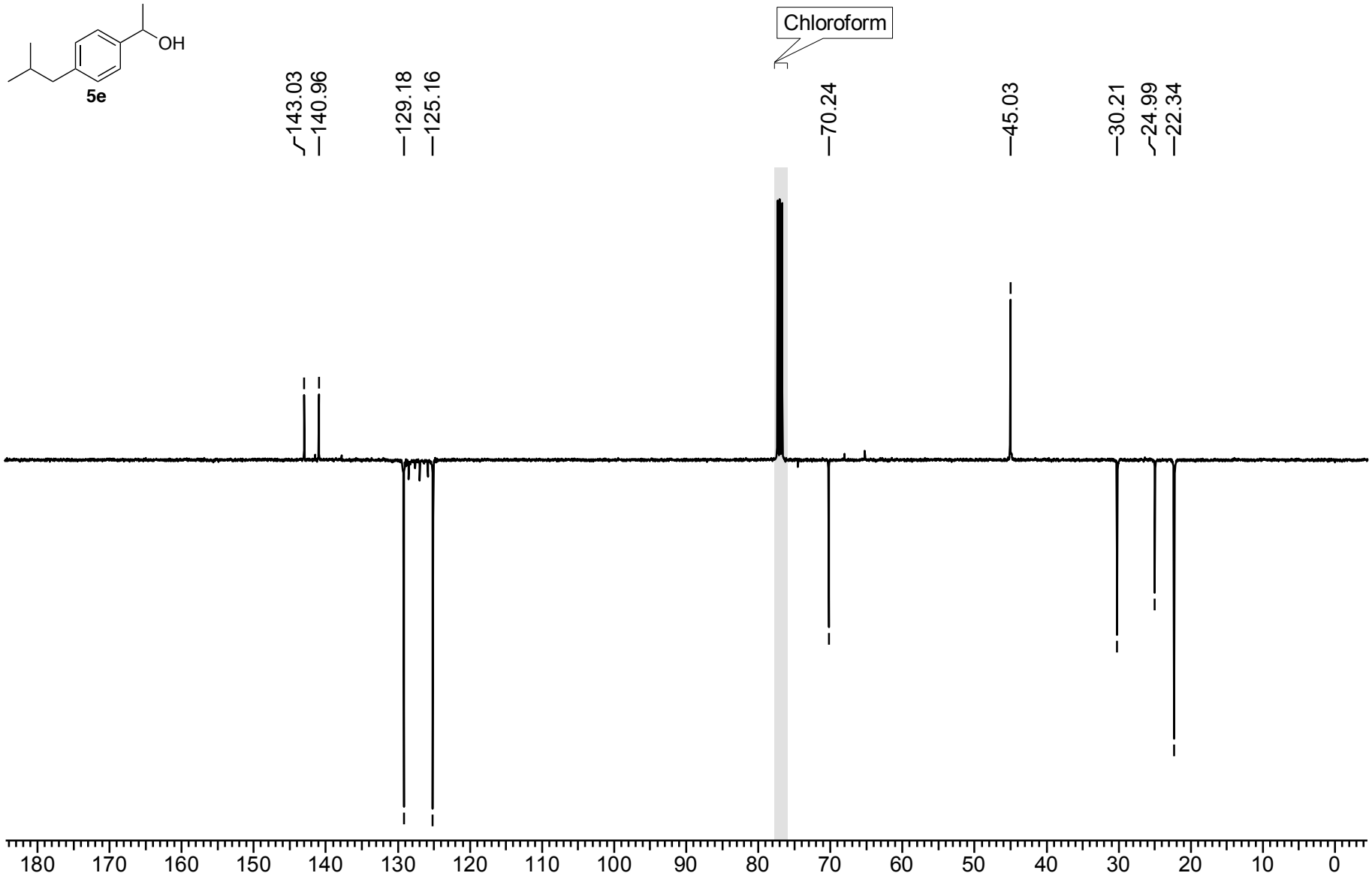

Figure S224. ^{13}C NMR APT (100 MHz, $CDCl_3$) spectrum of **5e**.

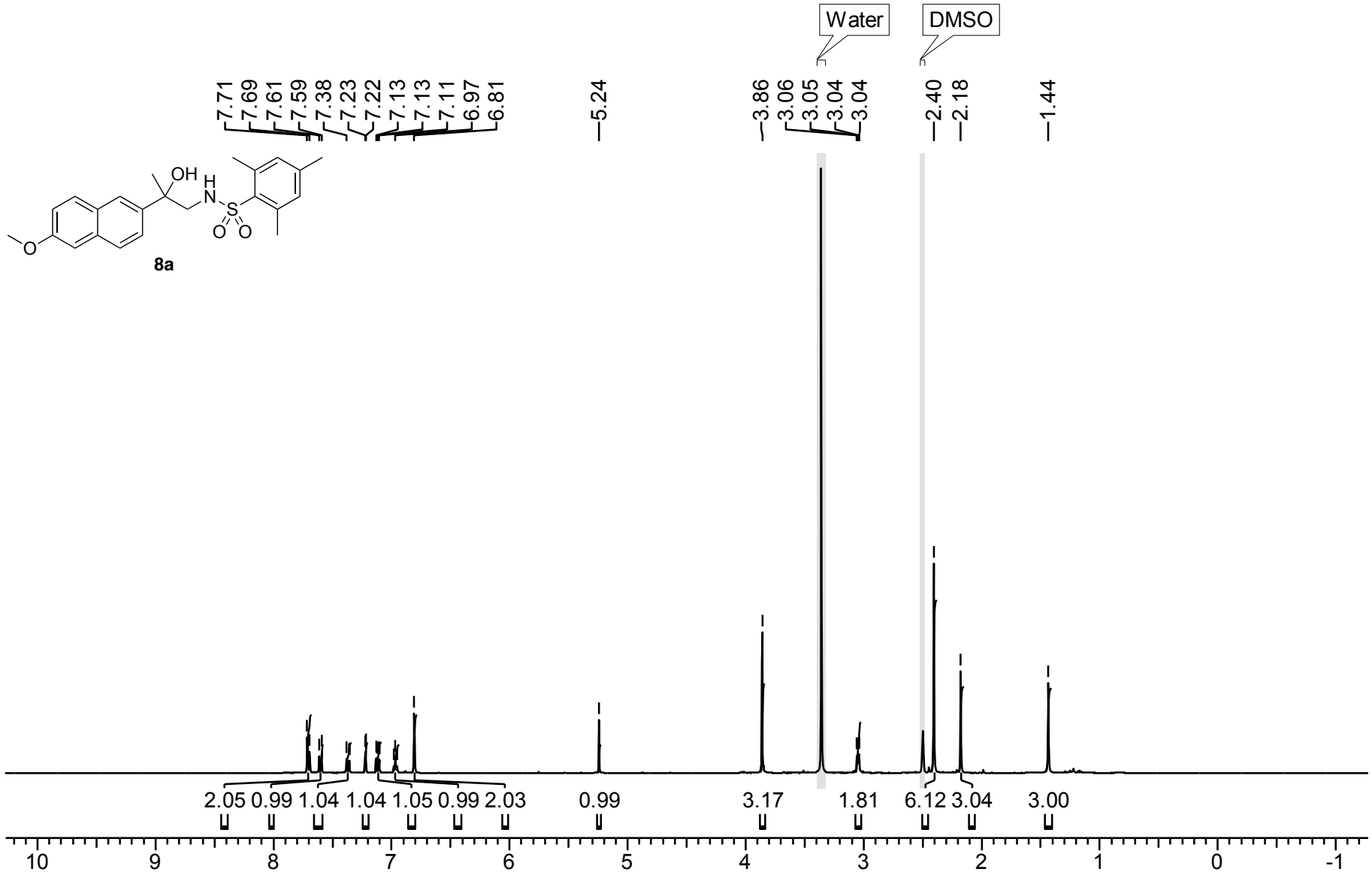

Figure S225. ^{1}H NMR (400 MHz, DMSO-d_6) spectrum of **8a**.

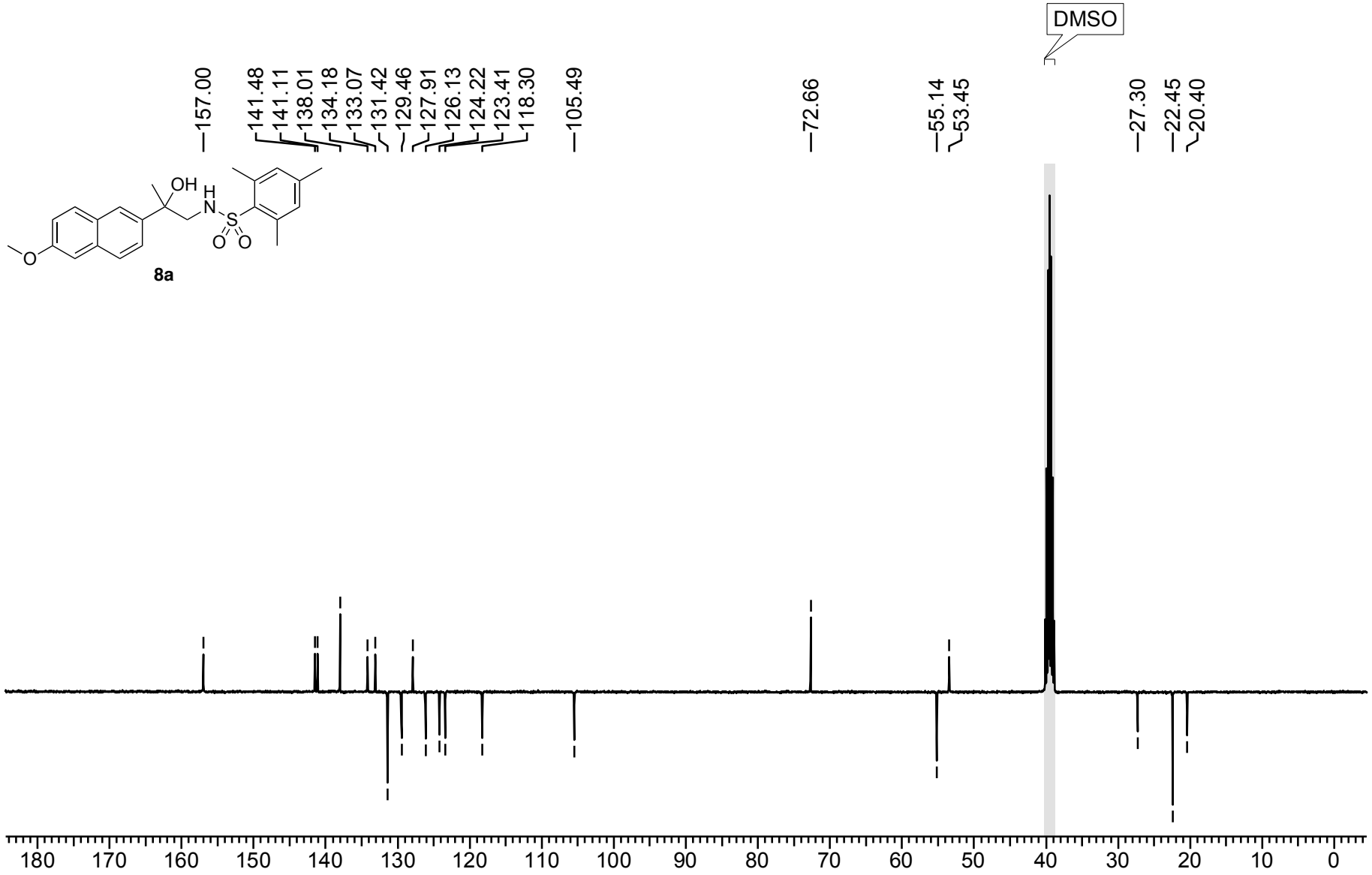

Figure S226. ^{13}C NMR APT (100 MHz, DMSO-d_6) spectrum of **8a**.

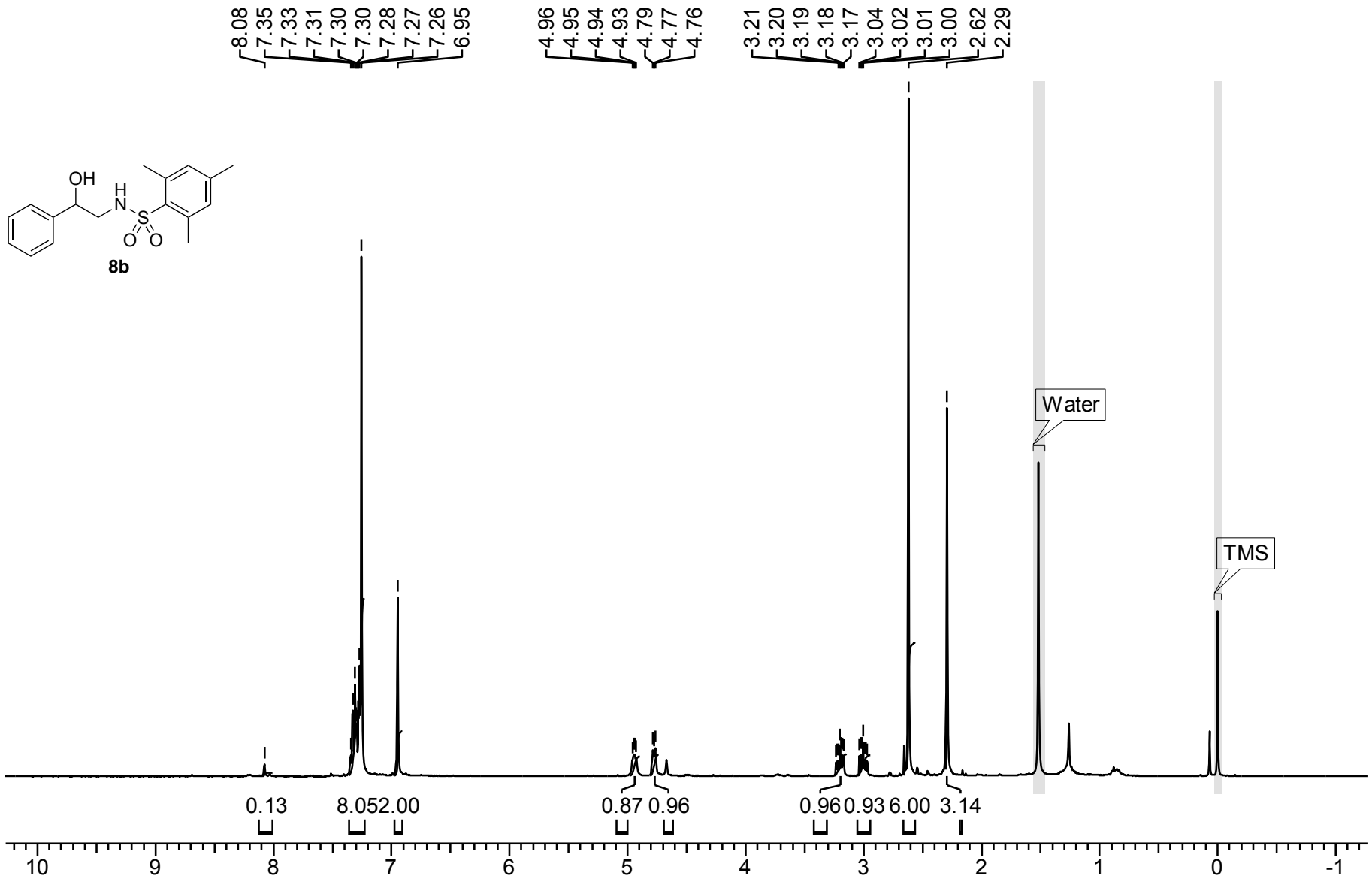

Figure S227. ^{1}H NMR (400 MHz, $CDCl_3$) spectrum of **8b**.

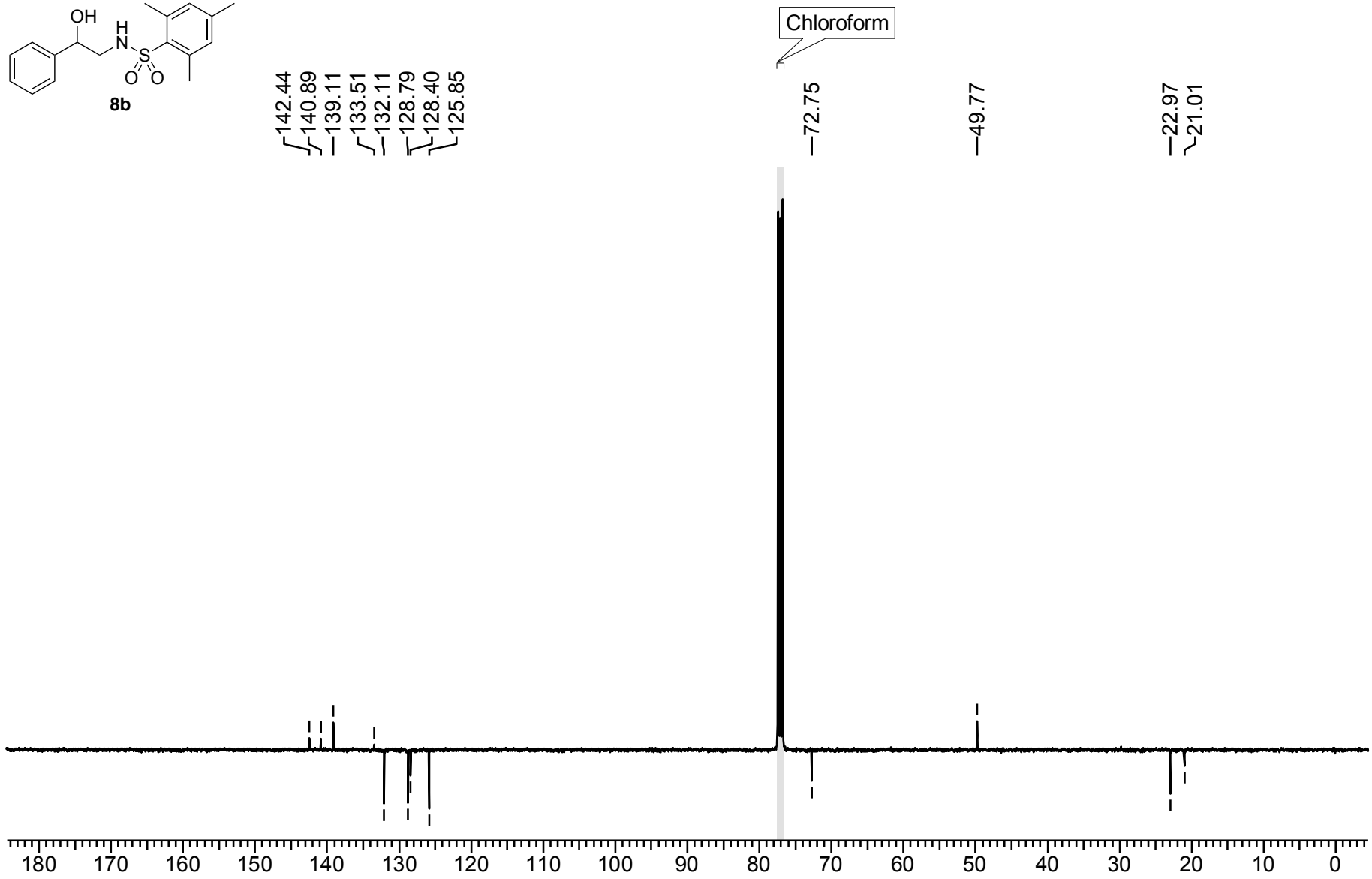

Figure S228. ^{13}C NMR APT (100 MHz, $CDCl_3$) spectrum of **8b**.

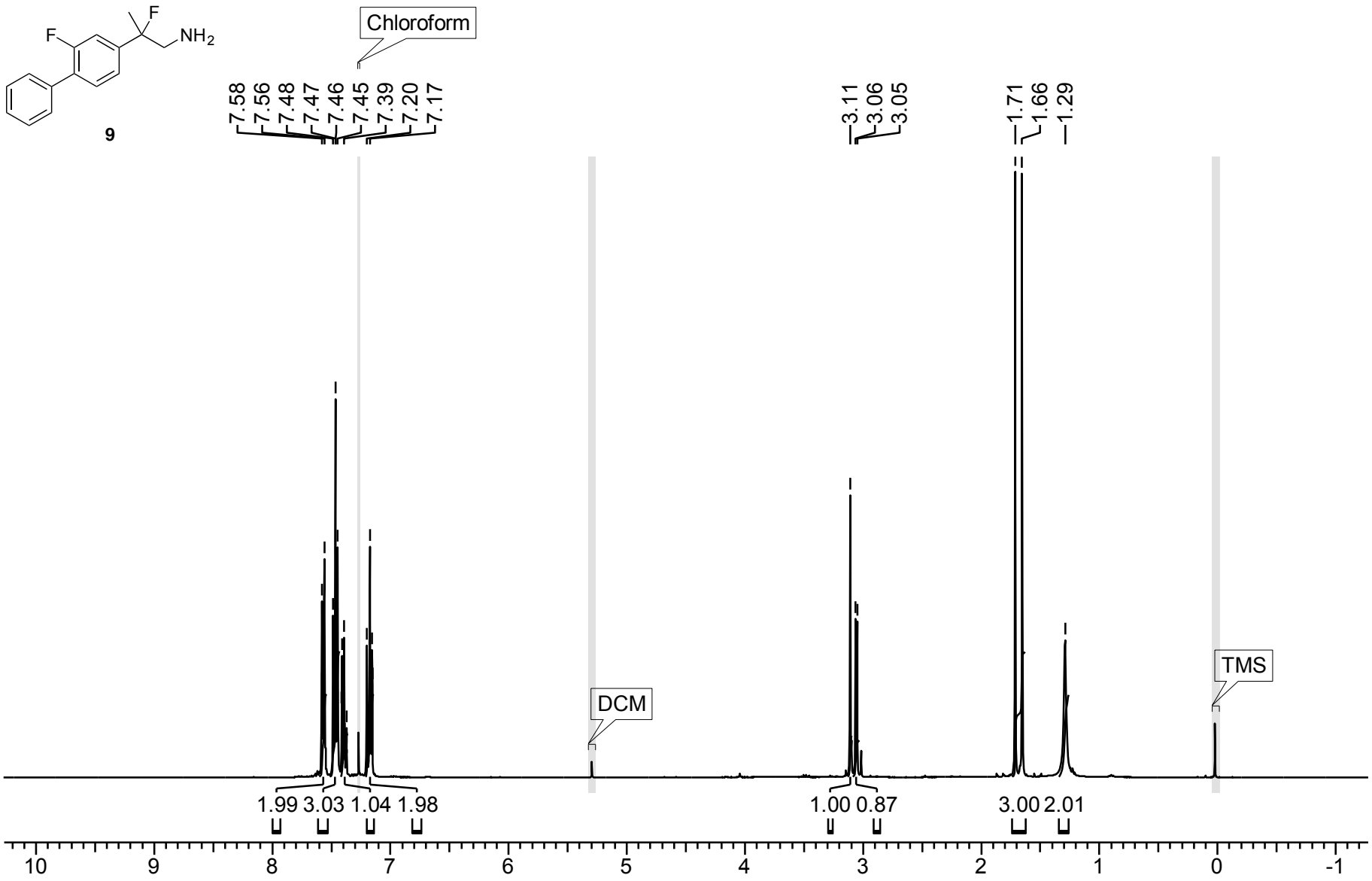

Figure S229. ^{1}H NMR (400 MHz, $CDCl_3$) spectrum of **9**.

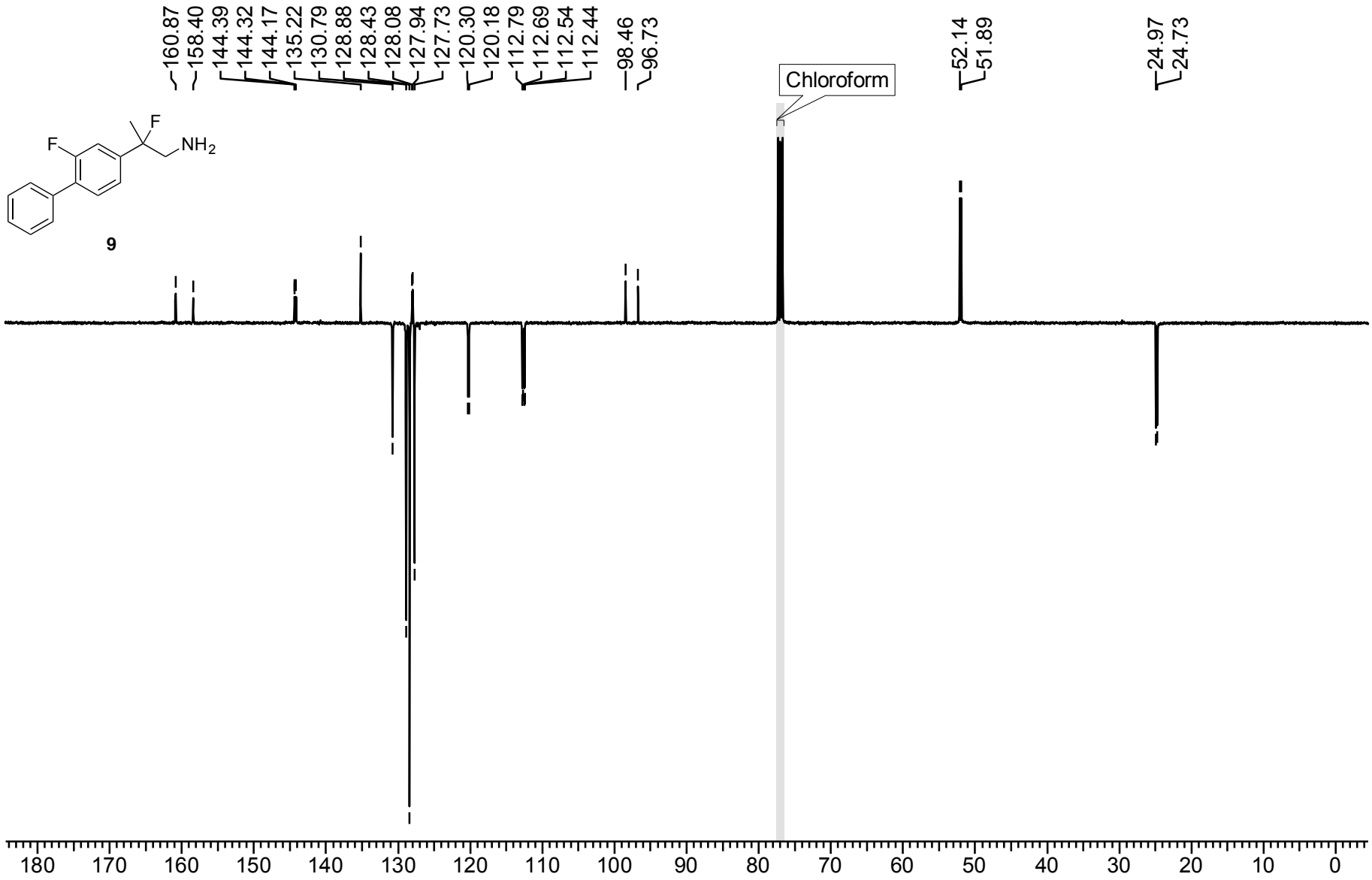

Figure S230. ^{13}C NMR APT (100 MHz, $CDCl_3$) spectrum of **9**.

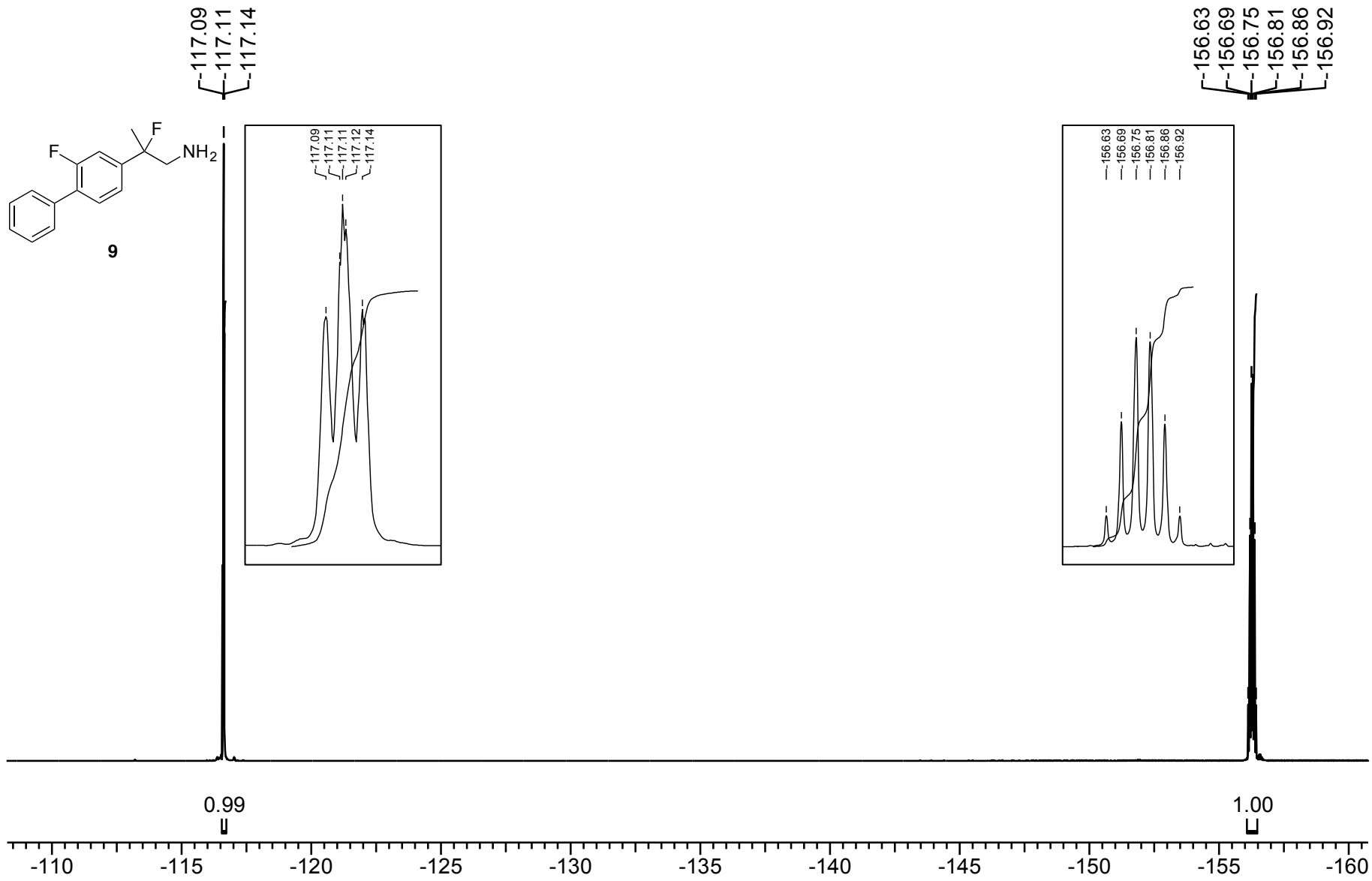

Figure S231. ^{19}F NMR (376 MHz, $CDCl_3$) spectrum of **9**.

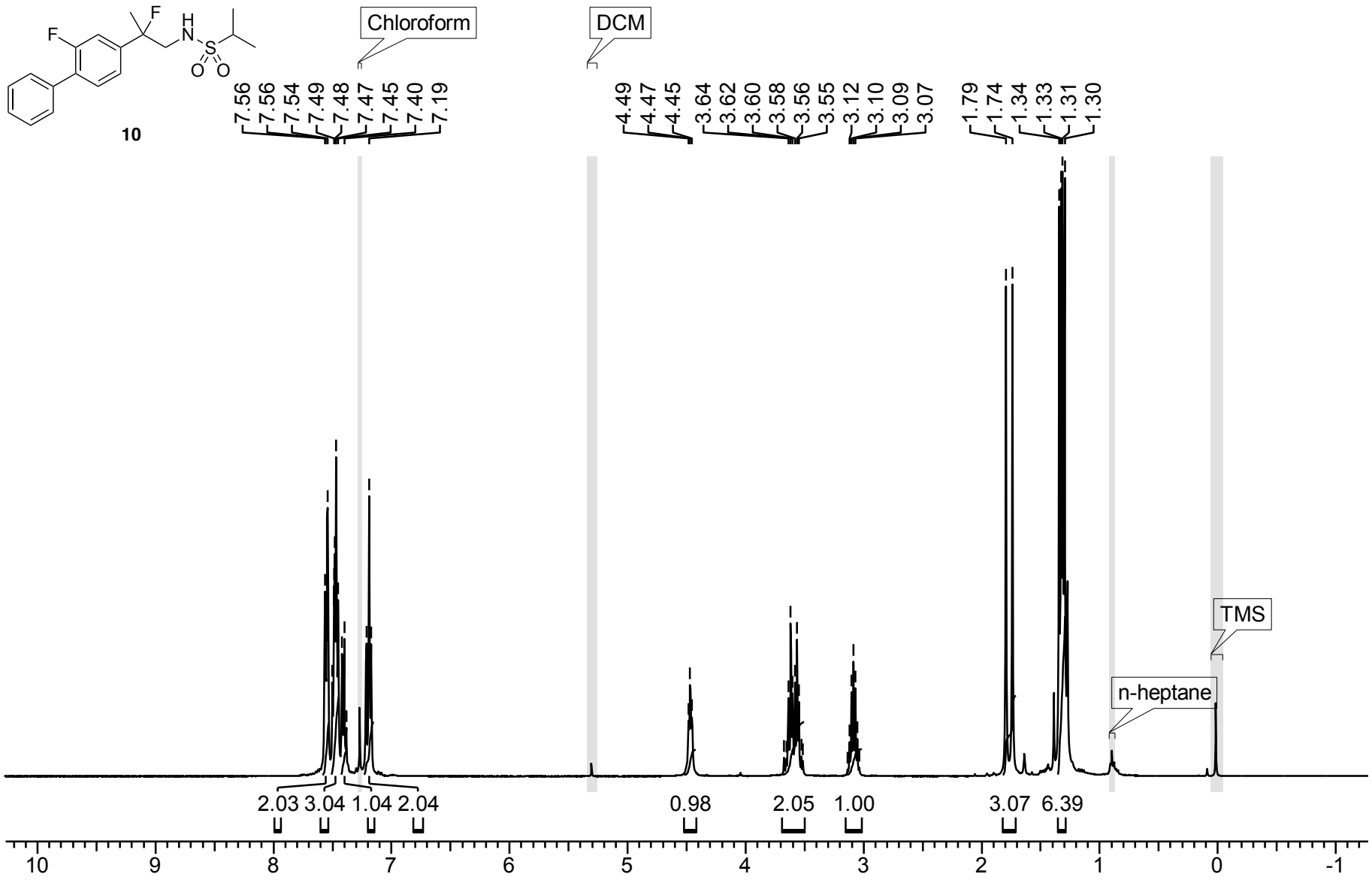

Figure S232. ^{1}H NMR (400 MHz, $CDCl_3$) spectrum of **10**.

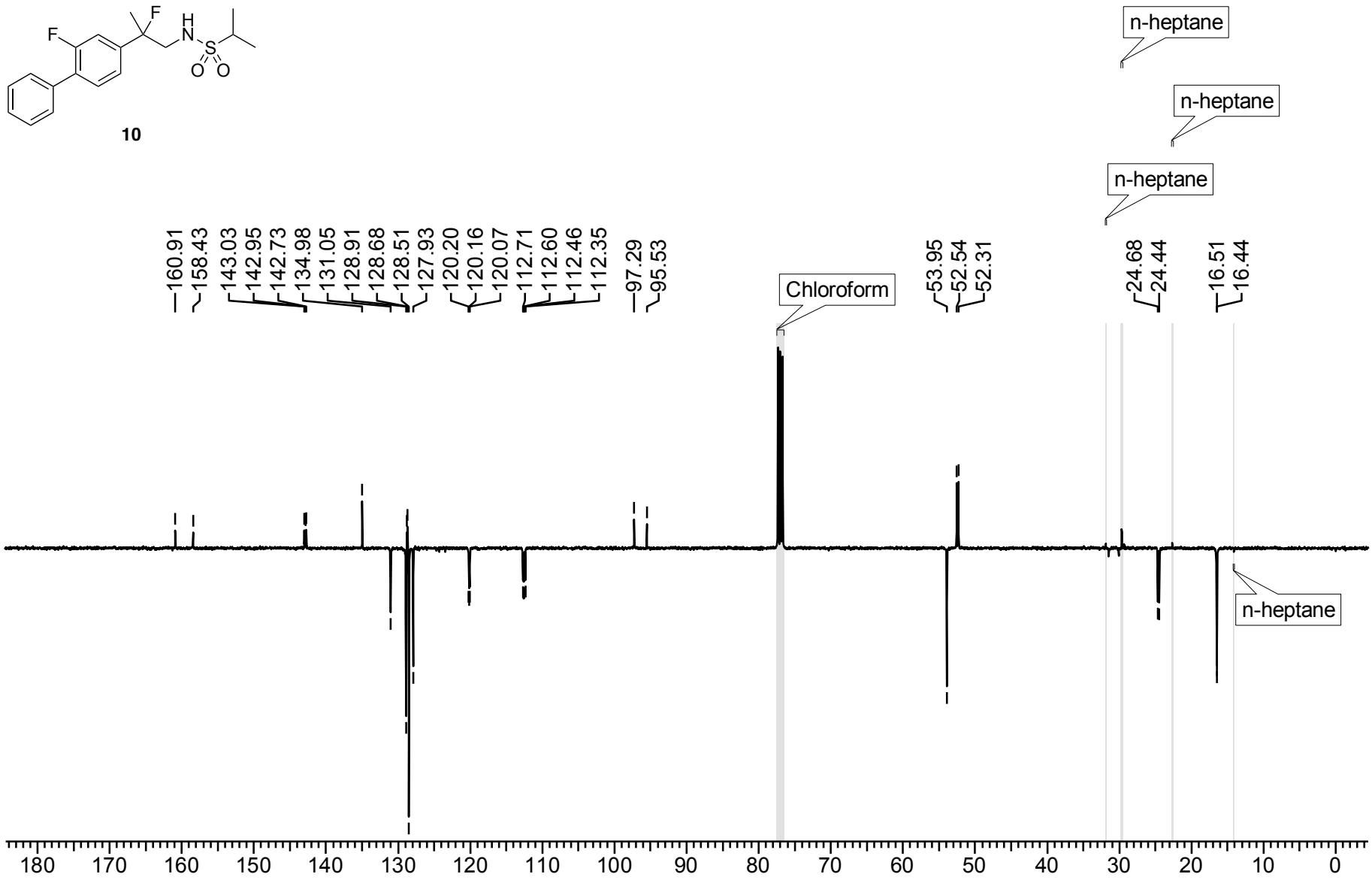

Figure S233. ^{13}C NMR APT (100 MHz, $CDCl_3$) spectrum of **10**.

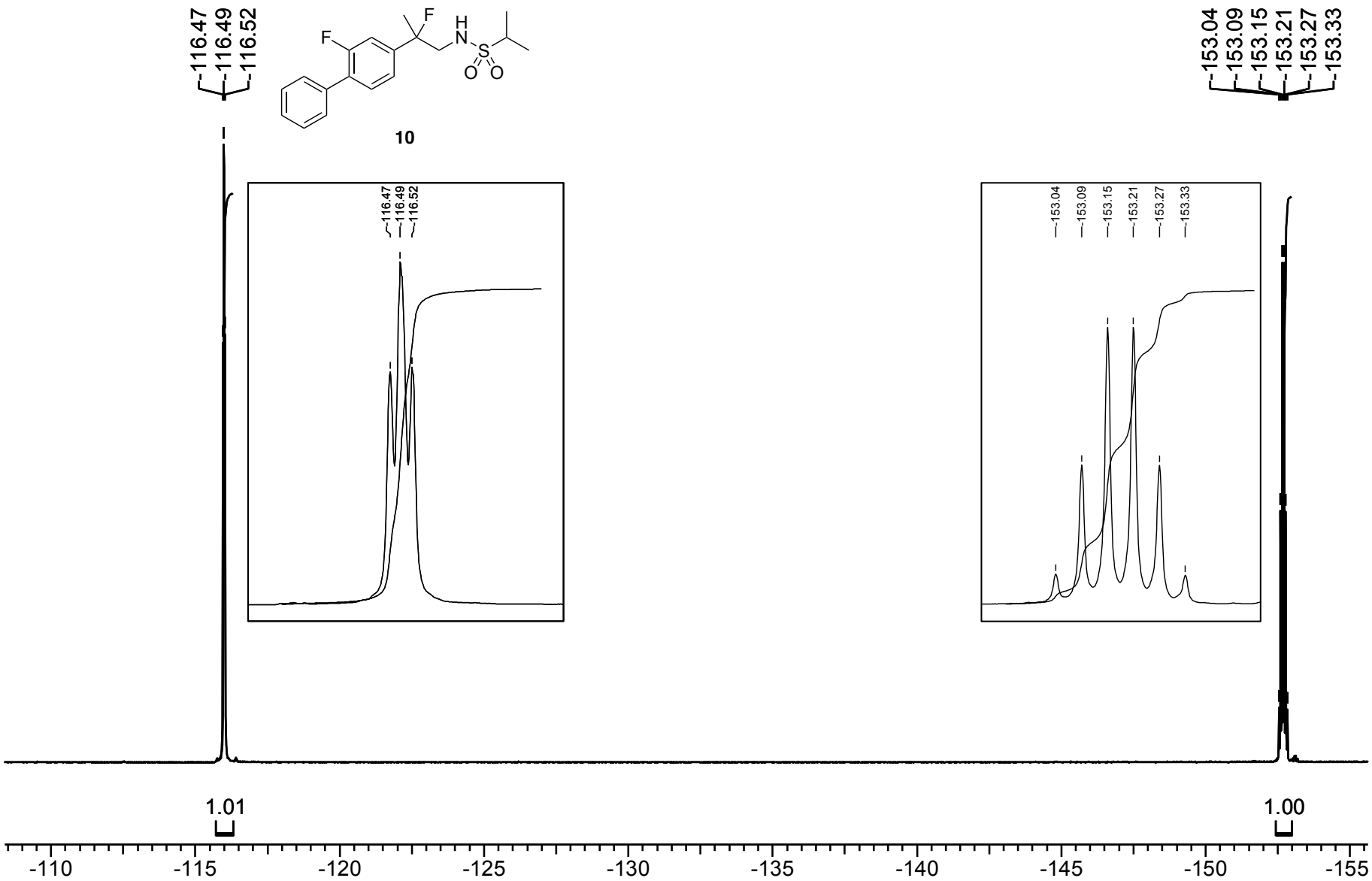

Figure S234. ^{19}F NMR (376 MHz, $CDCl_3$) spectrum of **10**.